A study of mechanisms of cell cycle regulation in the male gametophyte of *Arabidopsis thaliana*

Thesis submitted for the degree of Doctor of Philosophy

Said S. Hafidh

Department of Biology
University of Leicester
October, 2008

ABSTRACT

A study of mechanisms of cell cycle progression in the male gametophyte

Said Hafidh, 2008

The haploid male gametophyte of angiosperms has an integral role in the production of twin sperm cells necessary for the double fertilization, the essence of flowering plants. However, the mechanisms regulating sperm cell formation and cell fate specification has yet to be identified. In this study, the thesis investigates the function of key cell cycle regulators and presents characterisation of a novel pollen division mutant of Arabidopsis (*duo3*) that fails to produce twin sperm cells. In addition, the project also examines the activity of small RNA (smRNA) pathways as a potential mechanism that modulates native gene expression. Pollen cell-specific vectors were constructed to drive the expression of hairpin double stranded RNA (hp-dsRNA) as tools for investigating the activity of smRNA pathways, and their efficacy was tested by manipulating expression of key cell cycle regulators in Arabidopsis. Indeed, expression of hp-dsRNA intended to knockdown transcripts of Cyclin B1 members, revealed a putative role Cyclin B1 in microspore and germ cell division. Furthermore, analysis of a *Cyclin B1;1* reporter led to the identification of *DUO1* (a pollen specific R2R3 MYB protein) but not *DUO3* as a germ cell-specific regulator of *Cyclin B1;1* expression. This interaction was further verified by rescuing mutant *duo1* plants with Cyclin B1;1. Analysis of *DUO3* expression revealed restricted patterns confined predominantly in dividing tissues. Moreover, study of *Cyclin B1;1* reporter revealed mutant *duo3* cells to be impaired in degrading Cyclin B1;1 protein, suggesting a role in modulating Cyclin B1;1 activity. In summary, this work has highlighted a potential role of the Cyclin B1 family in the development of the male gametophyte. Use of *Cyclin B1;1* marker has demonstrated a first example of germ cell specific integrator of cell division and cell differentiation and a putative role of *DUO3* in germ cell division. A significant progress has been achieved in understanding smRNA pathways and the vectors generated will be exploited to gain more insight into the development of the male gametophyte.

Acknowledgments

I would like to thank Prof. David Twell for his excellent supervision, endless support and continuous encouragement throughout the project.

I would also like to thank all members of the Twell lab (2004-2008) for their friendship, scientific advice and for being a good team, Maxi-Borg in particular.
Warm thanks to members of the Biology Department for their support during the course of this project. Sincere gratitude to Peny Buttler, Sue, Steve, Judy and Tony for "putting up with me" throughout my PhD course.
I am very grateful to my mother, my late father and rest of my family for their patient and invaluable support. I would like to apologise for abandoning them in Africa to pursue my career. I am looking forward to seeing you more in the near future.

Special thanks must go to Pan Jerzy and Pani Maria for their wonderful and warm welcome in Rzeszow and providing me with "classic" facilities particularly "only hit records", salatka jarzynowa, filet z kurczaka, ziemniaki tluczone, and a classic PC from 1985 for writing my thesis, all had a significant contribution to the completion of my PhD project. I would like to extend my gratitude to Iza Wojcik and Marcin Stachurski for their wonderful support and entertainment.
I am grateful for this pleasant opportunity to express my sincere and warm thanks to my sweet "butterfly" Katarzyna Wojcik (Kitty) for her love, caring, entertainment and endless support during the PhD period. One of the best things that happened during this period was our first shared experience of Krakow, and Poland in general, which gave additional and joyful dimension to our relationship.

Table of Contents

CHAPTER TWO
Materials and Methods:

List of figures **Page**

List of tables **Page**

Abbreviations

aa	amino acid
bp	base pair
^{o}C	degrees centigrade
cm	centimetre
DEPC	diethyl pyrocarbonate
DNA	deoxyribonucleic acid
dNTP	deoxynucleotide triphosphate
DW	deionized water
EDTA	ethylenediaminetetraacetic acid
g	gram
GUS	b-glucuronidase
h	hour
kb	kilobase pair
l	litre
M	molar
MES	2-(N-Morpholino) ethanesulfonic acid
μl	microlitre
ml	millilitre
μM	micromolar
mM	millimolar
mg	milligram
MS	Murashige and Skoog
PCR	polymerase chain reaction
RNA	ribonucleic acid
rpm	revolution per minute
RT	room temperature
RT-PCR	reverse transcriptase-PCR
SD	standard deviation
TAE	tris-acetate EDTA
Tris	tris(hydroxymethyl)aminomethane
Triton X-100	(t-Octylphenoxypolyethoxyethanol)

U	enzyme units
v/v	volume per volume
WT	wild type
w/v	weight per volume

Chapter one

Introduction

1. Plant life cycle and formation of gametophyte generation

The life cycle of higher plants is well characterised by the postembryonic organ development which progress through a diploid vegetative generation to the haploid reproductive phase. This is in contrast to animal development, which possess a pre-laid embryonic pattern that defines the phases of development. The absence of germline lineage from the early stages of development, competence for flexible and reversible cellular differentiation, alteration of haploid and diploid generations and the evolution of a unique double fertilization process, are the key features that has defined the evolutionary success and dominance of flowering plants. The architecture of reproductive development in plants and animals are far from being similar. In animals, the primodial germ cell lineage is specified and set aside from the somatic cell lineage early during embryo development, whereas plants do not establish their germ cell lineage until at the later stages of development. The presence of a continual supply of undifferentiated cells at the shoot meristem with stem cell characteristics, allows the plant to switch somatic gene expression programmes and specify cell fate of stem cells destined to become germ cells (Caryl et al., 2003). Furthermore, the animal germ line produces meiotic products that instantaneously differentiate to produce haploid gametes. On the contrary, the haploid products of meiosis in the plant germ line undergo a further round of mitotic division to form the haploid gametophyte that is responsible for the production of gametes (sperm cells and egg cell, Figure 1.1). Plants seem to have reserved the reproductive decision later in development, as such, it will be fascinating to understand the molecular pathways through which plants and animals define their germ cell lineage and where the specificity of these pathways lies between the two kingdoms.

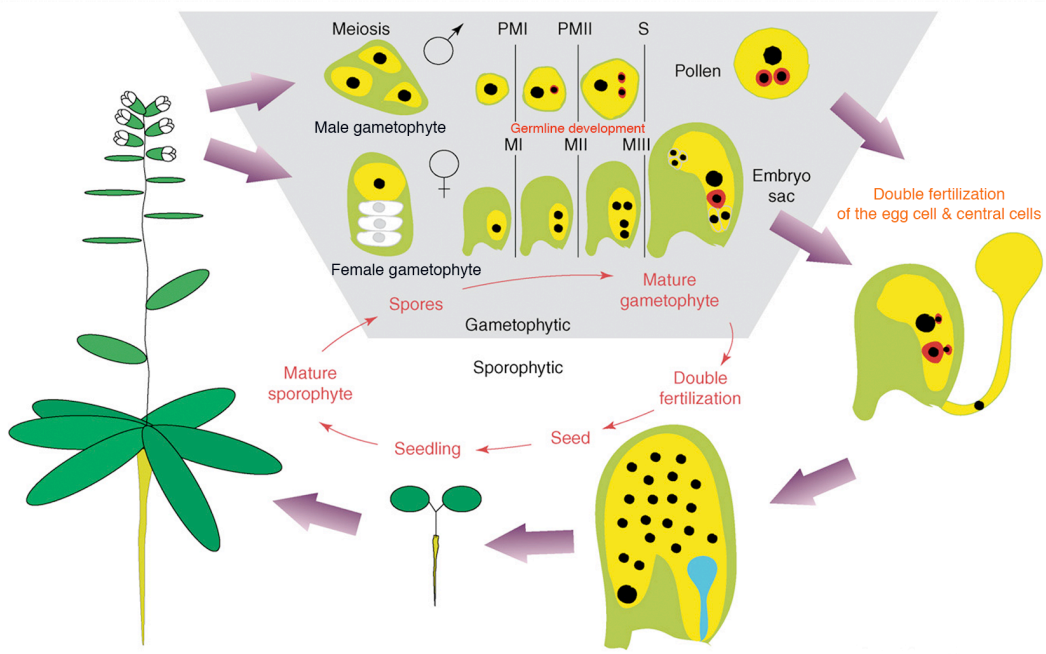

Figure 1.1 A model of life cycle of flowering plants and development of gametophyte generations.

The alteration of generation in flowering plants starts with the development of sporophyte as a dominant phase. The gametophyte generation (male and female gametophyte) is produced within the flowers of the sporophyte. Both forms undergoes two or three mitotic divisions to produce a set of sperm cells (marked red) and a vegetative cell in the male, and the egg cell (shown in red), surrounding synergid cells and central cell in the female gametophyte. The two sperm cells participate in the double fertilization following arrival in the embryo sac through a vegetative cell grown pollen tube. One sperm cell fuses with the egg cell to form the embryo, and the other fuses with the central cell to generate and endosperm. The newly formed zygote is nutritioned by the endosperm to generate a seedling that mark the start of a new life cycle.

(Image adapted and modified from Berger et al., 2006)

1.1 Overview

Development of the male gametophyte

The haploid male gametophyte (pollen grain) is a highly reduced haploid structure during the plant life cycle that is responsible for the production of twin sperm cells. The development of the male gametophyte is initiated in the anther of a stamen (the male reproductive organ) following differentiation of archesporial cells into sporogenous cells (Figure 1.2). The sporogenous cells then undergo a mitotic division to produce diploid meiocytes, also known as pollen mother cells. The progression of male gametophyte development from the pollen mother cell can be divided into two sequential phases, microsporogenesis and microgametogenesis. During microsporogenesis, the microsporocytes undergo meiosis to produce a tetrad of four haploid microspores enclosed in a callose wall. Completion of microsporogenesis and initiation of microgametogenesis is marked by the release of haploid unicellular microspores from tetrad by the activity of callase enzymes secreted by the inner layer of the locules (tapetum). Thereafter, the released microspores progress as independent entities from the sporophytic influences and mark the beginning of the male germline. During microgametogenesis, haploid microspores expand due to increase in vacuole size and number. This is accompanied by the fusion of smaller vacuoles to generate a large single vacuole that is associated with the displacement of the microspore nucleus to a peripheral position against the cell wall (Owen and Makaroff, 1995; Twell et al., 2006). Each polarised microspore undergoes an asymmetric division, termed Pollen Mitosis I (PMI), which result in the formation of cell-within-a-cell structure in which the two cells acquire distinct cell fates. A small generative cell is produced engulfed within the cytoplasm of a large vegetative cell. This is a unique feature of the male gametophyte development and has raised intriguing questions concerning how the distinct cell fate is achieved between the two cells that arise from the same cytoplasmic mass. Certainly, the asymmetric division of the

haploid microspore is known to be important for the correct generative cell fate specification, and vegetative cell fate is a default developmental pathway (Eady et al., 1995). After PMI, the vegetative cell exits the cell cycle and remains at G1 phase (Zarsky et al., 1992). The vegetative cell is necessary for nurturing generative cell development as shown by cell ablation studies (Twell, 1995) and most importantly to grow a pollen tube through the style (female reproductive organ) to deliver the two sperm cells to the embryo sac for double fertilization.

The generative cell with condensed nuclear chromatin migrates to the centre of the pollen grain and elongates to form a spindle-like shape. This structure is maintained by a cortical cage of microtubules aligned longitudinally to the long axis (Cai and Cresti, 2006). In Arabidopsis the generative cell undergoes a second mitotic division termed Pollen Mitosis II (PMII) to produce two identical sperm cells that remain associated with the vegetative cell nucleus (Lalanne and Twell, 2002). However, 70% of the flowering plants shed bicellular pollen grains and the tricellular state is achieved in a germinating pollen tube following successful pollination (Brewbaker, 1967).

The simplicity of the male gametophyte, the presence of a cell-within-cell structure with specialised cell fates, and the highly choreographed cellular processes, makes the male gametophyte an attractive model for studying molecular pathways regulating different aspects of cellular development. This pathway serves as an effective system in understanding control of cell cycle progression and cell specification, factors that determine cell polarity and differential gene expression between different cell types, and how are these events co-ordinated together. To date, advances in genetic and genomic technologies including the highly annotated *Arabidopsis thaliana* genome (The Arabidopsis Genome Initiative, 2000) and its associated databases, availability of comprehensive transcriptomic data sets including those from developing pollen and recent data from isolated sperm cells

(Honys and Twell, 2004; Borges et al., 2008) and identification of several gametophytic mutants, has lifted the boundaries and limits that had previously hindered the progress in understanding molecular mechanisms that govern male gametophyte development (Twell et al., 2006).

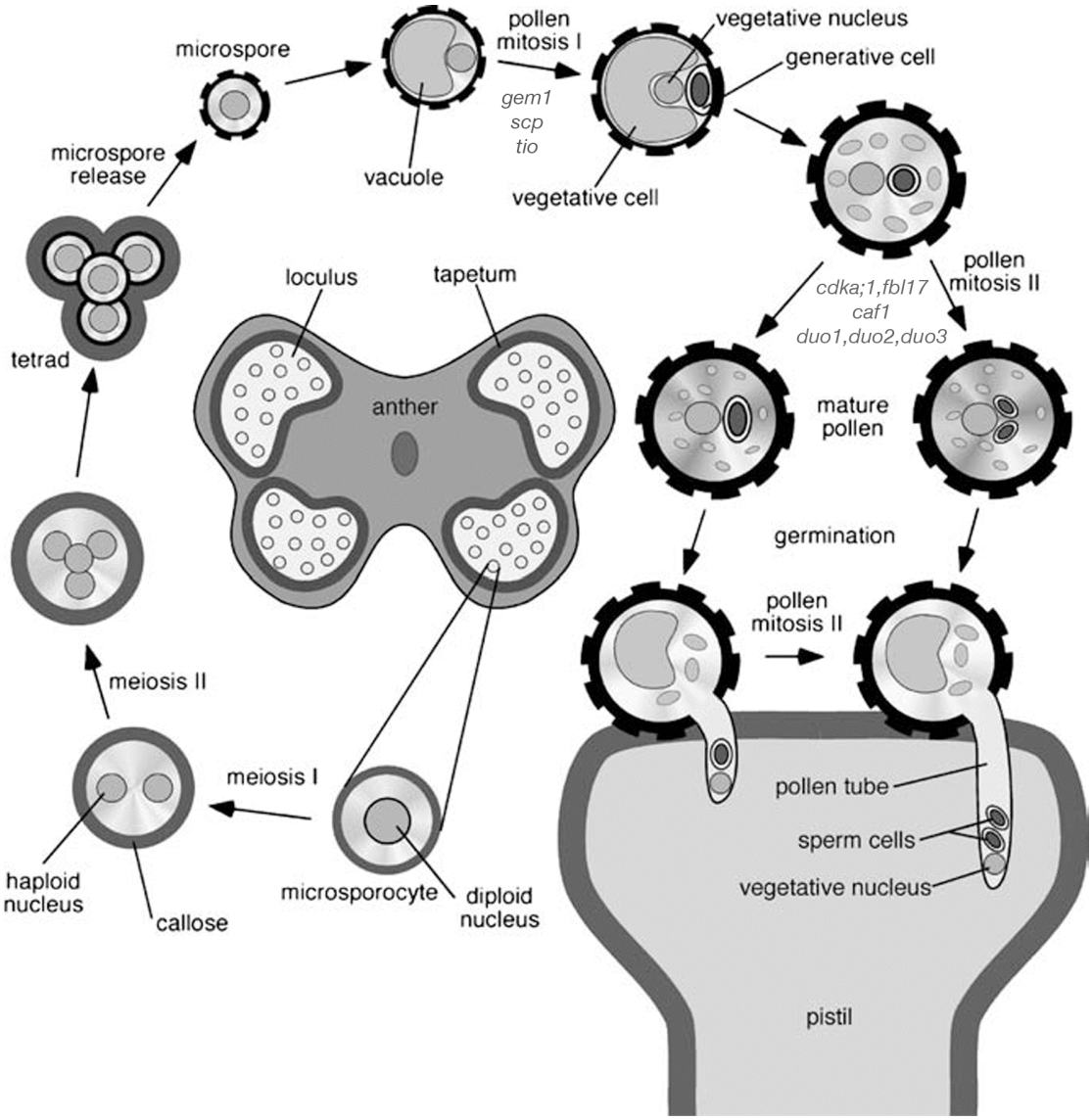

Figure 1.2 **Schematic representation of the male gametophyte development**.

Development of the male gametophyte is initiated following two nuclear divisions of the microsporocytes (megagametogenesis) to produce haploid microspores. Each micropsore undergoes an asymmetric division (pollen mitosis I) to produce a large vegetative cell and a small engulfed germ cell. Several mutations are known to disrupt the asymmetric division including *gemini pollen I* (*gem1*), *sidecar pollen* (*scp*) and *two-in-one* mutants (*tio*). In Arabidopsis, the germ cell undergoes a second symmetric division (termed pollen mitosis II) to produce a pair of sperm cells prior to pollen shed. In other flowering plant species (30%), the second mitotic division occurs within the pollen tube. The division of the germ cell and subsequent double fertilization event has recently been demonstrated to be under strict regulation by key cell cycle regulators such as *cyclin dependent kinase 1* (*cdka;1*) and *f-box like 17* (*fbl17*), chromatin remodelling proteins including *chromatin assembly factor 1* (*caf1*), and several DUO-like proteins, *duo pollen 1-3* (*duo1-3*).

(Figure adapted and modified from Twell et al., 2006)

2. Genetic analysis of male gametophyte development

Several genetic studies of mutants affecting male gametophyte development have provided substantial understanding and shed new light in identifying genes involved in cellular processes that are vital during male gametogenesis. With regard to this project that aims to provide more insight into the mechanism that control cell cycle progression and cell fate specification in the male gametophyte, studies describing pollen division mutants that affect different aspects of the cell cycle and their consequences on cell fate determination during male gametogenesis are discussed.

A: Mutants defective at PMI lack generative cell fate characteristics

Genetic screens in *Arabidopsis* for morphological mutants have identified several genes that affect microspore division and fail to produce tricellular pollen grains. *Sidecar pollen* (*scp*) was identified as a gametophytic mutant that affects microspore division symmetry (Chen and McCormick, 1996). Released microspores undergo premature symmetric division to produce two equal cells, with one of the daughter cells adopting a vegetative cell fate and the second daughter cell maintaining a microspore fate divides asymmetrically to produce a second vegetative cell and two sperm cells. These observations highlight the significance of asymmetric division for a correct cell fate specification. Similarly, *gemini pollen 1* (*gem1*) mutant was also shown to affect microspore polarity, asymmetric division and cell fate specialization (Park et al., 1998). GEM1 was later demonstrated to encode MAP215 family of microtubule binding protein, and was essential in stimulating growth of interphase, spindle and phragmoplast microtubule arrays (Twell et al., 2002). In *two-in-one* (*tio*), mutant plants shed binucleate pollen grains at pollen maturation with a vegetative cell fate, confirming that the vegetative cell fate is the default program and that germ cell fate needs to be established gametophytically (Twell et al., 1998). This suggests that presence of TIO is

necessary for complete asymmetric division and correct cell fate determination. TIO is the homologue of the Ser/Thr protein kinase FUSED, a key component of the hedgehog-signalling pathway in fruitflies and humans, and is has been shown to play essential role in centrifugal cell plate expansion (Lum and Beachy, 2004; Oh et al., 2005). Combining the findings of these studies, it is clear that defects in PMI progression can have adverse consequences on the subsequent division (PMII) and cell fate specification, and correct polarization of the microspore nuclei is a pre-requisite for generative cell fate. Takeda et al, (2005) showed that TCP16, a putative transcription factor belonging to the teosinte-branched, cycloidea, PCNA factor (TCP) gene family (Cubas et al., 1999), is required for normal microspore development. Expression of hair-pin dsRNA targeted to the TCP16 mRNA transcripts at the tetrad stage causes severe morphological abnormalities and degradation of genomic DNA (Takeda et al., 2006). TCP16 is predominantly expressed in microspores detected from tetrad stage and markedly increases in early unicellular stage (Takeda et al., 2006), however, the exact role played by TCP16 at the microspore stage remains to be established.

B: Regulators of germ cell division at PMII

Upon the asymmetric division of the unicellular microspore, the smaller germ cell produced is destined to become a progenitor of the twin sperm cells marking the beginning of the male germline. Following engulfment, migration, elongation into a spindle-like shape and condensation of its chromatin, the generative cell undergoes a single mitotic division (PMII) to produce two sperm cells that participate in the double fertilization event.

Thus far, no mechanisms have been verified at the molecular level that specifies the fate of the germ cell from the default vegetative cell fate. However several models have been proposed based on the significance of asymmetric division which implicate unequal

partitioning of the cell fate determinants that repress the germ cell fate in the vegetative cell and allow expression of germ cell specific genes (Eady et al., 1995). Recent transcriptomic studies of germ cell specific expressed transcripts generated from isolated germ cells of *Lilium longiflorum* (lily), led to the identification of a ubiquitous non-germ cell repressor protein, Germline Restrictive Silencing Factor (GRSF) that has been proposed to repress male germline specific gene expression in non-germ cells (Haerizadeh et al., 2006). Development of new techniques that allowed isolation of the male germ cell has led to a growing number of studies focused on understanding the transcriptomic profile of the male germline. As such, there is now evidence for extensive male germline gene expression in maize (Engel et al., 2005), lily (Okada et al., 2006), male germline specific expressed genes in Arabidopsis (Twell et al., 2006) and recently a near complete transcriptome from Arabidopsis sperm cells (Borges et al., 2008). These findings implicate the presence of regulatory networks that govern this specific pattern of germ cell development and gene expression.

An increasing number of mutations have been described in Arabidopsis that block germ cell division at PMII, producing bicellular pollen grains with a single germ cell associated with a vegetative cell nucleus. Most of the genes affecting germ cell division that have been described to date are essential components of the cell cycle machinery, reflecting the dominant cellular process undertaken by the germ cell in the production of two sperm cells. Cyclin dependent kinase of the A type family (CDKA;1) is a key regulator of the cell cycle machinery that operates from licensing DNA replication to entry and progression through mitosis. Mutations in CDKA;1 result in a pollen with a single germ cell at the mature pollen stage demonstrating an essential role in germ cell division (Nowack et al., 2006; Iwakawa et al., 2006a). Monitoring of DNA content of the *cdka;1* mutant pollen grains identified a significant delay of S-phase progression in a mutant germ cells. Furthermore, despite the lack of division, the mutant cell is capable of growing a pollen tube (demonstrating

independent functioning of the vegetative cell) and preferentially fertilizes the egg cell, illustrating that germ cell differentiation can be uncoupled from cell division. This preference of the mutant germ cell for fusion with the egg cell and exclusion of central cell fertilization, might be influenced by positional constraints, signalling within the embryo sac, or incomplete germ cell differentiation (Nowack et al., 2006).

Recent work has shown that mutation of the *F-box-Like 17* (*FBL17*) gene produces a similar phenotype to that of *cdka;1* mutant pollen grains (Kim et al., 2008). The F-box is a protein motif of approximately 50 amino acids that mediates protein-protein interaction and is one of the components of the SCF ubiquitin-ligase complexes composed of Skp1 and CUL1 that form the SKP1-CUL1-F-box (SCF) complex (Kipreos and Pagano, 2000). The SCF is an E3-ubiquitin protein ligase complex that is involved in the ubiquitination of substrates for 26S proteosome mediated proteolysis. F-box-like proteins have been shown to positively regulate CDKA activities by directing degradation of *CDKA* inhibitory proteins (Kip related proteins, KRPs), through the SCF complex. Similarly, during male gametophyte development expression of *FBL17* is excluded from the vegetative cell and preferentially expressed in the germ cell marking *KRP6* and *KRP7* proteins for degradation (Kim, 2008). Consequently, this removes inhibition of the *CDKA* activities and facilitates normal S-phase progression. In the absence of *FBL17*, the germ cell fails to degrade *KRP6* and 7 proteins and the persisting activities of *KRP6* and *KRP7* result in a slower S-phase and delay in a mitotic entry at PMII. Exclusion of *FBL17* from the vegetative cell allows continuous action of *KRP6* and 7 in inhibiting *CDKA;1* activities, and perhaps that might be one of the mechanisms that prevent the vegetative cell nucleus from progressing through the cell cycle. Thus, *FBL17* provides a differential cell cycle switch that defines the germ cell division competence and the quiescent state of the vegetative cell. It will be intriguing to understand if ectopic expression of *FBL17* in the vegetative cell will alter the inert fate of the vegetative cell.

Another class of mutants that have also been shown to affect male gametophyte development is the Chromatin Assembly Factor-1 (CAF1) pathway mutants that include *fas1*, *fas2*, and *msi1* (Wagner, 2003). CAF1 possesses chaperone activity for chromatin assembly at the DNA replication fork during S-phase progression and loss of *FASCIATA1* (*FAS1*) or *FASCIATA2* (*FAS2*) causes fasciations as a result of enlarged shoot apical meristem. Loss of *CAF1* activity in pollen causes delay and arrest of the cell cycle prior to PMI and PMII (Chen et al., 2008). Mutant bicellular CAF1 deficient pollen grains acquire correct germ cell fate and are able to equally fertilize the egg cell or the central cells, unlike mutant germ cells of *cdka;1* and *fbl17*. Thus, *CAF1* plays an essential role throughout pollen development and loss of its activity (*caf1*) has demonstrated that correct chromatin assembly is important for germline and sperm cell formation.

duo pollen mutants: a novel class of male germ cell division mutants

One of the fruitful outcomes from the Twell lab in pursuing the interest of understanding regulators that govern cell cycle progression in the male gametophyte, was the identification of a novel class of mutants termed *DUO POLLEN (DUO)*, whereby their presence is essential to allow entry and progression through PMII during germ cell division (Durbarry et al., 2005). *duo pollen* mutants progress normally through the asymmetric division of the unicellular microspores, however, in some *duo* mutants the resulting germ cell fails to enter PMII whereas others fail to progress through the mitotic phase of the cell cycle (Durbarry et al., 2004. PhD thesis). Heterozygous *duo1* and *duo2* mutant plants produce approximately 50% bicellular pollen (demonstrating high penetrance and gametophytic nature of the mutations), and contain a single germ cell at the mature pollen stage (Durbarry et al., 2005). Monitoring of DNA content of the mutant *duo* pollen during development showed that, whereas *duo2* mutant germ cells enter mitosis and arrest at prometaphase, germ cell nuclei that lack *duo1* activity complete S-phase but fail to enter PMII and remain arrested at G2/M

phase (Durbarry et al., 2005). *DUO1* belongs to the MYB transcription factor gene family that contains approximately 130 MYB genes identified in Arabidopsis (Jiang et al., 2004). It encodes an R2R3 MYB protein that is specifically localized in the germ cell nucleus (Rotman et al., 2005). Plant MYB proteins have been speculated to be involved in controlling a range of cellular processes including phenylpropanoid biosynthetic pathway, cellular morphogenesis, and signal transduction pathways (Martin and Paz-Ares, 1997), in contrast to the control of cell proliferation and cell differentiation as demonstrated in other kingdoms (Ito et al., 2001a). Deficiency of *DUO1* in the germ cell does not affect S-phase progression and mutant germ cell reach a DNA content of approximately 1.98C prior to PMII (Durbarry et al., 2005). However the mutant germ cells bypasses entry into PMII (demonstrated by a reduction of mitotic figures) and continue with a new round of DNA replication (Durbarry et al., 2005). The *duo1* mutant germ cell is unique compared to the germ cell mutants produced by *cdka;1* and *caf1* mutations in a way that it does not fertilize neither the egg cell nor the central cells. This suggests that the *duo1* mutant germ cells do not acquire sperm cell competence unlike *cdka;1* and *caf1* mutants. Thus, *DUO1* may have a dual role in regulating cell cycle progression and determination of the germ cell fate.

In an effort to provide further insight into the mechanisms regulating the ontogeny of the male gametophyte, characterization and identification of another *duo* mutant, *duo pollen3* (*duo3*), was also carried out. Here, some aspects of the *duo3* characteristics are discussed.

I. Identification, Characterization, and Isolation of *DUO POLLEN3*

Following identification of the *duo3* mutation in a morphological screen of pollen division mutants, characterization of +/*duo3* phenotype showed that reminiscent of the +/*duo1* phenotype, the *duo3* mutation results in approximately 50% bicellular pollen grains at pollen shed containing a round densely packed generative cell nucleus and a diffuse vegetative cell nucleus (Figure 1.3a). The bicellular nature of the *duo3* mutant pollen grains as opposed to binucleate phenotype was illustrated by transmission electron microscopy of sectioned duo3 pollen grain, which showed an intact cell membrane around the generative cell similar to wild type bicellular pollen grain (Figure 1.3b-e). The mutant pollen grains also possess a vegetative cell nucleus and a generative cell nucleus that are centrally positioned and remained in close association with each other, indicative of a normal formation of male germ unit (MGU) prior to PMII (Lalanne and Twell, 2002).

To establish the point of deviation during cell cycle progression of the mutant *duo3* germ cell from that of the wild type phenotype, DAPI nuclear staining was used to monitor DNA content of the wild type and the *duo3* germ cell nucleus by measuring the intensity of the DAPI stained nuclei. Prior to entry into PMII, the DNA content of the wild type germ cell at late interphase was identified to be approximately 1.95C (Durbarry et al., 2005). Post PMII, the newly formed sperm cells (telophasic sperm cell) contain 1C DNA content that later increases to 1.2C before anthesis. Results of the DNA content measurement showed that *duo3* mutant germ cell complete S-phase prior to PMII (with DNA content of 1.98C) but fail to progress through G2/M. Moreover, measurement of the *duo3* mutant germ cell at anthesis revealed an increase of DNA content to 2.42C, indicating that the mutant germ cell complete the DNA replication phase but then bypass mitotic entry and instead initiate another round of DNA replication. To emphasize these results, analysis of mitotic index between wild type and +/*duo3* pollen population at late bicellular stage was performed. Results showed that in +/*duo3* population the mitotic index figure was reduced by

approximately 50% compared to that of the wild type (Figure 1.3f), demonstrating a completion of S-phase but failure to enter mitosis. The genetic nature of the *duo3* phenotype was determined by analysing selfing +/*duo3* individuals and screen of progeny from reciprocal test crosses. Analysis of self progenies showed a 1:1 segregation between wild type and mutant plants, whereas reciprocal test crosses showed a transmission of the *duo3* phenotype only through the female. Thus, the reciprocal test cross demonstrated a male specific gametophytic block of *duo3* transmission. Furthermore, the male gametophytic specific effect of the *duo3* phenotype was further verified by crossing +/*duo3* as a female in the quartet mutant background (+/*duo3*;*qrt1*/*qrt1*) in which the four product of meiosis remain associated within a tetrad (Preuss et al., 1994). If the mutation is gametophytic specific, two members of the tetrad product would show the mutant phenotype considering the mutation is fully penetrant. In a case where the mutation is not fully expressed, the segregation of the wild type and mutant individuals in a tetrad will vary. Analysis of the F1 siblings at pollen shed by DAPI stain showed that approximately 98% of the tetrads contained two bicellular mutant pollen grains and two tricellular wild type pollen grains, whereas the remaining 2% posses one bicellular and three tricellular pollen grains (Figure 1.3g-h). These results demonstrate the male specific effect of *duo3* mutation and a normal development of the female gametophyte.

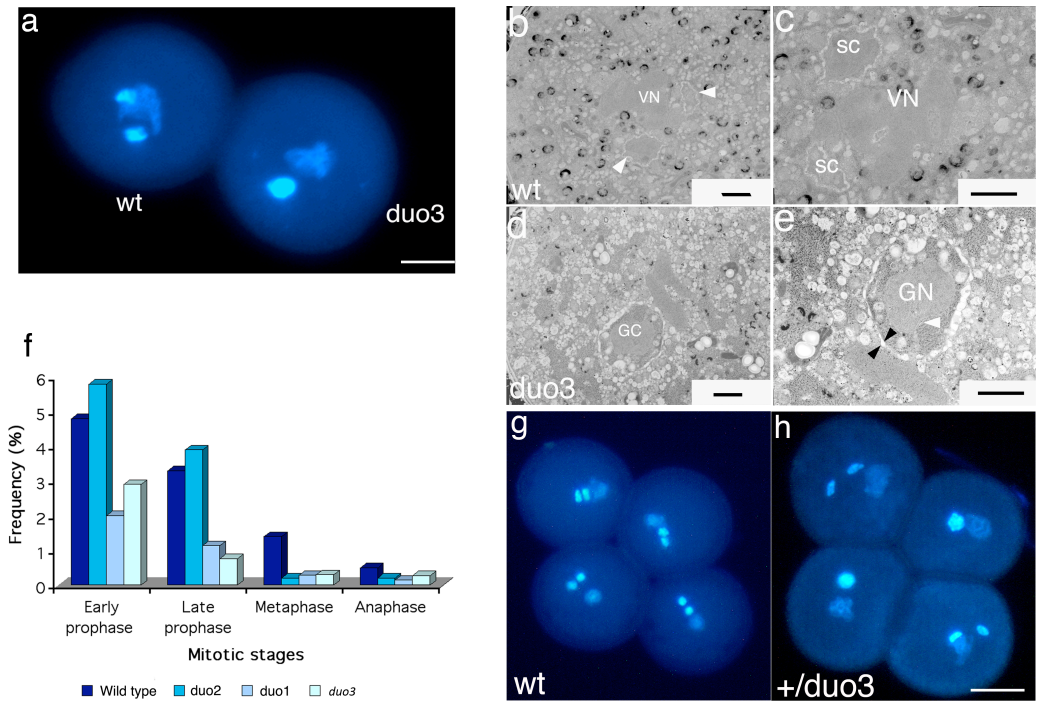

Figure 1.3 ***Phenotypic characterization of the duo3 mutation***
Heterozygous duo3 mutant plants were analysed cyctologically to establish developmental deviation from the wild type phenotype. (a) DAPI stains of wild type pollen grain showing two sperm cell nucleus and the vegetative cell nucleus (Anjusha Durbarry PhD thesis.,2004). Conversely, DAPI stain of the duo3 mutant pollen grains showed undivided germ cell nucleus with a vegetative cell nucleus. (b-e) Transmission electron micrographs of sectioned wild type and duo3 mutant pollen grains showing intact cell membrane of the sperm cells (b-c, white arrows) and the undivided generative cell (d-e, black arrows). (f) Analysis of mitotic progression of Pollen mitosis II in wild type and mutant duo1-duo3. Half of the pollen population in duo1 and duo3 mutant background failed to progress through G2 phase demonstrated by the reduced frequency of mitotic figures, whereas, duo2 showed normal progression through G2/M and arrested at the later stages. (g-h) Gametophytic nature of the duo3 mutation showing 1:1 segregation of the wild type:duo3 mutant phenotype in the quartet mutant background. Scale bars, (a) 5µm, (b-e) 1.4µm, (g-h) 10µm

II. Cloning of *DUO POLLEN3* gene and Identification of the mutant allele

The *DUO3* locus was identified within a 10kb region at the lower arm of chromosome 1 containing two putative genes. The identity of the *DUO3* gene was confirmed through complementation analysis in which a genomic fragment containing a promoter and the coding region of AT1G64570 locus was sufficient to complement the *duo3* phenotype, whereas, a similar region from AT1G64580 fail to complement. Thus, the AT1G64570 locus corresponds to the *DUO3* gene. Sequencing of the *duo3* mutant allele revealed a base pair substitution from Cytosine (C) to Thymine (T) at position +760bp converting Glutamine amino acid (CAG) into a premature stop codon (TAG;Figure 1.4a;Brownfield unpublished). As a result, a truncated protein of 253 amino acids is produced instead of a full-length 1239 amino acids. The AT1G64570 gene spans 5.7kb and contains seven introns and eight exons. The *DUO3* gene encodes a protein of 1239 amino acids with a predicted molecular weight of 137 kDa. Analysis of the protein sequence (http://hits.isb-sib.ch/cgi-bin/PFSCAN) predicted presence of three acidic rich domains, two at the N-terminus end and at the C-terminus end. Moreover, the DUO3 protein posses a Myb-like domain located in the middle of the protein. BLAST searches have revealed that the *DUO3* gene is unique in *Arabidopsis*, however a close homolog was also identified in rice, *OsDUO3* (Figure 1.4a).

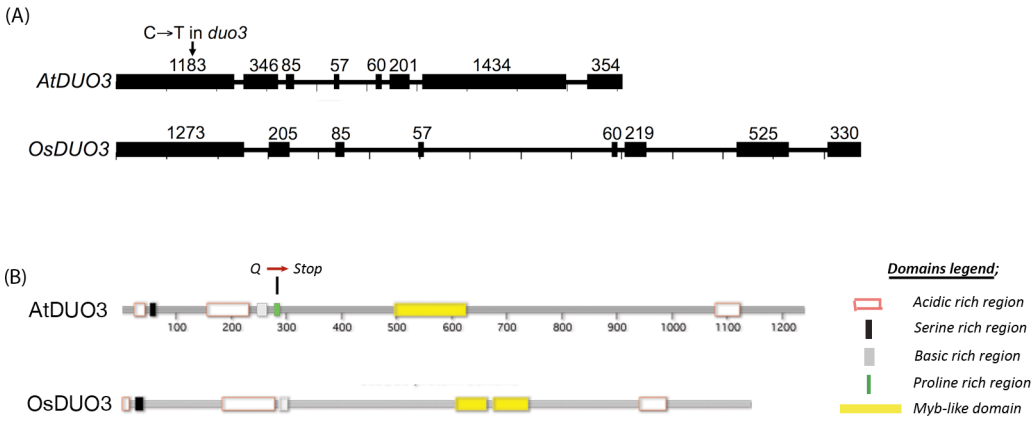

Figure 1.4 **Structure and conservation of the *DUO3* gene**
(A) Genomic structure of the *DUO3* gene from Arabidopsis (*AtDUO3*) and the rice homolog (*OsDUO3*) showing conserved exon-intron structures. Black boxes represent exons with the size of each exon in base pair indicated by the figure above it. Thick horizontal lines represent introns. The site of the duo3-1 mutation is indicated with an arrow. (B) Protein alignment showing conserved domains between the two homologs. Both proteins are drawn with the same scale. Each domain is indicated by the coloured square and the amino acid number is indicated below the AtDUO3 protein structure.

C: Male gametophyte as a model for studying cell cycle

The patterning of the male gametophyte is governed by only two division events, PMI and PMII. This results in a formation of a quiescent vegetative cell, a competent germ cell and two identical sperm cells that upon delivery into the embryo sac participate in double fertilization. This streamlined lineage of the male gametophyte and the formation of cell-within-cell structure with distinct cell fates outclass other cell types and make the male gametophyte as an attractive system for elucidating mechanisms regulating cell cycle progression and cellular patterning, and how these processes are synchronized together. The male gametophyte displays a cellular program whereby cellular processes progress in a highly choreographed and integrated manner. Any disruption of these co-ordinated processes can have severe consequences on the patterning of the male gametophyte and production of two sperm cells. Mutations affecting asymmetric division of the haploid microspores lose their cell fate and fail to produce a vigorous germ cell. This demonstrates a clear need of coordinating

progression of cell polarity before initiating cell division, as this event defines the fate of the daughter cells produced. Thus, by using the male gametophyte as a model system, one can evaluate the coordinating mechanisms that link cell polarity and the initiation of cell division increasing our understanding of the control of male gametophyte development. Moreover, at least three mutations have been described to date that affect germ cell division but with different downstream consequences. A mutant *cdka;1* produce a single germ cell with a "partial" sperm cell characteristics that is able to preferentially initiate fertilization of the egg cell and autonomous endosperm development. Whereas, *caf1* mutants also produce a single germ cell that is capable of fertilizing equally the egg cell or the central cell. In contrast, in the *duo1* mutation, the single germ cell produced fails completely to fertilize either of the female cell types. It is of no doubt that the process of cell division can be uncoupled from cell differentiation, but equally they can also be linked together by factors that play dual role on both processes. Thus by dissecting male division mutants, additional knowledge can also be gained by investigating the effect on other cellular processes. With the current advance of genetic, genomic and molecular technologies, dissecting mechanisms that regulate different aspects of cellular processes using the male gametophytic system would be more intriguing rather than challenging.

3. Cell cycle regulation during plant development

A: Introduction to the plant life cycle

Cell cycle is one of the most extensively studied biological processes across different species largely due to its importance in regulating growth and development, and the consequences of its deregulation results in many diseases. Considering the divergence of different species, studies of the mechanism of cell cycle control in different organisms has provided a universal picture on how the basic cell cycle machinery is operated, as well as demonstrating how this basic cell cycle machinery has been modified to cope with different environmental demands. The mechanisms of cell cycle control in plants share common features as of that of other eukaryotes. However, plants have extended families of some of the cell cycle regulators such as Cyclin dependent kinases (CDK) that are unique to plants, suggesting a much more complex mechanism perhaps to accommodate the postembryonic development and the plasticity of plant development in contrast to pre-embryonic laid developmental pattern observed in other eukaryotes.

The mitotic cell cycle consists of four sequential ordered phases that separate DNA replication from chromosome segregation (Figure 1.5). The widely conserved cyclin-dependent kinases (CDKs) from yeast, mammals and plants, and their cyclin subunits (Cyc) are the core components required for cell cycle progression, regulating transitions from Growth phase 1-to-DNA synthesis phase (G1/S) and from Growth phase 2-to-Mitotic phase (G2/M), as well as progression and exit from the cell cycle. The gap phases operate as check points to ensure accurate execution of the previous phase. Progression through the phases of the cell cycle is controlled by a specific combination of CDK-Cyc proteins, and their stage specific interaction is achieved through regulation of the abundance of cyclin proteins. Given appropriate arrays of internal and external signals, cells at G1 phase can be induced to enter S phase to initiate DNA replication. Completion of chromosome doubling triggers reorganization of the cytoskeleton in early G2 phase to generate a network of spindle cages

from opposite poles of the mother cell ready for chromosome separation into two daughter cells. In plants, entry into mitosis is preceded by rearrangement of transversely organised arrays of cortical microtubules into a narrow cortical ring, termed pre-prophase band, to mark the future division plane. The pre-prophase band is replaced with the mitotic spindles that separate the two sets of chromosomes to opposite poles, and the microtubules are recycled to form a phragmoplast that initiate the formation of new cell wall (Cytokinesis) between the two newly formed daughter cells (Kost et al., 1999). In some specialized plant tissues, cells cease (exit) from the normal cycling phases and undergo endoreduplication, a process characterised by repeated cycles of DNA replication (S-phase) without chromosome separation phase (Joubes et al., 2000).

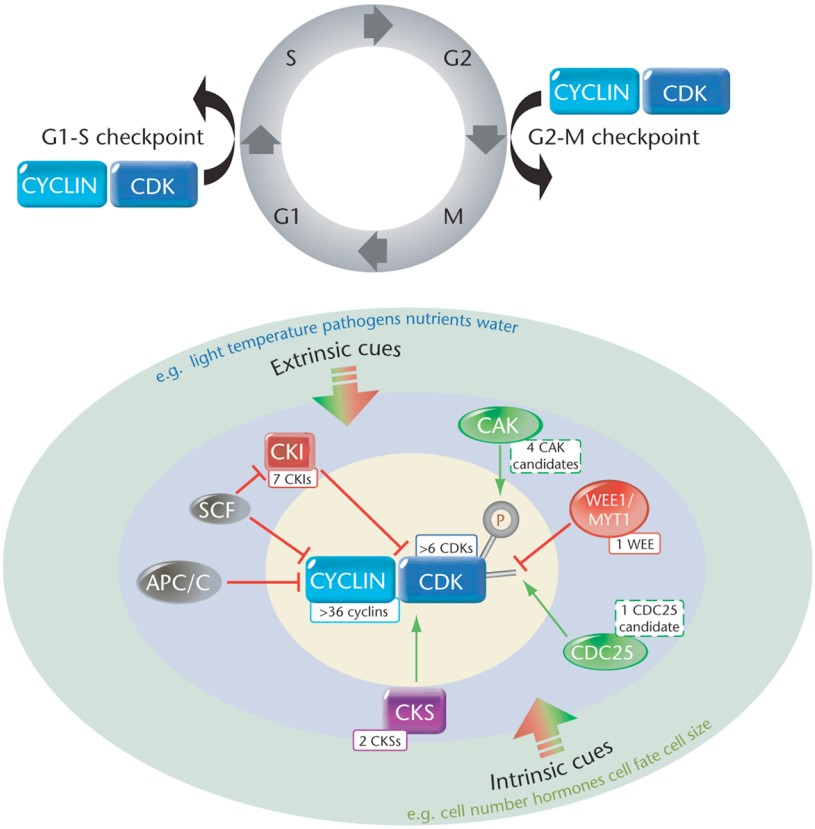

Figure 1.5. **Overview of the cell cycle pathway and the components involved in regulating transition between the cell cycle phases**.

Top panel; layout of the cell cycle progression highlighting phases of transition whereby cells in gap phase 1 (G1) undergo DNA synthesis (S), progress to gap phase-2 (G2), and complete the division cycle at the mitotic phase (M). Progression to the S- and M-phases are strictly regulated by CDK-cyclin complexes. Bottom panel; control of transition between the cell cycle phases by the CDK-cyclin complexes is itself under the influence of intrinsic and extrinsic signals dictating progression or arrest of the cell cycle.The major target in this pathway is the regulation of CDK activity by positive cofactors such as CDK activating kinases (CAK) and CDK subunit (CKS). Additional control by CDK inhibitors (CKIs) and negative and positive phosphorylation by WEE1 and CDC25 respectively, also mediate the activity of CDK in the control of cell cycle progression. The association of CDK with cyclins provides additional mechanism in regulating transition between cell cycle phases whereby degradation of cyclins and CKIs by the proteosome mediated pathways, Anaphase promoting complex (APC) and Skp, Cullin, F-box complex (SCF), is a major determinant of the fate of the cell cycle. Numbers in the white boxes indicate potential homologues of the animal regulators identified in Arabidopsis.

(Adapted from Kuijt et al., 2007)

B: Plant cell cycle machinery

As in all other eukaryotic organisms, progression through the cell cycle in plants is regulated by cyclin-dependent kinases (CDKs). CDKs are characterised by a heptapeptide motif consisting of Proline, Serine, Threonine, Alanine, Isoleucine, Arginine and Glutamic acid (PSTAIRE) that is highly conserved within the cyclin binding domain of the CDK protein. Yeast possesses only one CDK protein, cdc2 that regulate all phases of the cell cycle. However, higher eukaryotes possess more than one type of CDK that participate at different points of the cell cycle phases. With the exception of cdc2 of fission yeast; other CDKs are not highly conserved among eukaryotes and show variability in their cyclin-binding domain (Vandepoele et al., 2002). The main targets of CDKs include Retinoblastoma protein (RB), KIP RELATED family of proteins (KRPs), proteins involved in reorganization of cytoskeleton structure, nuclear membrane (such as lamins), transcriptional inhibition (example phosphorylation of TFIIIB) and the formation of the spindle apparatus.

A regulatory subunit of the CDKs, Cyclins, provides primary control of CDK activity and defines specificity during progression of the different phases of the cell cycle. Cyclin proteins are characterised for having a cyclin core motif composed of an approximately 100 amino acids cyclin box that act as a binding site for the associated CDK to form an active dimeric complex. Genome wide analysis has identified more than 32 cyclin genes in Arabidopsis with a putative role in cell division and have been classified into A, B, D and H classes based on their sequence similarity (Vandepoele et al., 2002; Wang et al., 2004). Other classes include type C, P, L and T (Torres Acosta et al., 2004). In a broad sense, A-type cyclins are detected in early S-phase, persist during S-phase progression, and are turned over before entry into G2/M. B-type cyclins are abundant at G2/M transition, are involved in mitotic entry and progression, and are destroyed prior to entry into anaphase. D-type cyclins on the other hand are thought to regulate the G1/S transition and do not show the cycling of transcript abundance. H-type cyclins have been proposed to be part of the CDK-activating kinase (CAK).

The complexity of the plant cyclins might be attributed to the plasticity of plants in response to intrinsic developmental signals and environmental cues.

The modulation of the cyclin proteins during cell cycle progression is the result of phase specific transcriptional regulation and protein turnover. A- and B-type cyclins posses a "destruction box motif" (D-box) at the N-terminal region that targets these proteins for destruction by the ubiquitin-dependent protein ligase complex, Anaphase Promoting Complex (APC/C) (Criqui et al., 2000). Whereas the D-type cyclins undergo proteosome degradation by another protein ligase complex termed Skp-Cullin-F-box containing complex (or SCF complex). This strict cell cycle modulation of the cyclin proteins is the basis for the unidirectional cell cycle progression and synchronous phase specific transition. Secondary regulation of the cell cycle progression involves modulation of CDK activity by dictating interaction with their specific regulatory subunit, cyclins. All CDKs contains a catalytic cleft with ATP and substrate binding sites positioned between the N- and C-terminal lobes. However, these binding sites remain restricted by the CDK loop known as the T-loop, and phosphorylation of a conserved threonine residue (activating phosphorylation) within the T-loop is essential for exposing the active binding sites. This positive phosphorylation event is performed by the CDK activating kinases (CAKs). Furthermore, CDK activities are also negatively regulated through inhibitory phosphorylation by a tyrosine protein kinase which belongs to the Ser/Thr family also known as WEE1 (Sun et al., 1999; Sorrell et al., 2002). Other proteins that regulate CDKs activity include inhibitors of CDK (ICK or CKI in animals) also known as Kip-related proteins (KRPs), which interact with both CDK and cyclin subunits (Wang et al., 1998). CDK subunit proteins (CKS) are also responsible for activating and inhibiting CDK activities by modulating scaffolding of CDK complex interactions with their substrate (Bourne et al., 1996). In turn, activation of the CDK complex leads to the phosphorylation of its downstream target such as histones H1, Retinoblastoma protein RBR

(a negative regulator of G1/S transition), and in other cases leads to the proteolysis of phosphorylated substrates either through the SCF or APC complexes.

C: Regulators of Plant cell cycle

1. Cyclin-Dependent Kinases (CDKs)

Cyclin-dependent kinases are the most conserved of the cell cycle regulators. The PSTAIRE motif is the main feature in the CDKs protein, and plant CDKs with the PSTAIRE motif are capable of complementing CDK deficiency mutants in yeasts (Ferreira et al., 1991; Hirayama et al., 1991). Plants possess only one gene that encodes the A-type CDK. It has been demonstrated that plant CDKA expression is mainly restricted to competent dividing tissues and is constitutively expressed throughout the cell cycle (Fobert et al., 1996; Menges and Murray, 2002a). These findings were supported by the overexpression of CDKA in tobacco that did not produce any dramatic effect (Hemerly et al., 1995). However, constitutive overexpression of an Arabidopsis CDKA negative dominant mutant that lacked kinase activity resulted in the production of a smaller plants due to a reduced rate of cell division (Hemerly et al., 1995). Monitoring cell cycle progression in this mutant background also demonstrated that CDKA activity can be detected at both G1/S and G2/M check points (Hemerly et al., 1995; Joubes et al., 2004; Porceddu et al., 2001). This evidence demonstrates that CDKA activity is not limited at the transcriptional level; rather its activity is post transcriptionally regulated. Recently, the essential role of CDKA in regulating entry into mitosis was demonstrated in the Arabidopsis male gametophyte. Analysis of a null +/*cdka-1* T-DNA insertion mutant showed a normal asymmetric division of the microspore into two heteromorphic cells, a vegetative cell and a generative cell. However, approximately half of the population failed to undergo the second mitotic division of the generative cell resulting in the production of a single germ cell instead of twin sperm cells (Iwakawa et al., 2006a;

Nowack et al., 2006). Analysis of DNA content demonstrated that the mutant germ cells undergo a slow S-phase and do not complete replication of the DNA prior to pollen shed. Thus, CDKA activity is essential for G1/S transition, S-phase progression and mitotic entry.

Another class of CDKs in plants are the B-type CDKs. This type of CDK is unique to the plant kingdom. The PSTAIRE motif present in A-type CDKs is substituted by either PPTALRE or PPTTLRE motifs dividing the B-type CDKs into two subgroups, CDKB1 and CDKB2 respectively (Vandepoele et al., 2002). Each subgroup contains two members (CDKB1;1, CDKB1;2 and CDKB2;1, CDKB2;2) that differ in their expression pattern during the cell cycle. The B-type CDKs are also characterised by cell cycle phase-dependent transcription unlike any other type of CDKs documented to date. Referring to experiments in several species including *Antirrhinum*, alfalfa, tobacco and Arabidopsis; transcripts of CDKB1 subgroup can be detected from the onset of S-phase, G2 and M-phase, whereas CDKB2 group is specifically expressed during G2 and M-phases (Reviewed by (Dewitte and Murray, 2003b; Inze and Veylder, 2006). Furthermore, accumulation of B-type CDKs has been shown to be restricted to dividing tissues and is distributed in a patchy pattern, indicative of a cell cycle phase dependent expression. B-type CDKs are likely to interact with D-type and B-type cyclins in regulating progression through S- and M-phases similar to CDKA. Overexpression of a dominant negative form of CDKB1 resulted in an increase in the proportion of cells with a tetraploid DNA content (4C) as a result of a block at G2/M transition (Porceddu et al., 2001; Boudolf et al., 2004). In addition, plants carrying the dominant negative form of CDKB1 also posses reduced numbers of stomatal complexes, that is associated with the increased expression of CDKB1;1 in the progenitor cells of stomata complexes (Boudolf et al., 2004).

Other CDK classes that are less documented include CDKD and CDKF. These types of CDKs are grouped with other two classes in Arabidopsis as CDK-activating kinases (CAKs;Inze and Veylder, 2006). Both CDKs possesses substrate specificity and unique interactions with cyclin subunits, and recently CDKF;1 has been shown to phosphorylate and activate CDKDs in

Arabidopsis (Shimotohno et al., 2004). Plants also posses C-type CDKs that are closely related to the mammalian cholinesterase-related cell-division controller (CHED), that possesses a PTAIRE or SPTAIRE motif. CDKC shows preferential expression in dividing tissues but not cell cycle-phase specific regulation. It has been shown that CDKC can interact with CYCT to phosphorylate Retinoblastoma related protein (RBR) as well as a C-terminal domain of RNA polymerase II (Inze and Veylder, 2006). Thus, CDKC has a putative role in transcription elongation and control of cellular differentiation by repressing RBR activity. Another class of CDKs with a SPTAIRE motif is CDKE. Unlike CDKC, CDKE is strictly restricted to dividing tissues and is identical to *HUA ENHANCER3* (*HEN3*;Inze and Veylder, 2006). In common with CDKC, CDKE has been shown to phosphorylate the C-terminal domain of RNA polymerase II, and following the analysis of *hen3* mutants, CDKE has been proposed to play role in cell expansion in leaves and cell-fate specification in floral organs (Wang et al., 2004).

2. Cyclins

Genome wide analysis of *Arabidopsis thaliana* revealed presence of approximately 32 cyclin encoding genes that are classified into four classes (Cyclin A, B, D and H-type cyclins) (Vandepoele et al., 2002; Wang et al., 2004). Furthermore, there are other 17 different cyclin genes that have been identified with a putative role in regulating cell cycle progression, that have been classified into type C, P, L and T subclasses (Torres Acosta et al., 2004). In general terms, transition through G1/S has been proposed to be regulated by D-type cyclins, A-type cyclins are thought to regulate S/M phase, whereas B-type cyclins have been demonstrated to regulate G2/M transition and progression through mitosis. Though some variations of this broad functional assignment of the cyclin proteins has been reported in some species (Inze and Veylder, 2006).

I: *A-TYPE CYCLINS*

Arabidopsis contains 10 different genes that encodes for the A-type Cyclins and they are classified into three subclasses, CYCA1, CYCA2 and CYCA3 classes (Chaubet-Gigot, 2000; Renaudin et al., 1996). In a broad sense, A-type Cyclins are expressed at the onset of S-phase progression and interact with A-type CDK to regulate S-phase progression primarily. Analysis of cell suspension culture from tobacco BY2 cells revealed an increased transcript abundance of the CYCA1 subfamily at mid-S phase, whereas the CYCA3 subclasses showed maximum expression at G1/S (Reichheld et al., 1996). In contrast to CYCA1/A3 subclasses, CYCA2 family members showed a broader pattern of expression. However, their kinase activities is known to be biphasic during the cell cycle progression. Transcript levels were high for CYCA2 during G1 and S-phase, peaked at G2 stage, and then dropped during M-phase. Whereas protein levels are low at G1 stage, increase during S-phase and remain constant during G2 and M-phase stages. This is in contrast to their kinase activity in which high activities were observed at mid S-phase, drop thereafter, and reach maximum again at G2/M transition (Roudier et al., 2000). This differential expression pattern of the A-type subfamilies suggests different biological functions among family members. Furthermore, subcellular localization of a CYCA3;1 protein GFP fusion detected GFP localization in the nucleus and nucleolus in cells undergoing S phase which disappeared in mitotic cells. A similar pattern was also observed for CYCA2 in alfalfa in which GFP was detected in the nucleus until prophase before disappearing during mitosis (Dewitte and Murray, 2003a). Several experiments have now demonstrated the essential roles play by the A-type cyclins during cell cycle progression. Overexpression of tobacco CycA3;2 results in accelerated cell division and lack of cell differentiation in Arabidopsis, whereas; in tissue culture, induction of CYCA2;3 inhibits regeneration of shoots and roots (Yu et al., 2003). This observation was accompanied by an increased expression of S phase specific genes and the formation of CDK-CYCA3;2 complex, suggesting control CDK-CYCA activity is essential for correct cell differentiation. Moreover,

yeast two hybrid experiments have demonstrated the ability of CYCA2 to interact with a maize Retinoblastoma protein in the presence of cyclin box, providing compelling evidence for the proposed role of A-type cyclins in S-phase progression (Roudier et al., 2000). In contrast to the induction of CYCA, knockout of CYCA2;3 results in a slight increase in DNA ploidy levels (Imai et al., 2006), whereas in *tardy asynchronous meiosis* (*tam*) mutant, substitution of a conserved amino acid in CYCA1;2 result in a slower cell cycle progression during male meiosis (Magnard et al., 2001;Wang et al., 2004). The occurrence of subtle phenotypes in both cases demonstrates possible functional redundancy among the A-type cyclin family members.

II: *B-TYPE CYCLINS*

The cyclin B family plays a conserved pivotal role during G2/M transition. Similar to A-type cyclins, B-type cyclins are also classified into three subclasses, CYCB1, CYCB2 and CYCB3, with a total of eleven members. The CYCB3 type subfamily differs from the other two classes due to the lack of a typical B-type destruction box motif (Vandepoele et al., 2002), a signature motif that leads to proteolysis upon cell cycle exit. B-type cyclins are among the first cell cycle proteins to be identified in plants and were isolated from carrot, soybean and Arabidopsis (Dewitte and Murray, 2003a). The expression of B-type cyclins has been extensively studied and several elements that are required for phase specific expression has been revealed together with some transcriptional factors required to achieve this pattern. Whereas A-type cyclins show an earlier expression at the onset of S-phase (G1/S transition) and their levels are controlled by cell cycle dependent proteolysis conferred by the N-terminal destruction box (Genschik et al., 1998), B-type cyclins shows maximum expression at G2/M before declining rapidly following exit from M-phase (Menges and Murray, 2002a). Recently, the mechanism underlying G2/M specific transcriptional regulation has received a

lot of attention in trying to identify the factors involved and the regulatory elements they bind to.

Studies in cell suspensions and in plants has demonstrated that transcripts for the B-type cyclins are detected as early as S-phase, rising at G2 phase, show enriched detection at G2-M and then are rapidly degraded as M-phase progresses (Menges and Murray, 2002b). This expression pattern was supported by the analysis of expression of full length AtCycB1;1 promoter with and without a destruction box motif fused to β-glucoronidase (Shaul et al., 1996b; Colon-Carmona et al., 1999a). The accumulation of GUS mRNA resemble the kinetics observed in cell suspension suggesting that the kinetics of B-type cyclins are conferred by transcriptional regulation (Shaul et al., 1996a; Trehin et al., 1999; Ito et al., 1997; Doerner et al., 1996). To understand the regulatory elements that are responsible for G2/M specific transcriptional enhancement, a promoter deletion analysis of *Catharanthus* CycB1;1-Luciferase was performed. This study led to the identification of nine-base pair element referred to as M-phase specific activator (MSA), containing a central core pentamer that is closely related to Myb-binding sites. Moreover, the MSA elements identified have been found to be conserved in a number of G2/M specific genes (Trehin et al., 1999; Ito et al., 1997). To date, three Myb containing proteins have been isolated from tobacco BY2 cells (NtMybA1, NtMybA2, and NtMybAB) using the MSA elements identified in *Catharanthus* as bait in one hybrid screen (Ito et al., 2001b). NtMybA1 and NtMybA2 were found to bind and activate MSA containing promoters, whereas NtMybAB antagonise NtMybA1 and A2 activity. This study suggests that MSA elements are conserved Myb binding sequences that are responsible for G2/M specific transcriptional regulation of the B-type cyclins. However, Myb transcription factors have a much wider role in plants other than controlling cell division. Therefore, it is still unknown what factors provides G2/M specific regulation of the Myb proteins that activate B-type cyclins. Furthermore, Myb proteins perhaps are not the only factors that regulate expression of B-type cyclins, as two interacting putative Myb-like

proteins containing a Myb binding domain, a Myc-type dimerization domain and a Leucine zipper motif were found to bind to the AtCycB1;1 promoter (Planchais et al., 2002a). Recently, another transcription factor **t**eosinte-branched **c**ycloidea, **P**CNA factor 20 (TCP20) has been isolated from Arabidopsis and has been shown to be necessary and sufficient to enhance transcription of AtCycB1;1 at the G2/M transition by binding to the enhancer elements (GCCCR motif) present in the promoter region of CYCB1;1 (Li et al., 2005a). The G2/M specific abundance of CYCB1;1 is also fine tuned through inhibition by other transcriptional repressors such as TOUSLED (Ehsan et al., 2004).

However, the situation at the protein level is far more complex. The accumulation of B-type cyclins is controlled by the proteolytic complex, the Anaphase promoting complex, and cyclins are degraded during metaphase into progression to anaphase in animals and in plants (Genschik et al., 1998). This pattern of CycB protein accumulation was observed in tobacco BY2 cells, whereby the protein levels were high at S/G2 stage and then dropped during M-phase progression (Criqui et al., 2000). Furthermore, analysis of CYCB1;1-CYCB1;1::GFP fusion construct in tobacco G2 cells showed cytoplasmic and nuclear localization of the protein. The GFP signal was then associated with the condensing chromosomes during prophase and was absent at anaphase and telophase as predicted (Criqui et al., 2001). In humans, CYCB1 is primarily localized in the cytoplasm but constantly shuttles between the nucleus and the cytoplasm during interphase, the protein is then rapidly translocated into the nucleus and becomes incorporated into the mitotic apparatus (Hagting et al., 1998; Furuno et al., 1999; Clute and Pines, 1999). This is in contrast with the human CYCB2 that is primarily bound to the Golgi apparatus in interphase and during mitotic progression (Jackman et al., 1995; Brandeis et al., 1998). This differential localization between the cyclin subfamily hints a possible specified roles between the cyclins in animals. Not surprising this concept can be extended into plant B-type cyclins as well. Studies for the role of B-type cyclins has demonstrated that microinjection of tobacco CYCB1;1 into Xenopus

oocytes can overcome their G2/M arrest and shift cells towards mitosis (Qin et al., 1996). Whereas overexpression of non-degradable CYCB1 in yeast and animals causes block of mitotic progression. Similar experiments using the tobacco non-degradable CYCB1;1 under the 35S promoter in tobacco BY2 cells and in plants, also showed a severe effect on mitotic progression, whereby cells showed defects in cytokinesis resulting in severe growth retardation, multinucleate cells, and endoreduplicated cells (Criqui et al., 2001; Weingartner et al., 2004a). Furthermore, ectopic expression of Arabidopsis CYCB1;2 but not CYCB1;1 shifts endoreduplicating trichome cells into mitosis which result in the production of multicellular trichomes (Schnittger et al., 2002). However, targeted overexpression of Arabidopsis CYCB1;1 in root meristems accelerated the rate of cell division and increased root growth (Doerner et al., 1996). Together these studies indicate that B-type cyclins are functionally involved in licensing the transition towards mitosis. Moreover, their degradation is essential for mitotic exit in other organisms but this does not appear to be a prerequisite in plants.

III: *D-TYPE CYCLINS*

D-type cyclins were originally identified based on their ability to complement yeast mutant deficient for G1 cyclins (Dahl et al., 1995; Soni et al., 1995) that are known to to show significant sequence divergence among their families. They were classified as D-type cyclins based on their low sequence similarity with the animal D-type cyclins and the presence of a LxCxEx motif located near the N-terminus that facilitates interaction with Retinoblastoma related (*RBR)* protein (Huntley et al., 1998). In addition, some of the *CYCD* members possess a putative PEST domain (Proline, Glutamic acid, Serine and Threonine rich region) that acts as a binding site for the interaction with the APC components during protein degradation. In Arabidopsis there are ten CYCDs that are classified into seven groups, termed *CYCD1* – *CYCD7*, with three members in *CYCD3* subclass, two members in *CYCD4* subclass and a single

member for the remaining subclasses (Vandepoele et al., 2002). Currently there are no D-type cyclin knockouts identified to have severe phenotypes suggesting a possibility of functional redundancy among the *CYCD* classes ((Campisi et al., 1999; Swaminathan et al., 2000). Only some specific D-type cyclin knockouts have been reported to show a slight delay in cell cycle reactivation in the root meristem during seed germination (Masubelele et al., 2005), whereas, a moss *cycD* knockout displayed developmental progression independent of the sugar supply without affecting growth rate, cell size, or plant size; this is in contrast to the wild type that in the presence of exogenous glucose sources exhibit prolonged growth of juvenile stages and retarded differentiation. This demonstrates that moss *CYCD* is not essential for cell cycle progression but it is required for linking development with nutrient availability (Lorenz et al., 2003). Initially D-type cyclins were proposed to be involved in regulating G1/S transition, however several evidence have now pointed to the extended role of D-type cyclins in G2/M transition. For instance, *CYD4;1* has been demonstrated to activate G2/M specific *CDKB2;1* in vitro, whereas ectopic expression of *CYCD3;1* in trichomes promotes S-phase progression as well as inducing mitosis (Inze and Veylder, 2006). Similarly, over-expression of tobacco *CYCD3;3* and snapdragon (*Anthirrhinum majus*) *CYCD1;1* in tobacco cell suspension culture (BY2 cells), induced S-phase entry and mitotic progression. However, caution needs to be taken in interpreting these results as some of the known G2/M regulators are under control of upstream factors involved in the previous phases. This is based on the observation that transcription of *CDKB1;1* that acts during G2/M is partially regulated by the G1/S specific E2F transcription factors (Inze and Veylder, 2006). In supporting a possible involvement of D-type cyclins in influencing the G2/M transition, some of the D-type cyclins have been identified to show peak expression at the G2/M boundary. Furthermore, kinase activities associated with *CYCD3;3* could be detected at G1/S and during G2/M transition (Nakagami et al., 2002). Thus, any positive effect on G1/S might also stimulate mitotic entry as well.

The expression of the D-type cyclins is variable among the family members; however the overall pattern seems to be associated with proliferating tissues and excluded from differentiating tissues. Arabidopsis *CYCD3;1* expression is abundant in proliferating shoot tissues such as meristematic tissues, young leaves and developing vascular tissues, whereas *CYCD4;1* expression is restricted to developing lateral roots, embryogenesis and vascular tissues (Dewitte and Murray, 2003a). Expression of the D-type cyclins has been proposed to provide a possible link between organ development and cell proliferation. In *Antirrhinum*, expression of two members of *CYCD3* homologs (*CYCD3a* and *CYCD3b*) is confined to the periphery of the inflorescence meristem, young floral meristem and the tips of older floral organs. Arabidopsis *CYCD3;1* expression is enhanced in plants over-expressing *AINTEGUMENTA* (a gene that regulates cell division in ovules and flowers, and encodes an AP2 domain transcription factor) which resulted in accelerated division rate and increased cell number in leaves. This is a similar effect to that of *CYCD3;1* over-expression, suggesting a common pathway between the expression of *AINTEGUMENTA* and that of *CYCD3;1* (Dewitte and Murray, 2003a). Moreover, it is well documented that expression of CYCDs is strongly influenced by plant growth hormones such as cytokinins, auxins, brassinosteroids, gibberellins and also presence of sugar (Inze and Veylder, 2006; Dewitte and Murray, 2003a). For instance callus growth in media deprived of cytokinin exhibit limited cell division due to reduced expression of CYCD3;1, conversely, over-expression of CYCD3;1 is sufficient to promote cytokinin-independent callus growth (Riou-Khamlichi et al., 1999). Similarly, Arabidopsis CYCD2;1 and CYD3;1 transcript abundance in BY2 cells was demonstrated to be sugar dependent and are induced in response to sugar supply (Riou-Khamlichi et al., 1999).

D: Cellular activities regulating cell cycle progression

1. CDK phosphorylation by **C**DK-**A**ctivating **K**inases (CAKs)

In addition to cyclin subunits, CDK activities are also regulated by CDK-activating kinases that phosphorylate Threonine 160 of the CDK T-loop resulting in conformational changes to allow greater recognition of the substrates. The first plant CAK was isolated in rice and was used as a probe to identify four CAK-encoding genes in Arabidopsis that were classified into two classes, CDKD and CDKF (Inze and Veylder, 2006; Dewitte and Murray, 2003a). CDKD is preferentially expressed during S-phase, requires association with H-type cyclins for activation and possesses kinase activity towards CDK and the C-terminal domain of RNA polymerase II (Fabian-Marwedel et al., 2002). By contrast CDKF is unique to plants in a sense that it does not phosphorylate RNA polymerase II subunit as other CAKs, and does not depend on H-type cyclin for activation, but it is capable of phosphorylating and activating CDKDs in Arabidopsis (Shimotohno et al., 2004). CAKs in plants have been shown to be essential factors in determining growth rate and correct cell differentiation by regulating overall CDK activities. The evidence comes from inducible co-suppression by sense and antisense down-regulation of AtCDKF activity that led to the premature differentiation of root meristems (Umeda et al., 2000), whereas, overexpression of rice CDKD;1 resulted in accelerated S-phase and increased growth rate of cell suspensions (Fabian-Marwedel et al., 2002).

2. CDK inhibitors (CKIs)

In addition to cyclin subunits, CDKs activities are also regulated by CDK inhibitors (CKIs) through inhibitory phosphorylation. This mechanism of regulating CDK activity is conserved across all species and several CKI encoding genes have been identified. Budding yeast contain three CKIs encoding genes; the Far1p that inhibits CDK activity at G1 phase, Sic1p that regulates CDK activity upon S-phase entry, and Pho81 that phosphorylates the CDK/cyclin complex and is involved in the control of gene expression under low phosphate conditions (Inze and Veylder, 2006). Whereas in animals, seven CKI genes have been identified and grouped into two major classes, the INK4 family and the Cip/Kip family (Inze and Veylder, 2006). The INK4 proteins have been demonstrated to inhibit CDKs involved during G1 phase whereas the Cip/Kip family of proteins have been shown to interact with a broad range of CDK/cyclin complexes involved in G1/S and G2/M transition. Plants also possess seven different CKI proteins that limit the activity of CDK/cyclin complexes. In contrast with other CKIs, plant CKIs comprise a 31 amino acid C-terminal domain that is responsible for interaction with CDK and cyclin proteins to induce the inhibitory phosphorylation. In addition to the C-terminal domain, plant CKIs also contain an N-terminal domain that has high homology with the animal Cip/Kip proteins, thus plant CKIs are also referred as Kip Related Proteins (KRPs). However, the first proteins identified were referred to as interactors of Cdc2 Kinase (ICK) (Inze and Veylder, 2006). It has been demonstrated that ICK1/KRP1, ICK2/KRP2 and ICK7/KRP7 and recently ICK6/KRP6 but not ICK5/KRP5 can interact with CDKA in a yeast two hybrid assay (Zhou et al., 2002; De Veylder et al., 2001). All the KRPs have been shown to interact with the CycD1, CycD2, CycD3 and KRP4 with CycD4; whereas their binding specificity was demonstrated in vivo in which the inhibitory effect caused by overexpression of ICK/KRP can be complemented by co-overexpression of D-type cyclins (Inze and Veylder, 2006; Dewitte and Murray, 2003a). In addition, the inhibitory effect of ICK1/KRP1 and ICK2/KRP2 on CDKA activity has been demonstrated in vitro (Wang

et al., 2000). Thus, evidence shows that the KRP proteins inhibit the kinase activity of the CDK/Cyc complexes by competing with the binding of the cyclin proteins to CDK, and also interact with CycDs to inhibit CDK/CycD complex formation and as a consequence inhibit S-phase progression. Furthermore, targeted over-expression of KRP1 results in ten-fold reduced cell number in petals with six-fold increased cell size, smaller serrated leaves and aberrant floral morphology; whereas similar experiment with KRP2 and KRP4 result in smaller serrated leaves, aberrant floral morphology and reduced cell number in leaves respectively (Zhou et al., 2002; De Veylder et al., 2001). KRP proteins are differentially regulated during cell cycle progression suggesting a phase specific roles for the different KRPs. KRP1 expression is detected in sucrose starved cells, decline upon entry into G1 but rises again following mitotic entry (Menges and Murray, 2002a). On the other hand, KRP2 is transiently expressed during G1 then disappears thereafter, whereas, KRP3 expression is restricted to mitotic cells only. The differential expression pattern of the KRPs implicate specific role for KRP1 in maintaining cells at stationary phase and fine tuning mitotic progression, whereas KRP2 may provide a licence for cell cycle re-entry.

3. RBR-E2F/DP interaction; a "three way" S-phase affair

Retinoblastoma protein (RB) is the most highly conserved cell cycle component across all species and its interaction with the adenovirus E2 promoter-binding factor (E2F) that form a dimer with the Dimerization protein (DP) has also been established as the most primitive conserved cell cycle pathway that licences the transition from G1-to-S phase. Arabidopsis encodes only a single retinoblastoma related protein (RBR) with two conserved sequence motifs that form the A/B pocket domain, which act as a docking site for the E2F transcription factors (Ach et al., 1997; Durfee et al., 2000). Moreover, *RBR* has been shown to interact with *CDK/CYCD* complexes in animals, binds to the conserved LxCxE motif of *CYCD* in plants

and also interact with RbAp48-like proteins (Huntley et al., 1998; de Jager and Murray, 1999).

In animals, the activity of RB is negatively regulated through phosphorylation by *CDK2/CYCA*, *CDK2/CYCE*, *CDK4/CYCD* and *CDK6/CYCD* complexes at G1/S transition and positively dephosphorylated by PP1 at the G2/M phase (Inze and Veylder, 2006). Whereas in plants, *RBR* is associated with kinase complexes that contain *CDKA* and D-type cyclins, and the phosphorylation of RBR has been demonstrated to be cell cycle-phase dependent (Nakagami et al., 2002). The Arabidopsis homologue of the Rb-interacting Rbp48-related protein, MSI1, has been shown to be part of the chromatin assembly factor (CAF) in conjunction with *FAS1* and *FAS2* encoded proteins (Kaya et al., 2001). Loss of MSI1 activity leads to deregulation of the meristem identity gene *WUSCHEL* which result in loss of differentiation of the shoot apical meristem, implicating a dual role of the RBR in cell cycle control and cellular differentiation (Dewitte and Murray, 2003a). Indeed RBR protein is essential in maintaining the differentiation of the root stem cells (Wildwater et al., 2005). Female megaspores develop through a series of mitotic divisions to produce a mature megagametophyte that consists of the egg cell and the central cell. Knockout of the *RBR* gene is detrimental for female gametophyte (megagametophyte) development resulting in excessive nuclear proliferation in the embryo sac and autonomous endosperm development prior to fertilization similar to the effect of *fertilization-independent seed* (*fis*) mutants; suggesting a role for RBR as a negative regulator of cell proliferation, specifically in this case preventing autonomous embryo and endosperm development in the absent of fertilization (Ebel et al., 2004).

FIS-class genes encode polycomb group proteins (PcG) that include *MEA*, *FIE*, *FIS2* and the Rbp48-related protein, *MSI1*, which controls cell proliferation in the megagametophyte and has been shown to interact with the RBR. Thus, RBR prevents cell proliferation in the embryo sac through association with the PcG group of proteins; indeed +/*rbr1-1*;+/*fis* double

mutants exhibit enhanced autonomous endosperm development compared to *+/rbr1-1* alone. This is a unique role of the RBR that exhibit negative regulation of cell proliferation through an E2F-DP independent pathway. Analogously, the *rbr1-1* allele also produced a segregant population of malformed dead pollen and viable pollen as well as reduced transmission of the *rbr1-1* allele through the male, implicating a putative role of RBR in the control of male gametophyte development (Ebel et al., 2004). Maize is the only example that possesses more than one gene encoding RBR proteins. The *RBR1* is expressed post-mitotically in endoreduplicating and differentiating cells, whereas, *RBR3* is exclusively expressed during mitotic phase of the endosperm development (Sabelli et al., 2005). Thus, it has been proposed that the differential expression pattern between the two RBR proteins implies division of labour whereby *RBR3* is required in cell cycle control and *RBR1* in cell differentiation.

The RB regulatory pathway involves negative regulation of the E2F transcription factors (through binding on E2F activation sites within the promoter), which controls the expression of its target genes required for entry into S-phase. Current knowledge has proposed that the RBR induced inhibition of the E2F target genes might be achieved through changes in chromatin structure of the target genes. Indeed, maize (*Zea mays*) RBR has been demonstrated to physically associate with histone deacetylase RDP3I (Rossi et al., 2003). Arabidopsis contains three families of E2F proteins (*E2Fa*, *E2Fb* and *E2Fc*), two DP proteins (*DPa* and *DPb*) and three DP/E2F-like genes (DEL, *E2Fd/DEL2*, *E2Fe/DEL1*, and *E2Ff/DEL3*) (Vandepoele et al., 2002). *E2Fa* and *E2Fb* can trans-activate reporter genes that possess E2F consensus *cis*-acting elements when co-expressed with *DPa* but not *DPb* (Kosugi and Ohashi, 2002). Similarly, transient overexpression of *E2Fa* and *DPa* induces quiescent mesophyll cells to re-enter S-phase (Rossignol et al., 2002), whereas, ectopic co-expression of *E2Fa* with *DPa* and *E2Fb* with *DPa* in transgenic plants induces continuous cell proliferation in differentiated cotyledon and hypocotyl cells; and stimulates cell division that results in shortening of the

cell cycle respectively (Inze and Veylder, 2006). In contrast, E2Fc acts as a transcriptional repressor of the E2Fa and E2Fb target genes, and its overexpression inhibits cell cycle progression reflective of its negative effect on the E2F's target (del Pozo et al., 2002). Unlike the E2F and DP proteins, DEL proteins possess two DNA binding domains that allow binding in a DP-independent manner as a monomer to repress transcription of E2F-activated promoters, and as such, act as a negative feedback loop for E2F's targets (Kosugi and Ohashi, 2002). Furthermore, DEL proteins also lack RB binding site, hence their activities are not under the control of RB unlike other E2F families. A combination of in silico analysis of the Arabidopsis genome for the presence of genes with canonical E2F binding site (TTTCCCGCC) and transcriptomic profiling has lead to the identification of 70 E2F putative target genes that were conserved between Arabidopsis and rice, and encode proteins involved in cell cycle regulation, DNA replication, and chromatin dynamics (Inze and Veylder, 2006). Some of the identified targets have been verified experimentally, including *MCM3*, *CDC6*, *CDT1a*, *PCNA*, *RBR*, and *RNR*. The E2F target genes are activated in specific cell cycle-phase, and analysis of DEL1 showed enhanced expression at G1/S, no transcripts were detected during S-phase, but the expression was enhanced again at G2/M transition; as such it was proposed that *DEL1* regulates the temporal expression of the E2F target genes (Mariconti et al., 2002). In contrast, overexpression of *DEL3* results in reduction of cell size without affecting cell differentiation in roots and hypocotyls, whereas, loss of *DEL3* leads to production of larger cells in the hypocotyl (Ramirez-Parra et al., 2004). These effects are directly linked to the misregulation of the DEL3 target genes, demonstrating an active role of *DEL3* in the control of cell division.

4. Proteolysis

Apart from the phase-specific expression of some of the CDK regulatory subunits, the cyclins, rapid proteolysis of the target cyclin proteins and specific combinations of CDK-cyclin subunits are the main mechanism that ensures unidirectional progression of the cell cycle. There are two main proteolytic pathways that are intimately dedicated to the cell cycle to mediate protein degradation during S-phase progression and upon exit of the mitotic phase. The Anaphase Promoting Complex (APC) and the Skp1-Cullin-F-box (SCF) related complex; are the two related complexes composed of E2 and E3 types of enzymes, that utilize the ubiquitin proteosome pathway to mark target proteins using highly conserved polypeptide ubiquitin to direct target proteins for degradation by the 26S proteasome (Vodermaier, 2004). The ubiquitination of the target proteins is performed by the combination of E2-ubiquitin carrying enzyme and E3-ubiquitin protein ligase that initiate interaction between E2 and the target protein (Pickart, 2001).

Cyclin proteins are the targets for degradation during cell cycle progression, and their degradation is facilitated by the destruction box motif located at the N-terminal that is recognised by the SCF/APC complexes and directed for proteasome degradation (Renaudin et al., 1996; Genschik et al., 1998). However other cyclins are degraded in a proteaosome independent pathway (Imai et al., 2006). The significance of the APC activity was demonstrated by the over-expression of non-degradable form of tobacco CYCB1;1. The mutated destruction box in this construct prevents CYCB1;1 from being targeted by the APC complex, as a result plants exhibit persistant CYCB1;1 resulting in severe growth retardation, abnormal development and production of cells with increased ploidy levels (Weingartner et al., 2004b). Similarly, ectopic expression of non-degradable CYCA2;3 that retains the cyclin protein after prometaphase results in dwarfism (Weingartner et al., 2003).

The E2/E3 conjugating enzymes does not provide specificity for protein degradation, instead APC substrate specificity is partially determined by two proteins, *CDC20* and *CDH1*. Five

genes have been identified in Arabidopsis that encode *CDC20*, as well as three *CDH1*-related proteins termed *CC52A1*, *CC52A2*, and *CC52B* (Inze and Veylder, 2006). It has been shown that *CC52B* is expressed during G2/M transition - to - M phase, whereas, *CC52A1* and *CC52A2* are expressed from the late M-phase until early G1 phase. Consistent with their distinct expression, the three *CC52* have been demonstrated to possess distinct functions based on their unique phenotypes in *Schizosaccharomyces pombe*. The pattern of expression and the distinct phenotypes of these APC specificity components suggest a continuous activity of the APC complex throughout the mitotic progression to maintain cell cycle phases "in check".

E: Progression through the cell cycle phases

The post-embryonic set up of plant development is exclusively dependent on cell proliferation to generate specialized tissues and organs to facilitate its growth. Thus, control of cell division during plant development is of primary importance due to the intricate connection between cell division and cell differentiation, which in turn determine tissue type, size, cell number, pattern of formation and the type of organ produced. Moreover, cell proliferation also provides a means for adaptation and escape of sessile plants from dramatic environmental changes. Thus, entry and progression through the cell cycle phases is determined by intrinsic and extrinsic signals.

I. G1-to-S-phase transition

The current model for the G1/S-phase transition has been proposed to be regulated by the CDKA-CycD complexes that exhibit inhibitory phosphorylation on the RBR protein. The transition event is initiated by external signals that induce transcription of D-type cyclins that allows formation of the CDKA-CycD complex. These complexes relieve transcriptional

inhibition of the E2F target genes required for S-phase progression by phosphorylating and block the binding of RBR protein to the promoters of E2F target genes. Furthermore, prior to entry into S-phase the inhibition of the CDKA kinase activity by the KRPs is released by degradation of the KRP proteins through the SCF complex, a process mediated by the F-box proteins (Kipreos and Pagano, 2000). Likewise, inhibitory phosphorylation of the CDKA protein by WEE1 is released by the phosphatase activity of CDC25. The negative regulation of CDKA activity is counteracted by the CAK's that phosphorylate CDKA and induce protein conformational changes for greater substrate recognition. These sequential events licence the progression from G1 to enter S-phase and complete DNA replication. The rate of S-phase progression is likely to be regulated by the balance of CDKA-CYCD activities and the presence of inhibitory factors, KRP's in particular, and turning over of CycD. In addition, E2Fc is known to be a competitive inhibitor of E2F activated genes through binding of E2F target sites within a promoter region and inhibiting their activation. As such, the expression of E2Fc, which is also CDKA-CycD dependent, is most likely to be involved as a negative feedback loop during S-phase progression. This phenomena can be observed upon over-expression of S-phase related factors such as CycD and E2F which result in shortening of the cell cycle (accelerating S-phase progression) demonstrated by the increase in cell number and reduction of cell size. Conversely, knockout of the CDKA and FBL17 activity result in a slower S-phase during pollen maturation illustrating that CDKA and FBL17 are the rate limiting factors during S-phase progression (Nowack et al., 2006; Iwakawa et al., 2006a; Kim, 2008).

II. G2-to-M-phase transition

Completion of DNA replication during the S-phase is followed by a G2 check point whereby cells monitor the replicated DNA for any errors during the replication process. Any incorrectly replicated DNA will cause the cell to arrest at the G2-phase until the damage is repaired. Once the checkpoint is completed, cells are licensed to enter the mitotic phase to undergo division. This “quality” checkpoint is referred as Decatenation.

Plant CDKs are constitutively transcribed during the phases of the cell cycle with the exception of B-type CDK. The B-type CDK is a plant specific family and shows a cell cycle dependent expression pattern with highest transcript and protein levels at G2/M (Bogre et al., 1997). This expression pattern indicates a potential role for CDKB in regulating G2/M transition. Certainly, manipulating expression of CDKB by down-regulating its transcript levels, results in an increase of the relative duration of G2 phase (Porceddu et al., 2001). In Arabidopsis, B-type cyclins interact with CDKA/CDKB to form a complex that is initially inactivated by WEE1 kinase through inhibitory phosphorylation of CDK at Thr14 and Tyr15. It has been proposed that the CyclinB-CDK complexes are later activated through the action of homologues of CDC25 phosphatase. The active cyclinB-CDK complex then associates with other proteins in coordinating the synthesis and arrangement of the mitotic spindle, disassembly of the nuclear envelope, condensation of the chromosomes, arrangement of the chromatids on the metaphase plate, and progression through the mitotic phase. Separation of the two daughter nuclei at anaphase and exit from the cell cycle is achieved through a destruction of the mitotic cyclins by the anaphase-promoting complex (APC).

III. Endoreduplication

Endocycle is a modified mitotic cycle whereby cells possess increased nuclear ploidy as a result of repeated rounds of DNA replication without intervening mitosis. Endoreduplication is a phenomenon that occurs in almost all plant cells and in specific cell types such as trichomes where they cease from mitotic cycles and lose the ability to re-enter mitosis. Endoreduplicating tissues contain a modified cell cycle machinery in which the regular control of cell cycle progression is abolished. For instance, CYCD is known to regulate transition from G1/S-phase, however, its expression is excluded in endoreduplicating tissues (Dewitte and Murray, 2003a). When CYCD3;1 is over-expressed in endoreduplicating tissues, it inhibits progression through the endocycle suggesting that normal G1/S control might not operate in these tissues. Furthermore, the inability of endoreduplicating cells not to enter the mitotic cycle might be explained by the lack of expression of key regulators of mitotic entry and progression, the cyclinB family. Indeed, ectopic expression of AtCycB1;2 in unicellular trichomes results in the formation of multicellular trichomes (Schnittger et al., 2002), an effect that mimics ectopic expression of CYCD3;1 in trichomes. It was later established that ectopic expression of CYCD3;1 induced endogenous CycB expression, consistent with the dominant role of CYCD3;1 in driving G1/S transition and commitment of cells to enter mitosis. Moreover, CCS52A essential component of the APC complex is detected in endoreduplicating cells, and its downregulation results in a reduction of endoreduplication cycle (Cebolla et al., 1999). It is still not very clear why cells cease from the mitotic cycle and enter the endocycle, and what are the advantages.

4. A framework of small RNA (smRNA) pathways in plants

Forward genetics has the advantage that the phenotype of the mutant provides a hint about the putative function of a gene. However, the completion of full genome sequencing in Arabidopsis and rice and the advent of large scale genome sequencing in other plant species such as maize have identified a large number of genes but without a known biological function. To date, reverse genetics has been the most effective way for elucidating gene function, but the biggest challenge has been to establish a general and effective method with little or no limitations for dissecting gene function and understand the regulatory network of cellular processes. Generation of T-DNA insertion lines such as the SALK, GABI-Kat and SAIL collections is a very useful strategy for discovery of gene function but is limited by gene redundancy, failure to target inserted elements to a gene of interest, multiple insertions and generation of lethal knock-outs that are not useful in dissecting the wider roles of gene of interest during development. Chemical mutagenesis with Ethyl-methane sulfonate (EMS) that involves whole genome random mutagenesis through a base pair substitution has also been exploited successfully. EMS has the advantage that it generates loss – or gain – of-function mutants, provides information in understanding the role of specific amino acids residues in protein function and most importantly, it generates hypomorphic alleles that are non-lethal essential for understanding gene function during plant growth, development and in response with other physiological factors. However, the drawback with EMS is it requires screening a large number of M1 populations (Jander et al., 2003) to achieve a genome saturation and detection of single-nucleotide polymorphisms or substitutions, which is laborious. Though this can now be overcome by Target Induced Local Lesions in Genomes (TILLING), a technology that involves an automated detection of polymorphisms in a mutant pool. Furthermore, because the EMS approach involves random mutagenesis, it can be difficult to obtain clean lines that are not associated with other linked phenotypes despite several backcrosses into wild type plants.

By contrast, the promise of small interfering RNA (siRNA) technology, a designated pathway of the small RNA machinery (smRNA) which has been widely and successfully explored in *C. elegans*, Drosophila and animals to down-regulate gene expression using self complementary hairpin-double stranded RNA is set to revolutionize reverse genetic approaches. Gene silencing through small interfering RNA (siRNA) also known as Post transcriptional gene silencing (PTGS) was first discovered in worms as a mechanism of gene silencing directed by dsRNA (Waterhouse et al., 1998). However, the silencing phenomenon was already described in plants as the co-suppression phenomena induced by a sense transgene that leads to the suppression of the transgene itself and the homologous endogenous gene. The discovery in plants came about following an observation that introduction of exogenous RNA such as RNA from virus infection or introduction of transgenes, resulted in silencing of the exogenous RNAs and homologous endogenous RNA molecules. The RNA silencing pathway operates by generating dsRNAs that are processed to produce short interfering RNA, which are then used to direct degradation of target mRNA (Figure 1.6). The components involved in this post-transcriptional gene silencing includes the RNAse III family protein (DICER) that recognises long dsRNAs and cleaves them into short 21-24nt siRNA duplexes with 2-nt overhangs at the 3'-hydroxyl end. A second critical component involved in RNAi pathway is RNA dependent RNA polymerase (RdRP) that enhances the RNAi effect and allows the inheritance of the silencing between generations. A third major component is a family of RNA nucleases termed Argonaute proteins which form part of RNAi-protein complex known as the RNA Induced Silencing Complex (RISC), which uses siRNAs onboard to guide targeted mRNA degradation. Other components that are known to function in smRNA pathways include HASTY, HEN1, HYL1, SERRATE and others that participate in import and export of proteins and RNAs that are essential for full PTGS activity.

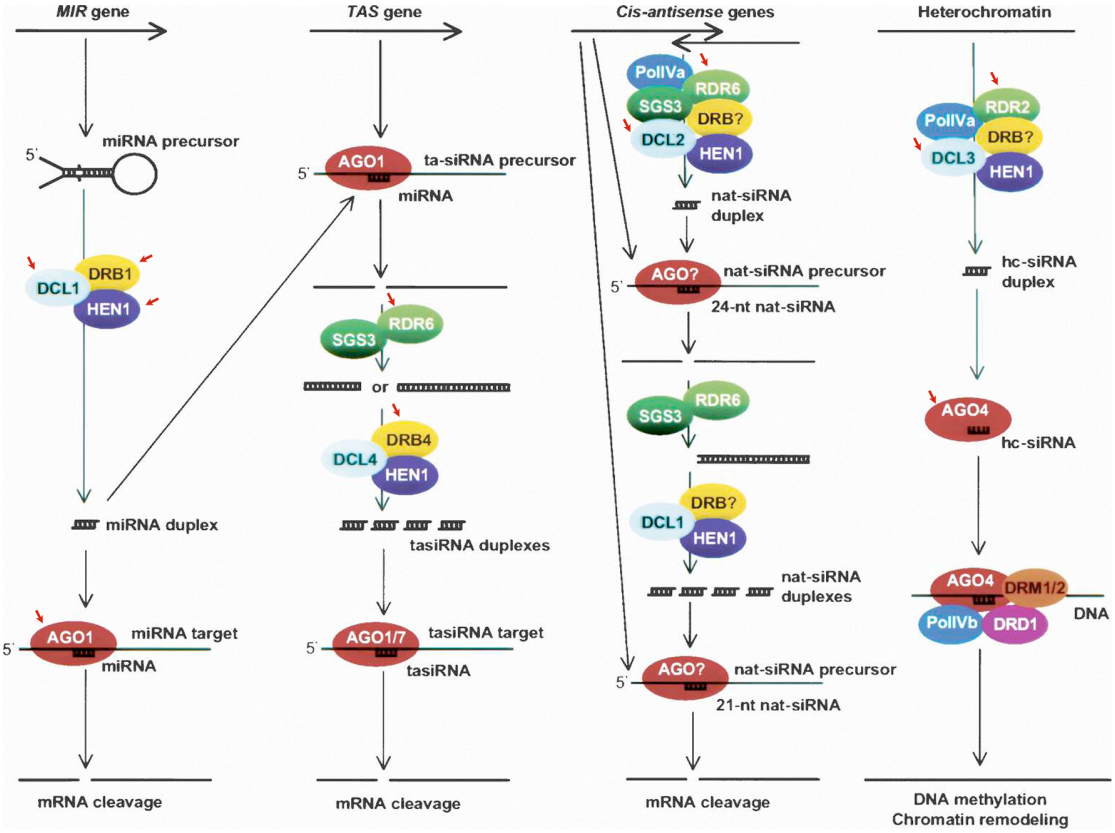

Figure 1.6. **smRNA pathways in plants**
Schematic representation of the different smRNA pathways involved in regulating gene expression and maintaining genome integrity during plant development. Unlike animals whereby the major mechanism is translational inhibition of the target mRNA; miRNA, ta-siRNA and nat-siRNA pathways in plants all leads to cleavage of the target transcripts mediate by the Argonaute complex (*AGO*). Where miRNA pathway merge with the ta-siRNA, arrow is used to indicate the linkage. The two arrows that originate from the nat-siRNA pathway indicate that the nat-siRNA precursor transcribed from this gene is used at different steps of the pathway. Key components marked with red arrows are also detected during pollen development. MIR, microRNA gene; *DRB*, double stranded RNA binding protein; *DCL*, *dicer-like*; *HEN*, *HUA ENHANCER*; *AGO, Argonaute*; *TAS, trans-acting siRNA*; *RDR, RNA dependent RNA polymerase*; *SGS, suppressor of gene silencing.*

(Image adapted and modified from Vaucheret et al., 2006)

A: Three major families of smRNA components

I. Dicer-like family (DCL)

DICER is one of the RNase III family members of nucleases that cleave dsRNA into 22nt RNA fragments with 3' overhangs of 2 to 3 nucleotides (Elbashir et al., 2001). DICERs are involved in the initiation of smRNA effects by digesting dsRNA into uniformly sized small RNA (siRNA) that are later used in the subsequent steps. These nucleases are conserved across all species and they are well characterised by having four distinct domains, a helicase domain, two RNase III motifs, a dsRNA binding domain and PAZ domain (Tabara et al., 1999; Catalanotto et al., 2000). DCL proteins play an essential role in the functioning of smRNAs and lack of DCL activity results in growth abnormalities as a consequence of de-regulated plant development.

II. RNA Dependent RNA polymerase family (RdRP)

RNA dependent RNA polymerases are known to be involved in the amplification of dsRNAs allowing continuous degradation of newly transcribed targets mRNA throughout development and in successive generations. Mutations in RdRP reduce smRNA effects specifically through failure of the amplification of siRNAs as an epigenetic agent that enhance the RNAi effect during development in plants and between generations in *C. elegans* (Lipardi et al., 2001; Sijen et al., 2001). In Arabidopsis there are six genes that encode RdRPs, *RDR1-RDR6*.

III. Argonaute family (ARG)

The discovery of the ARGOUNATE family of nucleases came about following an observation by Hammond et.al, (2001) who discovered that endogenous Drosophila genes in cultured S2 cells can be targeted in a sequence-specific manner following transfection with dsRNA (Hamilton et al., 1998). This phenomena of sequence/RNA directed nuclease activity on the

degradation of target mRNAs was mediated by the RNA-Induced Silencing Complex (RISC). The RISC is a multi component RNAi nuclease and was purified to homogeneity as a ribonucleoprotein complex. One of the proteins identified from this complex was Argonaute 2, a homologue of RDE1 protein that is required for dsRNA-mediated gene silencing in *C. elegans* (Hammond et al., 2001). Argonaute family members are characterised by poly-glutamine residues, PAZ and P-element induced wimpy testis (PIWI) domains, and have been linked both to the gene silencing phenomenon and to the control of development in various species. The major role played by the Argonaute proteins is the degradation of dsRNA after being recruited to the RISC complex following DICER activity and unwinding of the dsRNA by helicase enzymes. Therefore, Argonaute proteins have a downstream effect in the smRNA pathway and are essential for RNAi activity. There are ten genes that encode AGO-like proteins in Arabidopsis; however, not all of them have been demonstrated to have a role in the smRNA pathway.

B: Mechanisms and diversity of smRNA silencing pathways

A picture that was concealed for more than 15 years since its initial discovery has now unveiled following accumulation of a number of experimental lines of evidence in diverse organisms on the important role of the small non-coding RNAs in regulating the molecular machinery of eukaryotic cells. The initial discovery of plant transgene silencing by Baulcombe (2004) provided a glimpse of the existence of the RNA-mediated silencing pathway in plants. Plants similar to other organisms have made extensive use of the smRNA pathways in processes that include immune responses against parasitic viruses and transposable elements, the control of endogenous gene expression by transcriptional gene silencing through chromatin modification and post-transcriptional regulation involving transcript degradation and translational inhibition. In addition, plants exclusively depend on the smRNA pathways in defence against other exogenous nucleic acid invasion such as

transgenes, which form the basis of tools for functional genomics. The source of smRNAs initiation includes the microRNAs (miRNAs) encoded by endogenous loci, and small interfering RNAs (siRNAs) of different length that are synthesised by different mechanisms with divergent sources. These are commonly recognised as aberrant transcripts such as uncapped single stranded RNA or double stranded RNA derived from viruses, transgene constructs, transposable elements, repetitive DNA and genes in antisense configuration. As such, plant smRNA pathways are complex and diverse which impose a necessity in understanding the biochemistry and mechanisms by which the pathway operates in a number of organisms. To date, plants possess at least three smRNA silencing pathways that have been well documented and several lines of evidence have been accumulated demonstrating the contribution of each pathway to the overall control of genome integrity, endogenous gene expression and defence against exogenous nucleic acid invasion. Moreover, evidence has been compiled regarding the implication upon deficiency of these pathways on plant development.

I. MicroRNAs (miRNAs)

miRNAs play an essential role during development by fine-tuning organogenesis and controlling gene expression in response to biotic and abiotic factors. To date, there are more than 100 microRNA encoding genes proposed to exist in the Arabidopsis genome and they have been grouped into 25 distinct classes (Xie et al., 2005a). miRNAs are produced as single stranded of ~70nt long precursor RNAs (sRNA) with a distinct stem-loop structure, which are then processed by DCL1 into 20-24 nucleotides RNA species. It has been demonstrated that miRNAs induce post transcriptional regulation of their target transcripts *in trans* either by directing cleavage of the target transcript or by inhibiting translation of the target mRNA (Bartel, 2004). The indispensable role of the miRNAs during plant development has been demonstrated by over-expression or in loss-of-function mutants. For instance, temporal and

spatial expression of transcription factors required to specify floral organ identity and organ number, leaf shape, abaxial-adaxial leaf asymmetry and lateral root formation, are under strict control by MIRNA genes (Reviewed by (Brodersen and Voinnet, 2006). Furthermore, accumulation of key components of the PTGS pathways including the miRNA pathway, DCL1 and AGO1, are also under miRNAs regulation suggesting the existence of a negative feedback mechanism controlling the activity of PTGS components.

In both animals and plants, primary miRNA transcripts (pri-miRNA) are synthesised by RNA polymerase II with a characteristic 5' cap and a poly(A) tail (Xie et al., 2005a; Lee et al., 2004). In animals, synthesised precursor transcripts (pri-miRNA) acquire a fold-back stem loop structure that is cleaved at the base of the loop by the RNaseIII Drosha in association with DGCR8/Pasha within the nucleus to produce precursor miRNAs (pre-miRNAs). These are then exported to the cytoplasm by Exportin-5-dependent (Exp5) nuclear export (Reviewed by (Vaucheret, 2006). The exported pre-miRNAs are further cleaved by Dicer to form miRNA/miRNA* duplex with a 2'-hydroxyl termini overhangs at the 3'-end. Note, the duplex consists of a mature miRNA strand (miRNA) and its complementary strand (miRNA*). Once guided to the RISC complex, the miRNA strand which is partially base-paired at its 5'-end is loaded as a guide strand into the RISC complex, whereas, the miRNA* strand is degraded. Conversely, plant DCL1 also possesses Drosha and Dicer like activities and it was also localized to the nucleus (Kurihara and Watanabe, 2004). Furthermore, DCL1 has been shown to associate with HYL1 during the cleavage of pre-miRNAs, and the miRNA/miRNA* duplex produced is methylated by another protein HEN1, an S-adenosyl methionine (SAM) – binding methyltransferase, likely to protect the RNA duplex from degradation and or polyuridylation (Hiraguri et al., 2005; Yu et al., 2005). A plant homolog of Exp5, HASTY, has also been proposed to be involved in the export of miRNA/miRNA* duplexes and pre-miRNAs to the cytoplasm (Park et al., 2005). However, plants carrying *hasty* mutation showed a decrease in

miRNA accumulation in nuclear and cytoplasmic extracts, suggesting the existence of HASTY-independent miRNA export pathways.

Currently, the downstream effect of the miRNA-guided RISC complex in plants and in animals still needs clarification. To date, most animal miRNAs have been proposed to guide translational repression of their target transcripts, whereas, plant miRNAs induce AGO1-directed mRNA cleavage. Animal miRNAs show only limited complementarity with their target transcripts, whereas, plant miRNAs show a high degree of complementary with their targets. As such it is possible that both mechanisms might be operating in plants and in animals, the degree of which will depend on the complementary nature between the miRNA and the target transcript. Indeed, there was already an indication of miRNAs induced translational repression in plants where by miR172 was initially proposed to direct translational repression of *APETALA2* (*AP2*) mRNA following the observation of unchanged AP2 mRNA transcripts. However, this was later shown to be as a result of lack of a negative feedback loop by the *AP2* protein to inhibit its transcription (Aukerman and Sakai, 2003; Chen, 2004b). To the advantage of plant miRNAs possessing a high degree of complementarity, significant advances are being made in understanding the relationship between miRNAs and their target transcripts by artificially disrupting pairing between miRNA-target transcripts. A good example is the verification of *AGO1* as a target of miR168 that was demonstrated by rescuing miR168 resistant AGO1 plants with an artificially synthesised miRNA carrying compensatory mutations (Vaucheret et al., 2004).

II. Small Interference RNAs (siRNAs)

Apart from the MIR encoded siRNAs produced by DCL1 activity, plants also possess two other types of siRNAs. This include cis-acting siRNAs that are derived from transposons, repeat elements and heterochromatin, and are processed by DCL3; and another class of trans-acting siRNAs (tasiRNAs) that are derived from *TAS* genes and are processed by DCL4. The production of tasiRNAs is achieved through the activity of the miRNA pathway and the siRNA biogenesis pathway. The single stranded primary–tasiRNA possess a miRNA binding site which directs cleavage at a specific site and the products of which are then converted into dsRNA by RDR6-SGS3 RNA dependent amplification (Peragine et al., 2004). Good examples of MIR genes that target TAS primary RNAs are miR173 and miR390 (Xie et al., 2005a). The TAS-derived dsRNAs that are produced enter the siRNA biogenesis pathway and are sequentially processed into 21nt's tasiRNAs by DCL4 in association with dsRNA binding protein, DRB4 (Hiraguri et al., 2005; Adenot et al., 2006b). In common with miRNAs, ta-siRNAs are also methylated by HEN1 (Li et al., 2005b). tasiRNAs regulate transcription of their target genes by directing mRNA cleavage. Furthermore, ta-siRNAs have been demonstrated to function alongside miRNAs and target different members of the same gene family. This phenomenon was well demonstrated in an example whereby different members of the subfamily Pentatricopeptide repeat proteins (PPR) are targeted by either miR161 or TAS2 derived ta-siRNA, whereas, members of Auxin Response Factors (ARF) are targeted by either miR160, miRNA167, or TAS3 derived tasiRNAs (Reviewed in (Vaucheret, 2006). Studies of Arabidopsis *dcl4*, *rdr6* and *sgs3* mutants all showed acceleration of juvenile to adult phase transition suggesting a possible role of ta-siRNAs in regulating this transition (reviewed in (Brodersen and Voinnet, 2006). Indeed one of the well-characterised gene families that are involved in this process, the ARF transcription factors, are the targets of tasiRNAs although there is no clear evidence of the involvement of the only well characterised target (ARF3/ETTIN) in regulating juvenile to adult transition (Sessions, 1997). It has been proposed

that AGO1 and AGO7 form part of the RISC complexes that are involved in the degradation of the TAS2 and TAS3-derived target transcripts respectively. Evidence comes from the analysis of *ago7* mutant plants that showed reduced levels of TAS3-derived ta-siRNAs accompanied by an elevation of TAS3 ta-siRNAs target transcripts, but not TAS1 or TAS2 derived ta-siRNAs or changes on TAS1/TAS2 ta-siRNAs target transcripts (Allen et al., 2005; Adenot et al., 2006a).

What controls the accumulation of miRNAs (MIR) and ta-siRNAs (TAS)

The important role imposed by the miRNAs and ta-siRNAs in regulating gene expression during development was emphasized earlier, which involves controls of transcript abundance of the target genes and as a consequence often determines cell fate. As such, the control of *MIR* and *TAS* gene expression becomes critical in delivering appropriate downstream effects. Compared to the extensive coverage in understanding animal miRNA expression (Wienholds et al., 2005), so far only limited information is available about the expression pattern of *MIR* and *TAS* genes in plants and how are they regulated during plant development. Promoter fusion analysis of *MIR164c* and *MIR171* genes has revealed a tissue specific expression pattern, implying that transcriptional control of *MIR164c* and *MIR171* is partly imposed by their promoter regions (Parizotto et al., 2004; Baker et al., 2005). Moreover, in situ hybridization of *MIR165, MIR166*, and *MIR172* has also revealed tissue specific transcript accumulation; however, the mechanism responsible for this pattern is yet to be identified (Chen, 2004a; Kidner and Martienssen, 2005). In addition, control of *MIR* and *TAS* genes is also likely to occur at the post-transcriptional level. Indeed, mutations in the *SERRATE* gene resulted in the increased accumulation of precursor pre-miR165/166 and reduced accumulation of mature primary-miR165/166, implying that SERRATE is required for the post-transcriptional regulation of MIR165/166 (Grigg et al., 2005).

Other than inducing silencing of their target genes, miRNAs such as miR162/168 and TAS-derived siRNAs are also involved in the negative feedback loop that ensures controlled accumulation of MIR and TAS derived transcripts by directing cleavage of *DCL1* and *AGO1* transcripts (Jones-Rhoades et al., 2007; Xie et al., 2005b; Vazquez et al., 2004). Since *DCL1* is involved in miRNAs biogenesis and *AGO1* in mRNA cleavage, such feedback ensures fine control of miRNA levels. The role of *AGO1* in the control of miRNA accumulation was demonstrated in *ago1* mutants that result in the instability of miRNAs in the absence of AGO1 protein, whereas, expression of miR168-resistant *AGO1* mRNA result in an increase of *AGO1* transcript levels and an increase production of miRNAs particularly miR168, suggesting *AGO1* to be a limiting factor in miRNA accumulation (Vaucheret et al., 2004).

More than before, close attention and effort has now also been focused on understanding more of the mechanisms involved in regulating expression of the MIR and *TAS* genes and their accumulation in different cell types. On the other hand, since the ta-siRNA duplexes are generated from the single stranded (ssRNA) *TAS* transcripts by the action of RDR6, the duplexes possess both the RNA strand that is complementary to the primary *TAS* RNA (+ strand) and the a strand that is complementary to the *TAS* RNA (- strand). Thus, ta-siRNAs derived from both "+" and "-" strands are capable of targeting their target genes and have the potential to maintain a steady-state level of *TAS* transcript accumulation respectively (Vazquez et al., 2004). Mutants deficient in tasiRNA synthesis showed increased accumulation of the primary *TAS* RNA supporting the locus-specific feedback controlled *TAS* RNA synthesis (Vazquez et al., 2004).

III. Exogenous ta-siRNA pathway

Plants have adopted a well established system in regulating gene expression and RNA accumulation by inducing transcriptional inhibition, a mechanism referred as Transcriptional Gene Silencing (TGS), or by initiating RNA degradation post-transcription, also known as Post Transcriptional Gene Silencing (PTGS). These pathways are involved in diverse functions in plants from control of transposable elements to response to virus infection demonstrated by mutations in PTGS (Baulcombe, 2004). As such, the PTGS pathway is a dedicated RNA-based plant immune system that is responsible for protecting the genome from endogenous (transposons) and exogenous (virus and transgenes) nucleic acid invasion. This pathway acts through the action of cis- and trans- acting siRNAs derived directly from the genome or encoded by the invading source itself. The PTGS pathway was initially discovered in transgenic *Petunia* as a loss of both transgene (in both sense- and anti-sense orientation) and homologous endogenous gene expression (Napoli et al., 1990).

Despite the limited knowledge of how the PTGS pathway operates, the endogenous siRNA machinery is now being used routinely as a powerful tool for knocking down targeted endogenous gene expression in a tissue specific and temporally controlled manner (Reviewed by (Matthew, 2004). In Arabidopsis, silencing of specific endogenous transcripts can be achieved at low frequency using sense transgenes (S-PTGS) or at higher frequency using inverted-repeat transgenes (IR-PTGS) (Chuang and Meyerowitz, 2000; Beclin et al., 2002). The stronger effect induced by the IR-PTGS is due to the consequences of the inverted repeats that result in a folding of the transgene-derived RNAs into long dsRNA structures, whereas, the S-PTGS silencing effect relies on the ability of a transgene locus to produce particular species of single stranded RNA with aberrant features (such as lack of 5' capping). These are recognised by RDR6 in association with SGS3 and converted into dsRNA which leads to the subsequent degradation of the homologous transcripts (Smith et al.,

2000; Dalmay et al., 2000). Indeed, S-PTGS directed transgene-derived RNA degradation is induced in the Arabidopsis *xrn4* mutant (a 5'-3' exonuclease that degrades uncapped mRNAs) as a result of enhanced accumulation of uncapped transgene mRNAs which fuel their conversion into dsRNA by RDR6 RNA polymerases (Gazzani et al., 2004). Furthermore, imperfect integration of transgenes in the genome might result in a juxtaposed sense-antisense transgene orientation, and as a consequence produce a dsRNAs and trigger PTGS activity (Stam et al., 1997; Metzlaff et al., 1997). Two classes of siRNAs are produced as populations along the entire length of the IR-dsRNA transcripts, the 21-nt siRNAs that guide mRNA cleavage of the target transcript, and the 24-nt siRNA species that exclusively mediate chromatin modifications (Llave et al., 2002; Hamilton et al., 2002; Zilberman et al., 2003).

Biochemical analysis of the S/IR-PTGS effect has established that transgene-derived siRNAs are methylated by HEN1 and guide sequence specific ARGONAUTE1 (AGO1)-catalyzed mRNA cleavage (Boutet et al., 2003; Baumberger and Baulcombe, 2005; Qi et al., 2005). A question still remains of how the S-PTGS induces the silencing effect. A clue might be obtained from the observation that the PTGS components (AGO1, HEN1, RDR6, and SGS3) also participate in the RNA-based immune response against cucumber mosaic virus (CMV) infection (Boutet et al., 2003; Mourrain et al., 2000), raising the possibility that perhaps some of the transgene-derived RNAs produced during S-PTGS is likely to resemble those of viral RNAs during CMV infection and as a consequence activate the RNA based immune response.

IV. smRNA pathways and Chromatin modification

Chromatin modification has a profound effect on genome integrity and control of gene expression. DNA methylation in coding and non-coding parts of the genome plays a central role in genome organization, immobilization of transposable elements, and transcriptional gene silencing (Chan et al., 2005). Extending its arm on the control of gene expression and protection of the genome from exogenous nucleic acid invasion, there is significant growing

evidence that smRNA pathways are also involved in genome methylation through RNA-directed DNA methylation using a specific set of smRNA components dedicated to this process (Matzke and Birchler, 2005). The methylation process is accomplished through the action of siRNAs ~24nt long that confer sequence specificity towards their target sites and the activities of Dicer-like3 (DCL3), RNA-dependent RNA polymerase2 (RDR2), RNA polymerase IV and Argonaute4 (AGO4) protein (Zilberman et al., 2003; Xie et al., 2004; Onodera et al., 2005; Onodera et al., 2005). Lack or reduced activities of these components through mutation result in a significant reduction of siRNA accumulation and a decrease in DNA methylation of several endogenous loci including transposons and repetitive elements (Xie et al., 2004; Lippman et al., 2003).

There are four pathways of RNA-mediated chromatin modification that have been described so far, two of which, RNA-directed DNA methylation (RdDM) and RNAi-mediated heterochromatin formation, result in covalent modification of cytosines in DNA or of histones (Reviewed in (Matzke and Birchler, 2005). RdDM was initially discovered in viroid infected tobacco plants and was shown to be directed by smRNAs of 21-24nts (Wassenegger et al., 1994; Mette et al., 2000). The methylation effect is confined within the region of RNA-DNA homology, and depending on the degree of homology smRNAs can direct promoter methylation to shut down gene transcription and also methylation of cytosines in a normal CG symmetrical pattern as well as in asymmetrical configuration (Pelissier et al., ; Aufsatz et al., 2002). The process of RdDM is initiated by an RNA signal that directs DNA methylation by guiding a site-specific DNA methyltransferases to the target site, and thereafter, the methylation pattern initiated is maintained following histone modification which otherwise might be lost through rounds of DNA replication (Cao et al., 2003; Aufsatz et al., 2004). This maintenance of the methylation pattern is catalysed by DNA methyltransferases (MET1), Histone deacetylases (HDAC6), plant specific DNA methyltransferases CHROMOMETHYLASES

(CMT3), and H3 lysine 9 methyltransferases SUVH4 (KRYPTONITE;Reviewed in (Matzke and Birchler, 2005).

The first glimpse of RdDM in Arabidopsis was demonstrated in an experiment in which an introduced transgene carrying a promoter of a homeodomain transcription factor, Late-flowering (FWA) that also has a role in endosperm proliferation (Kinoshita et al., 2004) was silenced following methylation of two tandem repeats within the promoter region (Lippman et al., 2004). In wild type, the promoter of *FWA* is normally methylated and silenced by MET1 (Kinoshita et al., 2004; Soppe et al., 2000) presumably directed by siRNAs homologous to the tandem repeats which originate from transposons (Lippman et al., 2004). As a result its expression is restricted from other tissues except in the endosperm following demethylation by DEMETER (DEM), a DNA glycosylase required for the demethylation and activation of maternally imprinted genes *MEDEA* and *FWA* (Kinoshita et al., 2004).

Advances from this initial discovery and in-depth understanding of how RdDM induced DNA methylation of target sites came from the isolation of mutants that are defective in RdDM of a seed-specific promoter that was transgenically expressed in Arabidopsis. The screen led to the identification of DEFECTIVE IN RNA-DIRECTED DNA METHYLATION 1 (DRD1), a putative SNF2-LIKE chromatin remodelling protein (Kanno et al., 2004). This evidence points to the requirement of chromatin reconfiguration to allow access of RNA signals to the target DNA site (Reviewed in (Matzke and Birchler, 2005). Furthermore, a second SNF2-like protein, DECREASE IN DNA METHYLATION (DDM1) was identified in a screen of mutants that are deficient in DNA methylation of centromeric repeats and ribosomal DNA and have been shown to contribute to the maintenance of RdDM (Reviewed in (Matzke and Birchler, 2005). A direct demonstration of RdDM involvement in the methylation of the FWA promoter sequence was achieved by the introduction of dsRNA corresponding to the tandem-direct repeats within the *FWA* transcription start site into the mutant background of a *ddm1*-induced *fwa* epiallele. The outcome of the experiment was the de novo DNA methylation of

FWA tandem repeats that led to transcriptional suppression and phenotypic reversion of the *ddm1* phenotype (Kinoshita et al., 2007). It can be concluded that methylation of *FWA* direct repeats in wild type presumably driven by siRNAs originated from Short Interspersed Nuclear Elements (SINE) is sufficient to induce the epigenetic control of the *FWA* gene expression (Kinoshita et al., 2007). Thus, FWA RdDM provides the first example of an endogenous gene demonstrating RdDM of promoter sequences by transposon-derived siRNA.

C: smRNA silencing and control of gene expression in the male gametophyte

To date a comprehensive coverage and in-depth understanding of the diversity and mechanisms of smRNA pathways and how they operate in different context in somatic cells has been the focus of many experiments. Effort in addressing similar queries in the male gametophyte of flowering plants has received far little attention in contrast to animal germ line in which significant understanding of the smRNA pathways in governing the development of the germ cell lineage has been achieved. However, the knowledge gained cannot be strictly applied to the plant germlines since the specification of plant germ cell lineage is distinct from that of animals. In animals, the germ cell lineage is defined and set aside early during embryogenesis, whereas, plant germ cell lineage is specified later during development induced by change in gene expression of somatic stem cells. Currently, this difference in defining the germ cell lineage together with the differences in gamete formation between plants and animals has posed a fundamental question concerning how these two related processes are controlled at the molecular level.

smRNAs are fundamental to the regulation of eukaryotic endogenous gene expression either at the transcriptional level through chromatin modification or post-transcriptional through mRNA degradation or translational inhibition. As a result, by altering changes in

gene expression, smRNA pathways have become key determinants of cell fate in eukaryotes throughout the life cycle.

Genome wide analysis of Arabidopsis transcriptomic data from the four stages of male gametophyte development identified a total of 13,977 male gametophyte expressed mRNA, of which, 1358 genes were male gametophytic specific (Honys and Twell, 2004). Intriguingly, the progression of the proliferating microspores to terminally differentiated pollen was accompanied by a large-scale repression of early expressed genes (11,565) and activation of late expressed genes (8,788;Honys and Twell, 2004). Considering the short phase of transition from microspore development to division into two cells of different cell fate and the large scale transcriptional shut down; it is easy to speculate presence of an effective transcriptional regulatory mechanisms that would allow transcriptional repression and the rapid turnover of the remaining transcripts of the early expressed genes. With the limited knowledge on the mechanisms that regulate gene expression in the male germ line, one can hypothesize the possible involvement of smRNA pathways in modulating gene expression in the male gametophyte. Several studies in animals have demonstrated the importance of the smRNA function in the development and correct specification of germ line lineage. A Drosophila gene *PIWI* encodes a protein of AGO family and another PIWI subfamily member AUBERGINE, are both specifically required for spermatogenesis and oogenesis, and maturation of the oocytes respectively (Cox et al., 1998; Saito et al., 2006; Kennerdell et al., 2002). Findings by Saito et al. (2006) showed that Drosophila PIWI proteins functions in nuclear RNA silencing in association with repeat-associated siRNAs (rasiRNAs) derived from repetitive targets. Indeed, three PIWI subfamily members MIWI, MILI and MIWI2 from mice were identified to play roles in spermatogenesis (Carmell et al., 2007). In Arabidopsis there are 10 members of the AGO family, however, until now none of the members have been identified to act in a gametophytic manner. AGO1 and AGO10 are known to be involved in maintenance of the shoot meristem (reviewed in (Vaucheret, 2006), AGO4 is involved in the

biogenesis of siRNAs that are required in RdDM pathway and silencing of transposons (Zilberman et al., 2003), whereas AGO7 is involved in the induction of juvenile-to-adult transition during vegetative development (Peragine et al., 2004). AGO1 has also been implicated to have a role in reproduction by specifying meristem identity, flowering transition and flower organ identity through control of LFY, AP1 and AG encoding transcription factors (Kidner and Martienssen, 2005). In addition, AGO1 is responsible for the post-transcriptional silencing of CURLY LEAF (CLF), encoding a polycomb group protein that maintains the repression of KNOX genes and the floral organ identity genes AGAMOUS (AG) and APETALA3 (AP3) in vegetative leaves (Goodrich et al., 1997) and in pollen (Kidner and Martienssen, 2005).

The specification of germ line identity by ARGONAUTE proteins of the Piwi subfamily in flies and mammals involve a germ line specific class of small RNAs termed PIWI-interacting RNAs (piRNAs;Lin et al., 2007). piRNAs are specific to the germ line and unique in a sense that they are synthesised 24-31 nt long and do not require activities of RdRP or Dicer-like proteins for their production (Reviewed in (Matranga and Zamore, 2007). In flies, piRNAs are thought to originate from loci rich in transposons then act in *trans* to repress dispersed copies homologous to the trigger locus (Reviewed in (Matranga and Zamore, 2007). In plants, there are no homologs of PIWI subfamily despite having a larger ARGONAUTE family than animals. However, an exciting breakthrough came from the identification of Argonaute gene in rice with a direct role in sexual reproduction (Reviewed by (Grant-Downton and Dickinson, 2007). The discovery came from seed-sterile mutants that exhibit normal vegetative development but are defective in the generation of reproductive organs and progression through meiosis. One mutant line in particular, *meiosis arrested at leptotene1* (*mel1)*, was identified to have specific effect on the meiotic progression of the sporogenous cells in the anther (Reviewed by Grant-Downton and Dickinson, 2007). *MEL1* is a member of the AGO family and has been identified to be involved in regulating meiosis in plant germ cell by

maintaining germ cell identity through repression of somatic gene expression and heterochromatin modification. The expression of MEL1 was restricted to the cells that would undergo meiosis and become sporogenous cells. In conjunction with the above evidence, it was proposed that MEL1 confers germline fate by inducing chromatin modification and repressing somatic gene expression programmes in plant germ cells (Reviewed by (Grant-Downton and Dickinson, 2007). This proposition seems to fit with the knowledge of the function of Piwi subfamily in the specification of germ cell lineage in animals, and the discovery that plant AGO4 and AGO6 play essential roles in RdDM and chromatin modification (Reviewed by (Grant-Downton and Dickinson, 2007). The identification of MEL1 as a regulator of meiotic progression was not an intriguing discovery considering the knowledge of Piwi subfamily in the specification of animal germ cell lineage, however, the discovery indicates a common molecular switch involving smRNA pathways that regulates specification of germ cell lineages in animals and in plants despite the difference in their origin.

Thus, our current knowledge of the expression and function of smRNA components in plants has exclusively come from the study of mutants with sporophytic defects, whereas similar studies in the gametophyte generation have not been reported. To date, it is apparent that the essential roles played by the smRNAs pathways in the specification of germ cell lineage and production of gametes in animals is clear (Reviewed in (Matranga and Zamore, 2007). Yet nothing is known about the possible role of smRNAs in fate determination during plant gametogenesis. Recent studies of the pollen transcriptomic data suggested a transcriptional shutdown of small RNA components during pollen maturation, and a possible lack of smRNA activities in the male germ cells (Pina et al., 2005). However, this study only analysed a limited number of components, and there has been several reports on miRNA expression in maturing pollen, use of RNAi construct to knockdown pollen expressed gene and the recent discovery of the ARGONAUTE protein (MEL1) that has an indispensible role in premeiotic

mitosis and meiosis in rice (Grant-Downton et al., 2009). Furthermore, the recent generation of a genome-wide Arabidopsis sperm cell transcriptome revealed over-representation of a set of smRNA components involved in the RNA-directed DNA methylation (RdDM). This has led to the suggestion that distinct mechanisms might be involved in regulating the epigenetic state of the paternal genome by exploiting the RdDM machinery (Borges et al., 2008). As such, the unexplored male gametophyte developments in the context of expression and functionality of the smRNA pathways and the initial glimpse on the possible RNAi activity in pollen have sparked one of the objectives of my project.

Overview of the project objectives;

Several studies have demonstrated that CDKA-CycA/CycD complexes are involved in the phosphorylation of a retinoblastoma-related protein (RBR) that leads to the activation of genes regulated by E2F/DP transcription factors that are crucial in licensing S-phase. During G2, CDKA/CycB1 and CDKB/CycB1 complexes induce entry into mitosis to allow chromosome separation. The phosphorylation of kinase complexes on specific residues by the inhibitory kinases (such as ICK) and the degradation of mitotic cyclins through the ubiquitin mediated proteolysis that involves Anaphase promoting complex/Cyclosome (APC/C) allows exit from the cell cycle. In recent years, considerable progress has been made in unravelling the mechanism operating at the centre of plant cell cycle. Most of the key regulators involved in the activation of cell cycle components and their stage specific roles during cell cycle progression have now been established. However, most of these efforts have been solely focused on the model system cell suspension cultures and some studies in sporophytic tissues. Control of cell cycle progression in the male gametophyte from asymmetric division of the haploid microspores to fusion of twin sperm cells with the female gametes, requires a high level of synchrony between the cellular events, cell cycle in particular. The products of

male and female gametophyte (sperm cells, egg cell and central cells) coordinate their ontogenic events prior to fertilization through the cell cycle. Successful fusion of male and female gametes in the double fertilization event depends upon synchronous cell cycle progression during karyogamy. Friedman, (1991) showed that fusion of male and female gametes in Arabidopsis only occurs when the DNA content reaches a 2C level. Furthermore, several studies have demonstrated the significance of correct progression through PMI and PMII and its consequences in double fertilization. Thus, it is of significant importance to understand the mechanisms regulating cell cycle progression in the male gametophyte that are yet to be explored. It was hypothesised that key regulators that are involved in licencing mitotic progression in sporophytic tissues might also have n essetial role in the male gametophyte. Thus, the main objective of this project was to explore expression of essential regulators of the G2/M transition, the CycB family, during male gametophyte development. This involved use of publicly available pollen transcriptomic datasets and verification of the transcriptomic datasets by RT-PCR analysis. To get a more detailed view of the expression profile of the B-type cyclins, the expression of an existing cell cycle marker comprising the CycB1;1 promoter fused to destruction box and a reporter gene (Kindly provided by P. Doerner) was investigated to establish CycB1;1 expression pattern in vivo during pollen development. For a functional test to establish which of the B-type cyclin family members play a role during PMI and PMII, RNA interference (RNAi) vectors were used to down-regulate expression of CycB1 family members in specific cell types in pollen. The results of these experiments are presented in Chapter 3.

To extend the investigation of the mechanisms regulating cell cycle progression in the male gametophyte, *DUO POLLEN3* mutant was analysed in detail. To get a clear understanding of how *DUO3* participates in the control of germ cell division, one aspect of my PhD project objectives was to address the temporal and spatial patterns of *DUO3* expression during plant development and how it differs from the expression of the *DUO1* gene. In addition, to

establish the essential cell cycle role played by *DUO3* at PMII, the project was aimed to investigate the activity of a valuable mitotic marker (pCycB1;1-CycB1;1D-box::GFP in the *duo3* mutant background with the purpose of addressing the missing components that induce the G2/M arrest of the mutant germ cells in heterozygous *duo3* plants. Results of these studies are presented in chapter 5.

To address the expression pattern of smRNA components in the male gametophyte, the project aimed to uncover the profile of three key gene families encoding essential components of the smRNA machinery. Moreover, other genes that have also been demonstrated to play role in the smRNA machinery where included in this analysis with the purpose of demonstrating active expression of these components in the male gametophyte. In addition, the project also aimed further to test the functionality of the siRNA pathway by generating pollen cell-specific molecular vectors that would target genes of interest specifically in pollen. Results of the experiments undertaken to accomplish these objectives are presented in chapter 4.

5. Outline of the project aims and objectives

The initiation of this project was inspired by the need to gain more in-depth understanding of the cellular processes governing the formation of twin sperm cells, an important evolutionary aspect of angiosperms that has allowed the success and dominance of the flowering plants on land. The overall aims of this project were to uncover evidence for the molecular mechanisms imposed in the male gametophyte that control cell cycle progression and cell fate specification, and to establish whether smRNA pathways could possibly operate as a mechanism of transcriptional regulation during spermatogenesis. This was with the intention of contributing to the limited knowledge that exists to-date and to expand our understanding of the process of male gametogenesis. The project consists of three main

objectives, each is presented as a separate chapter. The key objectives of this project were as follows:

1. To investigate the role of B-type cyclins in regulating cell cycle progression through in the male gametophyte. This involved analysis of pollen transcriptomic datasets to establish the expression pattern of the family members and verification of their expression profiles by RT-PCR analysis. Two existing cell cycle markers comprised of *AtCycB1;1* promoter fused to a *CycB1;1* mitotic destruction box (D-box) –GUS fusion (pCDG), or AtCycB1;1:: GFP protein fusion (pCDGFP) were also explored to demonstrate the spatial and temporal expression pattern of *AtCycB1;1 in planta* during male gametophyte development. The activity of these constructs was exploited to investigate the nature of *duo1* and *duo3* mutations. Moreover, to determine whether CycB1 family participate in regulating cell cycle progression, pollen cell-specific constructs were generated to direct expression of targeted hairpin dsRNA to manipulate expression of CycB1 family members in specific cell types. Results of the experiment performed to achieve this objective are presented in Chapter 3.
2. The second part of this project involved investigation of the expression of components of the smRNA pathways in the male gametophyte and to determine the likelihood of these pathways to operate during pollen development. To accomplish this objective, investigation was initiated by analysing transcriptomic datasets to get a hint of the expression profile in pollen. These data were verified for many of the smRNA pathway components by RT-PCR analysis. In parallel, pollen cell-specific molecular vectors were generated for manipulating expression of target genes in different cell types of the male gametophyte. The vectors served a dual purpose; [1] to provide functional test of the siRNA pathway in pollen by expressing hairpin dsRNA to induce RNA-directed mRNA transcript degradation [2]

and as a tool for targeted mutagenesis specifically in the male gametophyte. Data from these experiments are presented in Chapter 4.

3. In building the network of factors regulating cell cycle progression in the male gametophyte, the project aimed to characterize the expression pattern of *DUO POLLEN3*, which is essential for germ cell division. This involved analysed transcriptomic datasets, verification of the observed pattern by RT-PCR and in situ histochemical localization *DUO3* promoter activities. Furthermore, to get an indication of role of *DUO3* during germ cell division, potential relationship between *DUO3* and *AtCycB1;1* was also investigated. This objective comprises Chapter 5 of the thesis.

Chapter 2

Materials and Methods

2.1 Materials used for the experiment

Plant materials were grown at the university botanic garden and brought in the lab prior bolting, once a week. All the chemicals used were purchased from Melford Lab (UK), Sigma chemical company Ltd, Fisher scientific, BioAgar (biogene.com), CALBIOCHEM, Promega, Lehle seeds, Duchefa Biochemie, DHAI PROCIDA, Qiagen and Bioneer. Enzymes and other reagents were obtained from Invitrogen, FINNZYMES, New England Biolabs (NEB), Novagen and Bioline

2.2 Preparation of plant materials

2.2.1 Media for plant tissue culture

Arabidopsis seeds were plated on Murashige and Skoog salt media (MS Duchefa Biochemie, Netherlands). 4.3g of MS salt were dissolved in 950ml of deionised water with no added sucrose (MS0) or with 1-3% (w/v) sucrose. The media pH was adjusted to 7.0 with 5N NaOH and autoclaved for 20 minutes at 120^0C and 15psi on liquid cycle. To make MS agar for plating, 0.6% (w/v) of bactor agar (BioAgar, Biogene limited, UK) was added before autoclaving.

2.2.2 Seed plating and growth conditions

Arabidopsis thaliana plants ecotype Columbia (Col-0) and Nossen (No-0) were grown either in soil in 3:1:1 compost (Levington$^{(R)}$): vermiculite: sand with 16 hours light at 22 ^{0}C, or plated on MS0 growth media. Seeds were surface sterilised with 70% (v/v) ethanol for 5 minutes followed by 100% (v/v) ethanol for 1 minute, and dried on sterile filter paper for 30 minutes. For the primary transformants, ~150mg of T1 seeds were plated on MS-0 media with appropriate selection. In the case of selection on soil, similar amount of seeds were sown on soil with appropriate selection. Non-transformed seeds were plated on MS-0 media without

selection. From the second generation of transformants, seeds were plated on MS10 (with 1% added sucrose). All seeds were stratified at 4 ^{0}C for three days, and then incubated in the growth room set at 21 ^{0}C with variable humidity and continuous light.

2.2.3 Antibiotics for selection of transformed plants

Antibiotic	Working concentration
Cefotaxime (Melford Lab, UK)	200 mg/ml
Benamyl (Melford Lab, UK)	10 mg/ml
Kanamycin (Melford Lab, UK)	50 mg/ml
Hygromycin (CALBIOCHEM)	20 mg/ml
Glufosinate ammonium [BASTA] (DHAI PROCIDA)	30 mg/ml

To make working stocks at desired concentration as listed above, antibiotics were dissolved in deionized water and stored at -20^{0}C.

2.2.4 Storage of plant materials

All isolated plant tissues (including roots, seedlings, shoot apex enriched tissues, rosette leaves, cauline leaves, flowers with mature pollen grains and siliques) for DNA and RNA extraction were weighed, flash frozen in liquid nitrogen and stored at –80^{o}C. Where necessary, GUS stained materials including seedlings and whole inflorescence buds were first fixed in 3:1 (v/v) ethanol: acetic acid for 4 hours and then cleared with 75% (v/v) ethanol overnight before storing at 4^{o}C prior to examination.

2.3 Bacterial culture and storage

2.3.1 Media for growth of bacteria

Escherichia coli (*E.coli*) and *Agrobacterium tumefaciens* (*A. tumefaciens*) were grown in Luria Bertani Broth media (LB Broth): 1% (w/v) tryptone, 1% (w/v) NaCl, 0.5% (w/v) yeast extract. For bacterial growth on plates, 1.5% (w/v) bacto-agar was added into the media before autoclaving. The media pH was adjusted to 7.0 with 5N NaOH and autoclaved for 20 minutes at 120^{o}C and 15psi on liquid cycle. When a ready mix media was used, no pH adjustment was necessary.

2.3.2 Bacterial strains

Escherichia coli (*E. coli*)

- DH5α
- DB3.1

Agrobacterium tumefaciens (*A. tumefaciens*)

- GV3101

2. 3.3 Growth conditions

After inoculation on plates or in liquid media with or without antibiotics, cultures were placed in an incubator (LEEC Ltd, UK) or orbital shaker (SANYO Gallenkamp, UK) at 220rpm set at 37^{o}C for *E. coli* and 28^{o}C for *A. tumefaciens* respectively. Cultures were grown over night, for two days or until desired optical density was reached.

2.3.4 Antibiotics for bacterial selection

Antibiotic	**Working concentration**	
	E.coli (DH5α / DB3.1)	*A.tumefaciens* (GV3101)
Rifampicin (Melford Lab, UK)	n.a	50 mg/ml
Gentamycin (Melford Lab, UK)	n.a	50 mg/ml
Spectinomycin (Melford Lab, UK)	100 mg/ml	100 mg/ml
Kanamycin (Melford Lab, UK)	50 mg/ml	50 mg/ml
Ampicillin (Melford Lab, UK)	30 mg/ml	30 mg/ml
Chloromphenicol (SIGMA)	30 mg/ml	20 mg/ml

2.3.5 Storage of bacterial strains

A single colony was used to inoculate 5ml LB media and grown as described in section 2.3.3. 700µl aliquot of the overnight bacterial culture was transferred to a cryogenic storage tube and was mixed with 300µl sterile 50% (v/v) glycerol. The cells were flash frozen in liquid nitrogen and stored at –80^{o}C. The strains were recovered by streaking a small portion of the frozen culture on solidified media containing appropriate selection and grown as required.

2.3.6 Preparation and transformation of competent cells

2.3.6.1 Preparation of competent *E. coli*

E.coli strains (DB3.1 and DH5α) were streaked out onto the LB medium containing 6% bactoagar and grown overnight at 37 ^{o}C. Individual clone was selected and grown in 5 ml of SOB medium (SOC media with $MgCl_2$ at a final concentration of 10µM) for overnight at 37^{o}C on a shaker (200 rpm). The SOC media consist of Bacto Tryptone, Bacto yeast extract, 5M NaCl, 1M KCl, 1M $MgCl_2$, 1M MgSO4 and 1M of glucose. A 2.5 ml aliquot of the overnight culture was added to 250 ml of the SOB medium in a 2L flask. The culture was grown at 37^{o}C with vigorous shaking (200-250 rpm) until the optimal density (OD) at A_{600} reaches 0.45. The cell suspension was transferred to sterile 250 mL bottles and chilled on ice for ten minutes. Cells were centrifuged at 2000 *g* (4000 RPM) for 10 minutes at 4^{o}C. The supernatant was discarded and the cells were resuspended in 60 ml of ice-cold TB solution (10mM of Piperazine 2-ethane sulphonic acid, 55mM $MnCl_2.4H_2O$, 15mM $CaCl_2$. $2H_2O$, 250mM KCl). The mixture was left on ice bath for 10 minutes and respin at 2000 *g* for 10 minutes at 4^{o}C. The pellets were resuspended gently (shaker 125 *rpm*) with 1.12 mL of 7% final concentration Dimethy lsulfoxide (DMSO). Cells were left on ice for 10 minutes and then aliquoted into Eppendorf tubes (200 µl/tube). Competent cells were flash frozen in liquid nitrogen and stored in -80 ^{o}C.

A: **Transformation of *E. coli***

For transformation of *E. coli*, 200µl aliquot from was removed from -80 ^{o}C freezer and thawed on ice for 10 minutes. 50µl of the competent cells was aliquot into four Eppendeorf tubes. 1µl (~125ng) of plasmid or half of the ligation / recombination reaction was added into a 50µl aliquot and incubated on ice for 30 minutes. The mixture was heat shocked in a water bath at 42 ^{o}C for 45 seconds, then transferred back on ice for further 2 minutes. 950µl of LB media was added and the culture was incubated at 37 ^{o}C for 1 hr with gentle shaking (200 rpm). 150µl of cells and 100ul of cell suspension were plated on LB agar containing correct antibiotics.

2.3.6.2 Preparation of competent *A. tumefaciens*

An *Agrobacterium* strain (GV3101) containing an appropriate helper T_i plasmid was grown in 5 ml of LB medium along with selective antibiotic overnight at 28^{o}C on a shaker (200 rpm). A 2 ml aliquot of the overnight culture was added to 50 ml of LB medium in a 250 ml flask. The culture was grown at 28^{o}C with vigorous shaking (250 rpm) until the OD_{600} reaches 0.5-1.0. The cell suspension was chilled on ice and centrifuged at 3000 *g* for 10 minutes at 4^{o}C. The supernatant was discarded and the cells were resuspended in 1 ml of 20 mm ice-cold $CaCl_2$ solution. A 100 µl aliquot of the cells was quickly dispensed into pre-chilled microfuge tubes, flash frozen in liquid nitrogen and stored at -80^{o}C.

B**:** **Transformation *of A. tumefaciens***

A single colony of Agrobacterium strain GV3101 containing an appropriate helper Ti plasmid (pMP90) was grown overnight as described in section 2.3.3 in a 5ml LB media containing 50 µg/ml Rifampicin and 50 µg/ml Gentamycin. Approximately 2 ml of the overnight culture was subculture into 50 ml LB media in a 250 ml flask with the appropriate antibiotics and shaken vigorously (250rpm) at 28 ^{o}C until the culture grew to OD600 of 0.5 to 1.0. The

culture was chilled on ice and then centrifuge at 3000g for 5 min at 4°C. Cells were resuspended in 1ml of 20mM ice-cold $CaCl_2$ solution. 0.1ml aliquots was dispense into pre-chilled 1.5ml microfugetubes, flash frozen in liquid nitrogen and stored at -80 °C.

For transformation of Agrobacterium, 0.5 – 1 μg of plasmid DNA was added into the frozen aliquot and incubated at 37 °C for 5 min to heat-shock the cells. 1 ml of LB media was added into the mixture, and then incubated at 28 °C in 200 revolution per minute (rpm) shaker for 2 – 4 hours.

The culture was then centrifuge for 30 seconds at 5000 rpm and the supernatant was discarded. Transformed cells were resuspended with the remaining solution and then spread on LB agar plate containing appropriate antibiotics. The plates were incubated at 28 °C for 2 days.

2.4 Isolation of nucleic acids

2.4.1 Isolation of genomic DNA

For isolation of genomic DNA, 1-2 cauline or rosette leaves were collected into the 1.5ml Eppendorf tube containing ~200 glass beads (Sigma, UK) of size 425-600 microns. The leaf tissues were flash frozen in liquid nitrogen and ground for 9 seconds in a silament amalgam mixer (Ivoclar Vivadent, UK) at room temperature. The grounded samples were mixed with 250μl of DNA extraction buffer (1.4 M NaCl, 3% (w/v) CTAB, 20 mM EDTA, 100 mM Tris-Hcl pH8), vortexed briefly and incubated for 15 minutes at room temperature. An equal volume of chloroform: IAA (24:1;250μl) was added and centrifuged for 10 minutes at 13000 rpm. The upper clear phase (~200μl) was transferred to a fresh Eppendorf tube, precipitated with 0.7 volume (~140μl) of isopropanol, incubated for 5 min at room temperature and then centrifuged for 7 minutes at 13000 rpm. The supernatant was discarded and the pellet washed with 1ml of 70% (v/v) ethanol before being centrifuged for 5 minutes at 13000 rpm.

The ethanol was discarded and the pellet was vacuum dried for 5 minutes or left at room temperature for 30 minutes to dry. The dried pellet was resuspended in 100 μl of deinonized water (DW) by incubating for 5 min at 55^0C. The mixture was then spun down at 13000 rpm to remove any unsuspended pellets, and then stored at -20^0C.

2.4.2 Isolation of total RNA

Isolation of total RNA was performed using RNeasy Plant Mini Kit (Qiagen, UK) according to the manufacture instructions. Tissue samples were collected from seedlings, shoot apex, root, rosette leaves, stem, flowers containing mature pollen and siliques, frozen in liquid nitrogen and stored at -80^0C. 50-100mg of frozen tissues were ground to fine powder in liquid nitrogen with 450μl of buffer RLT (a lysis buffer containing guandine thiocynate as denaturing agent) containing 10μl of β-mercaptoethanol. The mixture were left to thaw and ground further to a homogenius lysate. For RNA extraction from siliques, buffer RLC (which contains guanidine hydrochloride) was used instead due to excess secondary metabolites in siliques. The lysate was transferred into a QIAshredder spin column and collection tube and centrifuge for 2 minutes at 13000 rpm. The supernatant was then transferred to a new eppendorf tube containing 225μl of 100% ethanol. The mixture was then applied to an RNeasy mini column and centrifuged for 15 seconds at 10000 rpm. The flow-through was discarded and 700μl of buffer RW1 (containing small amount of guandine thiocynate and ethanol) was added to the column before being centrifuged for 15 seconds at 10,000 rpm. The RNeasy column was transferred to a new collection tube and 500μl of buffer RPE (Binding buffer consist of ethanol) was added to bind the RNA to the column membrane. The sample was centrifuge for 15 seconds at 10000 rpm and additional centrifugation was performed for another 2 minutes at 13000 rpm. The column was centrifuged for further minute to dry off the membrane, and the RNA was eluted with 30μl RNAse free water into a

1.5ml Eppendorf tube. RNA samples were quantified by spectrophotometry and verified by gel electrophoresis before being stored at -20^{0}C.

2.4.3 Quantification of total RNA

After the RNA extraction was completed, 1µl of the total RNA was loaded in 1.5% agarose gel to check the quality of the RNA. To measure the concentration of the RNA using a Philips, PU-8740 spectrophotometer at 260nm wavelength, the following criterion was used;

1 Abs unit$_{260}$ = 40µg/ml (when the RNA is suspended in water only).

Concentration (µg/ml) = 40 x Abs$_{260}$ x dilution factor

Total amount (µg) = Concentration (µg/ml) x total volume of extracted RNA (ml)

The above criterion is based on the extinction coefficient (a measure of how well RNA absorbs electromagnetic radiation) calculated for RNA in water. RNA samples were diluted 1/50 or 2/100 in RNAse free water and loaded in RNAse free quartz cuvette. A fixed wavelength (260nm) was selected and a blank was set using RNAse free water. The quartz cuvette was cleaned and dried, the RNA sample was loaded and placed in the appropriate cell. The reading (absorbance) was taken and recorded in an excel sheet. The process was repeated for the remaining RNA samples. The total concentration of the RNA was calculated with the above criterion using Microsoft excel software. The concentration of the RNA was verified by running a fixed calculated concentration according to spectrophotometer on 1.5% agarose gel.

2.4.4 Measuring RNA purity

The purity of the RNA was analysed by measuring the absorbance at 260 and 280nm, and then calculating the ratio between the absorbance values (Abs_{260} : Abs_{280}). For pure RNA, a ratio of 1.9-2.1 was expected if the RNA is suspended in buffer at pH 7.5 (10Mm Tris.Cl, pH 7.5) . If the RNA is dissolved in water, a lower ratio value was expected as water is not buffered and the pH interferes with absorbance (i.e. low pH result in low absorbance due to change in ionic concentration).

2.4.5 Isolation of plasmid DNA

Transformed plasmid DNA from *E. coli* and *A. tumefaciens* was isolated using QIAprep Spin Miniprep Kit (Qiagen, UK) according to the manufacturer instructions. An overnight culture was set up from a single colony in a 5ml LB medium for *E. coli* and 6 ml for *A. tumefaciens*. A 1.5 ml of the overnight culture was transferred into an Eppendorf tube and centrifuge for 1 minute at 13000 rpm. This step was repeated twice with culture from *E. coli* and four times with culture from *A. tumefaciens* to achieve a good yield of isolated plasmid. The supernatant was discarded and the pelleted cells were resuspended in 250 μl of buffer P1 (containing ethanol and Rnase) by brief vortexing or pipetting. For lysing the bacterial cells, 250 μl of buffer P2 (containing sodium hydroxide and blue lysate dye) was added to lyse the cells and the tube was gently inverted to achieve a homogenius blue mixture. For precipitation, 350 μl of buffer N3 (contains guanidine hydrochloride and acetic acid) was added and the suspension was mixed gently to precipitate cell debris and the associated bacterial chromosomal DNA. Lysed bacterial cells were centrifuged for 10 minutes at 13000 rpm and the supernatant was transferred into a QIAprep spin column and centrifuged for 1 minute at 13000 rpm. In addition, 500 μl of buffer PB (precipitation buffer containing guanidine hydrochloride an isopropanol) was added to the column and centrifuged for 1 minute at 13000 rpm. The column was washed with 750 μl of buffer PE (containing 70% (v/v)

ethanol) and centrifuge for 1 minute at 13000 rpm. The supernatant was discarded and the column was centrifuged for additional 1 minute at 13000 rpm. The column was then transferred into a clean 1.5 ml Eppendorf tube and 50 μl of buffer EB (elution buffer) was added to the middle of the column. The column was left for 1 minute before being centrifuge at 13000 rpm for 1 minute to elute the plasmid DNA.

2.5 DNA synthesis by polymerase chain reaction (PCR)

2.5.1 Primer design

Different primer sets were designed to amplify genomic DNA, cDNA, cloned products and vector sequences. Primers were designed either manually and or using the *primer3* programme (http://frodo.wi.mit.edu/cgi-bin/primer3/primer3_www.cgi).

For genomic and cDNA sequence amplification, primers were designed with length that ranged between 21– 25bp and melting temperatures between 60 – 65 ^{0}C. Where possible, a Guanidine and Cytocine nucleotides (GC clamp) was also included at the 3'- OH end to stabilize primer binding. The PCR products ranged in size between 250 – 1200bp for cDNA and genomic sequence.

For amplification of cloning products using conventional cloning, primer length was increased up to 30bp to accommodate tagged restriction sites (that facilitates cloning). For Gateway cloning products, primer lengths were as long as 37bp after addition of the 12bp adapter sites necessary for recombination. The GC clamp was not always included in these primer sets. The PCR products varied between 600bp – 1800bp with optimum melting temperature of 60^{0}C.

Primers were ordered from Sigma Aldrich, and resuspended in appropriate volume of deionised water to achieve a stock concentration of 100μM. A 20 μM and 10 μM working solution were prepared in water and stored at -20^{0}C.

2.5.2 PCR reactions

PCR reagents including Taq-polymerase, 10xNH_4 buffer (160 mM $(NH_4)_2SO_4$, 670 mM Tris-HCI (pH8.8 at 25°C), 0.1% Tween-20) and $MgCl_2$ were obtained from Bioline, whereas dNTP's were supplied from either Bioline or Invitrogen, UK. For amplification of cloning products, proof reading enzymes, KODHiFi (Novagen, UK) and Phusion (Finnzymes) DNA polymerases were used instead.

A 20 μl PCR reaction using Taq-polymerase was set up as follow;

PCR reaction mixture		Final concentration
DNA template	(genomic DNA)	1.0 μl	5 ng
20 μM primers forward		0.5 μl	0.5 μM
20 μM primers reverse		0.5 μl	0.5 μM
2 mM dNTPs		2.0 μl	0.2 mM
10xNH_4 Buffer		2.0 μl	x1
50 mM $MgCl_2$		0.8 μl	2 mM
Taq polymerase 5U/μL		0.2 μl	1U
Deionized water		13μl	

For amplification of cloning sequences by conventional method, PCR reaction was set up and kept on ice at all time;

KODHiFi PCR reaction mixture		Final concentration
Deionized water	17.8 μl	
2mM dNTPs	2.5 μl	0.2 mM
25mM $MgCL_2$	1 μl	1 mM
10xNH_4 Buffer no1	2.5 μl	1x
20pmol/μl forward primer	0.5 μl	0.2 μM
20pmol/μl reverse primer	0.5 μl	0.2 μM

Template DNA	1 μl	10 ng	plasmid
DNA	1 μl	15 ng	genomic DNA
KODHiFi DNA polymerase (2.5U/μL, Novagen)	0.2 μl		0.5U

For Gateway cloning, PCR reaction was set up in two steps as follow;

Phusion PCR reaction mixture		**Final concentration**	
PCR 1:			
Deionized water	14.2 μl		
5x High Fidelity buffer	5.0 μl		x1
10mM dNTPs	0.5 μl		0.2 mM
5mM $MgCL_2$	1 μl		1 mM
5pmol/μl forward primer	1.5 μl		0.3 μM
5pmol/μl reverse primer	1.5 μl		0.3 μM
Template DNA	1 μl	10 ng	plasmid
DNA	1 μl	15 ng	genomic DNA
Phusion DNA polymerase (2.0U/μL, Finnzymes)	0.3μl		0.6U
PCR 2:			
Deionized water	15.4 μl		
5x HF Buffer	10.0 μl		x1
10mM dNTPs	1.0 μl		0.2 mM
5mM $MgCL_2$	2.0 μl		1 mM
5pmol/μl F - attB adapter	8.0 μl		0.3 μM
5pmol/μl R - attB adapter	8.0 μl		0.3 μM
Template DNA	5 μl	Product of PCR1	
Phusion DNA polymerase (2.0U/μL, Finnzymes)	0.6 μl		1.2U

2.5.3 Amplification of DNA

The PCR conditions used varied according to the product size to be amplified, melting temperature of the primers and the type of product. Double stranded DNA was denatured either at 94^0C or 98^0C depending on the type of the template. Annealing temperature was normally set up 5^0C below the melting temperature and where necessary optimum annealing temperature was determined by gradient PCR. Extension time was set up at 72^0C for 30 seconds per 1kb on average. Numbers of cycles were adjusted for cloning products and diagnostic PCR products with minimum number of cycles for amplification of promoters and coding sequences.

Initial denaturation		94°C/98 °C	2 minutes
Thermal cycling			
	Denaturation	94°C/98 °C	15 seconds
	Annealing	50-60°C	30 seconds
	Extension	72°C	30 seconds per kb
	Final extension	72°C	5 minutes

The amplification steps were carried out on a thermal cycler and the DNA was amplified over 40 cycles. The PCR product was analysed by agarose gel electrophoresis.

PCR conditions using KOD HiFi and Phusion

KOD HiFi:

Initial denaturation	94°C/98°C	60 seconds
Denaturation	94°C/98°C	15 seconds
Annealing	50-60°C	30 seconds
Extension	72°C	30 seconds per kb
Final extension	72°C	3 minutes
	Repeat step 2 to 4 x29 (30 cycles total)	

Phusion:

PCR1;

Initial denaturation	98^{o}C	60 seconds
Denaturation	98^{o}C	20 seconds
Annealing	50-60^{0}C	30 seconds
Extension	72^{0}C	30 seconds per kb
Final extension	72^{0}C	5 minutes
	Repeat step 2 to 4 x9 (10 cycles total)	

PCR2;

1.	Initial denaturation	98^{o}C	60 seconds
2.	Denaturation	98^{o}C	20 seconds
3.	Annealing	45^{0}C	30 seconds
4.	Extension	72^{0}C	30 seconds per kb
		Repeat step 2 to 4 x9 (10 cycles total)	
5.	Denaturation	98^{o}C	20 seconds
6.	Annealing	50-60^{0}C	30 seconds
7.	Extension	72^{0}C	30 seconds per kb
		Repeat step 5 to 7 x19 (20 cycles total)	

2.6 Reverse Transcription PCR (RT-PCR)

First strand cDNA was synthesised with a standard amount of total RNA primed with oligo dT primers using Invitrogen First strand cDNA synthesis kit^{R} (Invitrogen, UK). 750ng of RNA isolated from sporophytic tissues (including 8-day old seedlings, root, shoot apex enrinched tissues, rosette leaves, inflorescence stem, flowers with mature pollen, and siliques of mixed age) and 1µg of RNA isolated from the four stages of male germ cell development was used for cDNA synthesis. 1/10th of the RT product was then used together with gene specific primers to determine transcript abundance for the gene of interest by PCR amplification (section 2.5.2).

2.6.1 RT-PCR reaction mixture

The RT-PCR reaction mixture was prepared in a 0.5 ml microfuge tube that was kept on ice, mixed and spun briefly. The presence of the target template was detected by analysing the RT-PCR product using agarose gel electrophoresis (section 2.7)

SuperScript III First-Strand Synthesis System for RT-PCR

1. **Denaturing step**

Mix 1		**Final concentration**
• RNA_{total}	x μl	750ng
• Oligo $(dT)_{20}$ (50 μM)	1 μl	2.5 μM
• dNTP mix (10 mM)	1 μl	0.5 mM
• Nuclease free water	to 10μl final volume	

   - Incubate at 65^0C for 5 minutes in the water bath, then place on ice for at least 1 minute

2. **Annealing step**

Mix 2		**Final concentration**
• 10x RT Buffer	2 μl	x1
• 25mM $MgCl_2$	4 μl	5mM
• 0.1M DTT	2 μl	10 mM
• RNaseOUT (40U/μl)	1 μl	40U

   - Add 9μl of Mix 2 into Mix 1 and incubate at 42^0C for 2 minutes in PCR machine

• SuperScript III RT (200U/μl)	1 μl	200U

3. **cDNA Synthesis**: (Performed in a PCR machine)

	Temperature	**Duration**
• Oligo dT primed	42^0C	50 minutes
• 2^0 RNA Oligo dT primed	50^0C	10 minutes
• Extension	70^0C	15 minutes

4. **Terminate reaction**:

	Temperature	Duration
• Incubate	85^0C	5 minutes

5. **Remove RNA**:
    - Add 1µl of RNase H and incubate at 37^0C for 20 minutes
6. **Store**:
    - Store the cDNA at -20^0C or can be used directly for PCR analysis.

2.7 DNA modification and agarose gel electrophoresis

2.7.1 Digestion of DNA with restriction endonucleases

Unless otherwise stated, restriction digestion of PCR product and plasmid was performed with a choice of enzymes and their appropriate buffer incubated at 37^0C for 1hr30min. For verification of cloned product, a 20µl total reaction was used, whereas for products to be recovered for conventional cloning, the reaction was doubled to 40µl. When more than one restriction enzyme had to be used, appropriate buffer was selected that gave optimal activity for both enzymes according to manufacturers instructions. In a case were the buffer is not appropriate for both enzymes, a single digest was performed and the product was gel purified (section 2.8.1) and used for the second digest. The digest reaction was set up as follow;

DNA	1 µg
10xBuffer	2 µl
Bovine serum albumin (BSA)	0.2 µl
Restriction enzyme (10 U/µl)	0.5 µl
Water (DW)	up to 20 µl

All the reagents used for the DNA digest were purchased from Bioline, UK.

2.7.2 Fractionation of DNA by agarose gel electrophoresis

Identification and purification of different DNA fragments size from PCR products, restriction digest and purified plasmids, was performed by agarose gel electrophoresis. A similar technique was also used for the visualization of extracted total RNA. An agarose gel was made up with 1x Tris-acetate buffer (TAE) supplemented with 0.5µg/ml ethidium bromide. Depending on the size of the DNA fragments, the concentration of agarose gels varied between 1% (w/v) to 2% (w/v) according to Sambrook et.al, (2001). Samples were mixed with gel loading dye (Orange G powder dissolve in 50% glycerol) prior to loading. The loaded gel was placed in the electrophoresis tank and a voltage of 5V/cm was applied to separate the fragments for approximately 30 minutes. The DNA / RNA fragments were visualized under UVP trans-illuminator (BioDoc – It^{TM} System, U.S.A) and the size and quantity of the DNA fragments were determined by comparing with a standard DNA ladder (NEB).

50 X TAE stock

242g Tris-base

57.1ml Glacial acetic acid

100ml of 0.5M EDTA

Made up to 1L volume of water

To make a working solution of 1x TAE, 20% (v/v) of the 50 X TAE stock was used to make 10x TAE. 10% (v/v) of 10x TAE was then used to make a final working solution of 1x TAE.

2.8 Purification of DNA for cloning and sequencing

2.8.1 Purification of DNA fragments from agarose gel

DNA fragments required for sequencing or cloning were purified from agarose gel using QIAquick gel extraction kits (Qiagen, UK) according to the manufacturer's instructions. The DNA fragment was excised from the agarose gel with a clean, sharp scalpel. The gel slice was weighed and three gel volumes (100mg = 100µl) of buffer QG was added. The sample was then incubated at 55^{o}C for 10 minutes with occasional vortexing to dissolve the gel. Once the agarose had dissolved completely, one gel volume of isopropanol was added to the mixture. The mixed sample was then pipetted into QIAquick column and centrifuge for 1 minute at 13000 rpm to bind the DNA. The flow-through was discarded and 500µl aliquot of buffer QG was added to the samples to remove all traces of agarose. The column was centrifuge for 1 minute at 13000 rpm and the flow-through was discarded. To wash the column, 750µl of buffer PE was added to QIAquick column and centrifuged for another minute at 13,000g. After discarding the flow through the QIAquick column was centrifuged for an additional 1 minute at 13,000g to remove any traces of remaining ethanol. The DNA was eluted with 30µl of buffer EB by centrifugation at 13000 rpm for 1 minute. Eluted DNA was stored at -20^{0}C.

2.8.2 PCR purification of DNA

Where primer sets used to amplify DNA fragment for cloning or sequencing showed high specificity (i.e, no non-specific bands being amplified) and the fragment size was larger than 100bp, QIAquick PCR purification kit (Qiagen, UK) was used instead of QIAquick gel extraction kits due to its higher recovery of purified DNA. Following the PCR reaction, five volume of buffer PB was added to the sample and the sample was thoroughly mixed and pipetted to the QIAquick spin column. The column was centrifuged for 1 minute at 13000 rpm and the flow through was discarded. 750µl of buffer PE was added and the column was centrifuged for 1 minute. The flow through was discarded and the column was centrifuged

for an additional 1 minute. 30μl of buffer EB was added to the column, and the DNA was eluted by centrifugation at 13000 rpm for 1 minute. Eluted DNA was quantified by running a $1/10^{th}$ on agarose gel alongside a standard DNA ladder. Quantified product was then used directly for ligation reaction or stored at -20^{0}C.

2.9 Ligation of DNA fragments

2.9.1 Ligation by conventional cloning

DNA fragments to be cloned into vector through ligation of compatible sticky ends were amplified by PCR with primers that incorporate the appropriate restriction sites on the DNA fragment to be cloned. Following the PCR reaction, the PCR product was purified by gel purification (section 2.8.1) or PCR purification method (section 2.8.2) depending on the specificity of the primers. Purified product was the digested with restriction enzymes to generate sticky ends. In some occasions, the digestion product was purified by QIAquick PCR purification kit to remove any remaining protein. Plasmid vector was also treated with the same combination of restriction enzymes and purified by QIAquick gel purification kit. The concentration of insert and the plasmid vector was determined by agarose gel electrophoresis with a standard DNA ladder (NEB). Insert and plasmid vector were recombined in a 10μl ligation reaction with a molar ratio of 3:1 insert to vector. The ligation reaction was incubated overnight at room temperature and 5μl of the reaction was transformed into *E. coli* (DH5α). Colonies were screened by colony PCR using flanking primers at the T-DNA border, and the recombinant plasmid was isolated and diagnosed by restriction digest and sequencing where appropriate. All reagents were purchased from NEB, UK.

Ligation reaction

Insert		xμl
Plasmid vector		xμl
10x T4 ligase buffer		1μl
T4 ligase		1μl
Deionized water		x μl
	Total	10 μl

2.9.2 Cloning by Gateway recombination

For high throughput DNA cloning, a Gateway recombination technology (Invitrogen, UK) was used instead of a traditional conventional cloning. DNA fragments were first amplified by PCR using primer pairs that incorporate the recombination sites (attB1 and attB2) at the 5' and 3'-OH end of the DNA fragment. Depending on the specificity of the primers, the PCR product was then purified either by QIAquick gel extraction kit or QIAquick PCR purification kit (section 2.8). The concentration of purified product together with the vector was determined by agarose gel electrophoresis using a standard DNA ladder. The PCR product was cloned into the expression vector in two subsequent steps.

Step 1: BP reaction

In this initial step, 125ng of the PCR product and 75ng of the donor vector (pDONR201 / pDONR207) were used in a BP recombination reaction to generate an intermediate clone (Entry clone) necessary for the second cloning step. Following overnight incubation at room temperature, the reaction was terminated with 0.5μl of proteinase K enzyme by incubating at 37^0C for 5 minutes. 2.5μl of the total reaction was used for transformation of *E. coli* (DH5α) and the colonies produced were screened by colony PCR using pDONRF/R primer set. Positives colonies were used to setup 5ml overnight culture and the plasmid was isolated

from the bacteria and verified by restriction digest and sequencing before being used for the second step cloning.

BP-reaction (Invitrogen kit)

PCR product	~125ng
pDONOR vector	~75ng
TE buffer	x μl
BP Clonase II	1 μl
	Total 5.0μl

Step 2: LR recombination reaction

Sequence verified entry clones were used to recombine the insert into the destination vector in a LR reaction. Approximately 125ng of the entry clone and 75ng of the desired destination vector was used in a second ligation reaction catalyzed by the enzyme LR clonase. The reaction was incubated overnight at room temperature and then terminated with 0.5μl of proteinase K enzyme by incubating at 37^0C for 5 minutes. 2.5μl of the total reaction was used to transform *E.coli* (DH5α) and the colonies were screened by colony PCR. 5 ml overnight culture was setup for positive colonies and recombinant plasmid was isolated and used for restriction analysis and sequencing where appropriate. Verified expression vectors were then mobilized into *A. tumefaciens* (GV3101) for transformation of Arabidopsis plants.

LR-reaction (Invitrogen kit)

Destination vector	~75ng
pDONOR vector	~125ng
TE buffer	xμl
LR Clonase II	1μl
	Total 5.0μl

2.9.3 Sequencing of PCR product

Purified PCR product or isolated recombinant plasmids were sent to the John Innes Centre Genome lab (JIC, Norwich. UK) for sequence confirmation. 50ng of PCR product or 150ng of plasmid DNA in a total of 20μl was sent for sequencing according to JIC sequencing instructions. Depending on the sequence requirement (max of 500bp per reaction), more than one set of primers at a concentration of 1.5 pmol/μl were sent together with the DNA to provide overlapping sequence information when more the 500bp of DNA fragment was analysed. Sequencing result in ABI format were downloaded from the JIC website (http://jicgenomelab.co.uk/account.html) and analysed with the *MacVector version 9.5.2* sequence analysis program (MacVector, U.S.A). Sequence pattern was confirmed by analysing alongside chromatogram files and the expected wild type sequence.

2.10 Cytological analysis

2.10.1 Visualization of spores nuclei with 4',6-diamidino-2 phenylindole (DAPI)

Pollen nuclear morphology was visualized by staining with 4',6-diamidino-2 phenylindole (DAPI) as described by Park et al., (1998). Mature pollen were collected from 4-5 fully open flowers in an Eppendorf tube containing 300 μl of 10 μg/ml DAPI staining solution (0.1 M sodium phosphate, pH 7; 1 mM EDTA, 0.1% (v/v) Triton X-100, 0.4 mg/ml DAPI; high grade, Sigma). Pollen grains were released into the DAPI solution by brief vortexing and centrifuged for 5 seconds in a picofuge (Stratagene, UK). 3μl of the pollen pellet was transferred to a microscope slide, gently pressed down with a cover slip, sealed with nail varnish to prevent sample from drying, and viewed with a fluorescence microscope (Nikon TE2000-E, Japan). For screening pollen from a large scale population, mature pollen from 1 – 2 single open flowers were collected into a 96–well microtiter plate containing 100 μl of DAPI solution. Pollen grains were released from the flowers by gentle tapping of the microtiter plate and pollen nuclei were visualised under an inverted epifluorescence microscope (Zeiss Axiophot 100).

For analysis of spores at earlier developmental stages, buds were dissected with needles sequentially arranged based on their position on the floral axis with +1 representing a first fully open flower and approximately -12 stage which represent early released microspores (Lalanne and Twell, 2002). Flowers buds were dissected on microscope slide into 5μl of DAPI solution using a dissecting microscope (Zeiss). Anthers were agitated with forceps and dissecting needle to release the spores, coverslip was mounted and gently squashed to flatten the samples, sealed with nail varnish and visualised with the fluorescence microscope.

DAPI staining solution

DAPI (10μg/ml)	8μl
GUS buffer (0.1 M $NaPo_4$ pH 7.0, 0.5 M EDTA, 10% (v/v) Triton)	10 ml

2.10.2 Fluorescein diacetate (FDA) staining for pollen viability

Pollen grain viability was determined cytologically by visualising cellular esterase activity with 0.1mg/ml fluorescein diacetate (FDA) in 0.3M mannitol (Eady et al., 1995). 1-2 open flowers were agitated into 96-well microtiter plate containing 100 μl of freshly made FDA stain. Pollen grains were incubated for 2 minutes at room temperature then examined with Fluorescein isothiocyanate (FITC) filter set on Zeiss Axiovert 100 at low power (x10/x20 objectives) to prevent photobleaching of fluorescein.

FDA stain

0.3 M Mannitol	990 μl
10 mg/ml FDA (in acetone)	10 μl

2.10.3 GUS staining

Transgenic plants carrying constructs that harbouring a GUS marker were analysed by histochemical assay to determine spatial and temporal activity of the β-glucurodinase (GUS) in different plant tissues. Tissues to be analysed, were collected in 96 well plates containing 150 μl of GUS buffer (0.1 M sodium phosphate (pH 7), 10 mM EDTA, 0.1% (v/v) Triton X-100) with 0.5 mM / 1 mM potassium ferricyanide and 1 mM 5-bromo-4-chloro-3-indolyl β-D-glucuronic acid (X-gluc; Biosynth). Materials were then vacuum infiltrated for 10 minutes and sealed with Nescofilm. To visualise GUS staining, plant tissues were incubated in variable length of time (depending on the promoter activity, approximately between 1-3 days) at

37°C, cleared with 70% ethanol, then washed in a series of 50% and 25% ethanol followed by deionized water before being stained for DAPI were necessary. Staining pattern was visualized under Zeiss dissecting microscope and images were captured with Nikon D100 digital camera mounted on Nikon TE 2000 fluorescence microscope.

2.10.4 Fixation of GUS stained tissues

Alternative procedure was applied whereby

tissues to be stained for β-glucurodinase activity were first fixed in a fixative solution to maintain the integrity of the cell and nuclear structure. This was mostly important in visualizing the elongated nucleus of the late bicellular pollen grain. Flower buds were first incubated in 0.37% (v/v) formaldehyde in 100mM sodium phosphate buffer (pH 7.0) for 30 minutes. After fixation, bud clusters were washed with phosphate buffer and incubated in 0.03% (v/v) Triton X-100 with phosphate buffer for 1 hr and then washed again with phosphate buffer. Bud clusters were then stained for GUS as described in section 2.10.4.

Fixative solution

Sodium phosphate buffer (pH 7.0)	100mM
Formaldehyde	0.37%
Triton X-100	0.03%

2.10.5 Capturing images

Images of fluorescent and GUS stained spores throughout pollen development were captured using a low light monochrome ORCA-ER ccd camera (Model C4742-95, Japan) and Nikon D100 colour digital camera (Model MH-18, Japan) mounted on Nikon ECLIPSE (Model TE2000-E, Japan) fluorescent microscope. For fluorescent imaging, Improvision – Openlab 5.0.2 software (Improvision, UK) was used to capture live images, and save the images in

LIFF and TIFF format. Images of GUS stained materials from sporophytic tissues were captured using a 3-CCD colour video camera (JVC, KY-F55B), linked to a Neotech IGPCI capture card and Image Grabber PCI 1.1 software on an Apple Macintosh computer. All images were then processed in Adobe Photoshop CS3 software.

2.10.6 Relative DNA measurements

The relative DNA content of the vegetative cell nucleus from wild type plants and transgenic plants transformed with construct pK7LAT52-hpRBR was measured based on DAPI fluorescence. The microscope was set up and images were captured with the ORCA-ER video camera using the Openlab 5.0.2 software. Fluorescence values were recorded by measuring fluorescence intensity per area with Openlab 5.0.2 software. Since the morphology of the vegetative nucleus is variable, the region of interest (ROI) was defined with a marquee that was unique for each pollen nucleus by outlining the area occupied by the vegetative cell nucleus. The net fluorescence value was obtained by recording the initial reading of the nucleus and subtracting a corresponding background reading from an identical ROI taken from the cytoplasm. The average fluorescence value calculated from the wild type was defined as a 1C DNA content, and this value was used to test if it was statistically significant different from the average fluorescence obtained from the mutant vegetative cell nucleus.

2.10.7 Statistical Analysis

To determine whether the average fluorescence value of the wild type vegetative cell nucleus and the average fluorescence value from the mutant vegetative nucleus were statistically significant different from each other, one-tailed *t-test* (Microsoft Excel software) was used (that DNA content from mutant vegetative cell nucleus is greater than that of wild type vegetative cell nucleus) assuming unequal variance (unequal population size) was applied. The Chi-square (χ^2) test was used to compare observed frequencies to expected

frequencies if null hypothesis (H_0) is true. The closer the observed frequencies are to the expected frequencies, the more likely the H_0 is true.

To test whether the proportion of wild type to mutant is the same (segregating 1:1) in the complemented +/*duo1* individuals, the following hypotheses were set up:

H_0: $f_w - f_m = 0$

H_1: $f_w - f_m = 0$

where f_w and f_m are proportions of wild type and mutant respectively.

The Chi-square test is:

$$chi-squared = \sum_{All} \frac{(f_o - f_e)^2}{f_e}$$ with (r - 1)(c - 1) degrees of freedom where f_e and f_o are the observed and expected frequencies respectively. r is the number of rows and c the number of columns.

2.11 Transformation of *Arabidopsis thaliana*

Arabidopsis plants were transformed by floral dipping and were grown under long day light regime. The primary bolt was clipped when the plants were approximately 2-5 cm tall. After 1 week, the siliques and fully open flowers were removed and the plants were ready for transformation. A single transformed *Agrobacterium* colony was selected and inoculated in 5 ml of LB containing appropriate antibiotic, the cells were allowed to grow overnight at 28^{o}C. A 1ml aliquot of the overnight culture was diluted in 400 ml of fresh LB media and the cells were grown for another 24 hrs in a shaker at 200 rpm at 28^{o}C. The cells were centrifuged at 5000 rpm for 20 minutes and the cells were resuspended in standard infiltration medium.

Infiltration medium

Half strength of MS salts (Sigma, UK)	2.165 g/L
Full strength of Gamborg B5 vitamins (Duchefa, Netherlands)	3.16 g/L
2-[N-Morpholino]ethanesulfonic acid (MES; Sigma, UK)	0.5 g/L
Sucrose (Sigma, UK)	50 g/L
Benzylaminopurine (1mg/ml) (Sigma, UK)	10 μL/L

Just before dipping, 300 μl of silwet L-77 (consist of Polyalkyleneoxide modified heptamethyltrisiloxane and allyloxypolyethyleneglycol methyl ether) was added per litre of culture. The Silwet L-77 improves cuticular penetration of the plant surfaces, hence aid in infiltration of the agrobacterium into the plant tissues. The above ground part of the plant was dipped in *Agrobacterium* solution for 2 minutes with gentle shaking. A transparent plastic propagator lid was kept on the tray of dipped plants to keep the humidity high for one day. The plants were watered after two days.

Chapter 3

Expression and Functional Analysis of B-type cyclins during Male Gametogenesis

3.1 Introduction

To get an insight into how cell cycle progression is regulated in the male gametophyte and which are the major components participating in this process particularly focusing on the G2/M transition and mitotic progression, the expression and functional analysis of B-type cyclins during spermatogenesis was investigated. Results from the analysis of pollen transcriptomic data provide an initial insight into how B-type cyclins are expressed during pollen development. Data from semi-quantitative RT-PCR analysis is discussed with regard to verification of the expression patterns observed from transcriptomic data. Furthermore, analysis of the expression of an existing cell cycle marker, AtCycB1;1 promoter driving expression of translationally fused CycB1;1 destruction box (D-box) and a β-glucuronidase reporter gene (GUS) named pCDG (Colon-Carmona et al., 1999a), is presented to illustrate its expression pattern and relation with a key pollen specific regulator of germ cell division, *AtDUO1*. To verify this relationship independently, complementation of the *duo1* mutant phenotype with AtCycB1;1 was performed. In addition, the fate of the rescued *duo1* mutant pollen grains was analysed and compared with the fate of mutant germ cells in *cdka;1* mutants- another key regulator of cell cycle progression affecting germ cell division.

To investigate the role of B-type cyclins in the control of sperm cell formation, targeted-down regulation of the CycB1 family using pollen cell-specific promoters to drive expression of hairpin dsRNA targeted to the four members of CycB1 family was also performed.

3.2 Expression of AtCycB1 family in the male gametophyte

Genes involved in cell proliferation at different phases of the cell cycle show different patterns of expression. Some genes show strict modulation of transcript abundance at specific stages that are then turned over at other phases of the cell cycle, whereas, other molecules are expressed constitutively throughout the cell cycle. B-type cyclins have been demonstrated to show oscillatory regulation with high transcript abundance at G2 and high

protein activity at the G2/M boundary (Menges and Murray, 2002a; Menges et al., 2005; Planchais et al., 2002b).

In this section, the expression profile of the CycB family members from microspore to mature pollen stages is presented. The analysis involves the use of pollen transcriptomic data, verification of the transcriptomic profiles by RT-PCR, and investigation of pAtCycB1;1-D.Box::GUS (pCDG) promoter activity and localization by histochemical assay during male gametophyte development. To determine the spatial and temporal activity of the pCDG construct, light and epifluorescence microscopy was used.

3.2.1 Expression pattern of CycB1 family from pollen transcriptomic data

Pollen transcriptomic data that is currently available in the public database (http://arabidopsisgfp.ueb.cas.cz) was examined to provide an initial insight into the expression pattern of the CycB1 family members. The array data was sourced from the Arabidopsis Gene Family Profiler database (aGFP;Dupl'akova et al., 2007), and the mean hybridization signals were obtained from normalized ATH1 Affymetrix chip data. Stringent criteria were used to filter the data to limit false positive signals in the analysis. The criteria involved the use of MAS5 instead of MAS4 as a detection call method, whereby a normalized value is given a “Present call” (Blue values) when the transcript detection is reliable on both chips (Figure 3.1A). When a signal is reliable on one chip but marginal or absent on the other, the detection call is classified as “Marginal” (Green values). A marginal signal on one chip that is absent on the other chip or a signal that is absent on both chips is classified as “Absent” (Grey values).

Analysis of the microarray data showed that the CycB1 family members have different expression patterns during male gametophyte development. AtCycB1;2 was excluded from the analysis as it is not represented on the ATH1 chip. AtCycB1;1 showed a trend common to many pollen expressed genes, with a high expression at the early stages of germline

development and repression at later stages (Honys and Twell, 2004). Maximum transcript levels were detected at the microspore stage, which was then reduced at the bicellular stage and totally absent at tricellular and mature pollen (Figure 3.1). AtCycB1;3 showed a different profile compared to that of CycB1;1, with higher expression at the microspore stage, reduced expression at bicellular and tricellular stages, and an increased transcript abundance at the mature pollen stage. However, the overall expression was not very different between stages. AtCycB1;4 showed a maximum signal at the microspores with an approximately two fold reduction at the bicellular stage, and minimal expression at the tricellular and mature pollen stage. The profiles revealed by the microarray data indicate that several CycB1 members could be good candidates as regulators of cellular proliferation during germ cell division.

A

Transcriptomic profile of the AtCycB family during male gametogenesis

AGI number	Gene name	UNM	BCP	TCP	MPG
At4g37490	AtCycB1;1	870.84	540.24	171	163
At5g06150	AtCycB1;2	-	-	-	-
At3g11520	AtCycB1;3	591.69	488	453	542.79
At2g26760	AtCycB1;4	784.55	464.67	231	233
At2g17620	AtCycB2;1	208	205	329	340
At4g35620	AtCycB2;2	248	247	339.06	453.23
At1g20610	AtCycB2;3	-	-	-	-
At1g76310	AtCycB2;4	475.36	403.73	548.5	410
At1g16330	AtCycB3;1	589.01	424.09	525.27	767.5

B

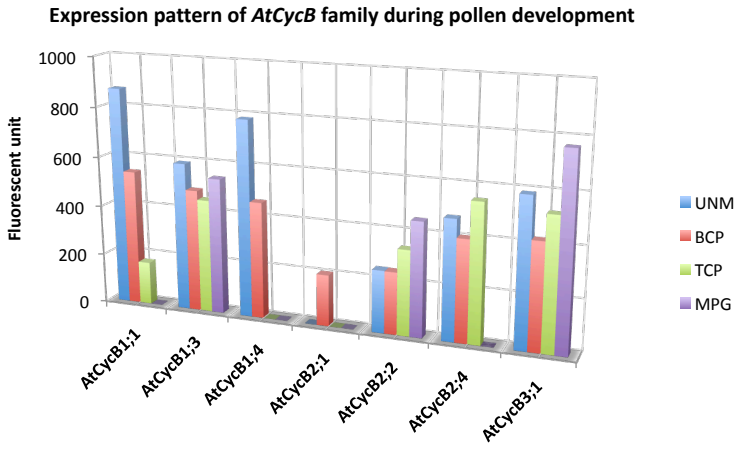

Figure 3.1. (A) Expression of CycB family during male gametophyte development predicted by microarray data. Mean hybridization signals were obtained from the aGFP database that contains normalized ATH1 affymetrix chip data (Duplakova et al., 2007). Mean values are colour coded according to detection call, blue = present call, green = marginal call and Grey = absent call. Detection calls were determined using MAS5 algorithm. The criteria used was, a present call (represent reliable detection on both chips), Marginal call (represent reliable signal on one chip and a marginal signal on the second chip), and an absent call (represent a marginal call in at least one of the chip or absent in one or both chips). UNM, unicellular microspore, BCP, bicellular pollen, TCP immature tricellular pollen, MPG, mature tricellular pollen. No data for AtCycB1;2 and AtCycB2;3 that have no corresponding probe sets on the ATH1 array. (B) Graphical presentation of CycB family expression profile at the four stages of pollen development. All absent call values were converted to zero.

3.2.2 Verification of expression of CycB1 members by RT-PCR analysis

Initial analysis of pollen transcriptomic data provided an insight into the predicted expression profiles of the CycB1 family with the exception of CycB1;2. To verify these expression profiles and to establish the expression pattern of CycB1;2, total RNA isolated from the four stages of pollen development was analysed by RT-PCR. cDNA was synthesised from 750ng of total RNA as described in chapter 2 (section 2.6). To examine the transcript abundance of the four members of CycB1 family, a 1/10 dilution of the synthesised cDNA was used with gene specific primers and the transcripts were amplified for 30 cycles.

Following RT-PCR analysis, CycB1;1 showed the same pattern as that observed in microarray data, with the highest transcript abundance in microspores that declines thereafter (Figure 3.2). CycB1;2 showed a steady decline in RNA accumulation throughout the first three stages of pollen development but interestingly showed an increase at mature pollen stage. A conflicting pattern with the microarray predicted pattern was observed for CycB1;3 in which maximum transcript abundance was observed at the microspore stage, which then drastically declined through bicellular and tricellular stages before disappearing completely in mature pollen. AtCycB1;4 showed a slightly different pattern from that revealed by the microarray data. RT-PCR revealed a strong signal at the microspore stage but the signal was slightly lower at the bicellular stage. Significant reduction of the RT-PCR signal at the tricellular and mature pollen stages was in agreement with the prediction by the transcriptomic data.

Examination of transcript abundance by RT-PCR has verified some patterns predicted from the microarray data and also revealed the new profile for CycB1;2 that was not known before. Where the conflict was observed between the two methods, it demonstrates the

importance of independently verifying the microarray data, and RT-PCR should be a decisive method when the there is discrepancy.

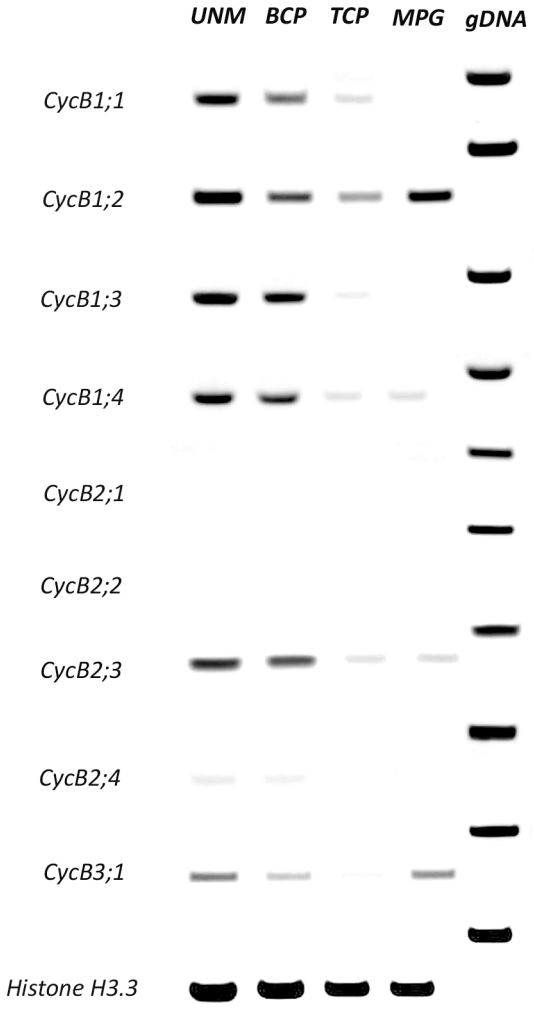

Figure 3.2. RT-PCR analysis of AtCycB family members during male gametophyte development.
Relative transcript abundance in uninucleate microspores (UNM), bicellular pollen (BCP), tricellular pollen (TCP) and mature pollen grains (MPG). Total RNA was isolated from the four pollen stages and 750ng of the RNA was converted to cDNAand used for the PCR reaction. For each gene, 30 cycles of PCR was performed in a three independent repeats. Histone H3.3 variant (At4g40040) was used as a positive control and primer efficiency was estimated from the genomic DNA template control. Comparison of transcript abundance can be made between stages for the same gene but not between genes, as primer efficiency between genes is not comparable.

3.2.3 Analysis of AtCycB1;1-D.Box::GUS (pCDG) during male gametophyte development

The expression pattern of the CycB1 family members revealed by the microarray data and RT-PCR analysis demonstrated the general expression pattern but did not provide an insight into the relative contributions of the vegetative and generative cell to the overall hybridization or amplification signal.

To understand the dynamics and spatial expression of CycB1;1, pCDG construct was exploited to examine how CycB1;1 promoter activity proceeded during pollen development. The vector contain a fusion of 1148 bp of putative CycB1;1 promoter and a coding sequence up to 116 amino acids, including a mitotic destruction box motif (D-box) and the coding region of the GUS marker (Figure 3.3A). The presence of the D-box ensures turnover of the CycB1;1::GUS fusion protein following exit from the cell cycle, hence the construct can be used to accurately report cells that are progressing through G2/M or exiting mitosis as well as reporting the kinetics of CycB1;1 expression during cell division.

Whole inflorescences from plants homozygous for the pCDG construct were stained for GUS activity. Inflorescence were incubated at the optimum concentration of 3mM X-gluc (5-bromo-4-chloro-3-indolyl-beta-D-glucuronic acid) with 0.5mM potassium ferricyanide ($K_2Fe(CN)_6$) in GUS buffer, then incubated for 36 hours at 37^0C. For more details of the procedure, see Chapter 2 (Section 2.10.4).

Analysis of the expression pattern was initially examined in the whole inflorescences. Strikingly, wild type inflorescences showed a very strong GUS activity in younger anthers containing spores of which the majority were at the unicellular microspore stage. The GUS staining was reduced dramatically in the proceeding anthers and was completely undetectable in older anthers (Figure 3.3B). To determine exactly where the GUS staining was localized within the pollen grains, anthers were dissected to release the spores from

anthers into a DAPI solution and then mounted with a cover slip and visualized under epiflouresence microscope.

A gradual increase of GUS activity was visualized in non-polarized microspores with maximum GUS activity observed in polarised microspores at late-prophase or metaphase (Figure 3.3C-I). The GUS staining was gradually reduced following completion of PMI and was absent by mid-bicellular stage in both cell types (Figure 3.3J-O). GUS activity then re-appeared prior to PMII and was localized specifically in the germ cell and not in the vegetative cell (Figure 3.3P). This GUS activity was then abolished following division of the germ cell into twin sperm cells at PMII (Figure 3.3Q).

Utilization of the labile pCDG construct has provided the first demonstration of the dynamic expression profile of AtCycB1;1 in vivo during male gametophyte development. Moreover, turnover of CycB1;1::GUS through the cell cycle has also provided indirect evidence for the APC activity in the male germ line. These results demonstrate key differences in division competence between the vegetative and generative cell.

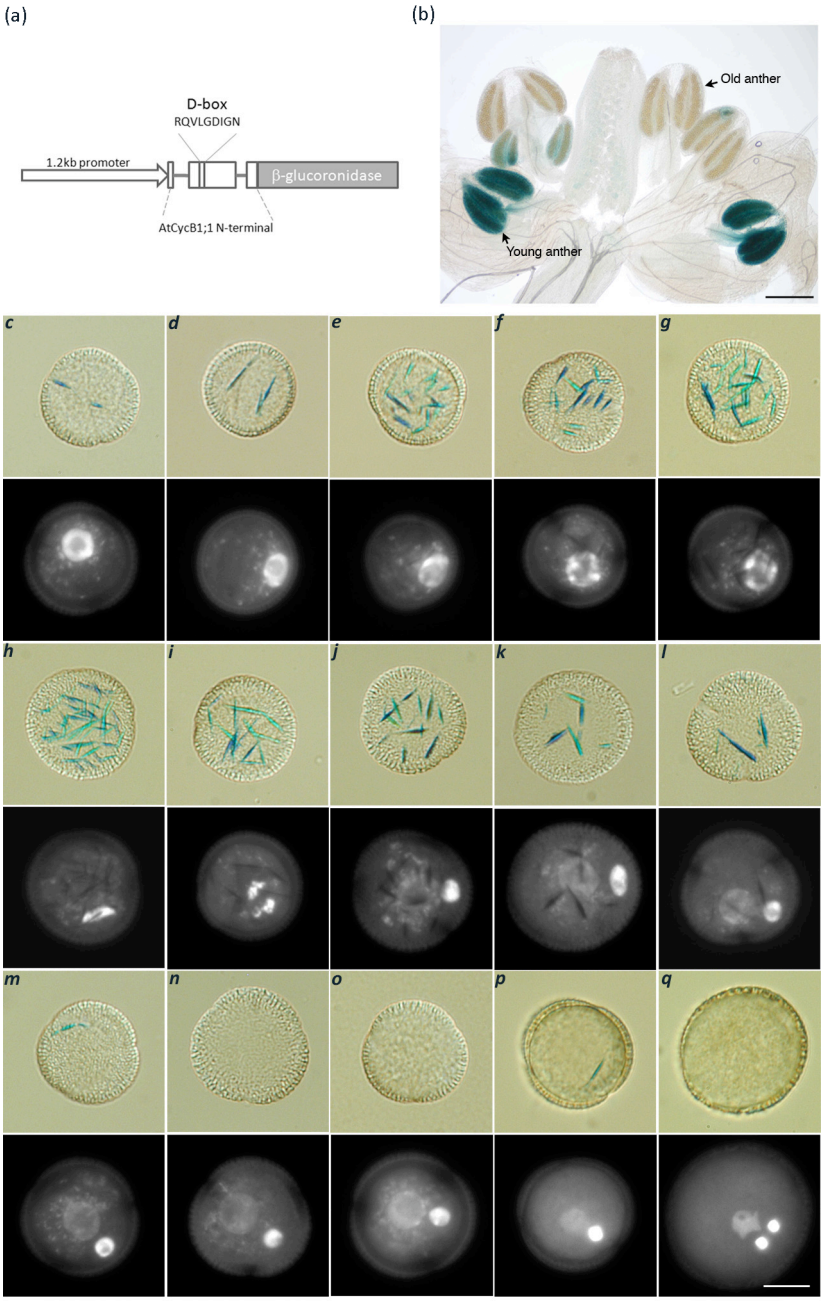

Figure 3.3. Dynamic expression of AtCycB1;1-D.box::GUS during sperm cell formation
(a) Schematic presentation of the pCDG construct showing *CycB1;1* promoter fused to a mitotic destruction box motif (D-box) and beta-glucuronidase marker (b) In situ GUS staining of an early flower bud from wild type plants carrying the pCDG construct showing strong AtCycB1;1::GUS activity in two young lateral anthers containing mostly late microspores, and weak or absent staining in older anthers containing bicellular pollen. Scale bar = 60 µm. (c-q) Brightfield images (upper panel) and corresponding DAPI images (lower panel) from dissected anthers show dynamic accumulation of GUS staining reflecting the pCDG activity during male gametophyte development; (c-i) microspore progression during the cell cycle up to late anaphase of pollen mitosis I (i) showing GUS micro crystals in the cytoplasm, (j-p) inherited GUS staining post PMI at early bicellular stage (j) showing beginning of protein turnover (k,l,m) indicated by reduced number of GUS micro crystals before disappearing completely at mid-bicellular stage (n,o), (p-q) newly GUS stained AtCycB1;1-D.box::GUS activity at late bicellular stage is confined to the germ cell and excluded from the vegetative cell as observed in five independent F2 individuals (p) before the second turnover post PMII at tricellular stage (q). Scale bar=10 µm

3.2.4 A novel Myb protein DUO1 is a regulator of AtCycB1;1 germ cell specific expression

The dynamic expression of cell cycle specific genes is achieved through transcriptional regulation and protein turnover predominantly through ubiquitin mediated proteolysis. Studies in humans, yeast and tobacco have illustrated that control of G2/M specific expression is mediated by the presence of MSA elements and enhancer GCCCR motifs present in proximal promoter region. Furthermore, it is now known that the MSA elements are the target binding sites for R3MYB containing proteins. However, plants also contain a specific class of MYB containing proteins that posses only two repeats (R2R3) which might also be essential for providing the G2/M specific expression. DUO1 protein has been one of the strong candidates for this role due to the fact that it is an essential regulator of G2/M transition in male germ cells and also possess R2R3 MYB repeats (Durbarry et al., 2005; Rotman et al., 2005). Secondly, the expression pattern of *DUO1* places it upstream of *CycB1;1* having a detectable expression at the early bicellular stage and increased expression thereafter (Rotman et al., 2005). Thus, in an effort to understand what provides phase specific expression of *CycB1;1* in the germ cell, it was prudent to test the relationship between *DUO1* expression and the expression of *CycB1;1*. In this way, one can understand how the modulation of *CycB1;1* activity is achieved during pollen development and simultaneously demonstrate if *CycB1;1* is the missing or one of the missing factors that causes the G2/M arrest of the germ cell nucleus in mutant *duo1* pollen grains.

To achieve this objective, plants homozygous for the pCDG construct were used as a pollen donor to introduce pCDG into +/*duo1* plants. Approximately 39 F1 individuals were generated and analysed for GUS activity as described in chapter 2 section (2.10.4). Analysis of the F1 wild type and +/*duo1* segregants indicated reduced CycB1;1::GUS expression in +/*duo1* background. Detailed analysis of individuals carrying the pCDG construct was carried out in the F2 generation. GUS staining in wild type inflorescences showed the normal

predicted pattern as described in Chapter 3 (section 3.2.3). To simplify the analysis, heterozygous +/*duo1* individuals homozygous for the pCDG construct where used for counting the proportion of pollen grains that showed GUS staining. Examination of the whole inflorescence did not reveal a clear difference between wild type and +/*duo1* plants. Stained inflorescences were dissected to score the percentage of unicellular microspores, vegetative cells and germ cells that are positive for GUS staining. Approximately 100% GUS staining was observed in unicellular microspores from wild type plants and plants heterozygous for *duo1* prior to pollen mitosis I (Figure 3.4). The GUS staining persists to early bicellular stage in both cells before it was turned over completely at mid bicellular stage. Until mid-bicellular stage, there were still no differences between wild type and +/*duo1* pCDG staining patterns. Pre-mitotic activity of the pCDG construct specifically in the germ cell was observed in approximately 100% of late bicellular pollen grains from wild type plants. However, this proportion was reduced to approximately half of the pollen population at early tricellular stage in pollen grains derived from +/*duo1* plants (Figure 3.4). These results were consistent in five independent F2 individuals. Subsequently, very weak or no GUS staining was observed following completion of pollen mitosis II in wild type tricellular pollen grains.

Strikingly, this experiment has demonstrated that *DUO1* (MYBR2R3) is an essential regulator of the G2/M specific expression of *CycB1;1* in the germ cell prior to division into twin sperm cells. Does *DUO1* recognise and bind directly to the MSA elements to regulate CycB1;1 germ cell specific expression? It remains to be established whether DUO1 acts directly on the CycB1;1 promoter or through an intermediate regulatory network.

(A) **Raw counts of the pCDG activity in wt and +/*duo1* during male gametophyte development**

Developmental stage	Staining	Counts of two wild type		duo1-1		duo1-2		duo1-3	
		counts	% gus stain	counts	% gus stain	counts	% gus stain	counts	% gus stain
UNM	+GUS	211	100%	416	98%	177	100%	358	100%
	-GUS	0		9		0		0	
		na		na		na		na	
EBCP	+GUS (VC)	158		101		202		229	
	+GUS (GC)	97	99%	60	100%	119	92%	168	100%
	-GUS	2		0		29		0	
MBCP	+GUS (VC)	164		66		113		39	
	+GUS (GC)	31	25%	13	28%	35	33%	9	25%
	-GUS	593		200		304		141	
LBCP	+GUS (VC)	17		21		17		4	
	+GUS (GC)	401	47%	67	19%	200	47%	139	56%
	-GUS	452		387		268		113	
TCP	+GUS (VC)	0		0		0		0	
	+GUS (GC)	569	92%	516	49%	248	41%	284	56%
	-GUS	51		534		354		222	
MPG	+GUS (VC)	0		0		0		0	
	+GUS (GC)	22	4%	0	0%	34	7%	448	0%
	-GUS	552		160		449		0	

(B)

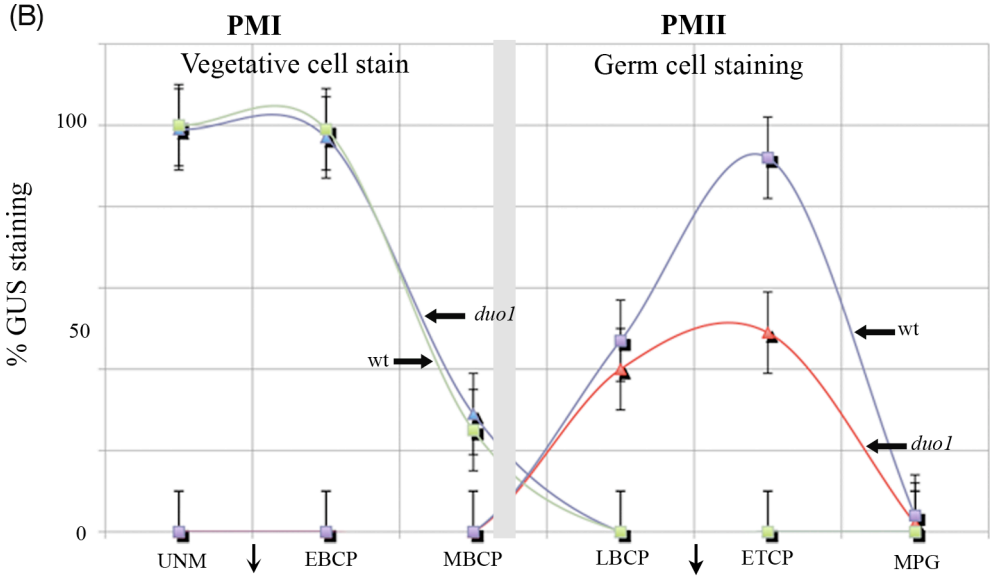

Figure 3.4. **Analysis of AtCycB1;1D.box::GUS activity in heterozygous duo1 plants**
(A) Table of raw data from the F2 population showing counts of two pooled homozygous wild type individuals and three independent heterozygous *duo1* plants. (B) Graph of average frequency of pollen grains that posses GUS activity in heterozygous *duo1* plants homozygous for the pCDG construct. The frequency of AtCycB1;1D.boxGUS activity at the microspore stage is similar in wild type and heterozygous *duo1* (data derived from three independent F2 siblings, n=7253). Whereas wild type show normal pCDG activity in the germ cell at early tricellular stage, the frequency of pCDG activity in the germ cell is reduced by approximately half in heterozygous *duo1* plants, corresponding to the proportion of mutant pollen grains. UNM;microspore, EBCP; early bicellular, MBCP;midbicellular stage, LBCP; late bicellular, ETCP; early tricellular, MPG; mature pollen.

3.3 Complementation of the *duo1* mutation by AtCycB1;1

The discovery of DUO1 as an essential regulator of CycB1;1 germ cell specific expression was a significant advance in dissecting the cascade of the cell cycle machinery involved in the control of male gametophyte development. The failure of +/*duo1* germ cells to progress through G2/M suggests a loss of essential molecules required to allow G2/M progression. To investigate whether CycB1;1 alone was sufficient to rescue the germ cell mitotic defect in +/*duo1* plants, 1.2 kb of the *DUO1* promoter was used to drive expression of a full length coding sequence of AtCycB1;1 in heterozygous +/*duo1* mutant plants.

In this section, the method used to generate the rescuing construct and the use of statistical analysis to determine efficiency rescue of +/*duo1* mutant phenotype is presented. The section also demonstrates the rescue of the +/*duo1* phenotype by AtCycB1;1 to be a dose dependent phenomenon. Further data are presented demonstrating that the rescue of the *duo1* germ cell division phenotype alone is not sufficient to generate competent twin sperm cells.

3.3.1 Generation of the rescuing constructs

Since the endogenous CycB1;1 promoter was under the control of DUO1 itself (Chapter 3, section 3.2.4), pollen cell-specific molecular vectors were explored to select an appropriate promoter to drive the expression of *AtCycB1;1* CDS in heterozygous +/*duo1* plants. A Gateway expression vector driven by 1.2 kb *DUO1* promoter was selected. The *DUO1* promoter is ideal due to its early bicellular germ cell specific expression which should allow enough time for the accumulation of *CycB1;1* transcripts prior to pollen mitosis II. A full length *CycB1;1* CDS (1283 bp) was amplified from cDNA using a thermally stable DNA polymerase with 3'-5' exonuclease activity in a two step Gateway PCR reactions as described in Chapter 2, (section 2.5.3). The amplified fragment was PCR purified and cloned into the

Gateway expression vectors in BP and LR gateway recombination reactions (Chapter 2, section 2.9.3) to generate the construct pBDUO1-AtCycB1;1. The verified construct (Figure 3.5A) was mobilized into *Agrobacterium* (GV3101) and introduced into heterozygous +/*duo1* plants through floral dipping.

3.3.2 *CycB1;1* is able to partially complement the germ cell division defect in *duo1* pollen

Seeds from pBDUO1-AtCycB1;1 transformed plants where sown on soil hydrated with 30 mg/L Basta to select resistance individuals. 112 primary transformants were generated of which 54 contain the heterozygous +/*duo1* mutation. DAPI stained mature pollen grains were counted for the segregation of bicellular and tricellular pollen phenotype by fluorescence microscopy.

The transformed plants where screened in three different sets with an interval of one month between each set. In a non-complemented state, the proportion of wild type : *duo* mutant pollen grains in +/*duo1* plants exert a ratio of 1:1. Whereas, in a fully complemented plants, the proportion of wild type : *duo* mutant pollen grains should revert from 1:1 to 3:1 ratio for an unlinked insertion. Counts of the wild type segregants harbouring the pBDUO1-AtCycB1;1 construct showed no deviation from the wild type phenotype, suggesting the introduced construct has no effect on wild type pollen grains (Figure 3.5). Counts of the first set of transformed +/*duo1* plants revealed 12/18 of the T1 individuals showed a significant reduction of the proportion of *duo1* mutant pollen grains. One particular individual (Line E3), showed a substantial reduction of the proportion of *duo1* mutant pollen grains from the expected 50% to 11% of *duo1* pollen grains (4.5:1 ratio of wild type : *duo1* pollen). Screening of the second set of transformed +/*duo1* plants again revealed 13/17 of heterozygous +/*duo1* plants with a significant *duo1* reduction, whereas, the third set produced 9/17 individuals with a reduced proportion of *duo1* mutant pollen grains with two lines showing

13% and 19% *duo1* mutant pollen grains. In summary, 34/52 representing (65%) of the primary transformants showed a significant reduction of the proportion of *duo1* mutant pollen grains at the mature pollen stage.

To verify statistically if the complemented +/*duo1* individuals showed a significant reduction of the *duo1* mutant pollen grains, thus deviating from the 1:1 segregation, a Chi-square test with a two-way contingency table and Yates correction at 0.5% level of significance was performed (http://statpages.org/#Comparisons). Chi-squared tests verified that 12/18 individuals from set one, 13/17 individuals from set two, and 9/17 individuals from set three, contained a ratio of WT:*duo* pollen population that were significantly different from the expected ratio of 1:1 of untransformed +/*duo1* plants at the 5% confidence level (Table 3.1). The E3 individual from set one and the two individuals from set three that showed the extremely significant reduction of the +/*duo1* phenotype, are proposed to possess more than one effective loci of the rescuing construct. To investigate whether the rescued mutant pollen grains were capable of transmitting the *duo1* mutant phenotype through the male, segregation seeds from selfed individuals was analysed and male transmission crosses where performed. Evidence from segregation analysis of four independent lines showed that the rescuing construct is transmitted normally through the male and the females with a 3:1 segregation ratio of resistance and sensitive plants (Table 3.2). However, only half of the population generated from all four lines possess a +/*duo1* phenotype (1:1 wild type : +/*duo1* plants). These results suggest that the rescued *duo1* pollen grains were not competent for fertilization and hence could not transmit the *duo1* phenotype through the male. Furthermore, the segregation data was further supported when pollen grains from the rescued heterozygous +/*duo1* plants were used as a pollen donor to cross to a wild type females. Only 50% of the F1 offspring were identified to contain the rescuing construct but none showed the *duo1* phenotype. These data suggest rescue of the division phenotype by DUO1-CycB1;1 but not differentiation into competent sperm cells.

To demonstrate whether the temporal and spatial expression of the rescuing construct was necessary for the complementation of the *duo1* phenotype, a control construct (pHLAT52-AtCycB1;1) was introduced into the +/*duo1* background whereby CycB1;1 was expressed in the vegetative cell instead of the germ cell. From the 39 primary transformants that were generated, none of the *duo1* individuals showed a significant reduction of the *duo1* phenotype, demonstrating the importance of correct spatial expression of CycB1;1 in the germ cell (Figure 3.5).

pBDUO1-CycB1;1 1st screen

		Pollen phenotype			
Line	Genotype	wt	duo	% *duo*	X^2 test
A5	+/+	262	2	1%	ns
B8	+/+	201	0	0%	ns
E2	+/+	215	1	1%	ns
A2	+/duo1	653	416	39%	***
A4	+/duo1	197	136	41%	**
A6	+/duo1	90	77	46%	ns
B3	+/duo1	652	405	38%	***
B4	+/duo1	142	88	38%	**
B5	+/duo1	204	148	42%	*
B7	+/duo1	207	145	41%	**
C4	+/duo1	237	171	42%	**
C5	+/duo1	223	159	42%	**
C8	+/duo1	192	158	45%	ns
D3	+/duo1	182	154	46%	ns
D5	+/duo1	252	184	44%	**
D6	+/duo1	1412	973	41%	***
D7	+/duo1	142	130	48%	ns
D8	+/duo1	212	180	45%	ns
E3	+/duo1	869	106	11%	***
E4	+/duo1	733	379	34%	***
E6	+/duo1	121	100	45%	ns
					12/18

pBDUO1-CycB1;1 2nd screen

		Pollen phenotype			
Line	Genotype	wt	duo	% duo	X^2 test
A3	+/duo1	221	118	35%	***
B1	+/duo1	326	197	38%	***
B2	+/duo1	213	138	39%	***
B3	+/duo1	241	164	40%	***
B4	+/duo1	275	169	38%	***
B5	+/duo1	210	113	35%	***
C2	+/duo1	224	165	42%	*
C3	+/duo1	348	192	36%	***
C6	+/duo1	293	147	33%	***
C7	+/duo1	271	140	34%	***
D2	+/duo1	222	191	46%	ns
D7	+/duo1	234	190	45%	ns
E2	+/duo1	224	133	37%	***
E3	+/duo1	207	197	49%	ns
E5	+/duo1	262	199	43%	*
E6	+/duo1	230	195	46%	ns
E7	+/duo1	257	194	43%	*
					13/17

pBDUO1-CycB1;1 3rd screen

		Pollen phenotype			
Line	Genotype	wt	duo	% duo	X^2 test
A3	+/duo1	204	179	47%	ns
A4	+/duo1	246	186	43%	*
A5	+/duo1	206	188	48%	ns
A7	+/duo1	200	176	47%	ns
A8	+/duo1	407	62	13%	***
B2	+/duo1	206	232	53%	ns
B3	+/duo1	245	171	41%	*
C2	+/duo1	219	209	49%	ns
C4	+/duo1	253	169	40%	***
C5	+/duo1	220	211	49%	ns
C6	+/duo1	409	96	19%	***
C7	+/duo1	205	204	50%	ns
D2	+/duo1	238	168	41%	*
D3	+/duo1	202	205	50%	ns
D5	+/duo1	237	178	43%	*
D7	+/duo1	246	185	43%	*
E2	+/duo1	223	142	39%	***
					9/17

pHLAT52-CycB1;1 (control)

		Pollen phenotype			
Line	Genotype	wt	duo	% duo	X^2 test
A2	+/duo1	276	264	49%	ns
A3	+/duo1	280	256	48%	ns
A6	+/duo1	320	308	49%	ns
A7	+/duo1	180	195	52%	ns
A8	+/duo1	214	172	45%	ns
B5	+/duo1	141	136	49%	ns
B7	+/duo1	240	236	50%	ns
C4	+/duo1	217	209	49%	ns
C7	+/duo1	211	215	50%	ns
C8	+/duo1	255	207	45%	ns
D5	+/duo1	212	210	50%	ns
D6	+/duo1	215	190	47%	ns
D8	+/duo1	221	229	51%	ns
E2	+/duo1	221	233	51%	ns
E3	+/duo1	227	214	49%	ns
E7	+/duo1	205	191	48%	ns
					0/16

Table 3.1: ***Counts of the % duo1 pollen grains from +/duo1 lines complemented with AtCycB1;1***.
Table shows counts obtained from DAPI stained spores of T1 +/duo1 complemented lines with AtCycB1;1 and control individuals transformed with LAT52-AtCycB1;1 construct. Following selection of primary transformants, individuals were screened for the presence of duo1 phenotype by DAPI stain using fluorescence microscope. Spores from each identified +/duo1 individuals and from the control lines were counted to analyse the percent proportion of duo1 mutant spores. Each count was then analysed by Chi-square test ($p < 0.05$) to determine if the ratio of wild type versus duo1 mutant spores is significantly different from the expected 1:1 ratio, hence complementation. Single asterisk (*) represent individuals which are statistically significant different from a 1:1 ratio with $p<0.05$, two asterisks (**) for $p<0.01$, three asterisks (***) for $p<0.001$, and (ns) for individuals who are not statistically significant different from 1:1 ratio. Bold figures at the bottom of Chi-square test column represent proportion of rescued individuals over the total population generated

Female	Male	F1 phenotype		TE^{male}	pptR:pptS	Ratio
		WT	+/*duo1*			
+/*duo1*	+/*duo1**	1912	1819	na	na	na
+/*duo1DC*[a]	+/*duo1DC*[a]	12	12	na	151:44	3:1
+/*duo1DC*[b]	+/*duo1DC*[b]	14	10	na	241:82	3:1
+/+	+/*duo1**	530	0	0	na	na
+/+	+/*duo1DC*[a]	34	0	0	16:18	1:1
+/+	+/*duo1DC*[b]	77	0	0	37:40	1:1

Table 3.2: Transmission of the *duo1* allele after introduction of DUO1-AtCycB1:1. When *duo1* heterozygotes are selfed the F1 progeny display a 1:1 ratio of WT to *duo1* plants. A similar ratio is observed when *duo1* heterozygotes partially complemented by DUO1-AtCycB1;1 (+/*duo1DC*) are selfed. The *duo1* allele is not transmitted through the male in either heterozygous *duo1* or *duo1* -complemented plants (+/*duo1DC*). The DUO1-AtCycB1;1 transgene (pptR) is transmitted as a single locus in selfed individuals and normally through the male when crossed to wild type female. TE^{male} represents the transmission efficiency of *duo1* through pollen calculated as; (mutant/ wild type X 100), na = not applicable. ^a,b data from two independent lines. * data taken from Durbarry et.al, 2005.

3.3.3 Rescue of *duo1* by AtCycB1;1 might be dosage dependent

When the pBDUO1-CycB1;1 construct was introduced into heterozygous +/*duo1* plants, none of the primary transformants generated showed the expected reversion from 1:1 to 3:1 wild type : *duo1* for an unlinked insertion. Instead, individuals showed a reduction of percent *duo1* mutant pollen from 50% to 33% with the exception of three lines that showed 11%, 13% and 19% *duo1* mutant pollen. These results indicate a partial rescue of the *duo1* phenotype by *AtCycB1;1*. Moreover, detailed analysis of the pollen population from the rescued individuals showed a proportion of spores (~10% - 15%) in which the generative cell nucleus exhibited a pre-prophase-to-late prophase arrest phenotype that is different with the G2/M arrest phenotype observed in untransformed heterozygous +/*duo1* individuals (Figure 3.5). Both, the partial rescue and the change in generative cell nuclear morphology phenotype provide a hint that the complementation of the *duo1* phenotype by *AtCyB1;1* may be dose dependent and CycB1;1 might be acting as a rate limiting factor. However, more experiments are needed to verify this hypothesis. Other possibilities that could explain the lack of full complementation are possibly the different strength of the *DUO1* promoter compared to the native CycB1;1 promoter and the lack of other factors that are also required for the G2/M transition.

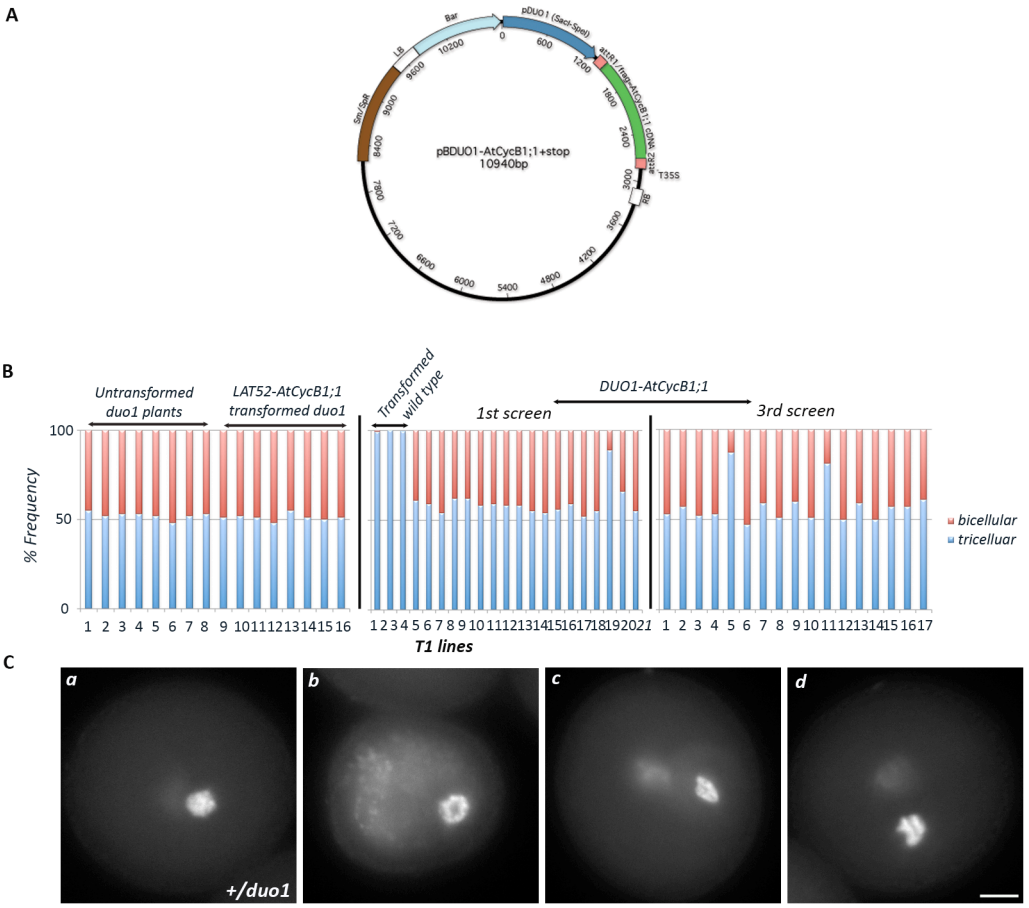

Figure 3.5. ***Rescue of duo1 germ cell phenotype by AtCycB1;1***
(A) Sequence map of heterozygous *duo1* rescuing construct showing 1.2kb *DUO1* promoter fused to a full length *AtCycB1;1* CDS. (B) Counts of three separate populations of untransformed heterozygous *duo1* plants (control) and the T1 individuals transformed with the rescuing construct (DUO1-AtCycB1;1) or rescuing control construct (LAT52-AtCycB1;1). Graph showing the frequency of tricellular and bicellular pollen grains. Note; maximum wild type frequency expected in untransformed or transformed control individuals is 50%. (C) Comparison of DAPI stain *duo1* mutant pollen grains at mature pollen stage (a) with those from individuals carrying the rescuing construct (b-d). A more condensed chromatin and change in nuclear morphology resembling that of late prophase was observed at a higher frequency in populations of rescued individuals compared to untransformed +/*duo1* plants. Scale bars 4 μm.

3.4 Germ cell fate specification in complemented individuals

In an effort to demonstrate the fate of the rescued *duo1* mutant pollen grains, the expression of germ cell differentiation markers were investigated. Three markers define the fate of the sperm cells including a sperm cell surface protein required for fertilization (GCS1/HAP2;Mori et al., 2006; von Besser et al., 2006) and a histone H3.3 variant (MGH3;Okada et al., 2005) that is specific to the germ cells were introduced into the complemented individuals. A vegetative expression marker (LAT52-H2B::RFP) was also introduced as a control. Moreover, to compare the fate of another cell division mutant alongside the rescued *duo1* mutant pollen grains, the germ cell division mutant (+/*cdka;1*) in which a single sperm cell is produced as a result of CDKA;1 depletion was investigated. In heterozygous *cdka;1* mutant background, the germ cell fails to proliferate and produces a single sperm-like cell that is fertile and is able to preferentially fertilize an egg cell and initiate embryogenesis (Nowack et al., 2006; Iwakawa et al., 2006b). These findings suggest that despite the failure of the generative cell to divide into two sperm cells, the single sperm-like cell acquires sperm cell fate. In comparison, the single sperm-like cell produced in heterozygous *duo1* mutant plants does not attain a sperm cell fate and fails to fuse with either egg cell or central cell (Brownfield et al., 2009). Furthermore, it has been demonstrated that *DUO1* is required for germ cell specific expression of AtCycB1;1, and a full length AtCycB1;1 is able to partially rescue a *duo1* division phenotype (Chapter 3 section 3.2.4 and 3.4.2). Therefore, CDKA;1 plays an essential role in germ cell division but it is uncoupled from the germ cell differentiation pathway.

To verify the speculation that a single sperm-like cell produced in heterozygous *cdka;1* mutant plants is a fully differentiated sperm cell, expression of germ cell specific markers, *GCS1*, *MGH3*, *DUO1*, and Generative cell Expressed 2 (*GEX2*), a sperm cell membrane associated protein (Engel et al., 2005), were also investigated to establish their expression

pattern in the mutant *cdka;1* pollen grains. Here results of the expression profile of germ cell specific markers in *duo1* rescued individuals and in *cdka;1* mutant pollen is presented.

In wild type background, all markers are detected in the germ cell from detached-early bicellular stage, accumulate in the germ cell thereafter, and persist to mature pollen stage (Brownfield et al., 2009). Analysis of F2 individuals from the rescued +/*duo1* plants homozygous for the marker genes showed normal activation of the marker genes in the wild type segregants (~99% GFP/RFP positive), whereas, only half of the population with +/duo1 phenotype showed expression of the marker genes (Figure 3.6). Furthermore, phenotypic analysis of the individuals analysed above showed a significant reduction of the *duo1* phenotype. Thus, despite the rescue of the *duo1* bicellular phenotype, the new class of rescued tricellular pollen grains did not have the capacity to activate expression of the sperm cell fate markers. This was demonstrated by the lack of increased proportion of tricellular pollen grains with detectable fluorescence at mature pollen stage.

Similarly, analysis of wild type F2 segregants from the +/*cdka;1* mutant background showed normal activation of the sperm cell fate markers with approximately 99% of the pollen grains with a wild type phenotype showing detectable GFP/RFP fluorescence (Figure 3.6 and 3.7). A similar proportion of the mature pollen grains in heterozygous *cdka;1* mutant plants were identified to activate the sperm cell fate markers correctly. Furthermore, the fluorescence signal in +/*cdka;1* plants was associated with wild type pollen grains and pollen grains with a single sperm-like cell demonstrating normal specification of germ cell fate in *cdka;1* mutant pollen grains.

In conclusion, unlike rescued *duo1* pollen grains that fail to express germ cell specification markers due to the absence of *DUO1*, single sperm-like cells generated following depletion of *CDKA;1* are capable of undergoing full differentiation and acquire sperm cell characteristics. Whereas, *CycB1;1* rescued *duo1* pollen grains does not acquire germ cell

fate, emphasising the role of *DUO1* as an integrator of cell division and cell fate specification in the Arabidopsis male germline.

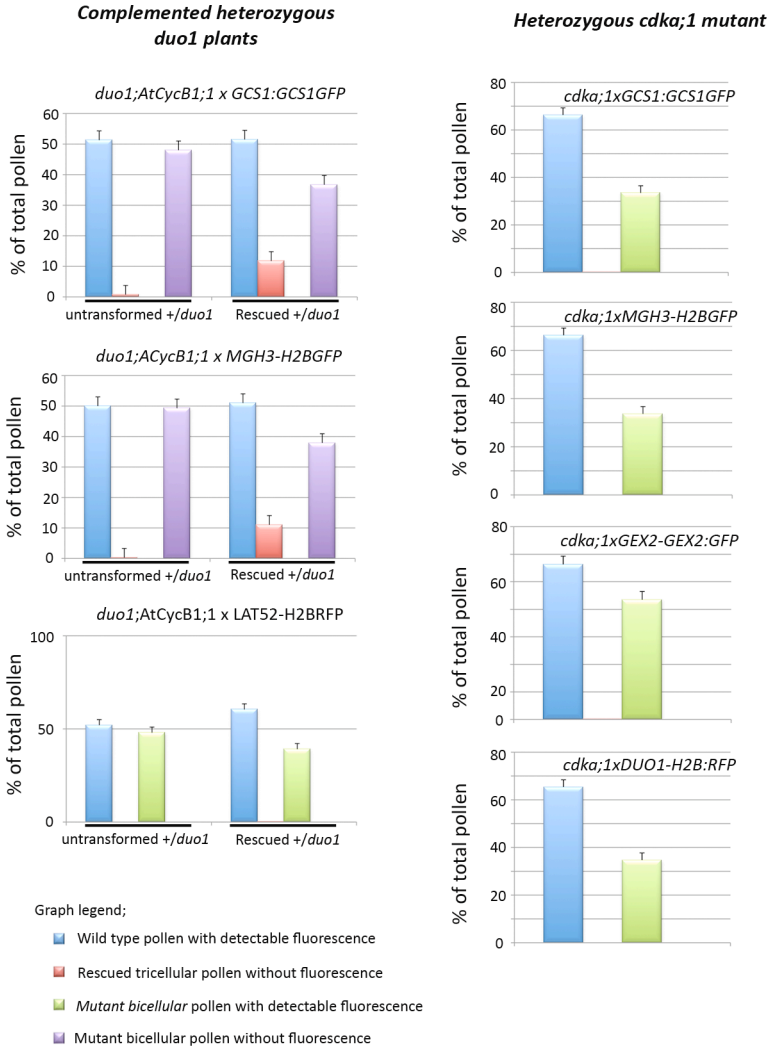

Figure 3.6. **Activation of germ cell markers in complemented *duo1* and *cdka;1* mutants**
Expression analysis of germ cell markers in heterozygous *duo1* plants complemented with DUO1-AtCycB1;1 and in the heterozygous *cdka;1* mutant background. Graphs showing the frequency of tricellular and bicellular pollen grains with and without detectable marker expression. (A-C) Germline markers are not activated in the rescued tricellular pollen. A maximum of 50% of marker expression is observed in tricellular pollen of untransformed +/*duo1* plants with approximately 50% wild type pollen. Whereas, in complemented lines, the 10% of the rescued tricellular pollen grains do not express germ cell markers. A non germ cell marker (C) is activated normally in all pollen types, indicative of the normal vegetative cell fate. (D-F) In contrast, all germ cell markers and a vegetative cell markers are expressed in the *cdka;1* pollen population. Each column represents average pooled data from three independent individuals homozygous for the marker genes and error bars showing standard deviation.

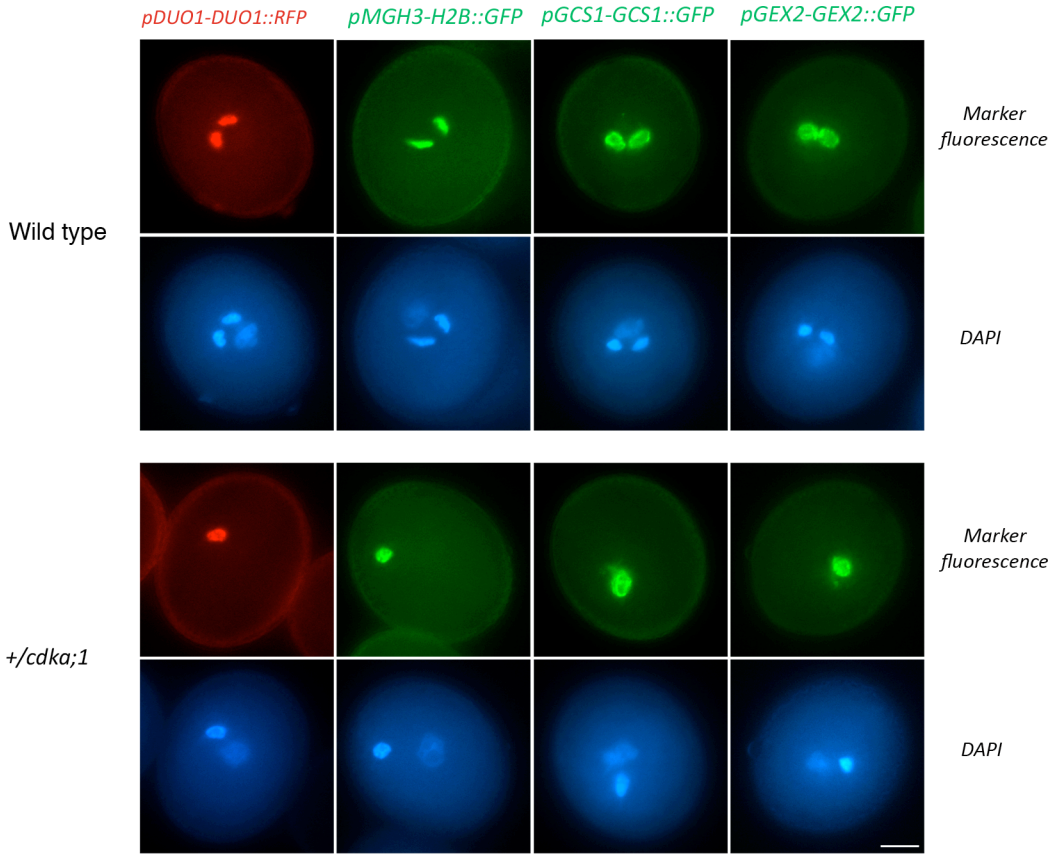

Figure 3.7. ***Expression of germ cell fate markers in cdka;1 mutant pollen***
Activity of germ cell specific expressed genes in heterozygous *cdka;1* plants. Mutant undivided germ cell showing normal activation of the markers (top panels) similar to wild type as observed under fluorescence microscope. Corresponding DAPI images are also shown (lower panels) to identify mutants and wild type pollen grains. Normal activation of the germ cell fate markers in heterozygous *cdka;1* plants signifying that *cdka;1* mutant germ cells acquire sperm cell fate and CDKA;1 activity is not required for fate specification. Scale bar 4µm

3.5 Manipulating expression of AtCycB1 family in pollen

Classification of cyclin proteins based on their sequence similarity indicates that plants posse's five different types of cyclins (Cyclin A, B, C, D and H) (Vandepoele et al., 2002). B-type cyclins have been well characterised as key regulators of CDKA activities during G2/M transition. NtCycB1;1 is able to overcome the G2/M arrest in Xenopus oocytes (Qin et al., 1996), and ectopic expression of CycB1;2 in endoreduplicating trichomes of Arabidopsis thaliana leads to multicellular trichomes (Schnittger et al., 2002). Moreover, constitutive overexpression of AtCycB1;1 promotes cell division in root meristems and increased root growth (Doerner et al., 1996). These studies indicate that B-type cyclins are the limiting factors during cell division and their modulation is critical for G2/M progression and normal rate of cell division.

There are three classes of B-type cyclins in Arabidopsis, Cyclin B1 family which consists of four members, (Cyclin B1;1, B1;2, B1;3 and B1;4), Cyclin B2 family which also consist of four members (Cyclin B2;1, B2;2, B2;3 and B2;4), and Cyclin B3 family which has only one member (CyclinB3). Analysis of pollen transcriptomic data and RT-PCR showed that all three classes of B-type cyclins are expressed during pollen development (Figure 3.1 and 3.2). To understand which of these cyclins participate in modulating CDKA activity during germ line development, a transgenic approach was used which involved expression of double stranded hairpin RNA interference (RNAi) using pollen cell-specific vectors to down regulate expression of the CycB1 family members. In this section, a strategy used to generate targeted RNAi constructs is presented and the detrimental consequences of expressing hp-CycB1 at the microspore stage and in the germ cell are discussed.

3.5.1 Generation of the hairpin dsRNAi constructs

Availability of the pollen cell-specific molecular vectors for manipulating gene expression provided tools to dissect the role of Cyclin B1 family during germ cell formation. Hairpin Gateway expression vectors containing a 1kb Microspore Specific Promoter 1 (MSP1;Honys et.al, 2006) and a 1.8kb Generative Cell Expressed 2 (GEX2) promoter were used to knockdown expression of Cyclin B1 family members in microspore and specifically in generative cell. A LAT52 driven CycB1-dsRNAi was also constructed as a control to demonstrate specificity of the effector constructs. Because of the possible functional redundancy among the family members, a strategy was adopted to design an RNAi fragment that would target all four members for degradation. A ClustalW alignment was performed based on cDNA sequence and a 179bp RNAi fragment was selected as the optimal region for targeting all four members (Figure 3.8). The selected region showed 100% identitiy with CycB1;1, 67% similarity with CycB1;2, 50% similarity with CycB1;3 and 60% identity with CycB1;4 respectively. Primers for amplification of the RNAi fragment were designed based on the CycB1;1 sequence and a two step gateway PCR reaction was performed using Biotaq DNA polymerase (Bioline, UK). The constructs were verified by a diagnostic restriction digest and selection on 30 ug/ml Chloramphenicol. Verified constructs (Figure 3.8) were transformed into *Agrobacterium* and introduced into wild type Col-0 plants through floral dipping (Chapter 2, section 2.3.6.2).

A

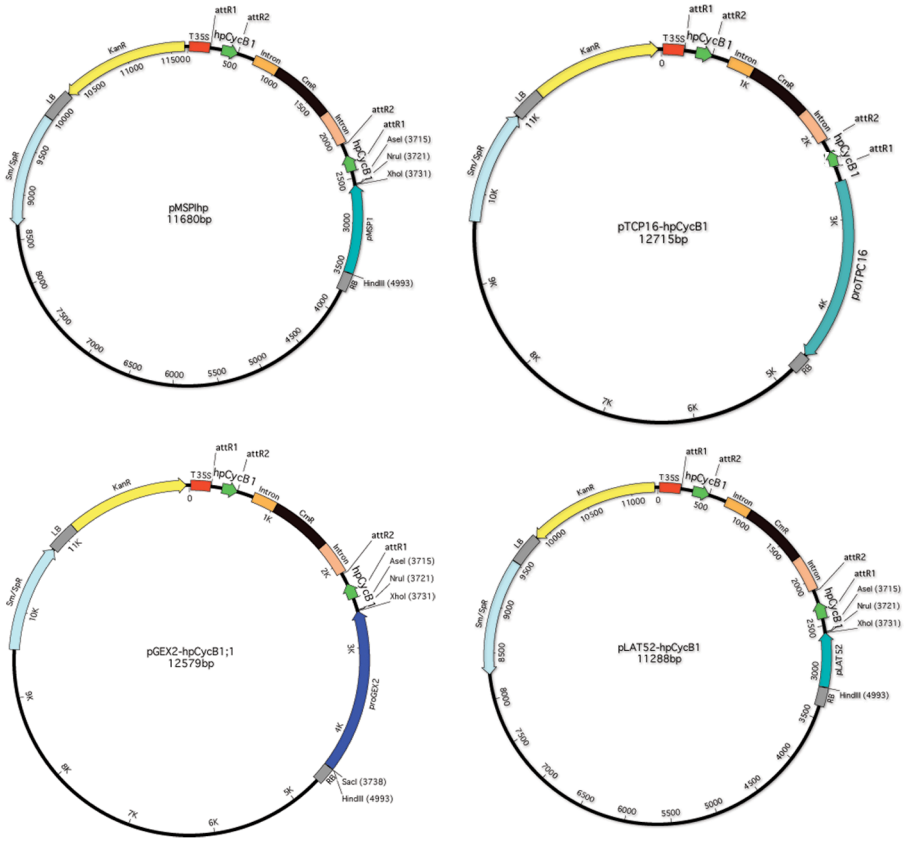

B

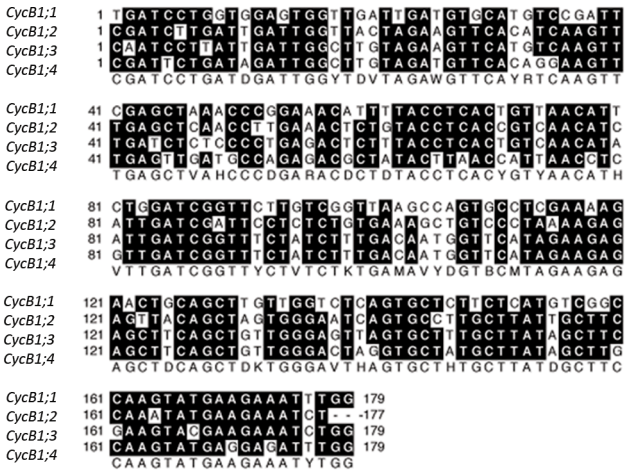

Figure 3.8. ***Construction of hpCycB1 RNAi vectors***
Gateway vectors were modified to accommodate pollen promoters for cell-specific target degradation of AtCycB1 mRNA transcripts. (A) Four constructs that where used to drive expression of hairpin dsRNA to induce transcript turnover of AtCycB1 family members at the microspore stage and bicellular stage specifically in the germ cell. The vectors were generated by modifying existing Gateway constructs. Pollen specific promoters were cloned by conventional restriction method, whereas, the target RNAi sequence were introduced by Gateway recombination in the inverted orientation. Prior to transformation into plants, all constructs were verified by sequencing and restriction analysis. (B) ClustalW alignment of AtCycB1;1, B1;2, B1;3, B1;4 CDS showing regions of high nucleotide similarity for multiple RNAi targeting. A segment comprised of approximately 179bp was selected for targeting mRNA degradation of the four cyclin members. attR1/attR2; recombination sites, hp;hairpin, pro; promoter, T35S; transcriiptional terminator, KanR; kanamycin resistance marker, Sm/SpR; spectinomycin resistance gene, LB/RB; left and right borders respectively.

3.5.2 Phenotypic characterization of hpAtCycB1 plants

To investigate the repercussion of hp-CycB1 expression during pollen development, mature pollen grains were analysed by light microscopy and simultaneously by DAPI stain with fluorescence microscopy to visualize nuclear morphology and establish if there is any deviation the deviation from the wild type phenotype. Where necessary, floral buds from selected individuals were dissected during development to establish the origin of the phenotype observed at the mature pollen stage.

3.5.2.1 **Prediction of the phenotype**

The wider role of B-type cyclins in licensing G2/M progression through the modulation of CDKA activity suggests a possibility of generating a range of abnormalities upon depletion of CycB1 transcripts. The activity of the B-type cyclins are initiated following G2 entry, from nuclear envelope breakdown in association with Cyclin A1, reorganization of microtubules and synthesis of mitotic spindles, and activation of APC to allow separation of the two new daughter nuclei and exit from mitosis. Therefore, progression through these phases is threshold dependent and lack or depletion of CycB1 is likely to inhibit G2/M entry or perturb mitotic progression and lead to failure of chromosome separation into two daughter cells. Hence, it was predicted that following degradation of CycB1 transcripts at the microspore stage, a pollen mother cell would fail to fail to enter G2/M or fail to progress through mitosis, depending on the extent of knockdown. This would result in a production of uninucleate microspore at pollen maturation or a G2/M – prophase arrest of the germ cell to produce a single sperm-like cell. With a limited knowledge on the consequences of CycB1 depletion, other unknown phenotypes were not ruled out as a possibility.

Based on the sequence similarity match between the RNAi fragment and the target gene coding sequences, it was predicted that the primary targets for knockdown would most likely be CycB1;1 and CycB1;2, and the less affected targets would be CycB1;3 and CyCB1.4.

Therefore, the generated phenotype following silencing are most likely to be the result of CycB1;1 / CycB1;2 deficiency.

3.5.2.2 **Microspore hpAtCycB1 expression leads to uninucleate microspore arrest**

To investigate the role of the AtCycB1 family at the first pollen mitosis (PMI), 32 primary transformants carrying the construct pK7MSP1-hpAtCycB1;1 were generated and screened for aberrant pollen phenotype. Screening of the primary transformants at the mature pollen stage for microspore division phenotype revealed 13 individuals with approximately 30% - 53% aberrant pollen phenotypes. The phenotype included a predicted prophasic - uninucleate arrest with highly condensed chromatin and visible foci arranged in a ring structure (Figure 3.9f), pollen grains with dispersed nuclear material (Figure 3.9g), and some collapsed pollen grains. To establish the origin of the phenotype, two lines with a single transgene insertion were selected and dissected back through development. It was observed that the mutant phenotype originates at the microspore stage showing partial collapsed pollen segregating among the wild type uninucleate microspores (Table 3.3). The severity of the phenotype increased at the bicellular stage with distinctive uninucleate microspore arrest, and totally collapsed pollen grains. At the tricellular and mature pollen stage, the dominant phenotype was largely collapsed pollen grains and a very small proportion of uninucleate microspore with dispersed nuclei forming a galaxy-type pollen grains.

This result indicates an important role for CycB1 in microspore division and that deficiency of CycB1 at this stage leads not only to microspore arrest but also triggers pollen death. Furthermore, considering the penetrance of the phenotype in some of the individuals, the outcome of this experiment also indicates that there is limited inheritance of CycB1 protein from pollen mother cells to allow the first microspore mitotic progression.

		Wild type phenotype			*Mutant phenotype*				
		Polarized UNM	BCP	MPG	UNM arrest	Aberrant	Partial collapse	Collapse	% total mutant
	Pollen stages								
Line B5	UNM	145	0	0	0	81	17	0	40% (n=243)
		60%			0%	33%	7%	0%	
	BCP	0	154	0	0	96	21	10	45% (n=281)
			55%		0%	34%	7.50%	3.50%	
	TCP	0	0	290	0	75	137	24	45% (n=526)
				55%	0%	14%	26%	5%	
	MPG	0	0	405	0	44	221	0	40% (n=670)
				60%	0%	7.00%	33%	0%	
Line D3	UNM	166	na	na	17	76	0	0	38% (n=259)
		63%			9%	29%	0%	0%	
	BCP	na	240	na	42	149	0	0	49% (n=431)
			52%		15%	34%	0%	0%	
	TCP	na	na	264	40	16	121	26	47% (n=467)
				53%	13%	3%	26%	5%	
	MPG	na	na	428	24	51	71	180	46% (n=7)
				55%	7%	7%	9%	23%	
Line D6	UNM	139	na	na	0	61	14	9	38% (n=223)
		62%			0%	28%	6%	4%	
	BCP	na	196	na	8	91	47	18	44% (n=360)
			54%		4%	25%	13%	5%	
	TCP	na	na	271	13	37	112	67	47% (n=500)
				52%	5%	7%	22%	13%	
	MPG	na	na	420	0	31	196	132	46% (n=778)
				54%	0%	4%	25%	17%	

Table 3.3. ***Developmental analysis of MSP1-hpCycB1 plants***
Counts of the pollen phenotypes during development to identify the origin of phenotype following introduction of the MSP1-hpCycB1 construct. The deviation of the wild type phenotype was observed as early as microspore stage including unicellular microspore arrest and some partially collapse pollen grains. The nature of the phenotypes are denoted by the sketch above. UNM; unicellular microspore, BCP; bicellular pollen, MPG; mature pollen grain.

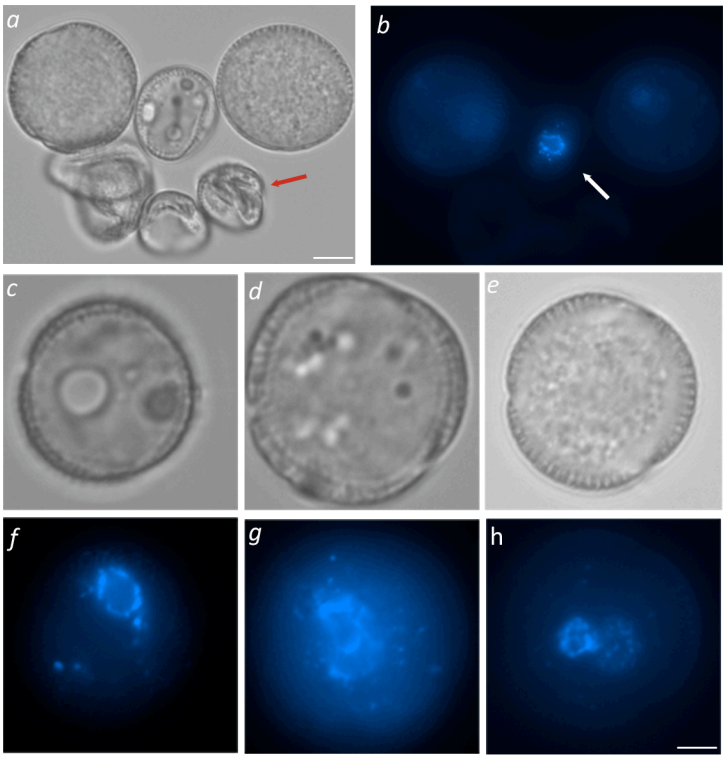

Figure 3.9. **Microspore phenotypic classes of MSP1-hpCycB1 plants**
Differential interference contrast (DIC) and fluorescence microscopy images of wild type and MSP1-hpCycB1 spores. (a-b) Light DIC image and corresponding DAPI stain micrograph showing wild type pollen grain, totally collapse pollen grain (red arrow) and a partially collapse microspore arrested pollen grain (white arrow), scale bar 1.2µm. (c-h) Bright field images (upper panel) of arrested uninucleate mic displaying aberrant pollen development and corresponding DAPI micrographs (lower panel) showing different phases of uninucleate prophase-arrest including initiation of DNA degradation (g). Scale bar 4µm

3.5.2.3 **Germ cell hpAtCycB1 expression leads to prophase arrest of the germ cell nucleus**

To investigate if CycB1 plays a role during division of the germ cell into twin sperm cells (PMII), 36 primary transformants were generated harbouring the germ cell specific construct pK7GEX2-hpAtCycB1;1 and screened for pollen division phenotypes. DAPI staining of the mature pollen grains from primary transformants identified 10 lines that had aberrant pollen phenotypes. Analysis of the aberrant lines with brightfield microscopy showed the presence of a small proportion of collapsed pollen grains and a much higher frequency of pollen grains, which appeared less mature than wild type pollen grains and distinctively containing

cytoplasmic vesicle-like inclusions (Figure 3.10). Screening of DAPI stained mature pollen revealed a significant proportion of pollen grains (~18 – 48%) with a predicted pre-mitotic generative cell nuclear arrest (Figure 3.10). To determine the point of arrest, DAPI stained mutant pollen grains from the heterozygous *cdka;1* mutation were compared along side. Clearly, the germ cell nuclear morphology observed in the *cdka;1* mutant pollen grains is distinct from nuclei in hpCycB1 pollen grains (Figure 3.10).

Furthermore, FDA staining was carried out on the mutant individuals to establish whether the aberrant pollen grains were viable. Staining of the mutant mature pollen grains showed partial or no staining, whereas, the wild type segregants within the mutant population showed normal staining (Figure 3.11). To establish if the construct introduced was responsible for the pollen phenotype observed, PCR analysis was carried out on wild type and mutant plants and individuals carrying the rescuing construct (pDUO1-AtCycB1;1) were used as a negative control. Indeed, PCR result demonstrated that all plants showing the pollen phenotype contained the pK7GEX2-hpAtCycB1;1 construct, implicating a linkage between the presence of the phenotype and presence of effector transgene. However, the presence of the transgene was not always sufficient to cause an effect, indicating variability in the effect of the transgene.

To determine the specificity of the phenotype generated with both constructs (pK7MSP1-hpAtCycB1 and pK7GEX2-hpAtCycB1), a control construct driving the expression of double stranded hpCycB1 in the vegetative cell (pK7LAT52-hpAtCycB1) was introduced into wild type plants grown in the same conditions as the other two effector constructs. From the 39 primary transformants that were generated, none of the individuals showed any aberrant pollen phenotype resembled that observed with hpCycB1 expression at the microspore stage or in the germ cell. This result demonstrated that the observed phenotype generated with pK7MSP1-hpAtCycB1 and pK7GEX2-hpAtCycB1 constructs in the microspore and in the germ cell is the consequence of stage and cell specific hpCycB1 expression. Following a

prophase arrest of the germ cell nucleus, these data suggest that a spatial and temporal expression of CycB1 in the germ cell is essential for twin sperm cell formation.

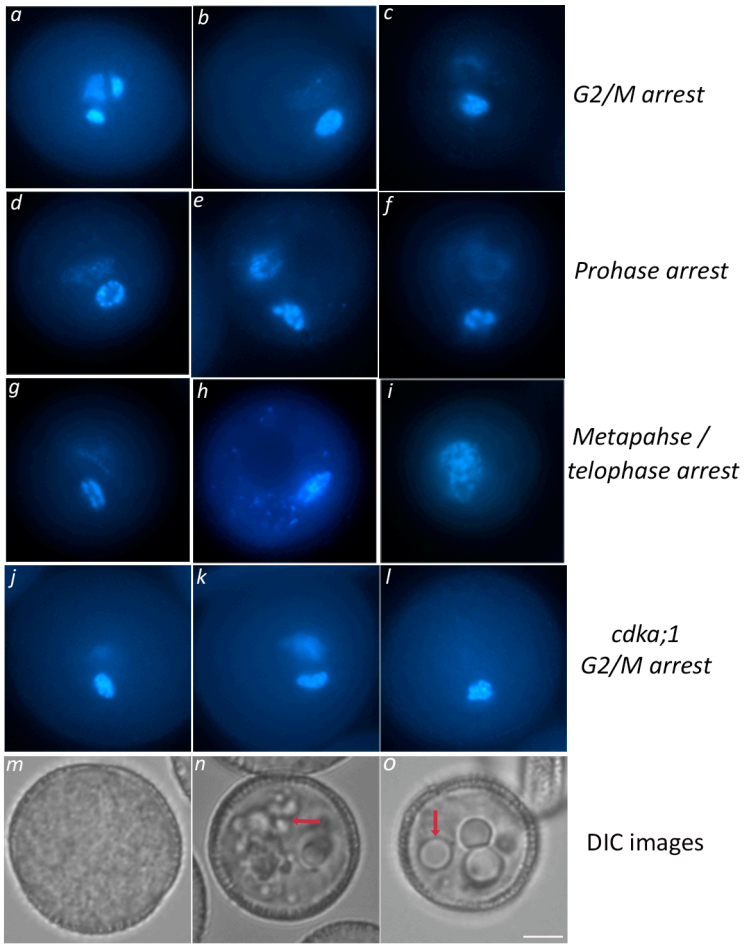

Figure 3.10. ***Germ cell specific phenotype of GEX2-hpCycB1 plants***
Phenotypic analysis of hpAtCycB1 plants at mature pollen stage. (a-i) DAPI images of wild type pollen grain with twin sperm cells (a) and aberrant pollen grains showing wild germ cell nucleus arrest at interphase (b-c), early-mid prophase (d-f) and late-prophase stage of the cell cycle (g-i). Some pollen grains also shows a sign of beginning of DNA degradation indicated by the dispersed DNA materials. (i). Whereas, analysis of *cdka;1* mutant pollen grains only shows interphase arrest (j-l). DIC images from the GEX2-hpCycB1 deficiency plants showing abnormal pollen development with a characteristic cytoplasmic inclusions, red arrows (m-o). Scale bar 5µm.

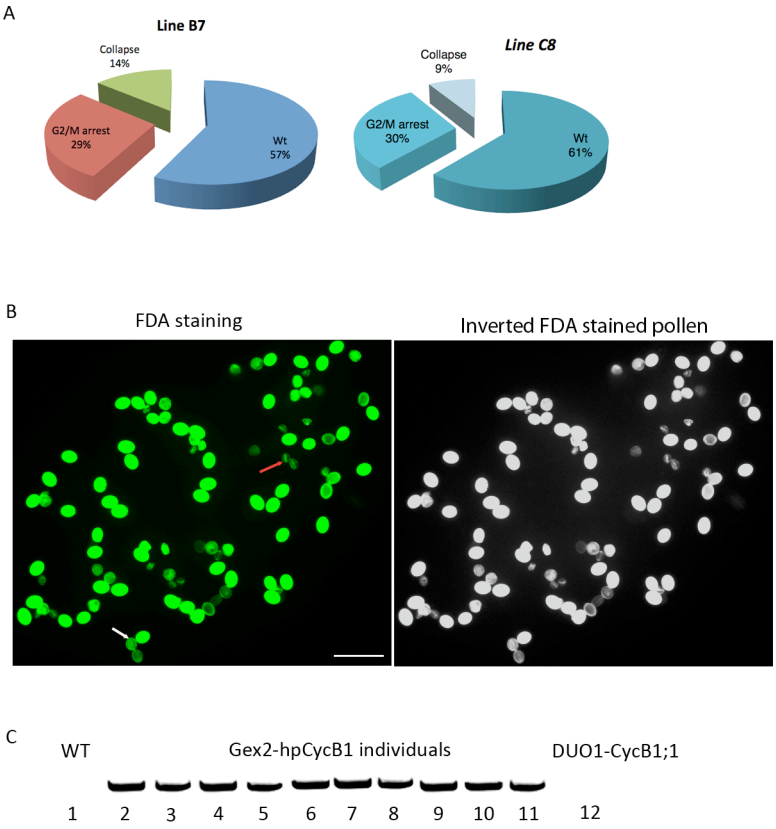

Figure 3.11. **Germ cell specific defect of hpCycB1;1 knockdown**
(A) Chart showing frequency of mutant phenotypic classes observed in GEX2-hp CycB1 plants during pollen maturation of two representative lines. (B) Fluorescein diacetate staining (FDA) of mature pollen population from plants harbouring pKGEX2-hpCycB1 constructs. White arrow represents less severe mutant pollen grains (partially staining) and red arrow represents severe form of the mutant pollen grains (no staining) with no DNA staining. (C) PCR analysis of selfed plants carrying the construct pK7GEX2-hpCycB1 to test the presence of the effector transgene in the mutant individual and absence in wild type control. Ten individuals derived from a T2 parent (C8) that display a bicellular arrest phenotype, and one untransformed wild type plant, and one transgenic plant harbouring a complementing construct (pBDUO1-AtCycB1;1), were PCR tested for the presence of pK7GEX2-hpCycB1 construct by amplifying a kanamycin resistance marker (NPT2). The analysis provided a linkage between the observed bicellular phenotype and the presence of the effector. Scale bar 1.1µm

3.5.2.4 **A single sperm-like cell is not competent for fertilization**

The distinct features that set apart flowering plants from others is the evolution of double fertilization that solely relies on the production of two sperm cells. Flowering plants are classified in two major groups, bicellular and tricellular species, depending on the timing of germ cell division in to twin sperm cells (Brewbaker, 1967). In both cases, a germ cell divides into two sperm cells prior to entry through the micropyle of the female gametophyte, in which one sperm cell fuses with the egg cell and the second sperm cell fuses with the central cells to produce an endosperm. Therefore, production of a single sperm cell will disrupt double fertilization and result in the production of aberrant seed. Evidence for the consequences of single sperm cell production has been demonstrated in the *cdka;1* mutant and in plants deficient in Chromatin Assembly Factor (CAF), in which a single sperm cell is produced as a result of failure of germ cell division (Nowack et al., 2006; Chen et al., 2008). In both cases, the mutants results in the production of aberrant seeds or arrest during ambryo development.

To investigate whether the single sperm cell produced following depletion of CycB1 in the germ cell is capable of undergoing successful fertilization, production of seeds was monitored from five selfed individuals carrying the construct pK7GEX2-hpAtCycB1;1 that drives CycB1 mRNA degradation specifically in the germ cell, and four independent individual lines from male and female back crosses to wild type. Matured green siliques and dried siliques were dissected and seeds were counted. In a wild type, on average, approximately 45-50 seeds are present per silique. Dissected siliques from the selfed mutant plants showed several gaps and a reduced number of seeds per silique (Table 3.4). The proportion of seeds present per silique from each mutant individual directly correlated with the severity of the pollen phenotype observed at the mature pollen stage with 52% maximum aborted seeds. The maximum proportion of the aborted seeds indicates that the effect is gametophytic specific. The aberrant seed phenotype included gaps, suggesting failure to fertilize, and

white stubs or aborted embryos demonstrating unsuccessful fertilization or failed embryogenesis. This observation indicates that a single sperm cell produced following hpCycB1 expression in the germ cell is not capable of fertilizing the egg cell and the central cell to produce a viable embryo. Nevertheless, the presence of white stubs suggests that the single sperm-like cell is not defective in growing a pollen tube and able to initiate fusion with the egg cell or the central cell mimicking the single sperm cell produced in the *cdka;1* mutant.

Parental genotype	Normal	Aborted	Undeveloped (white stubs)	Number of seeds counted	% seed gaps
ms1-1 x wt (No-0)	337	0	0	337	0.0
Line B7-D4*	292	6	41	339	13.9
Line B7-D8	272	13	159	444	38.7
Line C8-C3	178	23	134	335	46.9
Line C8-C7	182	20	181	383	52.5

Table 3.4. **Seed defects as observed in plants expressing pK7GEX2-hpCycB1 transgene**
Siliques generated from a male sterile female (ms1-1) that was pollinated by wild type pollen donor showed no abvious defect of seed development. However, mature siliques derived from selfed +/pK7GEX2-hpCyCB1 plants showed severe defect on seed development and early embryo abortion. The number of seed gaps observed varied depends on the severity of the pollen phenotype. *lines with severe pollen phenotype.

3.6 Summary

The results of experiment described within the chapter have demonstrated that B-type cyclins plays an important role during pollen development and deficiency of these key regulators is lethal to the male gametophyte function. Transcriptomic data in conjunction with the RT-PCR data provided an initial insight into the expression pattern of the CycB family. A spatial and temporal expression of AtCycB1;1 during pollen development was demonstrated using the well characterised pCDG construct. Furthermore, this cell cycle marker has also demonstrated the turning over of CycB1;1 in the vegetative and generative cell as well as providing hint for the activity of the APC/Cyclosome complex for the first time in the male gametophyte. The application of pollen cell-specific RNAi vectors, further indicated the important role played by the CycB1 family during pollen development. Interestingly, by exploring the pCDG cell cycle marker, a link between cell division and cell differentiation was established in which an R2R3MYB protein (DUO1), an essential regulator of G2/M transition of the germ cell (Durbarry et al., 2005), was identified to be crucial for CycB1;1 expression in the germ cell as well for the expression of sperm cell specific markers (Brownfield et al., 2009). This relationship was further verified by complementation of the *duo1* germ cell division phenotype with AtCYCB1;1 protein. Thus, B1-type cyclins are indispensible for the production of twin sperm cells and double fertilization.

Chapter 4

RNA interference (RNAi) Mediated Silencing and Male Germline Development

4.1 Introduction

Identification of gene function is a key objective of functional genomics that relies on techniques that have been established in molecular biology. Rapid completion of genome sequencing of several species have seen the need for establishing an effective, targeted and high throughput method for screening gene function. This has led to the exploitation of the small RNA pathways (smRNA), or RNA interference (RNAi), as a tool for reverse genetics. smRNA silencing also described as Post transcriptional gene silencing (PTGS) was first discovered in worms as a mechanism of gene silencing directed by dsRNA (Waterhouse et al., 1998), though, the RNAi phenomenon was already described in plants as a co-suppression phenomena induced by the introduction of transgene that leads to the suppression of the expressed transgene itself and the endogenous homologous gene (Napoli et al., 1990). The RNAi mechanism functions by directing degradation of target mRNA using small interfering RNAs (siRNAs) generated from the primary RNA transcript (priRNA). Major components involved in the RNAi pathway include; RNase III family (DICER) that cleaves double stranded RNA into short 21-24nt siRNA duplexes, RNA dependent RNA polymerases (RdRP) required for the replication of the siRNA duplexes to enhance the RNAi effect and allows inheritance of the silencing effect through generations, and a family of RNA nucleases termed Argonaute that form the RNA Induced Silencing Complex (RISC) which is responsible for the degradation of the target mRNA transcripts. Other components that participate in the RNAi pathway include HASTY, HEN1, HYL1, and SERRATE which are involved in cleavage, methylation and export of the generated siRNAs from the nucleus to the cytoplasm.

The ultimate aim of this project was to shed more light on the understanding of the cellular processes regulating gene expression in the male gametophyte particularly focusing on the RNAi mechanism as one of the PTGS pathways. The objective of the project was to analyse the expression pattern during male gametophyte development of some of the core components known to function in the smRNA machinery. In parallel, the project aimed at

developing RNAi-based pollen cell-specific molecular vectors that could be used to manipulate gene expression in specific cell types in pollen. These vectors would also allow functional verification of the activities of smRNA pathways in the male gametophyte as well as providing tools for pollen specific mutagenesis screens. In this chapter, evidence of the expression profiles of key smRNA components and functional verification of the potential smRNA activities during male gametogenesis of *Arabidopsis thaliana* is presented.

4.2 Understanding the smRNA pathway; Pollen expression profiles

To show if the RNAi mechanism operates during germ cell formation, it was important to first establish if some of the key components involved in the smRNA pathway are expressed during pollen development, and if so what their expression patterns are. The majority of pollen expressed genes show a common pattern with high transcript abundance at early stages of germ line development and a large-scale repression during pollen maturation (Honys and Twell, 2004). With a known role of RNAi mechanism in controlling transcript abundance and protein accumulation at pre-transcriptional and post-transcriptional level, it was predicted that most of the components involved in this pathway would show a corresponding profile to that of the target genes.

Here results of the expression pattern from microspore to mature pollen stage of three smRNA family proteins, DICER, RDR and ARGONAUTE, together with four other genes *HASTY*, *HEN1*, *HYL1* and *SERRATE*, which are the major components of the RNAi pathway, are presented. The pollen transcriptomic data used for this analysis is currently available in the public database, Arabidopsis Gene Family Profiler (aGFP;Dupl'akova et al., 2007). The microarray results presented were verified by semi-quantitative RT-PCR with RNA isolated from the four stages of pollen development.

4.2.1 Pollen transcriptomic profiles of smRNA components

Transcriptomic data that was obtained from aGFP database was normalized by ATH1 Affymetrix chip to obtain the mean hybridization signal. For detection calls, a MAS5 algorithm was used whereby a normalized value was given a "Present call" (Blue values) when the transcript detection was reliable on both chips (Figure 4.1). When a signal is reliable on one chip but marginal or absent on the other, the detection value is classified as "Marginal" (Green values). A marginal signal on one chip that is absent on the other chip is classified as "Absent" (Grey values).

A: DICER-LIKE family (DCL)

Dicer-like proteins play an essential role in the RNAi pathway and lack of DCL activity results in defects in the RNAi response. In an effort to uncover existence of the RNAi activity in pollen, expression profile of the four *DICER-LIKE* genes during germ cell proliferation was investigated. Analysis of a transcriptomic dataset covering four progressive stages of male gametophyte development showed that all four members of the *DICER* family have detectable hybridization signals in the male gametophyte. All the members showed a similar expression pattern particularly at the early stages, demonstrating a possibility of having a common response and regulatory pathway at least in pollen (Figure 4.1). *DCL1* showed a marginal call at the microspore stage and a reliable signal of similar intensity at the bicellular stage. Its expression pattern became unreliable and reduced from tricellular stage to mature pollen stage reflecting a common pattern of gene expression during pollen maturation. *DCL2* had a much more reliable profile with a strong reliable signal at the microspore stage, which was reduced at the bicellular stage. Low hybridization signal was marginally detected at the tricellular and in mature pollen stage. *DCL3* showed a very similar pattern to that of *DCL2* but with a slightly reduced detection value. *DCL4* did not show a reliable expression, only a marginal signal was detected at the bicellular stage. In addition, its expression did not reflect

the common pattern in pollen, instead, a persistent signal was observed throughout development.

B: Double stranded RNA Binding proteins (DRB);

To understand the expression profile of the DRB family members, pollen transcriptomic dataset was analysed for *HYL1* and its four close homologs, *DRB2*, *DRB3*, *DRB4* and *DRB5*. All five members showed diverse expression patterns with *DRB5* having no reliable signal throughout pollen development (Figure 4.1). *HYL1*, which has been functionally demonstrated to have strong interaction with *DCL1*, showed a marginal signal at the microspore stage and a reliable detection at the bicellular stage. Following germ cell division, no reliable expression of *HYL1* could be detected. Whereas, *DRB2* and *DRB4* showed a much more reliable transcript detection throughout the pollen stages with the exception of a marginal signal for DRB2 at the mature pollen stage. *DRB3* was only marginally detected at the tricellular stage, whereas *DRB5* showed no detection during germ cell development.

C: RNA Dependent RNA polymerases (RdRP) family;

RNA-dependent RNA polymerases (RdRP) have been proposed to be involved in the amplification of dsRNA that allow continuous degradation of newly transcribed target mRNA throughout development and in successive generations. In Arabidopsis, there are six genes that encode *RdRP*, however only four of those were represented on the ATH1 Affymetrix chip. Analysis of the transcriptomic dataset revealed that *RDR1*, *RDR2* and *RDR5* showed reliable hybridization signals at microspore and bicellular stages with highest expression exhibited by *RDR1*, followed by *RDR5* and *RDR2* respectively (Figure 4.1). In addition, all three genes showed unreliable signals at tricellular and mature pollen stages. In contrast, *RDR6* had a very reliable hybridization signal at the microspore stage, which was followed by a marginal signal at bicellular stage and unreliable signal at tricellular stage. Interestingly, the

RDR6 expression pattern differed significantly from the other three members by having its highest hybridization signal at mature pollen stage, and being the most abundant compared to the other three members despite its marginal status. Does this suggest a possible role of RDR6 post PMII and further on during pollen tube growth or after the double fertilization of the female gametes?

D: ARGONAUTE family;

The major role played by the Argonaute proteins is the degradation of dsRNA after being recruited to the RISC complex following *DICER* activity and unwinding of the dsRNA by helicase enzymes. There are ten *AGO*-like genes that have been identified in Arabidopsis, however, not all of them have been demonstrated to have a role in the RNAi pathway.

Transcriptomic profiles of the Argonaute family members can be classified into three major groups. The first group includes those members that show almost ten fold higher expression compared to those of the second and third group members respectively. The second group members show intermediate levels of expression, whereas, the third group are only marginally expressed or not reliably expressed. The highly expressed AGO members include *AGO1*, *AGO4* and *AGO5*, which showed up to ten fold higher expression levels at the microspore and bicellular stage compared to any other family members (Figure 4.1). Interestingly, their expression levels are reduced dramatically at the tricellular and mature pollen stage and are even absent in the case of *AGO5*. Second group members showed three different expression patterns. *AGO2* and *AGO10* showed reliable expression at the microspore and bicellular stage with no detectable expression at tricellular and mature pollen. A different expression profile is observed for *AGO6* and *AGO9* that showed a more steady and reliable expression throughout pollen development with the exception of a marginal call for *AGO6* at the tricellular stage. *AGO3* showed no detectable expression at the early stages of germ cell formation but a reliable expression at tricellular and mature pollen

stages, indicating a possible role in the germ cell or the vegetative cell after PMII. *AGO7* and *AGO8* are classified into a third group with marginal or no reliable hybridization signals. *AGO7* showed only a marginal call at the microspore stage and no detection thereafter, whereas, *AGO8* showed a marginal detection at the microspore and bicellular stage, no detection at tricelluar stage and interestingly a marginal call at mature pollen. It is most likely that *AGO7* and *AGO8* are not expressed or expressed at very low levels in the male gametophyte.

E: Other smRNA pathway proteins;

Several other proteins that have been reported to be actively involved in the functioning of the RNAi pathway are also expressed during male gametophyte development. Some of these proteins include *HASTY* (*HST)*, *HUA ENHANCER1* (*HEN1*), *SERRATE* (*SER*), *SILENCING DEFECTIVE3* (*SDE3*), EXORIBONUCLEASES *(XRN)*, *ATRL12*, 3′(2′),5′*-bisphosphate nucleotidase/inositol polyphosphate 1-phosphatase FIERY1* (*FRY1)*, RNA polymerase *IVa* (*NRPDA)1* and RNA polymerase *IVa* (*NRPDB2*), and *SUPRESSOR OF GENE SILENCING3* (*SGS3*). The majority of these molecules with the exception of *NRPDA1* show a common microarray expression pattern in pollen with highest hybridization signal at the microspore stage and reduced transcript abundance at bicellular stage (Figure 4.1). The hybridization signal then becomes only marginal for *HASTY* and *SERRATE* at the tricellular stage, and unreliable for other genes. At the mature pollen stage, no reliable hybridization signal can be detected, with the exception of *XRN3, ATRL12,* and *FIERY1* that show strong reliable signals at mature pollen stage. Whereas, *NRPDA1* is only marginally detected at the microspore stage then absent thereafter. Because of the existence of two NRPDA subunits, perhaps the activity of NRPDA1 is substituted by the NRPDA2 subunit during male gametophyte development.

Detection of reliable hybridization signals for smRNA pathway protein coding genes together with those of other protein families involved in the RNAi pathway, has demonstrated the

presence of a set of proteins that participate in different smRNA pathways and at different stages during smRNA processing. The evidence gathered is sufficient to hypothesise the presence of RNAi activity in regulating transcript abundance during male gametophyte development likely through RNA directed DNA methylation and mRNA cleavage of the target genes.

Gene name	AGI number	UNM	BCP	TCP	MPG
AGO1	At1g48410	2133.95	1848.25	397.95	170.57
AGO2	At1g31280	287.22	285.62	156.73	160.04
AGO3	At1g31290	304.9	285.69	472.95	419.21
AGO4	At2g27040	2091.62	1991.98	471.99	343.38
AGO5	At2g27880	1108.55	1291.59	637.54	627.57
AGO6	At2g32940	275.59	272.57	325.6	421.97
AGO7	At1g69440	213.13	186.66	195.18	181.91
AGO8	At5g21030	99.81	141.73	129.52	142.61
AGO9	At5g21150	467.73	555.86	350.13	388.55
AGO10	At5g43810	263.6	257.63	180.47	160.83
DCL1	At1g01040	383.67	379.76	258.39	117.84
DCL2	At3g03300	471.88	343.91	158.19	187.74
DCL3	At3g43920	329.50	278.45	139.17	149.76
DCL4	At5g20320	392.37	400.36	414.59	473.13
RDR1	At1g14790	406.04	309.84	128.16	174.81
RDR2	At4g11130	97.86	83.61	57.86	55.14
RDR5	At2g19930	266.96	222.24	275.7	305.81
RDR6	At3g49500	372.65	291.35	323.84	504.53
XRN2	At5g42540	831.718	731.1565	633.3585	721.956
XRN3	At1g75660	531.0125	507.3405	696.558	1152.33
XRN4	At1g54490	314.4415	296.7465	227.5515	174.832
ATRLI2	At4g19210	14750295	1501.96	822.6195	334.486
FIERY1	At5g63980	1923.605	1456	902.603	878.3135
HEN1	At4g20910	314.53	268.74	184.53	269.01
HEN2	At2g06990	398.7465	353.8315	274.9735	317.938
HEN family	At1g59760	850.402	751.662	338.2845	396.534
HEN family	At3g46960	1005.242	964.836	690.633	594.829
HEN family	At5g64390	173.17	181.0225	227.948	273.1375
SDE3	At1g05460	202.54	223.01	99.25	91.27
NRPDA1	At1g63020	309.47	255.8	235.87	264.07
NRPDB2	At2g40030	422.2	396.78	121.61	121.85
HYL1(DRB1)	At1g09700	204.24	197.88	239.51	336.43
DRB2	At2g28380	364.1	349.14	319.96	384.74
DRB3	At3g26932	167.38	138.12	221.38	229.89
DRB4	At3g62800	622.35	723.7	691.7	528.57
DRB5	At5g41070	233.84	215.2	351.69	379.18
HASTY	At3g05040	343.2	306.04	300.98	322.38
SERRATE	At2g27100	498.72	426.94	177.6	128.13
SGS3	At5g23570	317.1	285.66	56.53	68.6

Figure 4.1A. ***Transcriptomic profiles of smRNA components during pollen development***
Values shown represent mean normalized hybridization signals obtained from the aGFP database (Duplakova et al., 2007). A positive expression value is shown when there is a reliable hybridisation signal (Detection call "present", blue values) in both replicates. A present call in one chip but unrealiable or absent in the second chip, is defined as marginal (Green values). An expression value of "0" means that the hybridisation signal was unreliable (Detection call "absent" or "marginal", grey values) in at least one replicate or absent on both chips. AGI locus identification number is according to TAIR8 annotation. UNM, unicellular microspore, BCP, bicellular pollen, TCP immature tricellular pollen, MPG, mature tricellular pollen.

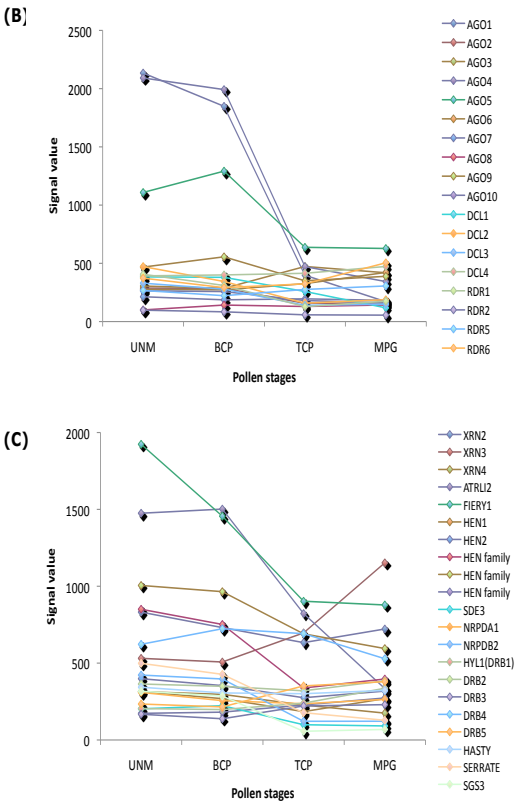

Figure 4.1(B,C). Graphical presentation of the pollen transcriptomic data showing pattern of transcript abundance of the small RNA components during male gametophyte development. Majority of the genes are expressed highly at the earlier stages at similar intensity and crushed to lower expression level towards pollen dehiscence.

4.2.2 Verification of the expression profile of smRNA components by RT-PCR

Following analysis of pollen transcriptomic data, an insight into the pollen expression profiles of several key RNAi components was obtained. To verify these observations independently, RT-PCR analysis was performed with RNA extracted from the four stages of pollen development according to Honys and Twell, 2004. For each gene, primer sets were design to span an intron and amplify a region of between 500-600bp for genomic DNA and ~300bp for cDNA (See primers list Appendix table 1). Primers efficiency and specificity were initially tested with genomic DNA and cDNA from seedlings. 750ng of total RNA isolated from the four pollen stages was used to synthesis cDNA and 1/10 of the cDNA dilution was used to analyse transcript abundance of each gene in a 30 cycles of PCR reaction as described in Chapter 2 section 2.6.

ARGONAUTE: Argonaute family members showed different patterns and levels of expression as depicted from the microarray data. Three major groups were identified, those that showed 2-5 fold higher expression levels compare to those of second and third group members; members that had intermediate level of expression; and those that were not reliably detected. With RT-PCR experiment, the expression pattern observed can also be classified into three major groups. The first group includes members that are expressed in all four stages of pollen development with highest expression at the earlier stages; members that were only expressed at microspore and bicellular stages but not detected at the later stages; and a third group that included members that were not detected at early stages but interestingly were detected later during pollen maturation. The first group consists of *AGO1*, *AGO4*, *AGO5* and *AGO9*. *AGO1* has highest transcript abundance at microspore and bicellular stage and a great decline but reliably detected at tricellular and mature pollen stage (Figure 4.2B). *AGO4*, *AGO5* and *AGO9* shows similar pattern of expression with highest expression

at the first two stages, reduced expression at the tricellular stage, and increased signal at mature pollen stage. Although, this is not very obvious for *AGO4*, as it difficult to judge clearly the difference of transcript abundance between tricellular and mature pollen stages. The second group consist of *AGO2*, *AGO6* and *AGO10*. All three genes show high transcript accumulation at microspore and bicellular stage but no detection at tricellular and mature pollen stage. *AGO3*, *AGO7* and *AGO8* belong to the third group. *AGO3* and *AGO7* are not detected throughout the pollen stages after the 30 cycles of PCR reaction, whereas, *AGO8* is also not detected at microspore, bicellular or tricellular stage, but show reliable detection at the mature pollen stage.

These results have verified and provide more evidence for the expression of Argonaute family members that was not obtained from the microarray data.

DICER-LIKE (DCL): Analysis of the microarray data showed that *DCL1* has a reliable detection only at the bicellular stage and a marginal call at the microspore stage. Whereas, *DCL2* and *DCL3* had reliable detection at the microspore and bicellular stages and a marginal calls at tricellular and mature pollen stages. Equally *DCL4*, showed only a marginal call at the bicellular stage. This pattern was verified by RT-PCR results with a slights different outcome. Following RT-PCR analysis, *DCL1* was detected at the microspore stage with an increased transcript accumulation at the bicellular stage (Figure 4.2C). But more markedly, *DCL1* showed highest expression at the mature pollen stage, a signal that was not detected by the microarray experiment. *DCL2* and *DCL3* showed a similar pattern as that observed with microarray data showing reliable detection at the microspore and bicellular stages, but no hybridization signal at the later stages. *DCL4* also showed a similar pattern to that predicted by the microarray data with no transcript detection throughout pollen development.

New critical information was again revealed by the RT-PCR for *DCL1* that was unveiled by the microarray data, and also verified the expression pattern for the other Dicer like genes.

RNA DEPENDENT RNA POLYMERASE (RDR): The four member of the RDR family, *RDR1*, *RDR2*, *RDR5* and *RDR6*, were reliably detected at the first two stages of pollen development according to the microarray dataset. The interesting pattern that was revealed by the pollen transcriptomic data was the exclusive marginal detection of *RDR6* transcript at the mature pollen stage that was not present at the tricellular stage. However, no information was obtained for the expression pattern of *RDR3* and *RDR4*, as the two genes were not represented on the Chip. Following RT-PCR reaction, *RDR1* showed exact pattern as that observed with the microarray data with maximum expression at the microspore stage, reduced expression at the bicellular stage, and no expression at tricellular or mature pollen stage (Figure 4.2E). *RDR2* again showed similar pattern as that of the microarray data, however, RT-PCR results revealed a clear transcript detection at the later stages. *RDR3* showed maximum transcript abundance at the microspore stage and a gradual decrease at bicellular and tricellular stage, but no transcript could be detected at the mature pollen stage. *RDR4* showed high transcript abundance at microspore and bicellular stage and a gradual reduction at tricellular and mature pollen stage. RT-PCR analysis for *RDR5* was consistent with the pattern predicted by the microarray data at the first two pollen stages, but noticeably, RT-PCR results revealed expression at the mature pollen stage that was not observed in pollen transcriptomic data. Unlike the pattern that was predicted by the microarray data for *RDR6*, RT-PCR results revealed strong transcript detection at the microspore and bicellular stage. This pattern continued with an approximately two-fold reduction at the tricellular and mature pollen stages.

In the case of RDR family, the increased sensitivity of the RT-PCR analysis provided valuable information particularly at the tricellular and mature pollen stages where no reliable signal was obtained by microarray analysis.

The presence of other genes that have also been demonstrated to be involved in the smRNA pathway including *HYL1*, *SERRATE*, *HASTY* and *HEN1*, were also verified by RT-PCR. *HYL1*

showed detectable transcripts at the microspore stage that increased at the bicellular stage (Figure 4.2D). No transcripts were detected at the tricellular or mature pollen stage. RT-PCR results for *SERRATE* showed a very similar pattern to that predicted by the pollen transcriptomic data with high transcript abundance at the microspore and bicellular stage, and reduced transcript levels at the tricellular stage (Figure 4.2D). However, RT-PCR provided additional information by demonstrating presence of transcripts at mature pollen stage. *HASTY* showed reliable expression level at the microspore stage in both experiments, reduced signal at bicellular stage, and lack of expression at tricellular and mature pollen stage (Figure 4.2D). *HEN1* showed a slightly different pattern from that observed with the microarray data with a detectable signal at the microspore stage, increased transcript level at the bicellular stage, and no detectable transcript at tricellular or mature pollen stages (Figure 4.2D).

In summary, microarray data from the four stages of pollen development has provided valuable information regarding the pattern of some of the components involved in the smRNA machinery. However, this data needed to be verified independently and fill the gaps for the missing genes that where not represented in the microarray experiment. The results of the RT-PCR experiment verified some of the the microarray data and added new information by providing the expression patterns for several genes that were not represented on the Affymetrix chip, and also revealed new patterns that were not reliably detected by the microarray.

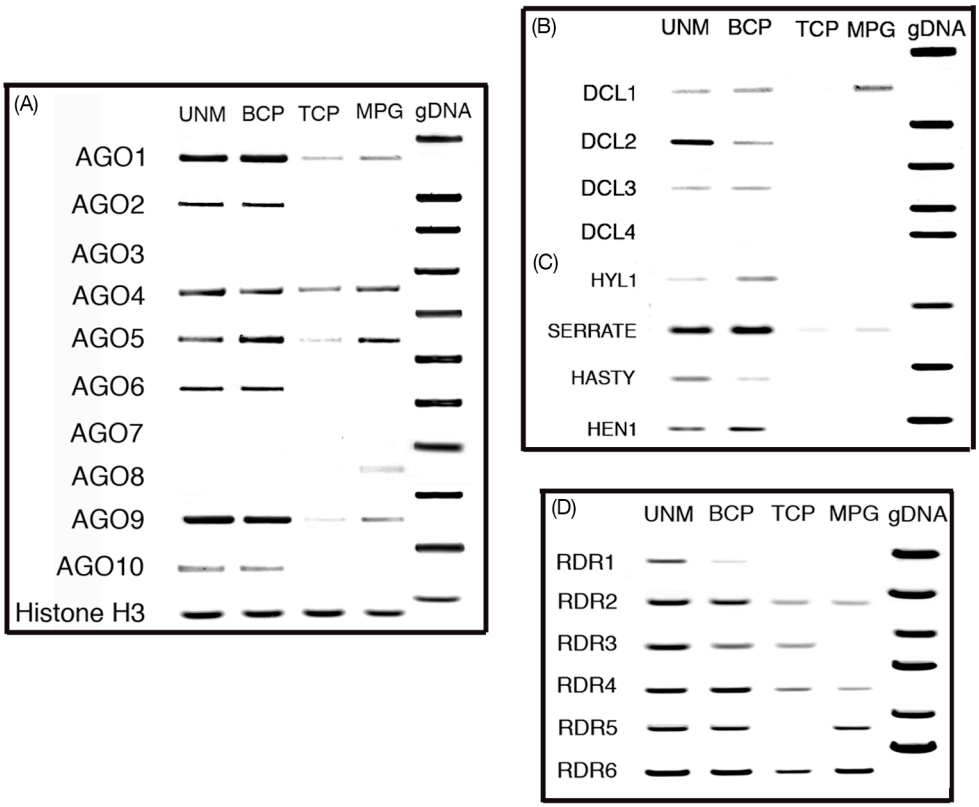

Figure 4.2. ***Expression pattern of smRNA components at the four stages of pollen development.***
Total RNA isolated from unicellular microspores (UNM), bicellular pollen (BCP), tricellular pollen (TCP) and mature pollen grains (MPG) were analyzed by RT-PCR. (A) A profile of the smRNA components showing (A) Argonaute family members; (B) Dicer-like 1-4 (DCL1-4); (C) HASTY, SERRATE, HEN1; (D) six members of the RNA Dependent RNA polymerase family (RDR). HISTONE H3 (AT4G40040) was used as a control to demonstrate equal input of the starting cDNA. The reproducibilty of these patterns was tested by amplifying target transcripts in three independent amplification reactions.

4.3 Construction of pollen cell-specific expression vectors

Investigating the expression pattern of key smRNA components in the four stages of male gametophyte development was an initial step in the investigation of whether the smRNA silencing pathways are functional in the male gametophyte. Analysis of the pollen transcriptomic data and RT-PCR experiments revealed that all key genes that have been identified to date to participate in the smRNA pathways shows reliable expression at different phases of pollen development. To test the functionality of these pathways, pollen specific vectors were constructed that would allow expression of hairpin dsRNA with the potential of inducing degradation of target mRNA transcripts in specific cell types during pollen development.

Prior to the initiation of this project, none of these tools existed, however, a subset of pollen specific expressed promoters were already identified. In this section, identification, selection and cloning of pollen cell-specific promoters together with cloning of the target sequences for functional test of RNAi activity in pollen is discussed.

4.3.1 Selection of pollen specific promoters

To identify pollen cell specific promoters that could be used to manipulate gene expression in a spatial and temporal fashion, two strategies were adopted; one was to explore the literature on the current knowledge of pollen expressed promoters, and the second was to analyse pollen transcriptomic data sets to identify promoters that were exclusively expressed in pollen.

At the beginning of this project, a number of male gametophyte specific expressed promoters that showed activity at different stages of pollen development were known. These include LAT52 and LAT59 promoters with specific high activity in the vegetative cell (Twell, 1990) and have been demonstrated to be highly active in a number of plant species. These promoters have now been widely used to drive gene expression specifically in pollen.

A few early expressed promoters active at the microspore stage have also been identified in different plant species. These include the tobacco *NTM19* promoter which has a strict microspore specific expression (Oldenhof et al., 1996; Custers et al., 1997), the *BnM3.4* promoter from rapeseed which is active in tetrad and microspores (Fourgoux-Nicol et al., 1999), the *invGF* promoter from potato which is active from late microspore stage (Maddison et al., 1999), and Arabidopsis the *BCP1*, *AtSTP2* and *TCP16* promoters which are active from tetrad stage (Li et al., 2005a; Xu et al., 1993; Truernit et al., 1999).

Furthermore, in the last few years, a small number of late expressed promoters including those that are specifically expressed in the germ cell and sperm cells have been identified. *GEX1* and *GEX2* were initially proposed to be specifically expressed in the germ cell and sperm cells with the exception of *GEX1*, which is also expressed in the vegetative cell and other sporophytic tissues (Engel et al., 2005). However, in the last few months, *GEX2* and *GEX3* have also been shown to be active in the egg cell of the female gametophyte (Alandete-Saez et al., 2008). *gcH3* and *gH2A* from *Lilium longiflorum* have also been demonstrated as sperm cell specific expressed promoters (Okada et al., 2005). *DUO1*, R2R3 MYB transcription factor that was isolated as a division mutant required for germ cell mitotic progression and sperm cell differentiation, has also been shown to be active from newly formed germ cells and in sperm cells (Durbarry et al., 2005; Rotman et al., 2005).

Other promoters that have also been identified to be pollen specific include *AtPTEN1* (Gupta et al., 2002), rapeseed *Bp10* (Albani et al., 1992), *AtSTP6* and *AtSTP9* (Scholz-Starke et al., 2003; Schneidereit et al., 2003), petunia *chiA* (van Tunen et al., 1990), *AtTUA1* (Carpenter et al., 1992), maize *Zm13* (Hamilton et al., 1992), *AtVEX1* (Engel et al., 2005) and tobacco *NTP303* (Weterings et al., 1995).

In addition to the use of literature, availability of transcriptomic data from microarray experiments covering various sporophytic and gametophytic tissues including the four stages of pollen development (Dupl'akova et al., 2007), now provides genome wide expression

profiles of over 20,000 genes from the Arabidopsis genome. Taking advantage of these facilities, transcriptomic analysis of the four stages of pollen development in comparison with sporophytic expression was performed to identify pollen specific expressed promoters. The aim of this exercise was to identify Arabidopsis microspore specific promoters that will allow manipulation of gene expression at the early stages of male gametophyte development. This work was exclusively done by Honys et.al, 2006. My involvement with the project was to explore one of the isolated candidate promoters (MSP1, AT5G59040) for its functional specificity prior to publication.

4.3.2 Modifying Gateway destination vectors

Construction of expression vectors with the implication of testing the activity of smRNA pathway involved modification of existing gateway binary plant transformation vectors (Karimi et al., 2002). The original destination vectors obtained contained a 35S tobacco mosaic virus constitutive promoter in the case of sense and anti-sense vectors (pB2GW7, pB2WG7, pH2GW7 and pH2WG7). And for the RNAi expression vector (pK7gwiwgL), the original vector had no cloned promoter; instead, the vector contained a linker region that contains restriction sites specific to the linker region to facilitate conventional cloning of promoters of interest. For detailed cloning procedures refer to Chapter 2 section 2.9. Briefly, to clone pollen specific promoters into the RNAi destination vector, 980bp upstream of *MSP1* coding region, 2kb of *TCP16* putative promoter region, 482bp of *LAT52* promoter fragment, and 1700bp of *GEX2* putative promoter sequence, were amplified by a proof reading thermally stable DNA polymerase (Kod-HiFi, Invitrogen) to introduce HindIII and XhoI restriction sites. A 1200bp of *DUO1* promoter fragment was amplified to introduce HindIII and NruI restriction sites. For sense and anti-sense vectors, similar size promoter fragments were amplified, but instead, SacI and SpeI restriction sites were introduced. The amplified promoters together with the vector backbones were digested, PCR purified and ligated with the destination vectors. Positives clones were subjected with PCR and restriction analysis.

Verified clones were then used in the LR reaction to introduce target gene sequence (Figure 4.3).

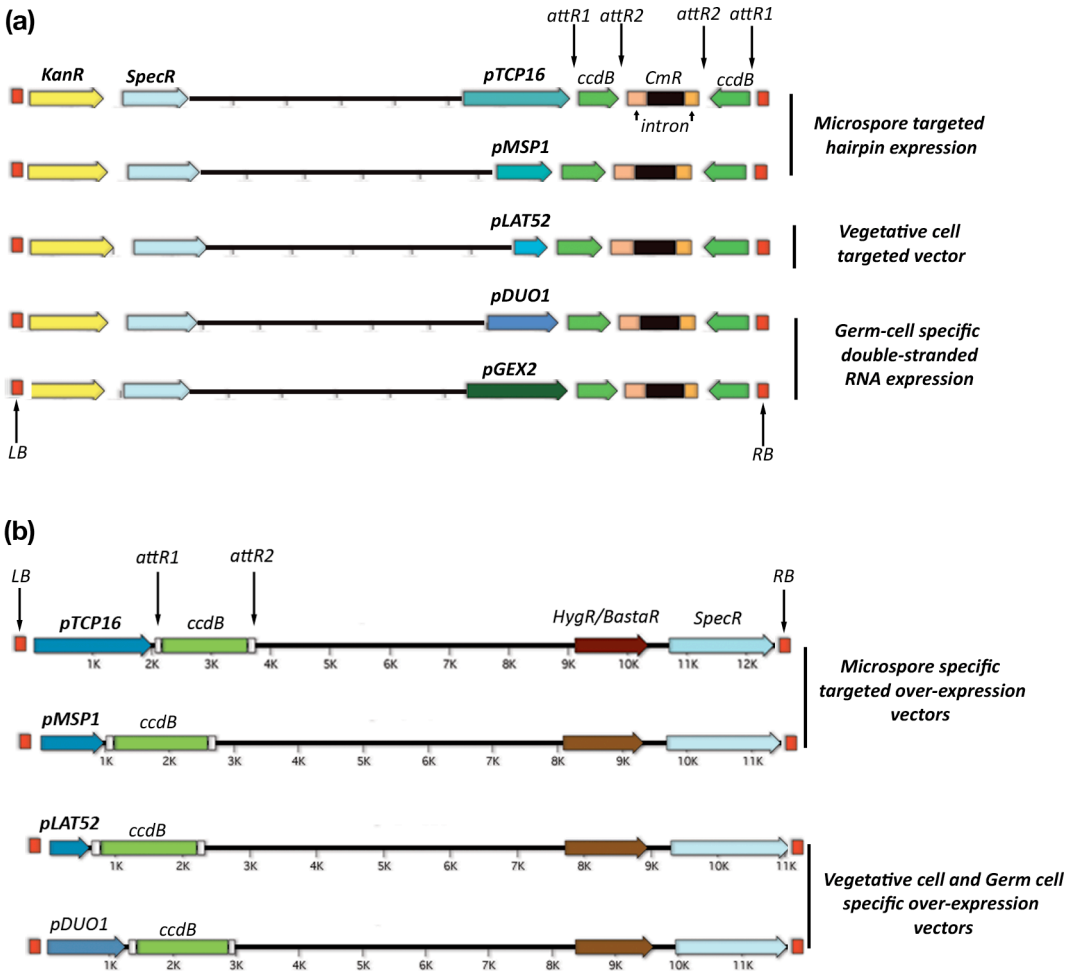

Figure 4.3. ***Pollen cell-specific expression vectors for manipulating gene expression***
Gateway destination vectors (pK7gwiwgL, pB2GW7 and pH2GW7 which possess pzp200 backbone) modified to accommodate pollen cell-specific promoters as tools for high throughput reverse genetic studies in the model male gametophyte of Arabidopsis thaliana.(a) Destination vectors used for the expression of dsRNA for down regulating target genes of interest in a temporal and spatial cotrolled manner through the RNAi-mediated pathway. (b) Expression tools for studying over-expression and ectopic expression of genes of interest during pollen development in specific cell types and at a define stage of pollen development.

4.3.3 Cloning target sequences

To ensure an informative outcome, a strategy was adopted which involves targeting known proteins that have been demonstrated to be essential in the progression of cell cycle and completion of cytokinesis during male gametophyte development. The target genes selected include *Two-In-One* (Oh et al., 2005), *CDKA-1* (Nowack et al., 2006) and *DUO POLLEN1* (Durbarry et al., 2005). In addition to the known targets, other genes were also targeted to address their role in specific cell types during pollen development. These include Retinoblastoma related (*RBR*) protein, an inhibitor of S-phase progression and chromatin remodelling in the female gametophyte, and AtCycB1 family which has been demonstrated to play essential role during G2/M transition and mitotic progression.

All target sequences were PCR amplified using gene specific primers tagged with recombination adapter sequences (attB1 and attB2; see Chapter 4 section 2.9.2). The PCR products were cloned into the donor vectors (pDONR207) to generate entry clones. Verified entry clones were then used in an LR reaction with the modified pollen cell-specific destination vectors to generate the final pollen expression vectors. All the constructs were verified by PCR analysis, restriction digestion and antibiotic selection particularly in testing the stability of the hair-pin structure in the RNAi vectors.

4.4 Functional analysis; Application of the tools

To test the molecular vectors that were generated with the intention of demonstrating the functionality of the RNAi mechanism during male gametophyte development, several vectors with cloned target sequences driven by pollen cell-specific promoters were introduced into wild type Col-0 plants through *Agrobacterium tumefaciens* mediated plant transformation (floral dipping). The vectors were designed to demonstrate RNAi activity in microspores using *TCP16* and *MSP1* promoters, RNAi activity in the vegetative cell using *LAT52* promoter and most importantly in the germ cell using *DUO1* and *GEX2* promoters.

Approximately 39 primary transformants were generated for each construct and analysed by bright field microscopy and by DAPI staining with fluorescence microscopy to detect aberrant phenotype.

4.4.1 smRNA activity at the microspore stage

To analyse the functionality of the RNAi pathway at the microspore stage, two constructs containing *TCP16* and *MSP1* promoters were used to drive expression of hairpin double stranded RNA for targeting *CDKA-1*, and *AtCycB1* mRNA transcripts. Results of the *AtCycB1;1* knockdown at the microspore stage are presented in Chapter 3.

CDKA-1 knockdown:

Analysis of DAPI stain mature pollen grains from primary transformants harbouring the pK7TCP16-hpCDKA-1 construct revealed 16/39 individuals (41%) that contain aberrant pollen phenotype (Table 4.1.). The phenotype range between 5% - 48% of aberrant pollen among individuals and the phenotypic classes observed include pollen grains with unicellular microspore arrest, pollen grains that were arrested at the bicellular stage, and a dominant proportion of collapsed pollen grains (Figure 4.4).

On the other hand, when a similar experiment was performed but this time using the MSP1 promoter (pK7MSP1-hpCDKA-1), only 4/32 individuals of the total population (12.5%) showed aberrant pollen phenotype (Table 4.1). Moreover, unlike the *TCP16* construct, individuals carrying the MSP1-hairpin transgene showed a phenotype that range between 5% - 13% maximum aberrant pollen grains. In this case, the phenotype observed was dominantly bicellular arrest and collapsed pollen, no unicellular microspore arrest phenotype was observed.

This analysis demonstrate that selection of appropriate tools taking into consideration the activity and its temporal pattern is essential and can result in a different outcome if wrongly applied. Nevertheless, applications of both constructs have indicated existence of RNAi

activity for modulating transcript abundance at the microspore stage. Further evidence of RNAi activity at the microspore is demonstrated by the pK7MSP1-hpCycB1 construct in Chapter 3.

		Bright field screen			***Nuclear staining screen (DAPI)***		
Line ID	Generation	Wt	Aberrant	% mutant pollen	Wt-Tricellular pollen	Bicellular pollen	% bicellular pollen
MSP1-hpCDKA							
1	T1	400	5	1.2%	300	0	0.0%
2	"	350	22	5.9%	400	3	0.7%
4	"	346	33	8.7%	263	11	4.0%
9	"	319	4	1.2%	507	75	12.9%
11	"	416	231	35.7%	307	3	1.0%
13	"	385	49	11.3%	382	6	1.5%
14	"	316	39	11.0%	477	24	4.8%
21	"	442	11	2.4%	212	4	1.9%
32	"	399	10	2.4%	219	3	1.4%
33	"	570	8	1.4%	254	5	1.9%
35	"	216	5	2.3%	274	24	8.1%
TCP16-hpCDKA							
2	"	213	21	9.0%	198	15	7.0%
3	"	167	5	2.9%	201	3	1.5%
11	"	254	16	5.9%	248	229	48.0%
13	"	178	20	10.1%	190	19	9.1%
14	"	211	13	5.8%	224	45	16.7%
16	"	207	9	4.2%	189	12	6.0%
22	"	284	223	44.0%	165	3	1.8%
30	"	188	14	6.9%	231	8	3.3%
34	"	257	122	32.2%	209	26	11.1%
35	"	195	138	41.4%	223	14	5.9%
36	"	216	167	43.6%	189	17	8.3%
39	"	242	9	3.6%	219	189	46.3%

Summary of the two microspore promoter activities in down-regulating CDKA expression

Construct name	*Generation*	*No of mutant plants*	*Frequency of the mutant plants*	*Pollen phenotype frequency (Range)*	*Phenotypic classes*
pK7MSP1-hpCDKA	T1	4/32	12.50%	5% - 13%	Bicellular arrest and Collapse pollen
pK7TCP16-hpCDKA	T1	16/39	41%	>5% - 48%	Microspore and Bicellular arrest, Collapse

Table 4.1. **Functional analysis of the CDKA role at the microspore stage by RNAi knockdown**
Two microspore specific promoters (MSP1 and TCP16) were used to drive the expression of double-stranded RNA targeted to CDKA transcript to test whether the smRNA pathway is functional at the microspore stage. Upper panel of the table shows some of the representative individuals generated from each construct and the phenotype observed. The lower panel of the table summaries the efficiency of the two promoter constructs in generating the *cdka;1* mutant phenotype. The MSP1 promoter showed weaker effect with only 12.5% of the T1 population posessed the mutant phenotype. In contrast, 41% of the population hourbouring the TCP16 driven hairpin construct showed the mutant phenotype.

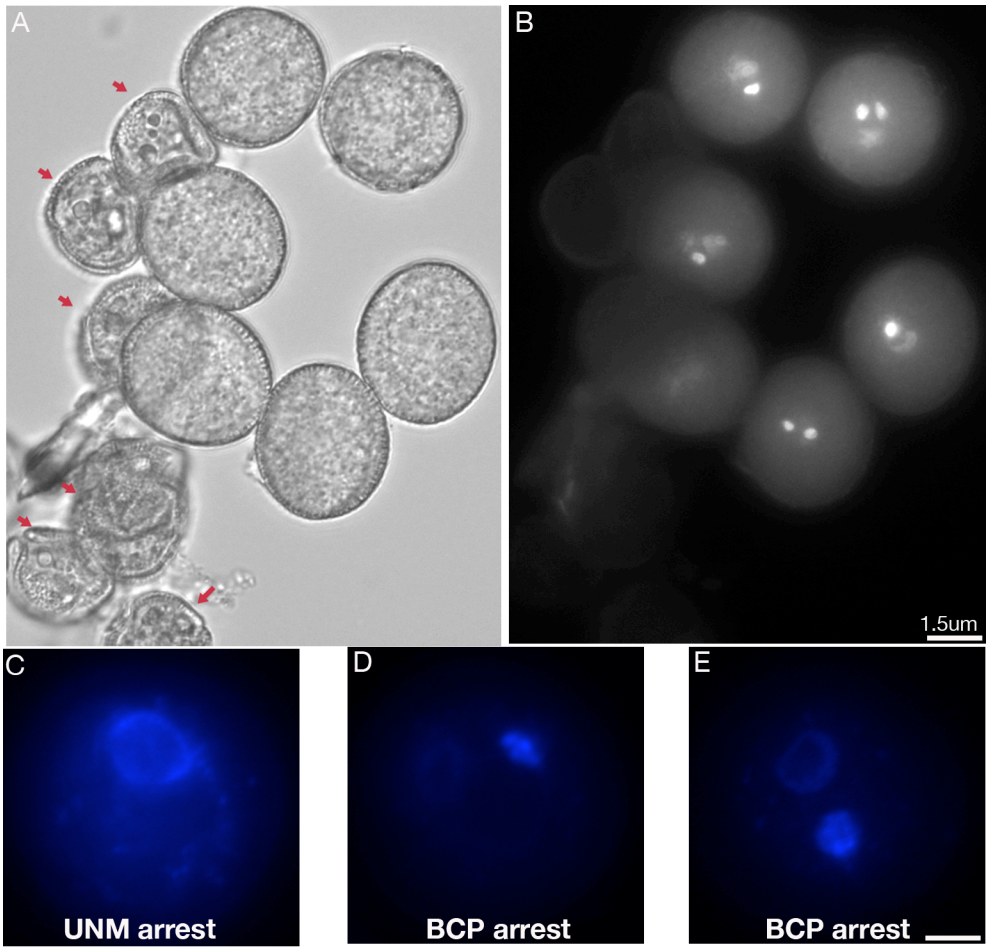

Figure 4.4. **Expression of pTCP16-hpCDKA at the microspore stage**
Analysis of CDKA role during microspore development. (A-B) DIC and corresponding DAPI images showing collapsed pollen phenotype (red arrows) as observed in primary transformants carrying the pK7TCP16-hpCDKA construct. Scale bar (C-E) Magnified DAPI stain florescence images show microspore and different degrees of bicellular arrest phenotypes of the CDKA deprived pollen grains. All images were taken at the mature pollen stage. Scale bar 5µm.

4.4.2 smRNA activity in the vegetative cell

The pollen cell-specific molecular vectors that were generated also equally provided an opportunity to test the activity of the RNAi pathway in the vegetative cell. The vegetative cell has been proposed to be blocked at G1-phase of the cell cycle following completion of PMI based on its DNA content, and fails to progress through another round of S-phase (Zarsky et al., 1992). Taking advantage of this opportunity, the strategy was to try to demonstrate existence of RNAi activity in the vegetative cell and simultaneously highlight a possible mechanism that blocks the vegetative cell at G1 and inhibit its progression through another round of S-phase. A well characterised inhibitor of S-phase progression, RBR, was selected as a putative candidate that may induce the vegetative cell G1/S block. A hairpin construct was generated to target RBR mRNA transcripts specifically in the vegetative cell using a LAT52 promoter. The construct generated, pK7LAT52-hpRBR was introduced into wild type Col-0 plants and primary transformants were analysed for deviation from the wild type phenotype.

Following analysis of 34 primary transformants, 18/34 individuals showed presence of collapsed pollen and a novel phenotype showing pollen grains with enhanced vegetative cell nucleus staining (Figure 4.5). The phenotypes range between 5% - 40% aberrant pollen. The occurrence of the phenotype was directly linked to the presence of the effector transgene through PCR analysis of genomic DNA extracted from the mutant plants (n=10). Analysis of the phenotype was extended further to the T2 generation and two sibling lines (Line A6 and B2) were studied in detail. Developmental analysis of these individuals revealed that polarization of the microspore nuclei was not perturbed in the mutant plants (Figure 4.5d). Furthermore, the origin of the collapsed pollen phenotype was observed from the bicellular stage and peaks towards mature pollen stage for the siblings of line B2 (29% - 35% collapsed pollen grains), and for siblings of line A6 the collapse pollen phenotype observed at the bicellular stage showed only a slight increase (25-28% collapsed pollen) to mature pollen

stage (Figure 4.5e). However, a reciprocal pattern was observed for the proportion of pollen grains with Increased Vegetative cell Fluorescence (I.V.F) phenotype. The I.V.F phenotype was initially detected from the tricellular stage for both lines and increased in mature pollen for line A6 siblings (16% – 27% mutant pollen), however this phenotype was reduced for the siblings of line B2 which showed 18% - 9% of mutant pollen grains. To verify the I.V.F phenotype observed, DNA content of the vegetative cell nucleus was estimated and compared between wild type pollen grains and pollen grains that posses the I.V.F phenotype by measuring fluorescence intensity of the vegetative cell nucleus. Following this analysis, a new class of pollen population was identified that contained increased DNA content compared to the average DNA content observed in the wild type population (Figure 4.5f). The average mean values (fluorescence unit) of the DNA content from the mutant populations were verified to be statistically significantly different from that of the wild type population (Chi-square test, $p<0.01$ at 5% significant level with Yates correction). The collapsed pollen phenotype verified what was already reported from the analysis of RBR T-DNA insertion, +/*rbr-1*, (Ebel et.al, 2004); however, the I.V.F phenotype is unique to the RNAi lines generated.

The presence of these predicted phenotypic classes following degradation of the RBR mRNA transcript, as a consequence what looks like releasing inhibition of S-phase progression, has also demonstrated existence and activity of the RNAi pathway in the vegetative cell.

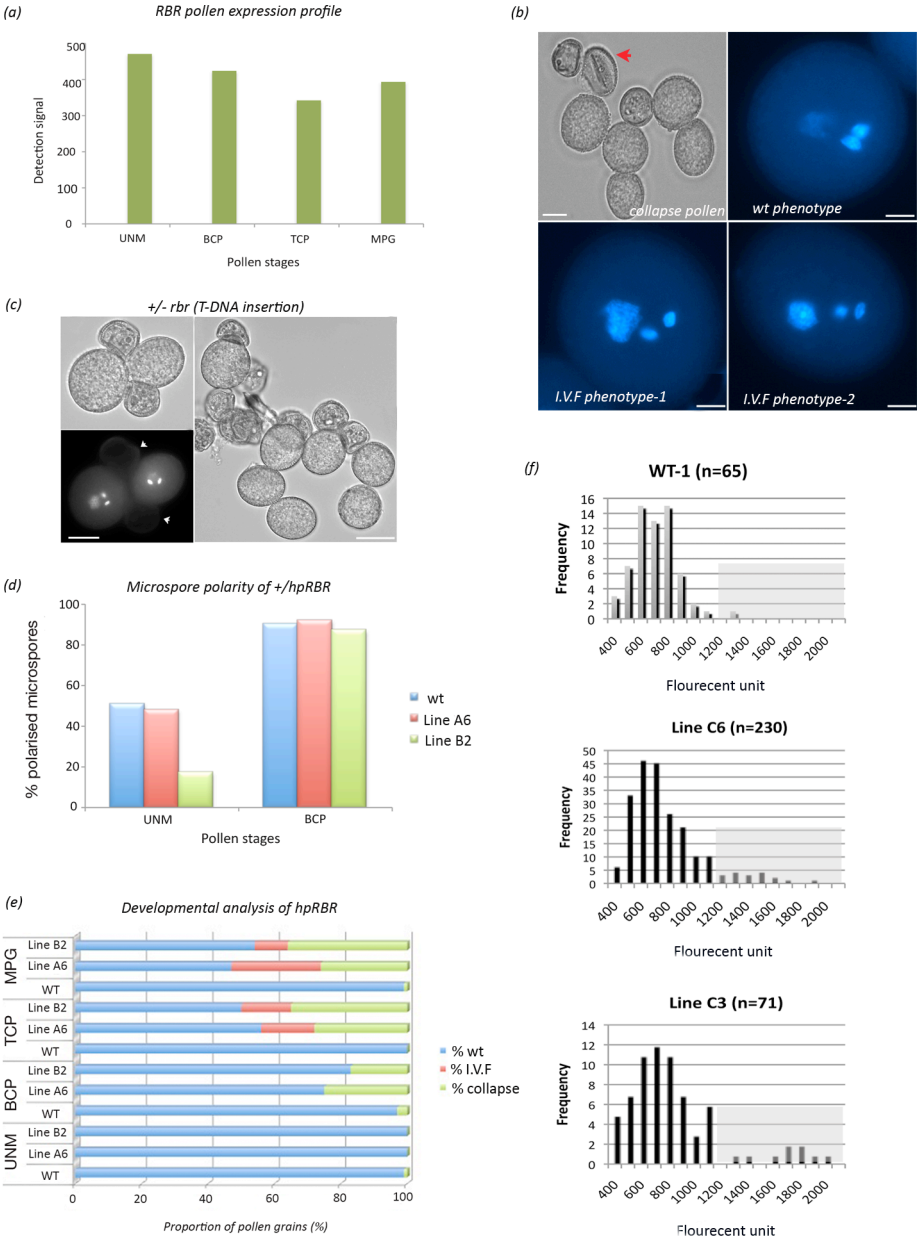

Figure 4.5. **Phenotypic classification of hpRBR plants during pollen development** Cytological analysis of plants carrying pK7LAT52-hpRBR expression vector to analyse role of RBR in the vegetative cell. (a) Pollen transcriptomic pattern of the RBR expression. (b-c) Identification of phenotypic classes by light and fluorescence microscopy of hpRBR individuals (b) and T-DNA carrying RBR allele (c); The two alleles posses a common collapse phenotype (red arrow in b, and white arrows in c), however, the Increased Vegetative nuclear fluorescence phenotype (I.V.F) is only observed with hpRBR lines. (d-e) Identification of the origin of the hpRBR phenotypic classes; (d) Normal polarization of the microspore nuclei in wild type and two independent lines of hpRBR individuals, (e) plot show the frequency of the phenotypic classes observed in hpRBR individuals during pollen development and the origin of the phenotype. Figure represent mean values of five siblings from two independent parents (Line A6 and B2) taken from the T2 generation. (f) Measurement of vegetative cell nucleus fluorescence at the mature pollen stage emphasizing the new class of pollen grain with the I.V.F phenotype that is not observed in the wild type. Bin range on the X-axis represent mean fluorescence unit. Fluorescence intensity was measured using Nikon 2000 fluorescence microscope and OpenLab 5.8 software.UNM; unicellular microspores, BCP; bicellular pollen, TCP; tricellular pollen, MPG; mature pollen grains. Scale bar 4µm.

4.4.3 smRNA activity in the germ cell

Pollen transcriptomic profiles of the majority of the genes showed reduced transcript abundance from bicellular stage and great transcript repression at tricellular and mature pollen stage. This gene expression shutdown might be achieved either through pretranscriptional repression by inhibiting transcription activation or through post-transcriptional repression by preventing transcript accumulation through mRNA degradation, or a combination of both mechanisms. To test weather germ cells possess RNAi activity in modulating transcript abundance, two germ cell specific promoters were used (*DUO1* and *GEX2*) to drive expression of hairpin dsRNA for targeting *DUO1*, *CycB1* and *Two-In-One* (*TIO*) mRNA transcript specifically in the germ cell. Results of *CycB1* knockdown in the germ cell are presented in Chapter 3.

AtDUO1 knockdown:

The DUO1 protein has been demonstrated to be essential for germ cell division at PMII in Arabidopsis (Durbarry et al., 2005; Rotman et al., 2005). To target the *DUO1* mRNA transcript for degradation, a 500bp fragment of *DUO1* coding sequence was cloned into the RNAi destination vector (in sense and anti-sense orientation) containing the *DUO1* promoter to generate pK7DUO1-hpDUO1 construct (Figure 4.6A). The construct was transformed into wild type Col-0 plants and primary transformants were screened for pollen phenotype.

Morphological screens for pollen division phenotypes of 40 primary transformants that were generated revealed 15/40 individuals that carried a *duo*-like phenotype at the mature pollen stage (Figure 4.6B). The phenotype observed included collapsed pollen and in some individuals the phenotype was pre-dominantly *duo*-like phenotype ranging between 4% - 27% *duo*-like pollen grains. The vegetative part of the primary transformants did not show any developmental abnormalities and the morphology of the vegetative cell was un-altered. Thus, the pK7DUO1-hpDUO1 construct shows specificity towards the germ cell expression as expected.

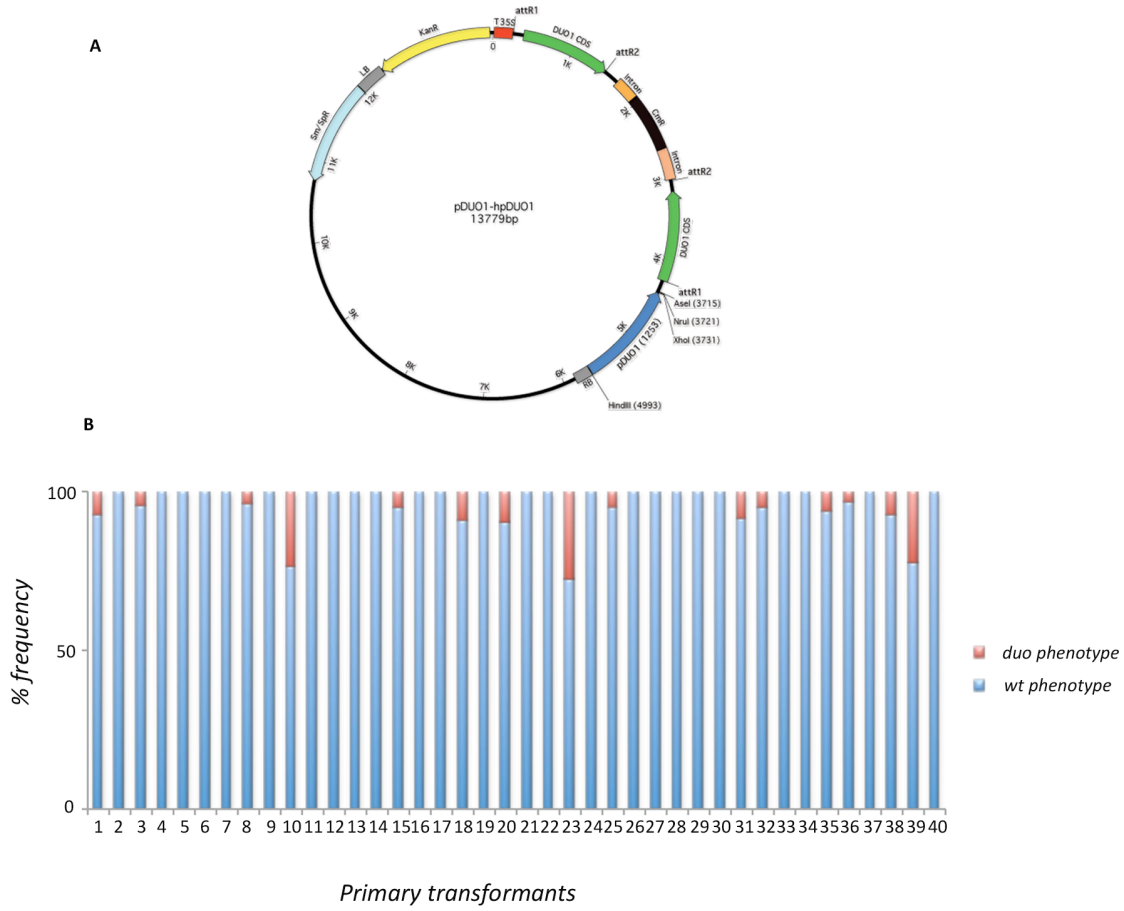

Figure 4.6. ***Germ cell specific RNAi-mediated silencing of the DUO1 transcription***
(A) Construct harbouring DUO1 promoter driving the expression of 500bp DUO1 derived sequences for directing clevage of DUO1 mRNA transcript accumulation by the PTGS mechanism. (B) Result of the primary transformants showing a duo-like phenotype following a light and DAPI screen of the mature pollen grains.

TIO knockdown

Previously, Oh et.al, 2006 demonstrated the role of *Two-In-One* (*TIO*) during microspore division in the male gametophyte and its role during cellularization of the female gametophyte. *TIO* was shown to be required for completion of cytokinesis (assembly of the entire phragmoplast wall) and separation of the two daughter nuclei. To address the role of

TIO in the male germ cell, 500bp of *TIO* genomic fragment from the 3'-end of the coding sequence was cloned into the RNAi vector harbouring a *GEX2* promoter to generate a pK7GEX2-hpTIOC construct (Figure 4.7A). The construct was transformed into wild type Col-0 plants and seeds were plated on kanamycin to select for transformants. DAPI screen under fluorescence microscope revealed 6/17 of the primary transformants generated possessed aberrant pollen phenotype that did not resemble the wild type phenotype (Figure 4.7B). The phenotype observed range between 34% - 47% mutant pollen and included collapsed pollen phenotype (in 2/6 of the mutant individuals), bicellular and uninucleate contained pollen grains (from 4/6 of the mutant lines). The vegetative development of the primary transformants generated did not vary much from that of the wild type, however, it should be noted that there were only a few primary transformants that were generated. With the current knowledge of *GEX2* promoter being active in the egg cell of the female gametophyte, it is possible that the pK7GEX2-hpTIOC construct also affects *TIO* transcript abundance in the female gametophyte which would result into embryo lethality hence generate less transformants

These findings have demonstrated the role of *TIO* in the male germ cell and provided independent evidence for the existence of RNAi activity in the male germ line.

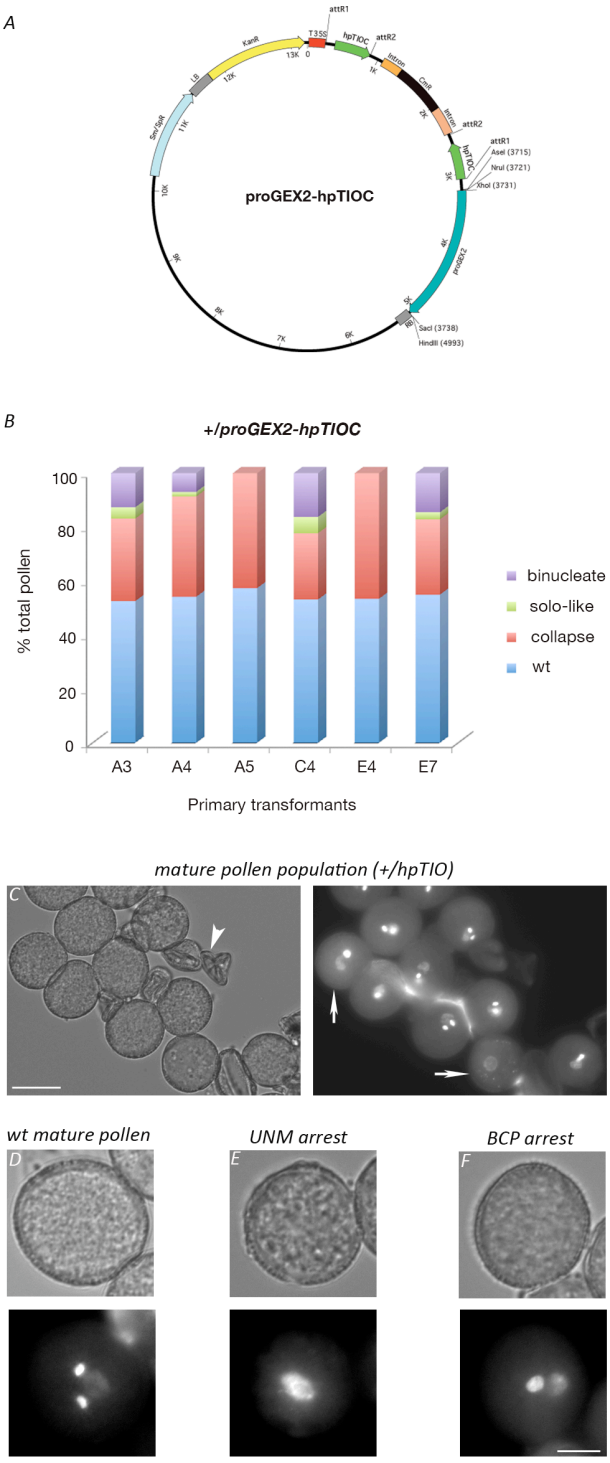

Figure 4.7. **Effect of the pGEX2-hpTIO in the male germ cell** Expression of hp-dsRNA directed to the *TWO-IN-ONE* mRNA specifically in the generative cell using *GEX2* promoter. (A) Map of the construct used to drive the expression of dsRNA for targeting *TIO* mRNA and direct cleavage. (B) Frequency of the phenotypic classes observed in primary transformants that express the pGEX2-hpTIO construct as observed at the mature pollen stage. 35% (6/17) of the primary transformants that were generated possess the aberrant phenotype (C) Micrographs of light and corresponding DAPI stain pollen population show phenotypic classes as observed at mature pollen stage; arrow head show a collapse pollen phenotype and the arrows on the DAPI image show a binucleate pollen grain and a microspore arrested nucleus. Scale bar 2um (D-F) High resolution light and DAPI micrographs show wild type, unicellular microspore arrested nuclei and a bicellular pollen grain respectively. Wt – wild type, UNM-unicellular microspore, BCP-bicellular. Scale bar 6um.

4.4.4 Testing vector specificity

To demonstrate precisely a cell specific role of a target gene of interest, it was essential to establish the specificity of the constructs used. To achieve this objective, control vectors were used in every experiment to express similar cloned target sequences as the experimental vectors but expressed either in a wrong tissue or at a wrong time.

The first construct to be used to test specificity of the promoters was the pK7LAT52-hpAtCycB1 that was used as a control for pK7MSP1-hpAtCycB1 and pK7GEX2-hpAtCycB1 hairpin constructs (see Chapter 3). *AtCycB1;1* which has been demonstrated to be required for germ cell division and also as one of the missing factors in *duo1* mutant pollen grains (Brownfield et al., 2009), is not expressed in the vegetative cell post PMI and possess no known function in the vegetative cell. Morphological screen of plants harbouring the pK7LAT52-hpAtCycB1 construct showed no aberrant pollen phenotype and no effect on the vegetative cell development. These studies illustrate the specificity of the *LAT52* promoter and provide independent evidence for the source of the unique phenotypic classes observed with pK7MSP1-hpAtCycB1 and pK7GEX2-hpAtCycB1 constructs bearing the same target sequence. Further evidence for the specificity of these tools was obtained from the effector constructs by displaying specific targeted effect as initially predicted. For instance, pK7LAT52-hpRBR plants show deviation from the wild type phenotype from the bicellular stage after the completion of PMII and not earlier. Furthermore, analysis of transgenic plants carrying pK7GEX2-hpAtCycB1 construct shows specific effect on the germ cell affecting germ cell division and not an earlier microspore division.

Together, the series of the experiments performed have highlighted the presence of essential components that have an active role in several smRNAs pathways. The detection of these components during male gametophyte development hints the presence of smRNA pathways as a mechanism of transcriptional regulation. Generation of the pollen cell-specific vectors was a prerequisite in testing the hypothesis that smRNA pathways are functional in

the male gametophyte of Arabidopsis thaliana. Application of these vectors in targeting genes with and without known biological role, have effectively address the presence of the smRNA pathways in pollen. The temporal and spatial specificity of the vectors have provided essential tools for specific manipulation of new target genes. As such, screen of genes essential for male gametophyte development can now performed in a more controlled manner.

Chapter 5

Characterization of *DUO POLLEN3*

5.1 Introduction

Morphological analysis of the *duo pollen3* (*duo3*) mutant identified that pollen grains deficient of *DUO3* activity fail to progress through PMII, and produce a single germ cell at pollen maturation. The *DUO3* gene was mapped at the lower arm of chromosome 1 and was identified as AT1G64570 locus encoding a MYB-like protein. Monitoring of DNA content demonstrated that the *duo3* mutant germ cells complete DNA replication but bypasses the mitotic phase of PMII, reminiscent of the *duo1* phenotype. The key question investigated in this project was how the expression of *DUO3* differs from that of *DUO1,* a novel R2R3 MYB protein that is also required for germ cell division (Durbarry et al., 2005). The project also aimed at understanding the relationship of *DUO3* with that of a G2/M regulator, AtCycB1;1, in order to understand the nature of the *duo3* mutation. To accomplish these objectives, the temporal and spatial pattern of *DUO3* expression during plant development was analysed using publicly available microarray datasets and was later verified by RT-PCR analysis. To characterize the tissue specific pattern of *DUO3* expression, a 1kb genomic fragment upstream of the *DUO3* start codon was fused with a β-glucuronidase (GUS) marker and introduced into +/*duo3* plants. The nature of the *duo3* mutant phenotype in which the germ cell fails to progress through mitosis was investigated by analysing the promoter activity of *AtCycB1;1* using the chimeric construct pAtCycB1;1-D-box::GUS/GFP, introduced in the +/*duo3* mutant background and through complementation of *duo3* mutant phenotype by *AtCycB1;1*.

5.2 Expression profile of *DUO POLLEN3*

To investigate the expression pattern of the *DUO3* gene, three approaches were used. Microarray data available in public databases were first investigated exploring different tissue types and developmental stages to give an initial insight of the *DUO3* expression profile. To validate the microarray data, RT-PCR analysis was performed from RNA isolated from different tissue types and from the four stages of pollen development. To further understand the tissue specific and temporal pattern of *DUO3* expression, a *DUO3* promoter – GFP::GUS fusion construct was generated and analysed by in situ histochemical GUS staining and fluorescence microscopy throughout plant development.

5.2.1 Transcriptomic pattern of *DUO POLLEN3* expression

Two independent public databases, aGFP (Dupl'akova et al., 2007) and Genevestigator (Zimmermann et al., 2004) were explored to establish the profile of *DUO3* expression. Transcriptomic data from aGFP was normalized by dCHIP and the present and absent calls were determined using MAS5 algorithm. Analysis of *DUO3* expression in sporophytic tissues with the AtGenExpress dataset from aGFP showed constitutive expression of *DUO3* throughout development with enhanced expression in isolated tissues such as shoot apex, xylem and cork (Figure 5.1A). Furthermore, study of *DUO3* pollen transcriptomic profile using NASC datasets accessible at aGFP showed a gradual increase of *DUO3* transcript accumulation from microspore to mature pollen stage (Figure 5.1A). Independent analysis was also carried out using the Genevestigator database by exploiting NASC and AtGenExpress datasets deposited. Again, a similar pattern of *DUO3* expression was also observed with Genevestigator (Figure 5.1B-D) covering an extensive collection of tissues allows high resolution profiles throughout development. The *DUO3* profile is compared with

that of a well characterized G2/M cell cycle marker, AtCycB1;1, to highlight the overlap expression pattern between the two genes.

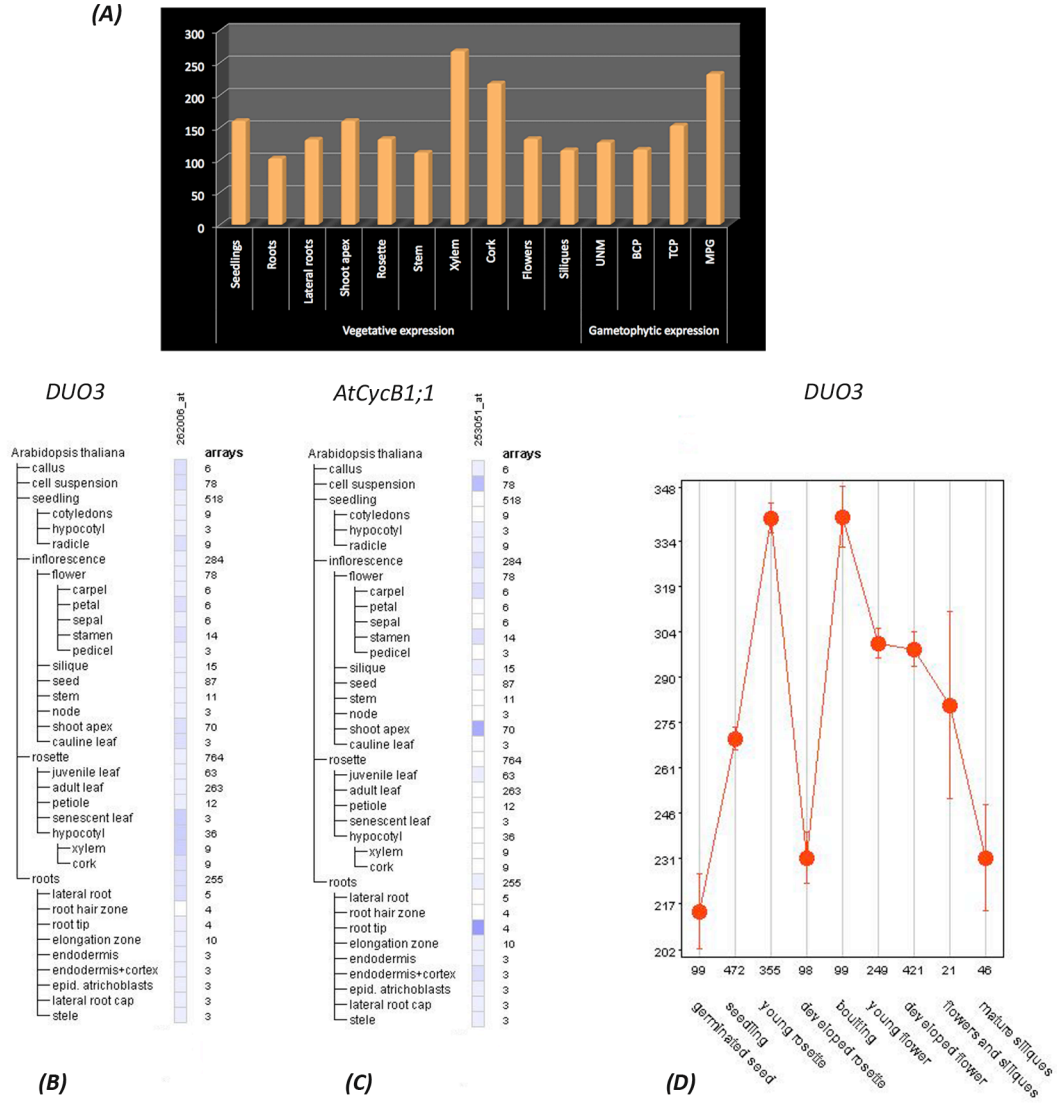

Figure 5.1 **Transcriptomic profile of DUO3 expression during development**
Affymetrix databases available as public resources that provide quantitative information of gene expression in a range of environment and different organs were mined to establish a comprehensive expression profile of the *DUO3* gene throughout plant development. (A) Wider expression of *DUO3* gene as determined by NASC microarray dataset obtained from Arabidopsis Gene Family Profiler (aGFP) database. Enhanced expression can be observed in some isolated sporophytic tissues, whereas, expression in the male gametophyte indicate a gradual increase towards pollen dehiscence. (B-D) Anatomical and developmental view of *DUO3* expression using AtgenExpress dataset obtained from the Genevestigator database. (B-C) Heat map showing abundance of *DUO3* transcript (strength of expression is indicated by the intensity of the purple squares) in comparison to that of a known cell cycle marker from Arabidopsis (AtCycB1;1). Though *DUO3* is not strictly cell cycle regulated (see analysis of *DUO3* promoter activity), it shows enhanced expression in tissues that are competent to divide. (D) Developmental profile of *DUO3* expression in the whole plant showing detection of *DUO3* transcript at all stages of plant development.

5.2.2 Verification of *DUO3* expression pattern by RT-PCR

Total RNA was extracted from several vegetative tissues including seedlings, roots, shoot apex enriched tissues, rosette leaves, and inflorescence stem, and from reproductive tissues including flowers containing mature pollen and siliques. A primer pair denoted SANTF and SANTR that was used for the RT-PCR analysis was designed to span exon1 and exon3 of the *DUO3* coding sequence and intervened by two introns, producing a cDNA fragment of 611bp and a genomic fragment of 725bp. 750ng of the total RNA was used to synthesise cDNA and 1μl of 1/10 cDNA dilution was used in a PCR reaction with SANTF/SANTR primers to analyse *DUO3* transcript abundance throughout plant development. *DUO3* transcript was detected at all stages of development and showed enhanced transcript accumulation in shoot apex enriched tissues (Figure 5.2). A histone H3 variant (At1g10980) that is constitutively expressed was used as a positive control to monitor equal input of cDNA from each tissue sample. The expression profile of *DUO3* observed with RT-PCR was in agreement with that predicted by the two independent microarray databases.

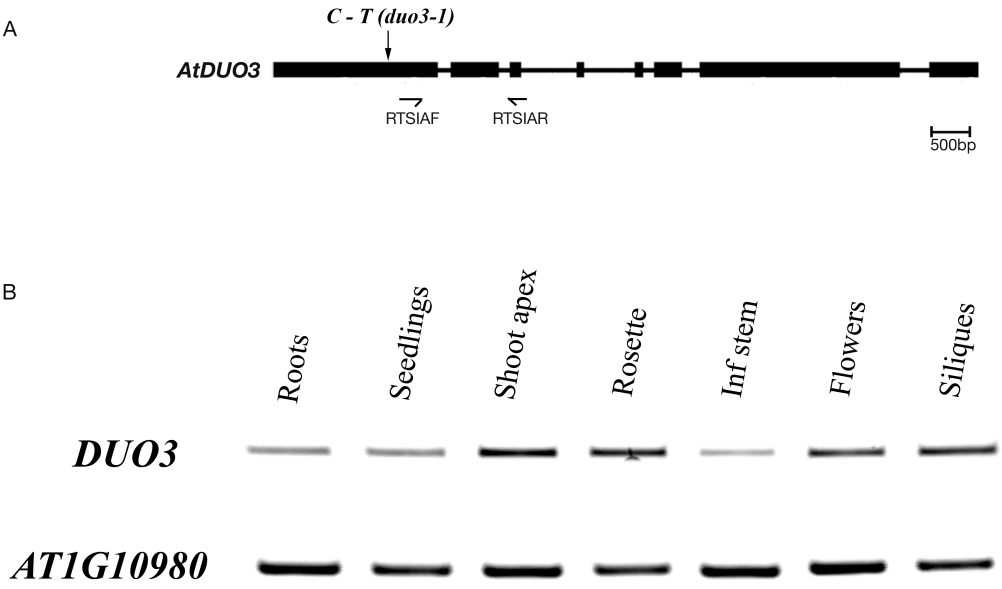

Figure 5.2 **Analysis of *DUO3* expression profile by RT-PCR**
Verification of *DUO3* expression pattern during plant development predicted by the microarray databases. Equal amount of starting RNA was used for each sample to provide a semi-quantitative measure of *DUO3* transcript abundance in different tissues. (A) *DUO3* gene structure showing position of the primers used in the RT-PCR reactions (black arrows). (B) Results of the RT-PCR reactions following amplification of *DUO3* transcript in a 30 cycles of PCR reactions. Abundance of *DUO3* transcript can be seen at different stages of plant development and enhanced detection in shoot apex enriched tissues. The RT-PCR result coincide that of the microarray data obtained from the public databases.

5.2.3 Promoter activity of *DUO3* during plant development

To investigate *DUO3* promoter activity and establish potential cell specificity and temporal regulation throughout plant development, approximately 1kb of *DUO3* sequence upstream of the translation initiation site was cloned by recombination (Invitrogen) into a Gateway destination vector (pKGWFS7) containing GFP::GUS reporter gene fusion. The final destination vector, *pDUO3-GFP::GUS* (Figure 5.3A) was introduced into the +/*duo3* mutant background through floral dipping. Plants generated were analysed by histochemical staining (GUS staining) and florescence microscopy (GFP) to investigate the profile of *DUO3* promoter activity. Following segregation analysis, 10 independent T2 lines with a single locus insertion were selected and plated on selection. Several tissues from different stages of plant development were collected and stained for GUS. *DUO3* promoter activity was detected in 10 day old seedlings in cotyledons and in the first true leaves exclusively associated with the vascular tissues (Figure 5.3B). The GUS activity was enhanced in the

shoot apex and in the leaf primordia (Figure 5.3C) consistent with the microarray and RT-PCR data. Analysis of whole root mounts revealed strong GUS activity in the root apical meristem and in the neighbouring cells localized in specific cell files, the pericyle and cortical cell layers, with a patchy pattern ("salt and pepper" stain) that fades towards the elongation zone of the root (Figure 5.3F-I). This pattern is similar to the GUS activity pattern observed with a labile mitotic G2/M marker AtCycB1;1::uidA construct, pCDG (Colon-Carmona et al., 1999b). Furthermore, GUS staining was also found to be associated with the vascular tissues of the primary root (Figure 5.3J). Similar analysis was also carried out by examining expression of the GFP marker. Again, an equivalent patchy expression pattern in the root tip was detected (Figure 5.3H-I). In addition to the activity at the root apical meristem, *DUO3* promoter activity was also detected in the lateral roots associated with the vascular tissues and strongly enhanced in the lateral root primodia and the pericycle (Figure 5.3K-L). The vascular staining pattern was maintained in rosette leaves and in the vascular tissues of the inflorescence stem (Figure 5.3D and Figure 5.3M). Analysis of reproductive organs also showed GUS staining in pedicel, vascular tissues of petals and sepals, and in anthers (Table 5.1). Moreover, careful analysis of in situ GUS stained 10 day old seedlings showed a consistent pattern of GUS activity localized in specific cell files in the primary roots and lateral root (Table 5.2). This pattern was reproducible between independent lines and through successive generations.

To analyse regulation of *DUO3* expression pattern during pollen development, a whole inflorescence was stained for GUS and individual buds were dissected in a DAPI staining solution to release the spores and stain the nucleus. Analysis of whole bud showed a gradual increase of GUS activity towards the older anthers (Figure 5.4B-C). Dissection of the anthers at different stages of pollen development showed weak *DUO3* promoter activity at the microspore stage, which then increased at the bicellular stage in both cells, vegetative and generative cell (Figure 5.4D, I-V). At the tricellular stage, GUS crystals increased in both cells

and continue to accumulate at mature pollen stage (Figure 5.4D, VI). Thus, analysis of *DUO3* promoter activity by histochemical staining has provided more insight in to the tissue specific expression of *DUO3* and its potential role during plant growth that implicates a likelihood of participating in cell proliferation.

	pDUO3-GFP::GUS			Mature flowers 0.5 mMFeCN;1mM X-gluc												
	Line	Pollen	Pollen (% +GUS)	Pedicel	Sepal	Petal	Filament	Anthers	Stigma	Style	Ovary	Rosette leaf	Seedlings	nR:nS	R:S
1	A1	+++	84%	++++	++	+	++	++	-	-	-	+++	++	186:15	12.4:1
2	A2	++	73%	++	+	++	++	++	-	-	-	++	+++	266:12	22:1
3	A4	++++	47%	++	+-	++	++	++	-	-	-	+++	++	157:48	3.2:1
4	B1	-		+-	+-	+	++	-+	-	-	-	++	+++	na	
5	B2	+++	88%	+	+	-++	++	++	-	-	-	+++	+++	192:15	13:1
6	B3	+-		+	+	-++	+	-++	-	-	-	+	++	na	
7	B4	++++	44%	+++	+	-++	++	++	-	-	-	+++	+++	102:35	2.9:1
8	C1	++++	49%	+	+	-	++	-	-	-	-	+++	+	96:30	3.2:1
9	C2	-		++	+	_	++	-	-	-	-	-	+++	na	
10	C3	++++	86%	+	+	-+	++	++	-	-	-	+++	++	219:15	15:1
11	C4	+++	89%	+	+	-+	++	++	-	-	-	+++	++	140:12	12:1
12	D1	+++	74%	+-	++	+	++	++	-	-	-	+++	++	167:42	4:1
13	D2	+-		+-	+-	+	-	-	-	-	-	+	+++	na	
14	D3	+-		++	-	+++	++	+++	-	-	-	+	+++	na	
15	E1	+++	86%	+	+-	++	-	++	-	-	-	+++	++	223:19	12:1
16	E2	++++	88%	+	-	++	+-	+++	-	-	-	+++	++	189:15	13:1
17	E3	+-		+-	+-	+	+-	+	-	-	-	+	++	na	
18	E4	+++	47%	++	+	++	+-	+++	-	-	-	+++	+++	121:35	3.5:1
19	A1	++		++	++	++	-	+-	-	-	-	+++	+	na	
20	A2	+-		+	++	+	-	+	-	-	-	+	+	na	
21	A3	+-		+	++	+	-	+	-	-	-	+	++	na	
22	A4	+		+-	+-	+	-	+-	-	-	-	+	++	na	
23	B1	++++	79%	+	+	++	+-	++	-	-	-	+++	++	126:21	6:1
24	B2	+++	82%	+	+	+-	+-	++	-	-	-	+++	++	297:18	17:1
25	B3	+		+	+-	+	+-	++	-	-	-	+	++	na	
26	B4	+++	90%	+-	+-	+	-	+++	-	-	-	+++	++	240:15	16:1
27	C1	+		+	+-	+	-	-	-	-	-	+	+++	na	
28	C2	+-		+	++	++	++	+-	-	-	-	+	++	na	
29	C4	++		+	+	++	++	++	-	-	-	+++	++	na	
30	D1	+-		+-	+-	+	+-	+	-	-	-	+	++	na	
31	D2	+		+-	+-	+	-	+-	-	-	-	+	++	na	
32	D3	++		+	+-	+	+-	+	-	-	-	+	+	na	
33	D4	++++	77%	+	+-	++	+-	++	-	-	-	+++	+	252:60	4.2:1
34	E1	+		+	+-	+	-	+-	-	-	-	+	+++	na	
36	E3	++		+	+-	+-	+-	++	-	-	-	+	++	na	
38	A1	++		+	+	+	+-	+	-	-	-	+	++	na	
39	A2	++++	52%	+	+	++	+-	+++	-	-	-	+++	++	102:30	3.4:1
40	A3	+		+-	+-	++	+	+	-	-	-	+	++	na	
41	C1	++	93%	+	+-	++	+-	+	-	-	-	+++	+++	137:8	17:01
42	C5	++++	87%	+	+	++	+-	++	-	-	-	+++	++	172:15	12:1
43	D4	+++	83%	+	++	+	+	++	-	-	-	+++	+	210:18	12:1

Table 5.1. Developmental analysis of *DUO3* 1kb promoter activity as examined by in situ histochemical GUS staining of seedlings, rosette leaves and reproductive organs of the T1 derived population. "+", "-", and "+-" designate present, absent, and moderate observed GUS staining respectively. The strength of GUS staining is indicated by numbers of "+" . "na" indicate data not available for that particular line. Individuals highlighted in red were also analysed in T2 generation. R:S indicates individual seedlings resistance-sensitive to kanamycin antibiotic

	0.5mM FecN + 1mM X-gluc/Incubated at 37°C								
Line ID T2 seedlings	Seedling number	Lateral root primordium	Vascular tissue of lateral root	Lateral root tip	Vascular tissue of primary- root	Primary root tip	Primary root cap	Segregation (Kan25)	Segregation (Ratio)
T1A4	1	+++	+	-	+ -/ ++/++	+	-	53:19	2.8:1
	2	++++	+	-	+ -/ ++/++	+	-		
	3	++/ - +/++	+-	-	+ ++	+-	-		
T1B2	1	+++	+-	-	+ -/ ++/++	+	-	114:2	57:1
	2	+++	+	+-	+ -/ ++/++	-	-		
	3	+++	++	+-	+ - /++/++	++	-		
T1B4	1	++++	+-	+-	+++/ - +/+++	++++	-	116:42	2.8:1
	2	++++	+	-	++/ - +/+++	+++	-		
	3	++++	+-	-	++/ - +/++	++	-		
T1C1	1	++++	++	++	++/ - +/++	+++	-	146:44	3.3:1
	2	+++	++	++	++	++	-		
	3	-	-	-	-	-	-		
T1C3	1	++	-	-	+ ++	+	-	210:56	3.8:1
	2	++	-	-	-/ -/ +++	++	-		
	3	+++	++	++	+ ++	++	-		
T1E2	1	++++	+	+	++/ - +/++	++++	-	224:5	44.8:1
	2	-	-	-	-	-	-		
	3	-	-	-	-	-	-		
T2B1	1	++++	++	++	++/ - +/+++	+++	-	225:33	6.8:1
	2	-	+-	-	-	-	-		
	3	-	+-	-	-	-	-		
T2D4	1	++++	++/ - +/++	++/ - +/++	++/+ -/ ++++	++++	-	156:33	4.7:1
	2	++++	+ -/ ++	+ -/ ++	++/+ -/ ++++	++++	-		
	3	++++	+++	+++	++++	++++	-		

Table 5.2. Analysis of pDUO3-GFP::GUS expression pattern in roots of 10 days old seedlings by GUS staining. Three seedling from each individual line were stained to analyse GUS activity in roots. "+", "-", and "+-" indicates present, absent, and moderate GUS staining. Where staining variability was observed within a seedling, more than one symbol was used to report the variability of GUS staining. Individuals derived from the first screen are denoted as (T1) followed by line identification (such as T1A4), and those derived from the second screen are denoted by (T2) followed by line identification.

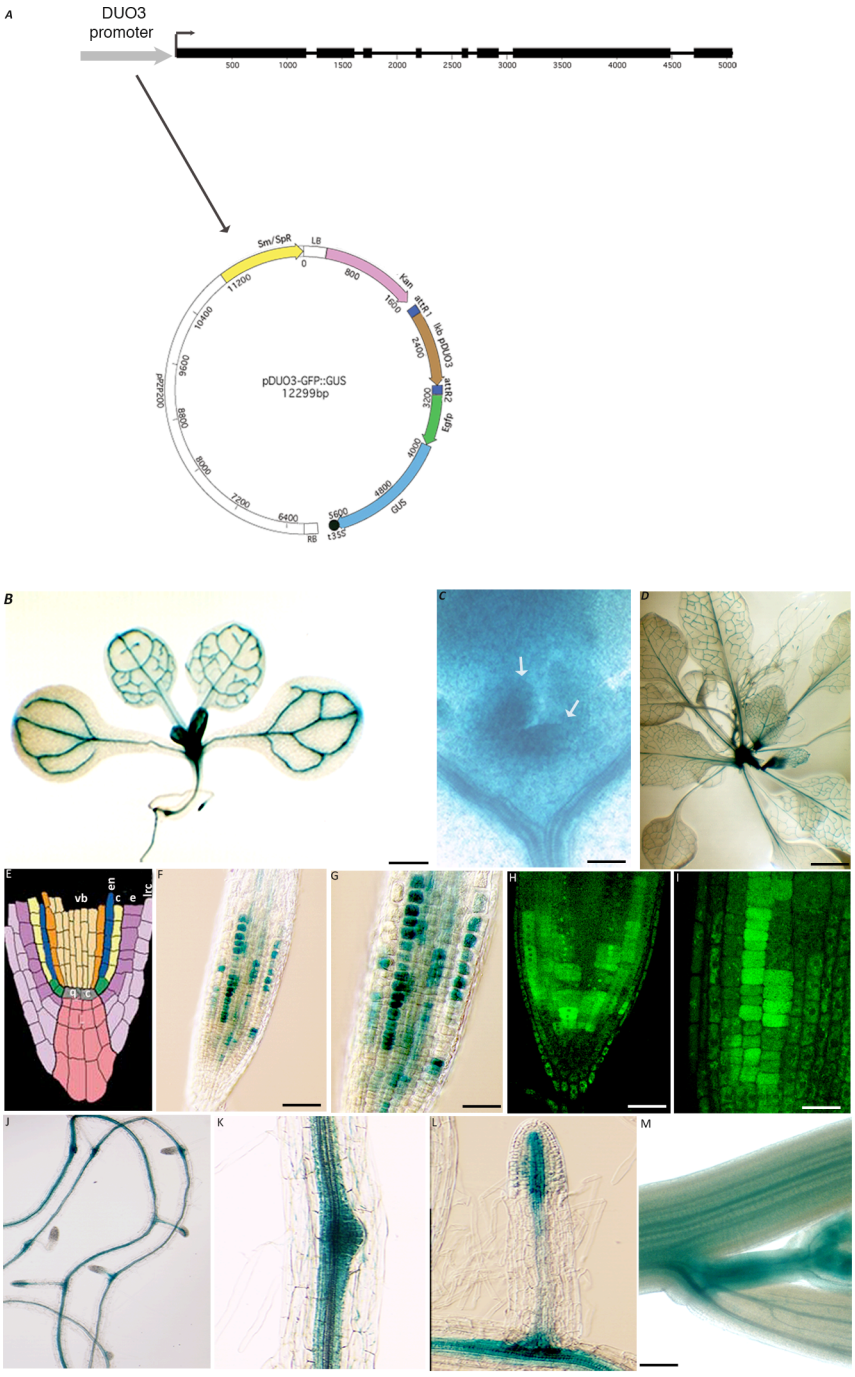

Figure 5.3 **Histochemical analysis of *DUO3* promoter driving GUS marker in sporophytic tissues**
Temporal and spatial pattern of *DUO3* promoter activity analysed by In situ histochemical GUS staining. (A) Sequence map of the pDUO3-GUS fusion construct; (B-C) restricted *DUO3* promoter activity in the vascular tissues of cotyledon leaves and first true leaves of the 10 days old seedlings showing enhanced expression in the shoot apex and leaf primordia (white arrows); (D) GUS staining at the rosette stage; (E-G) a cartoon of the root section illustrating regions of the root files that possess *DUO3* promoter activity as observed in (F) and (G) showing strong GUS staining in the epidermis, cortical layer and endodermis. vb;vascular bundle, en;endodermis, c;cortex layer, e;epidermis, qc;quiescent center; (H-I) fluorescence image of whole root mount showing *DUO3* expression pattern using a GFP marker; (J-L) strong *DUO3* expression in the lateral root and lateral root primordia; (M) light image showing conserved vascular pattern of *DUO3* expression in young stem as indicated by localized GUS staining following histochemical analysis of roots from 10 days old seedlings. The GUS staining reflects *DUO3* promoter activity (supported by another independent construct) without any influence from the nopaline synthase promoter that driving the selectable marker gene (Kan, nptII). Scale bars 1mm

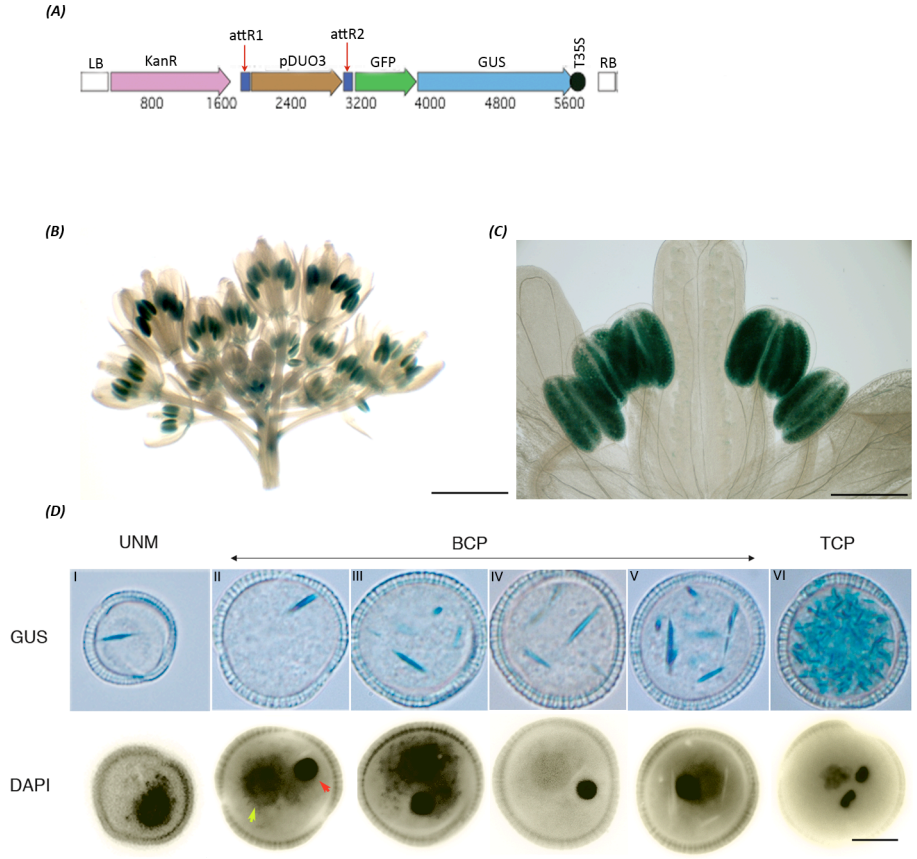

Figure 5.4 ***DUO3* promoter-reporter activity during male gametophyte development**
(a) Map of the 1kb *DUO3* promoter-GUS fusion used for analysing reporter activity in different cell types of the pollen (b) Whole inflorescence GUS staining showing reporter activity throughout pollen development and enhanced activity in the older anthers. Scale bar 5mm (c) Magnified view of the stained open flower showing strong staining in anthers. Scale bar 1mm (d) Bright field images (top panels) and corresponding inverted negative DAPI images (bottom panels) showing gradual increase in GUS staining from microspore (I), bicellular (II-V) and tricellular pollen (VI). At early bicellular (II), staining is only observed in the newly formed germ cell (red arrow) and not in the vegetative cell (yellow arrow), thereafter, GUS staining accumulates in both cell types. The selectable Kanamycin marker, nptII, is independently driven by nopaline synthase promoter. UNM;unicellular microspore, BCP; bicellular pollen, TCP; tricellular pollen. Scale bar 6µm

5.3 Investigating the Putative Role of *DUO POLLEN3*

To understand putative role of the *DUO3* gene, two strategies were engaged including analysis of hypomorphic alleles generated from Ethane methyl sulfonate (EMS) induced point mutations and correlation of *DUO3* with expressed cell cycle factors that might be regulated by *DUO3* gene. In this section, results from a morphological screen of vegetative and pollen division defect of *DUO3* hypomorphic alleles following EMS mutagenesis are presented. Furthermore, a study of the *DUO3* relationship with a known cell cycle regulator (*AtCycB1;1*) is also presented.

5.3.1 TILLING (Targeting Induced Local Lesions in Genomes)

TILLING is a reverse genetic strategy that uses an EMS mutagenesis procedure to generate allelic series of point mutations (McCallum et al., 2000). The TILLING strategy involves use of an endonuclease that preferentially cleaves mismatches in heteroduplexes between wild type and mutant sequences for high-throughput genomic screening for the presence of point mutations (single nucleotide polymorphism, SNP's) in a gene of interest. A 1500bp fragment from the 5'-end of *AtDUO3* genomic sequence was submitted to the Arabidopsis Tilling Project (ATP, http://tilling.fhcrc.org) for "coddling" to look for the presence of EMS induced point mutations. TILLING results reported a presence of 8 point mutations of which 7 were mis-sense mutations (Table 5.3). Lines were ordered from NASC and screened for the presence of mutant phenotypes. In most lines, no clear phenotypic effect was identified in the vegetative organs (Figure 5.5B-C) or in developing pollen that could be linked back to the *DUO3* point mutation. However, this in line N92261 3/19 of the generated individuals showed a significant proportion of *duo-like* phenotype that range between 34 – 47% mutant pollen grains (Figure 5.5D-F). Nonetheless, the observed phenotype was not reproducible in the second generation. The presence of the point mutation at the *DUO3* locus was confirmed by sequencing and by restriction digest of the amplified heteroduplexes from the

second generation (M5) using a derived Cleaved Amplified Polymorphic sequence (dCAPs) primer (Figure 5.5G-H). Thus, the amino acid changes identified appear not to affect DUO3 protein function.

Screen of the DUO POLLEN3 TILLING lines

			Observed phenotype	
Line	*Nature of mutation*	*Zygosity*	*Vegetative tissue*	*Pollen*
N93497	R146K	Homozygous	Abnormal vernalization on rosette leaves, plants produced tertiary inflorescence, short and bulky flowers, short siliques with seed gaps and dwarfism	No clear pollen phenotype was observed
N92439	G315E	Heterozygous		
N92261	D170N	Heterozygous		Bicellular pollen phenotype

Pollen phenotype from TILLING line N92261

Line	*Tricellular pollen*	*Bicellular pollen*	*Total pollen counts*	*% bicellular pollen*
T5A1	98	3	101	3%
T5A2	181	7	188	4%
T5A3	133	2	135	1%
T5A5	54	0	54	0%
T5B1	134	2	136	1%
T2B2	136	0	136	0%
T2B3	154	1	155	1%
T2B5	136	0	136	0%
T5C1	146	106	252	42%
T5C2	80	0	80	0%
T5C3	146	134	280	48%
T5C5	94	0	94	0%
T5D1	139	1	140	1%
T5D2	116	60	176	34%
T5D3	159	0	159	0%
T5D4	129	0	129	0%
T5D5	150	3	153	2%
T5E1	160	0	160	0%
T5E2	125	1	126	1%
T5E3	130	0	130	0%
T5E4	135	3	138	2%
T5E5	193	9	202	4%

N93729	R304K	Homozygous	Abnormal vernalization on rosette leaves, plants produced tertiary inflorescence, short and bulky flowers, short siliques with seed gaps and dwarfism	No clear pollen phenotype was observed
N92277	E424K	Homozygous		
N95567	A294V	Heterozygous		
N96131	G361R	Heterozygous		
N93424	Intron	Homozygous	Not ordered for analysis	-

Table 5.3

Phenotypic characterization of *DUO3* point mutations generated following EMS treatment. Plants showed a range of sporophytic abnormalities compared to the wild type plants. Only one line (N92261) was identified to show a male gametophytic effect. However the pollen phenotype observed was not reproducible and could not be linked back to the *DUO3* gene. The column marked "Nature of mutation" represent amino acid change of each mutant line and the co-ordinate within the DUO3 protein. Eight lines possessed a missense mutations and seven were ordered for analysis

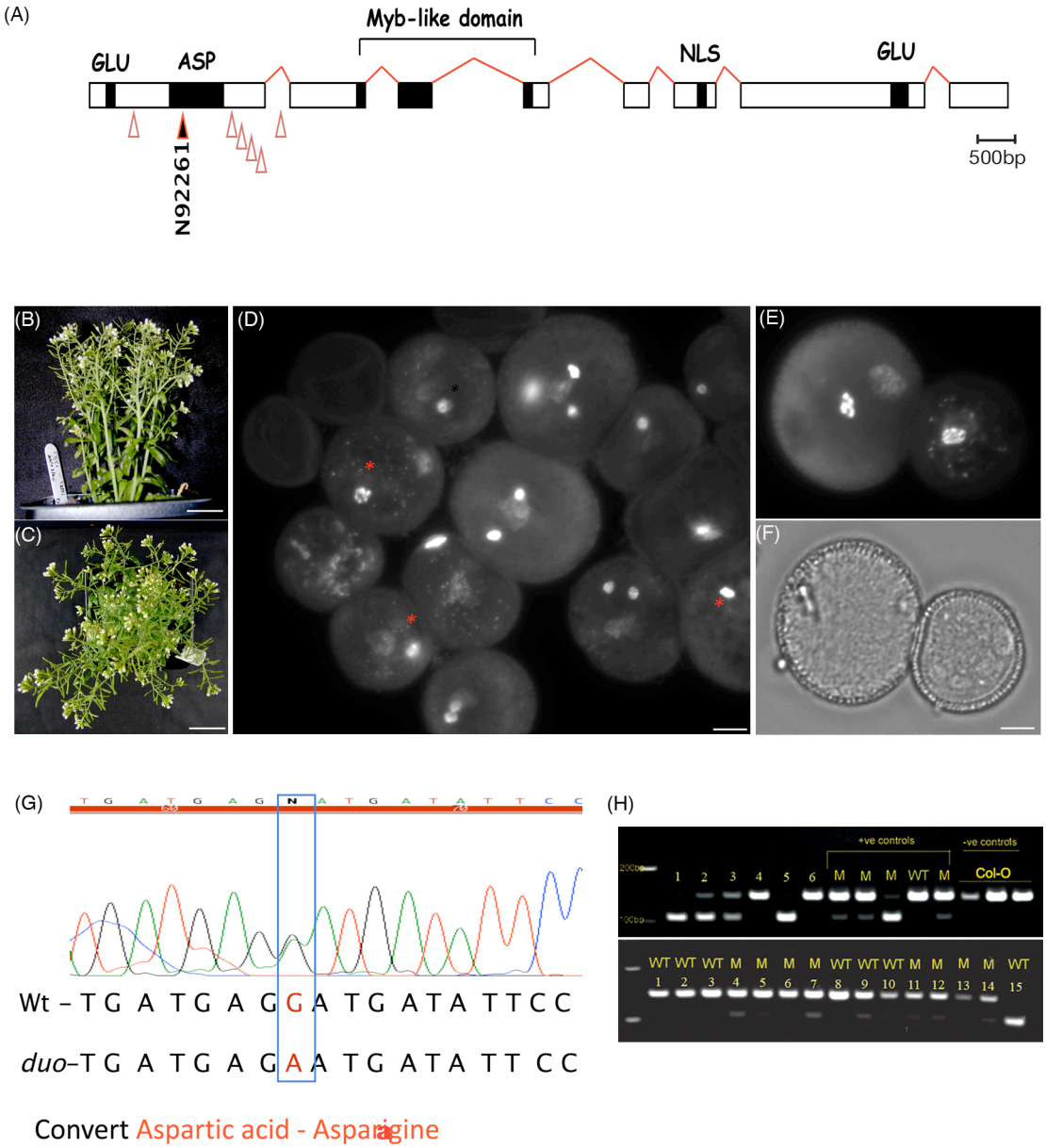

Figure 5.5 **Characterization of *DUO3* point mutations**
Phenotypic analysis of sporophytic and gametophytic developmental defects of plants carrying DUO3 point mutations (A) DUO3 genomic structure showing the seven alleles with identified missense mutations following coddling. Protein domains are indicated by filled squares, and point mutations are shown by wedges. (B-C) A representative of the individuals carrying point mutations (of the line N92261) showing normal vegetative development and formation of reproductive organs. Scale bar 3cm (D) DAPI stain of mature pollen grains population derived from line N92261 highlighting the presence of undivided germ cell nucleus (shown by asterisk). Scale bar 1µm (E-F) Detailed view of the mutant pollen grains showing arrest of the germ cell at pre-prophase stage of PMII. Scale bar 4µm (G) Snapshot of the chromatogram sequencing result verifying the presence of point mutation in line N92261 that convert aspartic acid into asparagine at amino acid 170 (D170N). (H) Molecular analysis by restriction digest of the individuals from line N92261 amplified with dCAPs primers. Top panel shows detection of wild type (4,6) and mutant individuals (1,2,3 and 5) with positive and negative controls. Bottom panel show segregation analysis for the presence of point mutation based on the phenotype. GLU; Glutamine, ASP; Asparagine, NLS; nuclear localization signal, WT; wild type, M; mutant

5.3.2 Role of *DUO3* as a regulator of cell proliferation

It was described earlier that cytological analysis of +/*duo3* plants identified mutant pollen grains that failed to progress through PMII and result in ~45% bicellular pollen grains with a compact generative cell at the mature pollen stage (see page 11 of the introduction Chapter). Furthermore, study of mitotic index figure showed a significant reduction (~50% of the population) in the frequency of pollen grains that failed to enter and progress through mitosis. Arrest at this point was further verified by DNA measurement of the generative nuclei, which showed a DNA content of ~1.98C, indicating completion of S-phase but blocked at G2/M transition. In light of these results, a relationship between *DUO3* and a key cell cycle regulator (*AtCycB1;1*) was investigated to test whether *CycB1;1* is one of the missing components in *duo3* mutant germ cells. In Chapter 3, a similar experiment was demonstrated in heterozygous +/*duo1* mutant plants. The same G2/M marker, pCDG (Figure 5.6A, (Colon-Carmona et al., 1999a), was crossed into the +/*duo3* background and F2 individuals homozygous for the pCDG marker was used for analysing *AtCycB1;1* activity in wild type and in +/*duo3* siblings. Score of percentage pollen grains from 5 independent +/*duo3* siblings positive for GUS staining showed normal pCDG activity (~100%) at the microspore stage prior to asymmetric division, reduced at early bicellular stage and almost absent by mid bicellular stage, similar in wild type and in heterozygous +/*duo3* siblings (Figure 5.6C). pCDG-dependent GUS staining was reinitiated at the late bicellular stage exclusively in the germ cell and showed normal activity in the wild type (~99%) as well as in heterozygous +/*duo3* mutant siblings. A similar marker (pCDGFP) that possess a GFP protein in place of GUS (see Figure 5.7) was also used alongside to provide independent evidence for the activity of CycB1;1 in *duo3* mutant cells. The main advantage of using the pCDGFP marker is that it allows analysis of live cells, which is important in identifying the change in germ cell morphology as it progresses through the cell cycle. Screening of five individuals heterozygous for the pCDGFP marker and three F2 siblings homozygous for pCDGFP showed

normal activity of AtCycB1;1 promoter in wild type and in heterozygous +/*duo3* individuals (See section 5.3.2.2). These results demonstrate that unlike *DUO1*, the presence of DUO3 protein is not required for the expression of AtCycB1;1 in the male germ cells of Arabidopsis.

(A)

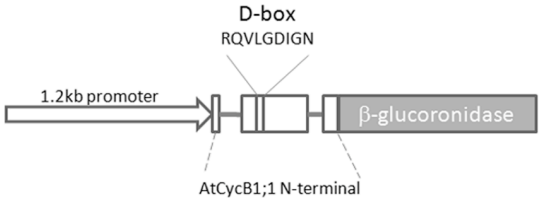

(B) **Developmental analysis of pCDG activity in heterozygous *duo3* mutant plants**

Developmental stage	*Staining*	*Counts of two wild type*		*duo3-1*		*duo3-2*		*duo3-3*	
		counts	% gus stain	counts	% gus stain	counts	% gus stain	counts	% gus stain
UNM	+GUS	211	100%	167	93%	208	99%	44	77%
	-GUS	0		13		1		13	
		na		na		na		na	
EBCP	+GUS (VC)	158		87		234		87	
	+GUS (GC)	97	99%	62	97%	112	100%	21	74%
	-GUS	2		4		0		39	
MBCP	+GUS (VC)	164		197		169		7	
	+GUS (GC)	31	25%	54	26%	42	29%	0	12%
	-GUS	593		731		524		50	
LBCP	+GUS (VC)	17		8		3		3	
	+GUS (GC)	401	47%	47	37%	46	23%	67	64%
	-GUS	452		92		168		40	
TCP	+GUS (VC)	0		0		0		0	
	+GUS (GC)	569	92%	255	93%	974	97%	575	96%
	-GUS	51		19		25		23	
MPG	+GUS (VC)	0		0		0		0	
	+GUS (GC)	22	4%	300	56%	37	24%	5	1%
	-GUS	552		237		114		388	

(C)

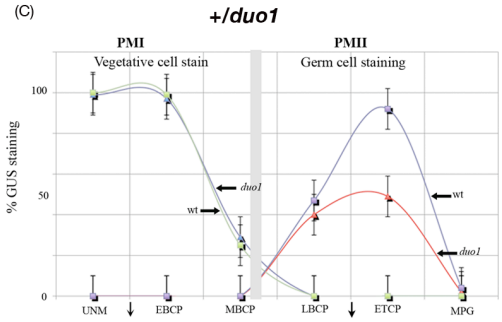

(D)

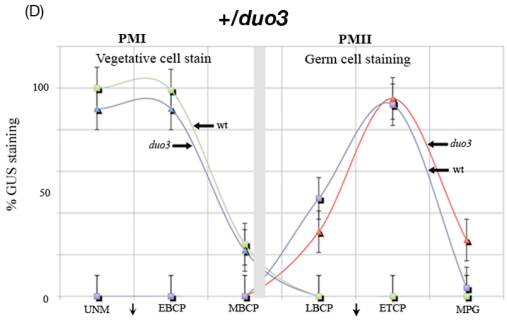

Figure 5.6 **Analysis of AtCycB1;1 dynamic expression in +/*duo3***
In situ GUS staining of the pCDG construct during male gametophyte development in wild type and in plants harbouring the *duo1* and *duo3* mutations. (A) Schematic presentation of the pCDG construct; (B) Counts of the GUS stained pollen grains in wild type and three individual plants heterozygous for the *duo3* mutant phenotype; (C,D) A plot of pCDG activity in wild type and mutant *duo1* and *duo3* during sperm cell formation similar to that of figure 3.5 for comparison purposes. The pCDG activity is off in the mutant *duo1* pollen grains represented by the 50% reduction at PMII compared to the wild type. (C) Conversely, pCDG activity is not altered in *duo3* mutant pollen grains. However, there is an implication of lack of GUS protein turnover emphasized by the detection of GUS at mature pollen in the +/*duo3* background but not in the wild type tricellular pollen grains. (n = 6292)

5.3.2.1 *AtCycB1;1* fails to rescue the *duo3* mutant;

To investigate the relationship between *AtCycB1;1* and *DUO3* independently, *AtCycB1;1* was introduced into the *duo3* mutation under the control of the *DUO1* promoter. Analysis of T1 transgenic lines showed no significant reduction in the frequency of *duo3* mutant pollen grains compared to the untransformed control individuals and plants transformed with the vegetative cell driven CycB1;1, pHLAT52-AtCycB1;1 (Table 5.4). The outcome of this experiment strongly suggests that CycB1;1 is not the missing factor in *duo3* mutant pollen grains, instead other factors associated with G2/M transition may be depleted.

			Pollen phenotype			
	Line	Genotype	wt	*duo*	*% duo*	X^2 test
Untransformed individuals	1	*+/duo3*	139	122	46%	ns
	2	*+/duo3*	198	177	47%	ns
	3	*+/duo3*	145	141	49%	ns
	A3	*+/duo3*	119	109	48%	ns
	A8	*+/duo3*	189	162	46%	ns
	B4	*+/duo3*	211	164	44%	ns
	B5	*+/duo3*	192	176	48%	ns
	B7	*+/duo3*	170	156	48%	ns
	B8	*+/duo3*	196	165	46%	ns
	C3	*+/duo3*	137	107	44%	ns
	C4	*+/duo3*	169	144	46%	ns
	D5	*+/duo3*	139	109	44%	ns
	E1	*+/duo3*	121	109	47%	ns
	E2	*+/duo3*	106	82	44%	ns
	E4	*+/duo3*	128	95	43%	ns
	E8	*+/duo3*	192	153	44%	ns
+/duo3;pBMGH3-CycB1;1::GFPHIS						
	A1	*+/duo3*	202	149	42%	ns
	A4	*+/duo3*	220	166	43%	ns
	A5	*+/duo3*	206	184	48%	ns
	A6	*+/duo3*	237	201	46%	ns
	B1	*+/duo3*	207	180	47%	ns
	B2	*+/duo3*	222	108	33%	s
	B5	*+/duo3*	211	170	45%	ns
	B8	*+/duo3*	237	176	43%	ns
	C3	*+/duo3*	205	154	43%	ns
	C5	*+/duo3*	235	195	45%	ns
	C8	*+/duo3*	213	169	44%	ns
	D7	*+/duo3*	228	187	45%	ns
	D8	*+/duo3*	258	200	44%	ns
	E3	*+/duo3*	208	178	46%	ns
	E6	*+/duo3*	245	191	44%	ns
+/duo3;pHLAT52-CycB1;1						
	A2	*+/duo3*	276	264	49%	ns
	A3	*+/duo3*	280	256	48%	ns
	A6	*+/duo3*	320	308	49%	ns
	A7	*+/duo3*	180	195	52%	ns
	A8	*+/duo3*	214	172	45%	ns
	B5	*+/duo3*	141	136	49%	ns
	B7	*+/duo3*	240	236	50%	ns
	C4	*+/duo3*	217	209	49%	ns
	C7	*+/duo3*	211	215	50%	ns
	C8	*+/duo3*	255	207	45%	ns
	D5	*+/duo3*	212	210	50%	ns
	D6	*+/duo3*	215	190	47%	ns
	D8	*+/duo3*	221	229	51%	ns
	E2	*+/duo3*	221	233	51%	ns
	E3	*+/duo3*	227	214	49%	ns
	E7	*+/duo3*	205	191	48%	ns

Table 5.4. Statistical analysis of *duo3* mutant pollen complementation by AtCycB1;1. The frequency of duo3 mutant pollen grains is comparable between transformed and untransformed lines X^2-chi-squared test with not signiifcant (ns) $p>0.05$ and statistically significant "s" $p<0.0001$. .

5.3.2.2 *duo3* mutant germ cells are impaired in *AtCycB1;1* turnover;

Study of pCDGFP activity in the +/*duo3* background revealed no correlation between *DUO3* and the activity of *AtCycB1;1* promoter. Instead, a significant proportion of bicellular *duo3* pollen grains (~15 – 30%) were observed to possess persistent GFP specifically in the mutant germ cell at the mature pollen stage unlike their wild type counterparts (Figure 5.7). Dissection of +/*duo3* spores during development showed an increased proportion of bicellular pollen grains with persistent GFP up to 45% at the tricellular stage, suggesting a more gradual degradation of GFP protein in mutant pollen grains (Figure 5.7D). An independent analysis of transgenic heterozygous +/*duo3* plants transformed with the *MGH3* driven *AtCycB1;1* construct (pBMGH3-AtCycB1;1::GFPHIS) with a purpose of complementing the *duo3* mutation, also displayed a persistent GFP (6/9 of the heterozygous T1 *duo3* individuals analysed) in the mutant *duo3* germ cells reminiscent to that observed with pCDGFP marker (Table 5.4, highlighted lines). In wild type, cyclin proteins undergo D-box - Ubiquitin mediated proteolysis through the Anaphase Promoting Complex, Cyclosome (APC) prior to progression into anaphase. Thus, it can be proposed that *duo3* mutant pollen grains are impaired in full APC activity in the germ cell. It should also be noted that the APC activity that leads to degradation of CycB1;1 in the vegetative cell is not compromised by the lack of germ cell division.

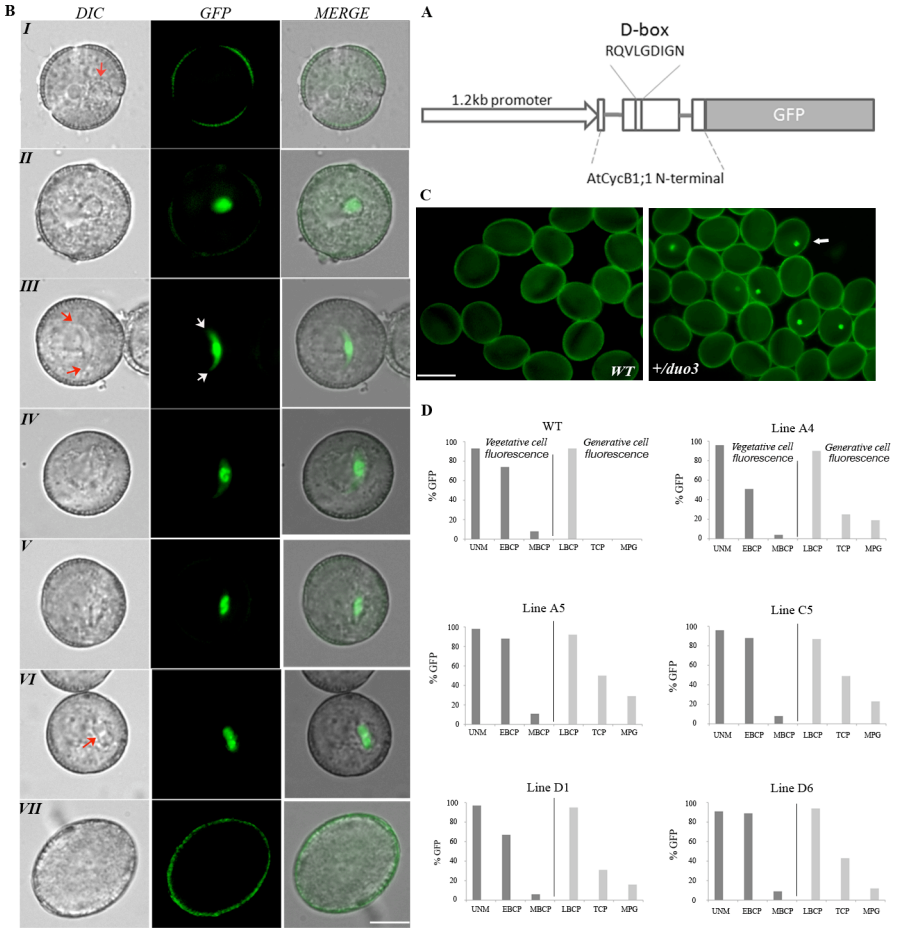

Figure 5.7 **Turnover of AtCycB1;1-GFP is impaired in mutant *duo3* pollen grains**
Activity of the pCDGFP expression pattern in wild type and in heterozygous *duo3* plants. (A) Schematic representation of the pCDGFP construct. (B) DIC, GFP fluorescence and superimposed images of the pCDGFP activity post PMI as observed in wild type pollen grains. (I) Absence of pCDGFP activity in newly formed germ cell (red arrow). (II-V) Newly initiated germ cell specific expression of the pCDGFP construct shows cytoplasmic and nuclear localization of the GFP (white arrows) during PMII. (VI) GFP fluorescence leftover in the newly formed sperm cells. The red arrow indicates a point of new sperm cell wall formation. (VII) Complete turnover of GFP protein at late tricellular stage. Scale bar 8µm (C) Fluorescence image showing mature pollen populations harbouring the pCDGFP construct with wild type phenotype and those that carry the *duo3* mutation. Persistant GFP is exclusively associated with the *duo3* mutant pollen grains (white arrow). Scale bar 6µm (D) Counts of pollen population expressing the pCDGFP marker during male gametophyte development expressed as percentages. Plots show normal activity of the pCDGFP marker in wild type and in +/*duo3* individuals prior to division of the germ cell; however, persistant GFP can be detected in +/*duo3* individuals at tricellular and mature pollen stages, consistent in four independent lines homozygous for the pCDGFP marker.

Chapter 6

DISCUSSION

A: B-type Cyclins are differentially expressed in the male gametophyte

The mechanisms that integrate cell cycle progression, chromatin remodeling and cell fate determination have remained unexplored in the male gametophyte where dramatic cell fate changes leading to gametogenesis occur over just two mitotic divisions. The first division of the haploid microspore produces a vegetative and a germ cell. Whereas the vegetative cell exits the cell cycle and produces a pollen tube, the germ cell undergoes a second mitotic division to produce two sperm cells that are transported down the pollen tube to undergo double fertilization. This reduced lineage of the male gametophyte provides an interesting model for dissecting the pathways through which these cellular processes are executed.

To understand the intrinsic network that regulates cell cycle progression at the molecular level, expression of B-type cyclins were investigated in the four stages of male gametophyte development. B-type cyclins have been demonstrated to be involved in the control of G2/M transition by pairing with *CDKA* and *CDKB* (reviewed by (Inze and Veylder, 2006). Thus, understanding their expression pattern in pollen was essential in investigating their potential role in the control of cell proliferation during male gametogenesis. Analysis of pollen transcriptomic datasets revealed that members of the B-type cyclins are expressed throughout pollen development with differential patterns of expression. These results were further supported by RT-PCR analysis of RNA isolated from the four pollen stages. *CycB1;1* and *CycB1;4* showed very similar patterns of expression with higher expression levels at the microspore and bicellular stage, and undetectable expression at the tricellular and mature pollen stages. This pattern coincides with that obtained from RT-PCR analysis. Loss of *CycB1;1* and *CycB1;4* expression at the later stages reflects the loss in pollen competence to undergo further cell proliferation. Probes for the *CycB1;2* were not present on the Affymetrix ATH1 microarrays, however, RT-PCR analysis revealed high transcript accumulation at microspore stage which then gradually decreased to tricellular stage and interestingly was elevated again at the mature pollen stage. This pattern of late expression

might suggest a dual role of *CycB1;2* in the male gametophyte as well as in the early division of the embryo following the double fertilization. The expression pattern of *CycB1;3* determined by the microarray analysis was in conflict with that predicted by the RT-PCR analysis. The transcriptomic profilefor *CycB1;3* showed a strong reliable hybridization signal at the microspore and bicellular stage, unreliable signal at the tricellular stage, and a high reliable signal at the mature pollen stage. RT-PCR results were in agreement at the first two stages, but showed significant decrease at the tricellular stage and no transcript was detected at the mature pollen stage. These results can be interpreted in two ways;(1) using the transcriptomic profile, *CycB1;3* seems to be co-expressed with *CycB1;1* and *CycB1;4* and therefore might act together with these in the control of cell cycle progression of the two pollen divisions. (2) Alternatively, with the profile predicted by the RT-PCR, the significance of the late expression of *CycB1;2* and *CycB1;3* might suggest a role in the control of pollen mitotic progression, potentially in the early mitotic division of the zygote following double fertilization. Together, these results provide the first description of B-type cyclin expression profiles during pollen development and present the opportunity to design future experiments in understanding factors regulating cell cycle progression in the male gametophyte.

B: Expression of *AtCycB1;1* is modulated with cell proliferation in the male gametophyte

The availability of the well characterized cell cycle marker, pCDG, provided an opportunity to address the temporal and spatial pattern of *CycB1;1 in vivo*. Following optimization of histochemical GUS activity, careful analysis of wild type Col-0 plants revealed a dynamic expression of *CycB1;1* promoter during pollen proliferation. Strong GUS activity was detected at the late microspore and early bicellular stage, which disappeared at mid-bicellular stage. Germ cell specific GUS activity then reappeared at the late bicellular stage,

which was completely excluded from the vegetative cell. As such, this marker has accurately reported the competent status of the two cells demonstrating one aspect of the differential cell fate between vegetative cell and the germ cell. Due to the nature of the construct (i.e. presence of the destruction box), this marker also reported the cell cycle status of the pollen mother cell and the germ cell showing high GUS activity at the G2/M phase and degradation following exit from mitosis. Moreover, the turnover of GUS activity between the two cells has emphasized indirectly the existence of APC activity in the male gametophyte, which was previously unknown. With this new insight, study of protein turnover in pollen through then the E3-Ubiquitin mediated 26S proteosome degradation pathways is now feasible and will provide more understanding of the mechanisms regulating protein accumulation and gene function. The first direct demonstration of E3-Ubiquitin mediated proteolysis in pollen was shown recently by Kim et al., (2008). The authors demonstrated the turnover of *KRP6* & *KRP7* proteins (inhibitors of *CDKA* activity) specifically in the germ cell by an F-box protein (*FBL17*), which forms part of the SCF complex (Kim, 2008). Thus, the pCDG construct has proven to be a valuable marker that can report cell cycle progression during pollen development. Its dynamic expression has also positioned *CycB1;1* as a strong candidate to regulate mitotic progression at PMI and PMII during male gametogenesis. It has promising future applications to study and understand characteristics of other division mutants affecting male gametophyte development.

C: Germ cell specific expression of *AtCycB1;1* is controlled by the R2R3 MYB transcription factor *DUO1*

Investigation of the *DUO1* phenotype established that the mutant *duo1* germ cells complete DNA synthesis phase (S-phase) but fail to enter mitosis (M-phase;Durbarry et al., 2005; Rotman et al., 2005), suggesting that *DUO1* may regulate the expression of essential G2/M factors. *AtCycB1;1* has been demonstrated to show enhanced expression at G2/M phase of the cell cycle (Menges and Murray, 2002a; Colon-Carmona et al., 1999a). In addition, earlier studies in this project showed reliable expression of the CycB1 family and specific and dynamic expression of *CycB1;1* during pollen cell proliferation. Thus, expression of *AtCycB1;1* using the pCDG construct was investigated as a potential target of *DUO1*. Analysis of pCDG activity in polarized microspores from wild type and heterozygous *duo1* plants showed ~100% GUS staining, indicating normal expression of *CycB1;1*. Germ cell pCDG activity was also observed to be normal in pollen from wild type plants; however, the expression was reduced by approximately half in pollen populations from heterozygous *duo1* plants. This result indicates that DUO1 is essential for the specific expression of *AtCycB1;1* in germ cells. Studies of the *CycB1;1* expression in other tissues has identified R1R2R3 MYB transcription factors (which bind to MSA elements in *CycB1;1* promoter regions) to be essential for the G2/M specific expression of *AtCycB1;1* (Ito et al., 2001a). Moreover, the expression of *CycB1;1* is enhanced by the co-activator TCP family of transcription factors (*TCP20*) which bind to GCCCR motifs (Li et al., 2005a). The discovery of the requirement of *DUO1* for *CycB1;1* expression in the germline has provided a first example of a plant germline specific R2R3 MYB transcription factor that promotes mitotic progression during spermatogenesis.

To independently verify the essential role of *DUO1* in controlling *CycB1;1* expression, the full length *CycB1;1* coding sequence was expressed specifically in the germ cell in an attempt to rescue the *duo1* germ cell mitotic defect. The majority of the transformed individuals (63%) showed a significant reduction in undivided germ cells and a subsequent increase in the

tricellular pollen grains with twin sperm cells. This implicated that expression of *CycB1;1* in the mutant germ cell is sufficient to rescue the *duo1* deficiency and promote germ cell division. However, the efficiency of rescue was incompletely penetrant. Genetic analysis predicts that in the case of 100% rescue efficiency, the presence of a single effector transgene is expected to reduce the 50% bicellular phenotype in heterozygous *duo1* pollen populations to 25% bicellular pollen. This was not observed in the lines generated; instead, a lower efficiency rescue was observed ranging between 35% - 44% bicellular pollen at pollen maturation. The explanation for this inefficient rescue might be the result of weak activity of the *DUO1* promoter that fails to produce the native amount of CycB1; 1, or the absence of other factors that are also essential for the G2/M transition and are in the regulatory network of DUO1 protein. It remains to be clarified whether enhanced expression of CycB1;1 will be sufficient to increase the rescue efficiency of *duo1* division defect.

Studies of germ cell fate determination in the *duo1* mutant have also established that *DUO1* is essential for the expression of germ cell fate markers (Brownfield et al., 2009). To investigate whether the rescued *duo1* mutant pollen also acquire the fate of a germ cell, germ cell markers were introduced to the rescued plants. It was identified that despite the partial restoration of the division competence, the rescued tricellular pollen grains fail to activate the germ cell markers. By contrast, a similar analysis in the *cdka;1* single germ cell mutant showed normal activation of the marker genes, illustrating that progression through cell division and cell differentiation can be uncoupled. Thus, together these results accentuate the essential role of *DUO1* as an integrator of germ cell division and cell fate specification.

D: Expression of hp*AtCycB1* is detrimental for mitotic cell cycle progression

Progression through the two mitotic divisions in the male gametophyte is highly co-ordinated and only few division mutants that perturb this process have been described (Twell et al., 2006). To address the role of CycB1 family members in regulating these two division events, an RNAi approach was used to knockdown their expression specifically at the microspore stage and in the germ cell. Due to possible functional redundancy, a common sequence was used to direct degradation of all family members. Cytological analysis revealed a significant role of the CycB1 family in the formation of twin sperm cells. Expression of hairpin dsRNA at the microspore stage led to the prophasic unicellular microspore arrest, induced DNA degradation and eventually caused pollen death. By contrast, expression of the same fragment specifically in the germ cell led to prophasic germ cell nuclei arrest and a low frequency of pollen cell death. This effect was identified to be specific as expression of the RNAi fragment in the vegetative cell did not induce such effects. FDA staining revealed that the mutant pollen grains were only partially viable, and thus, were unlikely to undergo double fertilization and initiate embryogenesis. It remains to be established if the single germ cell produced can correctly express cell fate markers and is capable of fertilizing indiscriminately either female gamete. Overall, this work has provided evidence of a novel function of CycB1 family as a positive regulator of cell proliferation during the development of the male gametophyte.

E: A glimpse of the smRNA activity in the male gametophyte

The key aim of this project was to unveil and understand the expression patterns of essential components of the smRNA machinery to provide evidence for the function of smRNA pathways in eliciting the rapid transcriptomic changes and chromatin remodelling that accompanies male gametophyte development. Previous analysis has suggested a cessation of active expression of smRNA components in mature pollen of *Arabidopsis thaliana* (Pina et al., 2005). However this study investigated only a subset of the key components involved,

thus providing a rather limited conclusion. The analysis of microarray data from different stages of pollen development carried out in this project has revealed a significant presence of key smRNA pathway components throughout pollen development. Investigation of essential proteins with confirmed or putative roles in smRNA pathways showed consistent patterns of expression with high transcript abundance at the early stages and a decline in expression at the late stages of pollen development, but importantly, continuous expression of some of these genes until mature pollen stage. Furthermore, expression of many of these components with demonstrated functions in smRNA pathways, including *DCL1*, *AGO1*, *AGO4*, *RDR2*, *RDR4* and *RDR6* were verified by RT-PCR analysis and identified to show expression throughout all stages of male gametogenesis (Grant-Downton et al., 2009).

One of the essential components involved in the smRNA pathways is the DCL protein that is involved in the biogenesis of siRNAs from long dsRNA transcripts. Members of the *DCL* gene family showed early activity and loss of expression following germ cell division, reflecting the general pattern of gene expression during pollen maturation (Honys and Twell, 2004). However, this is with the exception of *DCL1*, which showed persistent expression in mature pollen. This observation suggests a role for DCL1 in substituting the function of other DCL proteins at pollen maturation (Gasciolli et al., 2005). An alternative explanation for the lack of expression of other *DCL* genes is the inheritance of stable proteins from the bicellular stage that are employed during the later stages.

ARGONAUTE family proteins have been implicated in the cleavage of miRNA and siRNA and the maintenance of genome integrity through heterochromatin formation. The expression pattern of the *AGO* family members during pollen development is diverse with more than five genes showing persistent expression in mature pollen. *AGO1*, *AGO4*, *AGO5* and *AGO9* are expressed at all four stages of pollen development; *AGO2*, *AGO6*, and *AGO10* are expressed only at the first two stages; whereas *AGO7* and *AGO8* are excluded in the male gametophyte. *AGO1* is involved in several smRNA pathways and shows partial redundancy

with *AGO10* (Lynn, 1999). *AGO1* is expressed highly at microspore and bicellular stage and persists at lower levels in tricellular and mature pollen stage. Whereas, *AGO10* expression ceased at the bicellular stage. Since *AGO10* expression is confined to stem cells in sporophytic tissues, its expression in pollen might reflect the loss of stem cell characteristics following germ cell division with the later roles being substituted by *AGO1*. *AGO5* is the Arabidopsis representative of the plant specific *MEL1* subfamily that has been demonstrated to be essential for reproduction in rice (Nonomura et al., 2007) and recently has been shown to bind siRNAs derived from intergenic regions of the genome (Mi et al., 2008). Thus, the elevated expression of *AGO5* at the mature pollen stage might reflect its role in chromatin remodelling during gametogenesis, which is accompanied by a great change in chromatin states of the vegetative cell and sperm cells. These results provide evidence to suggest that AGO proteins might be actively involved in the cleavage of miRNA and siRNA and in guiding heterochromatin formation during male gametophyte development. *AGO5* could also be involved in epigenetic mechanisms such as RNA-directed chromatin changes to induce the reproductive cell fate in sporogenous tissues required for Arabidopsis male gametophyte development.

RNA-dependent RNA polymerases are essential in amplifying the RNAi effect and allowing its inheritance through generations. RDR family members are also constitutively expressed with the exception of *RDR1* and *RDR3*, which cease their expression at the bicellular and tricellular stages respectively. *RDR5* showed an unusual pattern with reliable expression at the first two stages, absence at the tricellular stage, and then strong reappearance at the mature pollen stage. The significance of this unusual pattern is yet to be clarified. A homologue of *RDR2* is required for propagation of paramutation in maize (Alleman et al., 2006), thus, abundance of RDR transcripts throughout pollen development might have a critical role in the transmission of epigenetic information through successive generations.

A recently generated transcriptomic dataset from isolated sperm cells of Arabidopsis has shown enriched representation of genes involved in RNA-directed DNA methylation (RdDM), maintenance of DNA methylation, and active demethylation (Borges et al., 2008). These included *AGO9*, *DDM1*, *DRB4*, *MET1* and *SUVH5*, all demonstrated to be involved in DNA methylation. Furthermore, expressions of two other key components that are involved in the biogenesis of siRNA (*DCL1* and *AGO5*) were also detected at high levels in sperm cells. The transcriptomic data showing the expression of *DCL1*, *AGO5* and *AGO9* in sperm cells coincides with the RT-PCR results obtained in the analysis of the smRNA components (Chapter 4, Figure 4.2). These results suggest a possible role of smRNA pathway in *de novo* methylation in sperm cells nuclei. Other key components with defined roles in the smRNA pathways including *HYL1*, *SERRATE*, *HASTY* and *HEN1* are also expressed during male gametogenesis. Overall, this evidence has highlighted the expression of essential smRNA components, which strongly suggests potential smRNA activities in modulating gene expression and controlling the chromatin epigenetic state of the male germline.

F: New pollen cell-specific RNAi vectors are invaluable for studying gametophytic gene functions

The effective study of male gametophyte development has been impeded due to the inability to manipulate expression of genes of interest in a rapid and efficient manner. The lack of molecular vectors with temporal and spatial specificity that are applicable specifically in pollen for studying gene function was overcome in the course of this project. These vectors have made a significant contribution in unraveling the role of key molecules involved in the cell cycle progression during male gametogenesis. The effectiveness of these tools in manipulating gene expression in different cell types of pollen and the invaluable contribution that has been made to the understanding of the networks that govern male germline development, are well supported. To date, manipulating gene expression in

specific pollen cell types has been made possible and substantial progress in identifying factors with key role in the male gametophyte is within grasp.

Since the completion of Arabidopsis genome sequencing project and its annotation (The Arabidopsis Genome Initiative, 2000), the functional identification of annotated genes has become increasingly important. Many 1000s of insertion lines have been generated and are currently available; however, to date this has not provided sufficient coverage of all the genes identified hence impeding comprehensive studies of gene function. To help overcome this impediment, this project aimed to generate molecular vectors that can be applied to manipulate gene expression specifically in pollen to understand the role of specific genes during male gametogenesis. The RNA interference-based Gateway vector (pK7gwiwgL) obtained from the Flanders Institute for Biotechnology (VIB), Gent, Belgium (Karimi et al., 2005), was modified to accommodate pollen cell-specific promoters. Current information from the literature was used to select appropriate promoters for driving the expression of cloned sequences. Target fragments were cloned in a juxtaposed orientation using the Gateway cloning system (Invitrogen, Carlsbad, CA), which facilitates quick and efficient construction of vectors. Another key component of these RNAi vectors is the presence of intron within the hairpin structure, which has been demonstrated to increase the efficiency of RNAi effect (Wesley et al., 2001). Taken together, the male gametophyte lineage of Arabidopsis is now equipped with new precision tools that make use of the smRNA pathways in the male gametophyte to manipulate gene expression on a large scale and address protein function. These tools are especially valuable in cases of functional redundancy whereby elimination of more than one gene is necessary to observe phenotypic effect.

Within this project, application of these vectors has proven successful in accomplishing the main objective of this project. Using these vectors, the role of the CycB1 family in regulating progression through PMI and PMII was successfully demonstrated despite possible functional redundancy among the family members. Within this project, RBR1 was also

identified to impede vegetative cell nucleus progression through the cell cycle. This discovery was achieved following targeted knockdown of *RBR1* specifically in the vegetative cell using the LAT52-hpRNAi construct. The effect of this construct was specific to the vegetative cell, demonstrating the precision of the tools used. Moreover, generation of these vectors has provided a functional test of the smRNA pathways following the discovery that key components of these pathways are expressed in the male gametophyte.

In light of success of the RNAi technology, there has been concern on its application particularly in pollen. Recently, analysis of a T-DNA insertion of the MADS-box transcription factor gene that is expressed during pollen development (*AGAMOUS-LIKE18*, *AGL18*) and analysis of several *AGL18* RNAi lines, revealed a pollen lethality phenotype associated with some of the RNAi lines (20%) that was not detectable in the *AGL18* T-DNA knockout insertion (Xing and Zachgo, 2007). The authors of this study suggested that the pollen lethality observed in *AGL18* RNAi lines was not caused by the loss of *AGL18* function; instead, it is a common phenomenon that occurs in RNAi populations. Additional investigation has shown that transformation of any vector including empty vectors showed up to 10% of the transgenic population with 20-50% aborted pollen grains (Xing and Zachgo, 2007). The origin of these abnormal pollen grains was traced back to uninucleate microspore stage. Thus, the authors are convinced that at least 10% of Arabidopsis transgenic plants produce 20%-50% nonviable pollen grains in anthers, and this phenomenon is independent of the construct type used for transformation. This observation was quite obscured in comparison to that of the RNAi lines generated in this project and several transgenic lines that express marker genes that were also generated in a similar way (communication with other lab members).

The presence of aberrant pollen grains in the RNAi population was observed in some individuals. However, this did not represent the dominant phenotype and in some cases the appearance of the aberrant pollen could be linked with the presence of effector transgene in RNAi and in T-DNA lines of the same gene of interest. For example, introduction of GEX2-

hpCycB1 RNAi construct in wild type Col-0 plants led to the mitotic arrest of the germ cell nuclei represented by 30%-40% of the total population, and 5%-10% of aberrant (collapsed) pollen in some siblings (see Chapter 3 for more details). Of the 35 T1 transgenic lines generated, only three individuals possessed these other aberrant pollen phenotypes with one individual that showed a significant proportion (~46%) of aberrant pollen. In contrast, expression of the same RNAi fragment in the vegetative cell (LAT52-hpCycB1) in which *CycB1;1* is not expressed, did not lead to significant aberrant pollen (< 1%, similar to wild type plants) in the 39 T1 individuals analysed.

Furthermore, expression of a hairpin RNAi fragment targeted to *RBR1* mRNA specifically in the vegetative cell (LAT52-hpRBR1), resulted in aberrant pollen grains and pollen grains with the increased vegetative nuclei fluorescence (IVF) as predicted (Chen et al., 2009). The aberrant phenotype represents between 10%-20% of the total population. The occurrence of the aberrant pollen could be traced to the bicellular stage demonstrating the specificity of the LAT52 promoter (Chen et al., 2009). The IVF phenotype was detected from the tricellular stage and increased at the mature pollen stage (see Chapter 4 for more details). Similarly, analysis of an *RBR1* T-DNA insertion line also showed a significant proportion of aberrant pollen grains in consecutive generations. Moreover, analysis of other constructs that possess marker gene only (e.g. pDUO3-GFP::GUS, pCycB1;1-D.box::GFP, and many more) did not show development of any aberrant pollen grains. These observations suggest that the occurrence of the collapsed pollen grains as a result of transformation is a random effect and not necessarily the aftermath of the expression of hpRNAi constructs. Moreover, the collapsed pollen observe by Xiang et al, (2007) might have been influence by growth conditions, an element that was not addressed. As such, the tools generated have been applied to successfully manipulate expression of the target genes as intended and have proved very useful in addressing gene function in a temporal and spatial manner during male gametophyte development.

In the near future, these vectors will be used to analyse function of multiple genes with known function in other tissue types, those without a known biological role and gene families with multiple members that are potentially functionally redundant. In effect, the advantage of the tools generated is, several hypomorphic alleles can be generated with a range of knockdown capacity, which will provide more insight into the kinetics of protein function without interfering with the sporophytic gene expression. The Gateway cloning technology will allow high-throughput screening of genes of interest, and in-turn, lead to quick progress in building the intrinsic regulatory network in male gametophyte development and increase our understanding of the cellular processes at the molecular level.

G: *DUO3* is a novel regulator of germ cell cycle progression

A screen for pollen division mutants led to the identification of the *duo pollen* genes that specifically affect germ cell division in the male gametophyte. *DUO3* was identified as a novel gene that results in germ cell division defects reminiscent of that of the *duo1* mutation (Durbarry et al., 2005). However, *DUO3* was mapped to a different chromosomal location and was identified as an independent locus (AT1G64570). Cytological analysis of plants carrying the *duo3* mutation showed that male germ cells in *duo3* pollen fail to divide, resulting in bicellular pollen with a single germ cell at pollen maturation. Furthermore, analysis of mitotic index and monitoring of DNA content demonstrated that *duo3* mutant germ cells complete the DNA replication phase prior to PMII in synchrony with the wild type germ cells. However entry into mitotic phase of PMII is blocked, and instead *duo3* germ cells initiate another round of DNA replication (Durbarry et al., PhD thesis 2004). These phenotypic characteristics are unique to *duo1* and *duo3*, but are in contrast to other germ cell division mutants such as *duo2*, *cdka;1* and *caf1*, whereby mutant germ cells enter PMII

but fail to progress through mitosis or experience a slow S-phase respectively (Nowack et al., 2006; Chen et al., 2008; Durbarry et al., 2005). Several studies have demonstrated that in higher eukaryotes entry and progression through mitosis is arbitrated minimally by *CDKA* and its B-type cyclin subunits (Reviewed by Inze, 2007). Thus, lack of entry into mitosis by the *duo3* mutant germ cells indicates that essential cell cycle regulators or other factors that modulate their activities are likely to be impaired in the mutant germ cell. To investigate if this might be the case, the activity of a key G2/M regulator *CycB1;1* was investigated in the mutant *duo3* background.

H: Expression of *DUO3* is not restricted to the male gametophyte

Analysis of transcriptomic datasets revealed abundance of *DUO3* transcripts throughout vegetative development with enhanced expression in shoot apex and cork, and a gradual increase during male gametophyte development. The microarray pattern was verified by RT-PCR. With the potential role of *DUO3* in regulating cell cycle progression in mind, the transcriptomic profile of *DUO3* was compared alongside that of a known cell cycle regulator, *CycB1;1,* throughout development. Where enhancement was observed with *CycB1;1* in certain tissues, the profile correlates with that of *DUO3* although not at the same level. As such, it can be proposed that *DUO3* might have a wider role in regulating cell cycle progression not only in the germ cell but also in sporophytic tissues. Indeed, rescue of the *duo3* phenotype specifically in pollen to generate a homozygous *duo3* mutation, resulted in abnormalities of seedling germination that eventually led to death (Brownfield et al., 2009). *In vivo* analysis of *DUO3* promoter-reporter activity by GUS staining, correlated with the profile predicted by microarray data and RT-PCR, showing strong staining throughout development restricted to the vascular tissues of developing seedlings and rosette leaves.

The staining was strongly enhanced in the shoot apex of 10-day-old seedlings specifically localized in the leaf primordia, highlighting increased *DUO3* activities in tissues rich in division competent or dividing cells. Furthermore, constrained *DUO3* promoter activity was also observed in the primary roots and in the lateral roots of seedlings where GUS staining was restricted to tissues of the root apical meristems and localized in specific cell files including the pericycle and the cortical cell layer. The staining within these cell files occurred in a patchy or "salt and pepper" pattern that fades towards the areas of elongation and differentiation, By contrast, staining in the lateral root was confined consistently in the lateral root primordia. Thus, the patchy pattern and the restricted *DUO3* promoter activity within tissues that are competent to divide recapitulate the patterns observed with known cell cycle regulators (Colon-Carmona et al., 1999a). This correlation supports the possible role of *DUO3* in regulating cell cycle progression.

The expression of *DUO3* in the male gametophyte was distinct compared to its profile that was observed in the sporophytic tissues. All results of the expression analysis showed a gradual increase in expression during pollen development, which does not reflect the proliferation state of the male gametophyte. Does *DUO3* have other roles apart from regulating cell cycle progression in the male germ cell? A weak expression signal at the microspore stage does not seem to signify a role of *DUO3* at PMI, since *duo3* mutant pollen grains progress normally during microspore division, although this might be explained if there is inheritance of RNA or protein from the pollen mother cell sufficient to allow normal progression through PMI. Knockdown of *DUO3* transcripts at the microspore stage would provide an approach to address this question.

I: Turnover of CycB1;1D-box::GFP is impaired in *duo3* mutant germ cells

Study of the relationship between *DUO3* and *AtCycB1;1* with the purpose of elaborating the nature of *duo3* mutation, revealed that expression of *AtCycB1;1* does not depends on the presence of *DUO3*. Intriguingly, the AtCycB1;1D-boxGFP marker (pCDGFP) appeared to persist in the *duo3* mutant pollen but not in the wild type sperm cells. In cells that undergo mitotic division, exit from mitosis is marked by the degradation of *CycB1;1* protein through the Ubiquitin-26S proteosome mediated proteolysis involving the Anaphase Promoting Complex (APC). Evidence for ubiquitin-mediated proteolysis in the germline was demonstrated by the turnover of *CDKA* inhibitors, *KRP6* and *KRP7,* by the F-box-Like protein (*FBL17*), which demonstrates the essential role of *FBL17* in modulating the rate of S-phase progression in the germ cell (Kim, 2008). Could the APC activity in the *duo3* mutant germ cell be impaired? Perhaps *DUO3* is required to enhance the expression of an essential component to allow full APC activity in the germ line, and thus in the absence of *DUO3* only a reduced APC activity can be achieved. Alternatively, in wild type, the activation of APC occurred during exit from mitosis. Thus, since *duo3* mutant pollen does not enter mitosis (Durbarry et al., PhD thesis 2004), the APC pathway is never activated due to lack of correct mitotic signals. One of the future perspectives of this project will be to investigate the activity of the APC complex in *duo3* mutant cells by analysing expression of the key components in the mutant germ cells. In addition, a screen of APC mutant alleles should be done to analyse any division defects in pollen, also combining these mutant alleles with the *duo3* mutation to determine possible enhancement of the *duo3* phenotype, will aid in understanding the role of *DUO3* in cell cycle progression during male gametogenesis.

Conclusion

The discovery of the important role of CycB1 family in governing mitotic progression in the male gametophyte has been a stepping-stone towards the understanding of the entire network that regulates cell cycle progression during pollen development. The role of *DUO1* (R2R3 MYB) in regulating *CycB1;1* expression has increased our understanding of the *DUO1* role in the male germline, helping to build the network through which *DUO1* regulates its target genes. More importantly, for the first time an R2R3 MYB transcription factor, DUO1, has been identified as a male germline specific regulator that links cell division and cell fate determination. Completion of Arabidopsis genome sequencing has set a challenge to understand the function and interplay of genes during plant development. Established methods that involve chemical mutagenesis, T-DNA and transposon tagging, have been very useful in screening individual gene functions. However, these methods induce random mutagenesis, and have hence proved to be laborious in identifying mutants in each gene and tracking down the gene responsible for that particular mutation. On the other hand, the exploration of the RNAi technology has made a significant contribution in studying gene functions in plants that can overcome the problem of functional redundancy among family members. This technology has revolutionized the study of genes in *C. elegans* and in *Drosophila*, and currently it has been applied for the whole genome screening in *C. elegans*. The construction of pollen cell-specific RNAi vectors has proved to be very useful for studying gene function in the male gametophyte, particularly for addressing roles in a selected cell type. The use of these tools and the demonstration of the existence of critical smRNA components during pollen development have opened a “new file” in building up molecular evidence for the involvement of smRNA pathways in regulating patterns of gene expression and chromatin organisation during male gametogenesis. In expanding the complex networks that control transition through the cell cycle phases of the male gametophyte, characterization of *DUO3* expression has highlighted wider roles for *DUO3* in

regulating both entry into PMII and a role associated with cells competent to divide in sporophytic development. Furthermore, the failure of *duo3* mutant germ cells in degrading a mitotic product (CycB1;1::GFP) has implicated a role for *DUO3* in the activation of APC activity and provided opportunity to explore the relationship between *DUO3* expression and the activation of the APC complex. Together, these results presented in this thesis have fulfilled the key objective of the project and made a significant contribution towards the understanding of the cellular processes imposed in regulating the formation of twin sperm cells for double fertilization.

Appendix

Primer sequences used in polymerase chain reactions (PCR)

Primer name	Primer sequence
CycB project	
CycBRNAiF	AAAAAGCAGGCTTGATCCTGGTGGAGTGGTTG
CycBRNAiR	AGAAAGCTGGGTCCAAATTTCTTCATACTTGGCCG
CycB1;1cDNAF	AAA AAAGCAGGCTTCATGATGACTTCTCGTTCGATTGTTC
CycB1;1cDNAR	CAAGAA AGCTGGGTCCTA AGCAGATTCAGTTCCGGTCAAC
CycB1;1cDNAR-Stop	CAAGAA AGCTGGGTCGTA AGCAGATTCAGTTCCGGTCAAC
AtCycB1;1F	ATGGTGC ACTATTTGGCTGAG
AtCycB1;1R	GATTCAGTTCCGGTCAACAA AGC
AtCycB1;2F	C CTCACCGTCA ACATCATTG
AtCycB1;2R	ATCATCCCCA ATTCAGCAAG
AtCycB1;3F	TCTTGCTGCTGTGGAATACG
AtCycB1;3R	TTCAAGATTCCCCAAAATGG
AtCycB1;4F	GAAACAACCACAGCAG CAGA
AtCycB1;4R	CGTCTCTGGC ATCAACTCAA
AtCycB2;1F	AGGAGGTTTCGGTTCCTGTT
AtCycB2;1R	GGAAACCGAAGCATCTCGTA
AtCycB2;2F	TTGCATTGCTCTTAGCTTGC
AtCycB2;2R	AACGACGCCAAGATCTCAAG
AtCycB2;3F	CGGCCTCAGC AATCTACACT
AtCycB2;3R	GAAACCCAGCTGGTTCAGTT
AtCycB2;4F	GTTCATCAAC ATATCGCGAG
AtCycB2;4R	CTGGTTTTGCTCCAATCCTC
AtCycB3;1F	GATCAGCATATCCGCAGAATC
AtCycB3;1R	CAAGACTGCGACGTTACTGC
AtCDKA;1F	CAG GCTAGAGCAG GAGGATG
AtCDKA;1R	ATGTCCTGACAGGGATACCG
MYB3R4F	GCAAGTTTCAACCCCAAGAA
MYB3R4R	TCTCCCCAGGACTGAAAATG
CYCB1.1RTF2	AAGAGAAACGCAGTACCAAAGC
CYCB1.1RTR2	ATATTCCACAGCTGCGAGGT
DUO1-CycB1;1/F	ATCCAACCGCCACTACAAAA
DUO1-CycB1;1/R	GGTTTCCCAGCCACTTTCTT
smRNA project	
AG01 forward	TTCAGGGCACTTCTCGACCTG
AG01 reverse	AGCTGGGAGTGGCCTCACTG
AG02 forward	GACCGAGCGGTGGTGAAATC
AG02 reverse	GCCTCCATCTGCATCCCAAG
AG03 forward	CTGGAAACCAGCCTCCAAGG
AGO3 reverse	TCCACCGTTGTCATGTTTGG
AGO4 forward	AAGCACCAGTGCCATTTCTG
AGO4 reverse	AACCCCAACAGGCAAACAAG
AG05 forward	CCCTGAGCAACACGGGAATC
AG05 reverse	TAGTAGCGGGCACGGAATGC
AGO6 forward	TGTTGTGGACACCAAGATCG
AGO6 forward-Col	TGTCGTGGACACCAAGATCG
AGO6 reverse	TCTGGAACTTTCCCGTCCTC

AGO7 forward	GATCGGTTGGTCCATCGAG
AGO7 forward-Col	GATCGGTCGGTCCATCGAG
AGO7 reverse	TGATCAGAGCTGCCTCCAATACTC
AG08 forward	GCGGTTGTGAGCTCCAGAGAG
AG08 reverse	GGGCTTTCGGTTTGGAAGAAC
AG09 forward	CTATCTCTGCGCCCATGCTG
AG09 reverse	AGGTGGCACAGGGACTGCTC
AG010 forward	ACAGAAGCGTCACCACACACTCG
AG010 reverse	CGTGCTCGAAATGCTGCAAG
RDR1F	GGTTCCGCCAAGAACGTCTG
RDR1R	TGTTGGCTTATCCGGTTTCTCC
RDR2F	GCGAAATGGACCCTCCAATG
RDR2R	TCAAACCGTTCCAGAAAATCAGG
RDR3F	AAGGGGGCTAAGGTTGATCTCC
RDR3R	CGCTTGGGACATTTCACTTCG
RDR4F	TTCTTGGATTAATCTTTGACACTGTGG
RDR4R	GTGCAAGGGCCTTTGGGTAG
RDR5F/3	CAAGCCAGCTTTCCCCAGAAG
RDR5R/3	GACCGGCTCATCTTCGAAACAC
RDR6F	GAAAAGCTATCCGGCCATGC
RDR6R	CCGACCCAAGATTTTGTTCGAC
HYL1F	GGGAATTAGCAAAATCCAGTGAGC
HYL1R	GGATCGCTAAAAGAGCAGTTCTCC
SERRATE-F	AAGTTGGGTATGATGCATTTGGTG
SERRATE-R	TTCCTCTGGAGCATCTAGGTCTTG
HEN1-F	AGCTTGCAACGTCAAATCTGCTAC
HEN1-R	ATGCCCATTGATTGAACTGTTCTC
HASTY-F	ACTAGCAGCCCCAAAGAACAAAAG
HASTY-R	TGACATGGAAGCTTTGGTTAGAGG

Pollen cell specific molecular vectors

DUO1F SacI	AAGATCTAGACGTCCGAAGTTTCCCTCTTGG
DUO1R SpeI	TTTTACTAGTCGCTAATCGATCTCTCTCTCG
GEX2-F XbaI	CCGGTCTAGATTCTTACATCGGATGGATTCAC
GEX2-R SpeI	CAGATGGACTAGTTAACCCT TCACAACAAGAG
LAT52-F SacI	GTATTGAGCTCTGATCGATTCTGGGTCATTTG
LAT52-R SpeI	GAGCACTAGTGCCTTTGCCATTTTAAATTGG
GEX2-F SacI	CTCAGAGCTC TTCCCTTCAC AGGTTTC
GEX2-F HindIII	GGTCAAGCTT CTTACATCGG ATGGATTCAC
GEX2-R XhoI	CTAACTCGAG GGTACATTAA CCCTTCACAA C
LAT52-F HindIII	TCAGAAGCTTTTGAGGAATG ATCGATTCTG G
LAT52-R XhoI	CCATCTCGAG GAAATTTTTT TTTTGGTGTG TG
proDUO1-F HindIII	GAAAAAGCTTAAC GTCCGAAGTT TCCCTCTTG
proDUO1-R XhoI	TTCCCTCGAG CTAATCGATC TCTCTCTCG
proDUO1-F Sa-AS	GAAGGTCGAC GGCGCGCCTT AACGTCCGAA GTTTCC
MSP2-F SacI	GTCAGAGCTC ATGAAAAATT GTATGTTAGT CTAC
MSP2-R SpeI	GTATACTAGT GTGTGTGTAT TTATAAGGG
MSP2-F HindIII	TGTCAAGCTT CATGAAAAAT TGTATGTTAG TCTAC
MSP2-R XhoI	TGTACTCGAG TGTGTGTGTA TTTATAAGGG
proDUO1-R NruI	TTCCTCGCGACGCTAATCGATCTCTCTCTCG
DUO3-R PstI	TCGTCTGCAG TCTCCAGCGC TTCCTCAAG
MSP2-F SacI	GTCAGAGCTCATGAAAAATTGTATGTTAGTCTAC
MSP2-R SpeI	GTATACTAGTGTGTGTGTATTTATAAGGG

LAT52-F SacI	TCAGGAGCTCTTGAGGAATG ATCGATTCTGG
LAT52-R SpeI	CCATACTAGTGAAATTTTTTTTTTTGGTGTGTG
Targets for testing tools	
TIONF	AAAAAGCAGGCTATGGGTGTCGAGGATTATCATGTG
TIONR	AGAAAGCTGGGTTCACATAGCTTAACGACAGAGCCAG
TIOCF	AAAAAGCAGGCTCAGCGCTCTTGCGGAACATCAAATC
TIOCR	AGAAAGCTGGGTCATAGTGAGCAATGTTAGCCTCAGG
CDKAF	AAAAAGCAGGCTATGGATCAGTACGAGAAAGTTGAG
CDKAR	AGAAAGCTGGGTCAGCAAGCTTCAGTGAGTTTG
RBR-RNAiF	AAAAAGCAGGCTCTGGAAGAGACGTCCATCTC
RBR-RNAiR	AGAAAGCTGGGTCGCTGCTCTGCCCATATGTC
RBR/RT-PCRF	GATGGGAGCACTTGCGATGAAG
RBR/RT-PCRF	CTTGACCACAAACTGAGGTAACTC
DUO3 project	
D3CDS5'	5'-ATGAAATCTCTGGATCAAGTAG-3'
D3CDS3'	5'ACAATACTTGGACTTGTTTCCG
RT-PCR primers	
asDUO3-Exon1-F	5'-AAAAAGCAGGCTTCATGAAATCTCTGGATCAAGT
asDUO3-Exon1-R	5'-AACCCAGCTTTCTCGTCAGAAACATCAACTAGA
RTDUO3F	5'-GCCTTACCGAGACCCATCATTACTGC
RTDUO3R	5'-GAACCCCCTGGGTCTCTGTTTGCAG
RTSIAF	5'-CTCTTTGTGCACTTGATCATTCACG
RTSIAR	5'-GCTCGCCTTTACTAGGAAGAAACC
RNAi knockdown	
DUO3-RNAiF+attB1	5'-AAAAAGCAGGCTTAGAGGGCAGACAAGGAAAGGAG
DUO3-RNAiR+attB2	5'-AGAAAGCTGGGTCATCAGTCTC CAGCGCTTCC
DUO3-F XhoI	5'-CAAACTCGAGAGGGCAGACA AGGAAAGGAGG
DUO3-R EcoRI	5'-CCTCGAATTC AGTCTCCAGC GCTTCCTCAA G
DUO3-F SpeI	5'-CATTACTAGTGTTCCCCAAACCTTAGAGGGCAG
DUO3-R ClaI	5'-CGTCATCGATCTCCAGCGCTTCCTCAAGTTC
DUO3 TILLING	
TILL1-5'	5'-CTGAGGAAGATGATGCAATCTGCAAAC
TILL1-3'	5'-CGATGATGCTGAACCAGTGACAAG
TILL2-5'	5'-CAATAAATGGCTTCACTCAAGCCCAA
TILL2-3'	5'-TTGGGCTTGAGTGAAGCCATTTATTG
dCAP TILL1F	5'-TGTCAACTGAGGAAGATGATGC
dCAP TILL1R	5'-CTCATCATCGACATTAGGAATAGAAT
dCAP TILL2R	5'-CGGTATTCTTCCTCATCATCGACATTAGGAATATGAT
duo3-1 dCAP-F	5'-CAACATAAGCACTAAGCGACGTCCTGTGACCAGG
General primers	
attB1 adaptor	GGGGACAAGTTTGTACAAAAAAGCAGGCT
attB2 adaptor	GGGGACCACTTTGTACAAGAAAGCTGGGT
gent-NPT2/F	AGCGGCGATACCGTAAAGCA
gent-NPT2/R	GTCCGGTGCCCTGAATGAAC

Bibliography

Ach R, Durfee T, Miller A, Taranto P, Hanley-Bowdoin L, Zambryski P, Gruissem W (1997) RRB1 and RRB2 encode maize retinoblastoma-related proteins that interact with a plant D-type cyclin and geminivirus replication protein. Mol Cell Biol **17:** 5077-5086

Adenot X, Elmayan T, Lauressergues D, Boutet S, Bouché N, Gasciolli V, Vaucheret H (2006b) DRB4-Dependent TAS3 trans-Acting siRNAs Control Leaf Morphology through AGO7. Current Biology **16:** 927-932

Alandete-Saez M, Ron M, McCormick S (2008) GEX3, expressed in the male gametophyte and in the egg cell of Arabidopsis thaliana, is essential for micropylar pollen tube guidance and plays a role during early embryogenesis. Mol Plant **1:** 586-598

Albani D, Sardana R, Robert LS, Altosaar I, Arnison PG, Fabijanski SF (1992) A Brassica napus gene family which shows sequence similarity to ascorbate oxidase is expressed in developing pollen. Molecular characterization and analysis of promoter activity in transgenic tobacco plants. The Plant Journal **2:** 331-342

ALLEMAN M, SIDORENKO L, MCGINNIS K, SESHADRI V, DORWEILER JE, WHITE J, SIKKINK K, CHANDLER VL (2006) An RNA-dependent RNA polymerase is required for paramutation in maize. Nature(London) **442:** 295-298

Allen E, Xie Z, Gustafson AM, Carrington JC (2005) microRNA-Directed Phasing during Trans-Acting siRNA Biogenesis in Plants. Cell **121:** 207-221

Aufsatz W, Mette M, Matzke A, Matzke M (2004) The role of MET1 in RNA-directed de novoand maintenance methylation of CG dinucleotides. Plant Mol Biol **54:** 793-804

Aufsatz W, Mette MF, van der Winden J, Matzke AJM, Matzke M (2002) RNA-directed DNA methylation in Arabidopsis. Proceedings of the National Academy of Sciences **99:** 16499-16506

Aukerman MJ, Sakai H (2003) Regulation of Flowering Time and Floral Organ Identity by a MicroRNA and Its APETALA2-Like Target Genes. Plant Cell **15:** 2730

Baker CC, Sieber P, Wellmer F, Meyerowitz EM (2005) The early extra petals1 Mutant Uncovers a Role for MicroRNA miR164c in Regulating Petal Number in Arabidopsis. Current Biology **15:** 303-315

Bartel DP (2004) MicroRNAs Genomics, Biogenesis, Mechanism, and Function. Cell **116:** 281-297

Baulcombe D (2004) RNA silencing in plants. Nature **431: 356-**363

Baumberger N, Baulcombe D (2005) Arabidopsis ARGONAUTE1 is an RNA Slicer that selectively recruits microRNAs and short interfering RNAs. PNAS **102:** 11928-11933

Beclin C, Boutet S, Waterhouse P, Vaucheret H (2002) A branched pathway for transgene-induced RNA silencing in plants. Curr Biol **12:** 684-688

Bogre L, Zwerger K, Meskiene I, Binarova P, Csizmadia V, Planck C, Wagner E, Hirt H, Heberle-Bors E (1997) The cdc2Ms Kinase Is Differently Regulated in the Cytoplasm and in the Nucleus. Plant Physiol **113:** 841-852

Borges F, Gomes G, Gardner R, Moreno N, McCormick S Feijo JA, Becker JD (2008) Comparative transcriptomicsofArabidopsis thaliana sperm cells. Plant Physiol 148:1168-1181

Boudolf V, Barroco R, Engler JA, Verkest A, Beeckman T, Naudts M, Inze D, De Veylder L (2004) B1-Type Cyclin-Dependent Kinases Are Essential for the Formation of Stomatal Complexes in Arabidopsis thaliana. Plant Cell **16:** 945-955

Bourne Y, Watson MH, Hickey MJ, Holmes W, Rocque W, Reed SI, Tainer JA (1996) Crystal structure and mutational analysis of the human CDK2 kinase complex with cell cycle-regulatory protein CksHs1. Cell **84:** 863-874

Boutet S, Vazquez F, Liu J, Béclin C, Fagard M, Gratias A, Morel JB, Crété P, Chen X, Vaucheret H (2003) Arabidopsis HEN1 A Genetic Link between Endogenous miRNA Controlling Development and siRNA Controlling Transgene Silencing and Virus Resistance. Current Biology **13:** 843-848

Brandeis M, Rosewell I, Carrington M, Crompton T, Jacobs MA, Kirk J, Gannon J, Hunt T (1998) Cyclin B2-null mice develop normally and are fertile whereas cyclin B1-null mice die in utero. PNAS **95:** 4344-4349

Brewbaker JL (1967) The distribution and phylogenetic significance of binucleate and trinucleate pollen grains in the angiosperms. Am J Bot **54:** 1069-1083

Brodersen P, Voinnet O (2006) The diversity of RNA silencing pathways in plants. Trends in Genetics **22:** 268-280

Brownfield L, Hafidh S, Borg M, Sidorova A, Mori T, Twell D A Plant Germline-Specific Integrator of Sperm Specification and Cell Cycle Progression. PLoS Genetics (2009).

Cai G, Cresti M (2006) The Microtubular Cytoskeleton in Pollen Tubes: Structure and Role in Organelle Trafficking. PLANT CELL MONOGRAPHS **3:** 157

Campisi L, Yang Y, Yi Y, Heilig E, Herman B, Cassista AJ, Allen DW, Xiang H, Jack T (1999) Generation of enhancer trap lines in Arabidopsis and characterization of expression patterns in the inflorescence. The Plant Journal **17:** 699-707

Cao X, Aufsatz W, Zilberman D, Mette MF, Huang MS, Matzke M, Jacobsen SE (2003) Role of the DRM and CMT3 Methyltransferases in RNA-Directed DNA Methylation. Current Biology **13:** 2212-2217

Carmell MA, Girard A, van de Kant HJG, Bourc'his D, Bestor TH, de Rooij DG, Hannon GJ (2007) MIWI2 Is Essential for Spermatogenesis and Repression of Transposons in the Mouse Male Germline. Developmental Cell **12:** 503-514

Carpenter J, Ploense S, Snustad D, Silflow C (1992) Preferential Expression of an [alpha]-Tubulin Gene of Arabidopsis in Pollen. Plant Cell **4:** 557-571

Caryl AP, Jones GH, Franklin FCH (2003) Dissecting plant meiosis using Arabidopsis thaliana mutants. J Exp Bot **54:** 25-38

CATALANOTTO C, AZZALIN G, MACINO G, COGONI C (2000) Gene silencing in worms and fungi. Nature **404:**245

Cebolla A, Vinardell JM, Kiss E, Oláh B, Roudier F, Kondorosi A, Kondorosi E (1999) The mitotic inhibitor ccs52 is required for endoreduplication and ploidy-dependent cell enlargement in plants. EMBO J **18:** 4476-4484

Chan S, Henderson I, Jacobsen S (2005) Gardening the genome: DNA methylation in Arabidopsis thaliana, Nat. Rev.Genet **6:** 351–360

Chaubet-Gigot N (2000) Plant A-type cyclins†. Plant Mol Biol **43:** 659-675

Chen X (2004a) A MicroRNA as a Translational Repressor of APETALA2 in Arabidopsis Flower Development. Science's **303:** 2022-2025

Chen Z, Tan JLH, Ingouff M, Sundaresan V, Berger F (2008) Chromatin assembly factor 1 regulates the cell cycle but not cell fate during male gametogenesis in Arabidopsis thaliana. Development **135:** 65-73

Chen Y, McCormick S (1996) sidecar pollen, an Arabidopsis thaliana male gametophytic mutant with aberrant cell divisions during pollen development. Development **122:** 3243-3253

Chen Z, Hafidh S, Poh SH, Twell D, Berger F (2009) Proliferation and cell fate establishment during Arabidopsis male gametogenesis depends on the Retinoblastoma protein. PNAS **106**:7257-7262

Chuang CF, Meyerowitz EM (2000) Specific and heritable genetic interference by double-stranded RNA in Arabidopsis thaliana. Proceedings of the National Academy of Sciences **97:** 4985-4990

Clute P, Pines J (1999) Temporal and spatial control of cyclin B1 destruction in metaphase. Nat Cell Biol **1:** 82-87

Colon-Carmona A, You R, Haimovitch-Gal T, Doerner P (1999) Spatio-temporal analysis of mitotic activity with a labile cyclin-GUS fusion protein. The Plant Journal **20:** 503-508

Cox DN, Chao A, Baker J, Chang L, Qiao D, Lin H (1998) A novel class of evolutionarily conserved genes defined by piwi are essential for stem cell self-renewal. Genes Dev **12:** 3715-3727

Criqui MC, Parmentier Y, Derevier A, Shen WH, Dong A, Genschik P (2000) Cell cycle-dependent proteolysis and ectopic overexpression of cyclin B1 in tobacco BY2 cells. The Plant Journal **24:** 763-773

Criqui MC, Weingartner M, Capron A, Parmentier Y, Shen WH, Heberle-Bors E, Bogre L, Genschik P (2001) Sub-cellular localisation of GFP-tagged tobacco mitotic cyclins during the cell cycle and after spindle checkpoint activation. The Plant Journal **28:** 569-581

Cubas P, Lauter N, Doebley J, Coen E (1999) The TCP domain: a motif found in proteins regulating plant growth and development. The Plant Journal **18:** 215-222

Custers JBM, Oldenhof MT, Schrauwen JAM, Cordewener JHG, Wullems GJ, van Lookeren Campagne MM (1997) Analysis of microspore-specific promoters in transgenic tobacco. Plant Mol Biol **35:** 689-699

Dahl M, Meskiene I, Bogre L, Ha D, Swoboda I, Hubmann R, Hirt H, Heberle-Bors E (1995) The D-Type Alfalfa Cyclin Gene cycMs4 Complements G1 Cyclin-Deficient Yeast and Is Induced in the G1 Phase of the Cell Cycle. Plant Cell **7:** 1847-1857

Dalmay T, Hamilton A, Rudd S, Angell S, Baulcombe DC (2000) An RNA-Dependent RNA Polymerase Gene in Arabidopsis Is Required for Posttranscriptional Gene Silencing Mediated by a Transgene but Not by a Virus. Cell **101:** 543-553

de Jager SM, Murray JAH (1999) Retinoblastoma proteins in plants. Plant Mol Biol **41:** 295-299

De Veylder L, Beeckman T, Beemster GT, Krols L, Terras F, Landrieu I, van der Schueren E, Maes S, Naudts M, Inze D (2001) Functional analysis of cyclin-dependent kinase inhibitors of Arabidopsis. Plant Cell **13:** 1653-1668

del Pozo JC, Boniotti MB, Gutierrez C (2002) Arabidopsis E2Fc Functions in Cell Division and Is Degraded by the Ubiquitin-SCFAtSKP2 Pathway in Response to Light. Plant Cell **14:** 3057

Dewitte W, Murray JA (2003b) Plant cell cycle. Annu Rev Plant Biol **54:** 235-264

Doerner P, Joergensen JE, You R, Steppuhn J, Lamb C (1996) Control of root growth and development by cyclin expression. Nature **380:** 520-523

Dupl'akova N, Renak D, Hovanec P, Honysova B, Twell D, Honys D (2007) A rabidopsis Gene Family Profiler (aGFP)--user-oriented transcriptomic database with easy-to-use graphic interface. BMC Plant Biol **7:** 39

Durbarry A, Vizir I, Twell D (2005) Male germ line development in Arabidopsis: duo pollen mutants reveal gametophytic regulators of generative cell cycle progression. Plant Physiol **137:** 297-307

Durfee T, Feiler HS, Gruissem W (2000) Retinoblastoma-related proteins in plants: homologues or orthologues of their metazoan counterparts? Plant Mol Biol **43:** 635-642

Eady C, Lindsey K, Twell D (1995) The Significance of Microspore Division and Division Symmetry for Vegetative Cell-Specific Transcription and Generative Cell Differentiation. Plant Cell **7:** 65-74

Ebel C, Mariconti L, Gruissem W (2004) Plant retinoblastoma homologues control nuclear proliferation in the female gametophyte. Nature **429:** 776-780

Ehsan H, Reichheld JP, Durfee T, Roe JL (2004) TOUSLED Kinase Activity Oscillates during the Cell Cycle and Interacts with Chromatin Regulators. Plant Physiol **134**: 1-12

Elbashir SM, Lendeckel W, Tuschl T (2001) RNA interference is mediated by 21-and 22-nucleotide RNAs. Genes Dev **15:** 188-200

Engel ML, Holmes-Davis R, McCormick S (2005) Green Sperm. Identification of Male Gamete Promoters in Arabidopsis. Plant Physiol **138:** 2124-2133

Fabian-Marwedel T, Umeda M, Sauter M (2002) The Rice Cyclin-Dependent Kinase-Activating Kinase R2 Regulates S-Phase Progression. Plant Cell **14:** 197-210

Ferreira P, Hemerly A, Villarroel R, Van Montagu M, Inze D (1991) The Arabidopsis Functional Homolog of the p34cdc2 Protein Kinase. Plant Cell **3:** 531-540

Fobert P, Gaudin V, Lunness P, Coen E, Doonan J (1996) Distinct Classes of cdc2-Related Genes Are Differentially Expressed during the Cell Division Cycle in Plants. Plant cell **8:** 1465-1476

Fourgoux-Nicol A, Drouaud J, Haouazine N, Pelletier G, Guerche P (1999) Isolation of rapeseed genes expressed early and specifically during development of the male gametophyte. Plant Mol Biol **40:** 857-872

Furuno N, den Elzen N, Pines J (1999) Human Cyclin A Is Required for Mitosis until Mid Prophase. J Cell Biol **147:** 295-306

Gasciolli V, Mallory AC, Bartel DP, Vaucheret H (2005) Partially Redundant Functions of Arabidopsis DICER-like Enzymes and a Role for DCL4 in Producing trans-Acting siRNAs. Current Biology **15:** 1494-1500

Gazzani S, Lawrenson T, Woodward C, Headon D, Sablowski R (2004) A Link Between mRNA Turnover and RNA Interference in Arabidopsis. Science **306:** 1046-1048

Genschik P, Criqui MC, Parmentier Y, Derevier A, Fleck J (1998) Cell Cycle-Dependent Proteolysis in Plants Identification of the Destruction Box Pathway and Metaphase Arrest Produced by the Proteasome Inhibitor MG132. Plant Cell **10:** 2063-2076

Goodrich J, Puangsomlee P, Martin M, Long D, Meyerowitz EM, Coupland G (1997) A Polycomb-group gene regulates homeotic gene expression in Arabidopsis. Nature **386:** 44-51

Grant-Downton R, Dickinson H (2007) Germlines: Argonautes Go Full Cycle. Current Biology **17:** 919-921

Grant-Downton R, Hafidh S, Twell D, Dickinson HG (2009) Small RNA Pathways Are Present and Functional in the Angiosperm Male Gametophyte. Molecular Plant **2**: 500-512

Grigg S, Canales C, Hay A, Tsiantis M (2005) SERRATE coordinates shoot meristem function and leaf axial patterning in Arabidopsis. Nature (London) **437:** 1022-1026

Gupta R, Ting JTL, Sokolov LN, Johnson SA, Luan S (2002) A Tumor Suppressor Homolog, AtPTEN1, Is Essential for Pollen Development in Arabidopsis. Plant Cell **14:** 2495-2507

Haerizadeh F, Singh MB, Bhalla PL (2006) Transcriptional repression distinguishes somatic from germ cell lineages in a plant. Science **313:** 496-499

Hagting A, Karlsson C, Clute P, Jackman M, Pines J (1998) MPF localization is controlled by nuclear export. EMBO J **17:** 4127-4138

Hamilton A, Voinnet O, Chappell L, Baulcombe D (2002) Two classes of short interfering RNA in RNA silencing. EMBO J **21:** 4671-4679

Hamilton AJ, Brown S, Yuanhai H, Ishizuka M, Lowe A, Solis AGA, Grierson D (1998) A transgene with repeated DNA causes high frequency, post-transcriptional suppression of ACC-oxidase gene expression in tomato. The Plant Journal **15:** 737-746

Hamilton DA, Roy M, Rueda J, Sindhu RK, Sanford J, Mascarenhas JP (1992) Dissection of a pollen-specific promoter from maize by transient transformation assays. Plant Mol Biol **18:** 211-218

Hammond SM, Boettcher S, Caudy AA, Kobayashi R, Hannon GJ (2001) Argonaute2, a Link Between Genetic and Biochemical Analyses of RNAi. Science **293:** 1146-1150

Hemerly A, de A Engler J, Bergounioux C, Van Montagu M, Engler G, Inzé D, Ferreira P (1995) Dominant negative mutants of the Cdc2 kinase uncouple cell division from iterative plant development. EMBO J **14:** 3925-3932

Hiraguri A, Itoh R, Kondo N, Nomura Y, Aizawa D, Murai Y, Koiwa H, Seki M, Shinozaki K, Fukuhara T (2005) Specific interactions between Dicer-like proteins and HYL1/DRB-family dsRNA-binding proteins in Arabidopsis thaliana. Plant Mol Biol **57:** 173-188

Hirayama T, Imajuku Y, Anai T, Matsui M, Oka A (1991) Identification of two cell-cycle-controlling cdc2 gene homologs in Arabidopsis thaliana. Gene **105:** 159-166

Honys D, Twell D (2004) Transcriptome analysis of haploid male gametophyte development in Arabidopsis. Genome Biol **5 (11):** R85

Huntley R, Healy S, Freeman D, Lavender P, de Jager S, Greenwood J, Makker J, Walker E, Jackman M, Xie Q (1998) The maize retinoblastoma protein homologue ZmRb-1 is regulated during leaf development and displays conserved interactions with G1/S regulators and plant cyclin D (CycD) proteins. Plant Mol Biol **37:** 155-169

Imai KK, Ohashi Y, Tsuge T, Yoshizumi T, Matsui M, Oka A, Aoyama T (2006) The A-Type Cyclin CYCA2; 3 Is a Key Regulator of Ploidy Levels in Arabidopsis Endoreduplication. Plant Cell **18:** 382-396

Inze D, Veylder LD (2006) Cell Cycle Regulation in Plant Development. Annu Rev Genet **40:** 77-105

Ito M, Araki S, Matsunaga S, Itoh T, Nishihama R, Machida Y, Doonan JH, Watanabe A (2001a) G2/M-Phase-Specific Transcription during Plant cell Cycle Is Mediated by c-Myb-Like Transcription Factors. Plant Cell **13:** 1891-1905

Ito M, Marie-Claire C, Sakabe M, Ohno T, Hata S, Kouchi H, Hashimoto J, Fukuda H, Komamine A, Watanabe A (1997) Cell-cycle-regulated transcription of A-and B-type plant cyclin genes in synchronous cultures. The Plant Journal **11:** 983-992

Iwakawa H, Shinmyo A, Sekine M (2006a) Arabidopsis CDKA; 1, a cdc2 homologue, controls proliferation of generative cells in male gametogenesis. The Plant Journal **45:** 819-831

Jackman M, Firth M, Pines J (1995) Human cyclins B1 and B2 are localized to strikingly different structures: B1 to microtubules, B2 primarily to the Golgi apparatus. EMBO J **14:** 1646-1654

Jander G, Baerson SR, Hudak JA, Gonzalez KA, Gruys KJ, Last RL (2003) Ethylmethanesulfonate Saturation Mutagenesis in Arabidopsis to Determine Frequency of Herbicide Resistance. Plant Physiol **131:** 139-146

Jiang C, Gu X, Peterson T (2004) Identification of conserved gene structures and carboxy-terminal motifs in the Myb gene family of Arabidopsis and *Oryza sativa* L. ssp. indica. Genome Biol **5 (7):** R46

Jones-Rhoades MW, Borevitz JO, Preuss D (2007) Genome-wide expression profiling of the Arabidopsis female gametophyte identifies families of small, secreted proteins. PLoS Genet **3:** 1848-1861

Joubes J, Chevalier C, Dudits D, Heberle-Bors E, Inze D, Umeda M, Renaudin JP (2000) CDK-related protein kinases in plants. Plant Mol Biol **43:** 607-620

Joubes J, De Schutter K, Verkest A, Inze D, De Veylder L (2004) Conditional, recombinase-mediated expression of genes in plant cell cultures. The Plant Journal **37:** 889-896

Kanno T, Mette MF, Kreil DP, Aufsatz W, Matzke M, Matzke AJM (2004) Involvement of Putative SNF2 Chromatin Remodeling Protein DRD1 in RNA-Directed DNA Methylation. Current Biology **14:** 801-805

Karimi M, De Meyer B, Hilson P (2005) Modular cloning in plant cells. Trends Plant Sci **10:** 103-105

Karimi M, Inze D, Depicker A (2002) GATEWAY vectors for Agrobacterium-mediated plant transformation. Trends Plant Sci **7:** 193-195

Kaya H, Shibahara K, Taoka K, Iwabuchi M, Stillman B, Araki T (2001) FASCIATA Genes for Chromatin Assembly Factor-1 in Arabidopsis Maintain the Cellular Organization of Apical Meristems. Cell **104:** 131-142

Kennerdell JR, Yamaguchi S, Carthew RW (2002) RNAi is activated during Drosophila oocyte maturation in a manner dependent on aubergine and spindle-E. Genes Dev **16:** 1884-1889

Kidner CA, Martienssen RA (2005) The role of ARGONAUTE1 (AGO1) in meristem formation and identity. Dev Biol **280:** 504-517

Kim HJ, Oh SA, Brownfield L, Hong SH, Ryu H, Hwang I, Twell D, Nam HG (2008) Control of plant germline proliferation by SCFFBL17 degradation of cell cycle inhibitors. Nature **455:** 1134-1137

Kinoshita T, Miura A, Choi Y, Kinoshita Y, Cao X, Jacobsen SE, Fischer RL, Kakutani T (2004) One-Way Control of FWA Imprinting in Arabidopsis Endosperm by DNA Methylation. Science **303:** 521-523

Kinoshita Y, Saze H, Kinoshita T, Miura A, Soppe WJJ, Koornneef M, Kakutani T (2007) Control of FWA gene silencing in Arabidopsis thaliana by SINE-related direct repeats. The Plant Journal **49:** 38-45

Kipreos ET, Pagano M (2000) The F-box protein family. Genome Biol **1:** REVIEWS3002

Kost B, Mathur J, Chua NH (1999) Cytoskeleton in plant development. Curr Opin Plant Biol **2:** 462-470

Kosugi S, Ohashi Y (2002) Interaction of the Arabidopsis E2F and DP Proteins Confers Their Concomitant Nuclear Translocation and Transactivation. Plant Physiol **128:** 833-843

Kurihara Y, Watanabe Y (2004) Arabidopsis micro-RNA biogenesis through Dicer-like 1 protein functions. Proceedings of the National Academy of Sciences **101:** 12753-12758

Lalanne E, Twell D (2002) Genetic Control of Male Germ Unit Organization in Arabidopsis. Plant Physiol **129:** 865-875

Lee Y, Kim M, Han J, Yeom KH, Lee S, Baek SH, Kim VN (2004) MicroRNA genes are transcribed by RNA polymerase II. EMBO J **23:** 4051-4060

Li C, Potuschak T, Colon-Carmona A, Gutierrez RA, Doerner P (2005a) Arabidopsis TCP20 links regulation of growth and cell division control pathways. Proceedings of the National Academy of Sciences USA **102:** 12978

Li J, Yang Z, Yu B, Liu J, Chen X (2005b) Methylation Protects miRNAs and siRNAs from a 3′-End Uridylation Activity in Arabidopsis. Current Biology **15:** 1501-1507

Lipardi C, Wei Q, Paterson BM (2001) RNAi as Random Degradative PCR siRNA Primers Convert mRNA into dsRNAs that Are Degraded to Generate New siRNAs. Cell **107:** 297-307

Lippman Z, Gendrel A, Black M, Vaughn M, Dedhia N, McCombie W, Lavine K, Mittal V, May B, Kasschau K (2004) Role of transposable elements in heterochromatin and epigenetic control. Nature (London) **430:** 471-476

Lippman Z, May B, Yordan C, Singer T, Martienssen R (2003) Distinct mechanisms determine transposon inheritance and methylation via small interfering RNA and histone modification. PLoS Biol **1:** E67

Llave C, Kasschau KD, Rector MA, Carrington JC (2002) Endogenous and Silencing-Associated Small RNAs in Plants. Plant Cell **14:** 1605-19

Lorenz S, Tintelnot S, Reski R, Decker EL (2003) Cyclin D-knockout uncouples developmental progression from sugar availability. Plant Mol Biol **53:** 227-236

Lum L, Beachy PA (2004) The hedgehog response network: sensors, switches, and routers. Science **304:** 1755-1759

Lynn K (1999) The PINHEAD/ZWILLE gene acts pleiotropically in Arabidopsis development and has overlapping functions with the ARGONAUTE1 gene. Development **126:** 469-481

Maddison AL, Hedley PE, Meyer RC, Aziz N, Davidson D, Machray GC (1999) Expression of tandem invertase genes associated with sexual and vegetative growth cycles in potato. Plant Mol Biol **41:** 741-752

Magnard JL, Yang M, Chen YCS, Leary M, McCormick S (2001) The Arabidopsis Gene Tardy Asynchronous Meiosis Is Required for the Normal Pace and Synchrony of Cell Division during Male Meiosis. Plant Physiol **127:** 1157-1166

Mariconti L, Pellegrini B, Cantoni R, Stevens R, Bergounioux C, Cella R, Albani D (2002) The E2F Family of Transcription Factors from Arabidopsis thaliana NOVEL AND CONSERVED COMPONENTS OF THE RETINOBLASTOMA/E2F PATHWAY IN PLANTS. J Biol Chem **277:** 9911-9919

Martin C, Paz-Ares J (1997) MYB transcription factors in plants. Trends in Genetics **13:** 67-73

Masubelele NH, Dewitte W, Menges M, Maughan S, Collins C, Huntley R, Nieuwland J, Scofield S, Murray JAH (2005) D-type cyclins activate division in the root apex to promote seed germination in Arabidopsis. Proceedings of the National Academy of Sciences USA **102:** 15694-15699

Matranga C, Zamore PD (2007) Small silencing RNAs. Current Biology **17:** 789-793

Matthew L (2004) RNAi for plant functional genomics. Comp Funct Genomics **5:** 240-244

Matzke MA, Birchler JA (2005) RNAi-mediated pathways in the nucleus. Nature Reviews Genetics **6:** 24-35

McCallum CM, Comai L, Greene EA, Henikoff S (2000) T argeting I nduced L ocal L esions IN G enomes (TILLING) for Plant Functional Genomics. Plant Physiol **123:** 439-442

Menges M, de Jager SM, Gruissem W, Murray JAH (2005) Global analysis of the core cell cycle regulators of Arabidopsis identifies novel genes, reveals multiple and highly specific profiles of expression and provides a coherent model for plant cell cycle control. The Plant Journal **41:** 546-566

Menges M, Murray JAH (2002) Synchronous Arabidopsis suspension cultures for analysis of cell-cycle gene activity. Plant J **30:** 203-212

Mette M, Aufsatz W, van der Winden J, Matzke M, Matzke A (2000) Transcriptional silencing and promoter methylation triggered by double-stranded RNA. EMBO J **19:** 5194-5201

Metzlaff M, O'Dell M, Cluster P, Flavell R (1997) RNA-Mediated RNA Degradation and Chalcone Synthase A Silencing in Petunia. CELL **88:** 845-854

Mi S, Cai T, Hu Y, Chen Y, Hodges E, Ni F, Wu L, Li S, Zhou H, Long C (2008) Sorting of Small RNAs into Arabidopsis Argonaute Complexes Is Directed by the 5′ Terminal Nucleotide. CELL **133:** 116-127

Mori T, Kuroiwa H, Higashiyama T, Kuroiwa T (2006) Generative Cell Specific 1 is essential for angiosperm fertilization. Nat Cell Biol **8:** 64-71

Mourrain P, Béclin C, Elmayan T, Feuerbach F, Godon C, Morel JB, Jouette D, Lacombe AM, Nikic S, Picault N (2000) Arabidopsis SGS2 and SGS3 Genes Are Required for Posttranscriptional Gene Silencing and Natural Virus Resistance. Cell **101:** 533-542

Nakagami H, Kawamura K, Sugisaka K, Sekine M, Shinmyo A (2002) Phosphorylation of Retinoblastoma-Related Protein by the Cyclin D/Cyclin-Dependent Kinase Complex Is Activated at the G1/S-Phase Transition in Tobacco. Plant Cell **14:** 1847-1857

Napoli C, Lemieux C, Jorgensen R (1990) Introduction of a Chimeric Chalcone Synthase Gene into Petunia Results in Reversible Co-Suppression of Homologous Genes in trans. Plant cell **2:** 279-289

Nonomura KI, Morohoshi A, Nakano M, Eiguchi M, Miyao A, Hirochika H, Kurata N (2007) A Germ Cell Specific Gene of the ARGONAUTE Family Is Essential for the Progression of Premeiotic Mitosis and Meiosis during Sporogenesis in Rice. Plant Cell **19:** 2583-94

Nowack MK, Grini PE, Jakoby MJ, Lafos M, Koncz C, Schnittger A (2006) A positive signal from the fertilization of the egg cell sets off endosperm proliferation in angiosperm embryogenesis. Nat Genet **38:** 63-67

Oh SA, Johnson A, Smertenko A, Rahman D, Park SK, Hussey PJ, Twell D (2005) A divergent cellular role for the FUSED kinase family in the plant-specific cytokinetic phragmoplast. Current Biology **15:** 2107-2111

Okada T, Bhalla PL, Singh MB (2005) Transcriptional Activity of Male Gamete-specific Histone gcH3 Promoter in Sperm Cells of Lilium longiflorum. Plant Cell Physiol **46:** 797-802

Okada T, Bhalla PL, Singh MB (2006) Expressed sequence tag analysis of Lilium longiflorum generative cells. Plant Cell Physiol **47:** 698-705

Okada T, Endo M, Singh MB, Bhalla PL (2005) Analysis of the histone H3 gene family in Arabidopsis and identification of the male-gamete-specific variant AtMGH3. Plant J **44:** 557-568

Oldenhof M, Groot P, Visser J, Schrauwen J, Wullems G (1996) Isolation and characterization of a microspore-specific gene from tobacco. Plant Mol Biol **31:** 213-225

Onodera Y, Haag JR, Ream T, Nunes PC, Pontes O, Pikaard CS (2005) Plant Nuclear RNA Polymerase IV Mediates siRNA and DNA Methylation-Dependent Heterochromatin Formation. Cell **120:** 613-622

Owen HA, Makaroff CA (1995) Ultrastructure of microsporogenesis and microgametogenesis inArabidopsis thaliana (L.) Heynh. ecotype Wassilewskija (Brassicaceae). Protoplasma **185:** 7-21

Parizotto EA, Dunoyer P, Rahm N, Himber C, Voinnet O (2004) In vivo investigation of the transcription, processing, endonucleolytic activity, and functional relevance of the spatial distribution of a plant miRNA. Genes Dev **18:** 2237-2242

Park MY, Wu G, Gonzalez-Sulser A, Vaucheret H, Poethig RS (2005) Nuclear processing and export of microRNAs in Arabidopsis. Proceedings of the National Academy of Sciences **102:** 3691-3696

Park SK, Howden R, Twell D (1998) The Arabidopsis thaliana gametophytic mutation gemini pollen1 disrupts microspore polarity, division asymmetry and pollen cell fate. Development **125:** 3789-3799

Pelissier T, Thalmeir S, Kempe D, Sanger H, Wassenegger M Heavy de novo methylation at symmetrical and non-symmetrical sites is a hallmark of RNA-directed DNA methylation. Nucleic Acids Res **27:** 1625-1634

Peragine A, Yoshikawa M, Wu G, Albrecht HL, Poethig RS (2004) SGS3 and SGS2/SDE1/RDR6 are required for juvenile development and the production of trans-acting siRNAs in Arabidopsis. Genes Dev **18:** 2368-2379

Pickart CM (2001) Mechanisms underlying ubiquitination. Annual Review of Biochemistry **70:** 503-33

Pina C, Pinto F, Feijo JA, Becker JD (2005) Gene family analysis of the Arabidopsis pollen transcriptome reveals biological implications for cell growth, division control, and gene expression regulation. Plant Physiol **138:** 744-756

Planchais S, Perennes C, Glab N, Mironov V, Inzé D, Bergounioux C (2002a) Characterization of cis-acting element involved in cell cycle phase-independent activation of Arath; CycB1; 1 transcription and identification of putative regulatory proteins. Plant Mol Biol **50:** 109-125

Porceddu A, Stals H, Reichheld JP, Segers G, De Veylder L, de Pinho Barro^ co, R., Casteels P, Van Montagu M, Inze D, Mironov V (2001) J Biol Chem **276:** 36354-36360

Preuss D, Rhee S, Davis R (1994) Tetrad analysis possible in Arabidopsis with mutation of the QUARTET (QRT) genes. Science **264:** 1458-1460

Qi Y, Denli AM, Hannon GJ (2005) Biochemical Specialization within Arabidopsis RNA Silencing Pathways. Mol Cell **19:** 421-428

Qin LX, Perennes C, Richard L, Bouvier-Durand M, Tréhin C, Inzé D, Bergounioux C (1996) G2-and early-M-specific expression of the NTCYC1 cyclin gene in Nicotiana tabacum cells. Plant Mol Biol **32:** 1093-1101

Ramirez-Parra E, Lopez-Matas MA, Frundt C, Gutierrez C (2004) Role of an atypical E2F transcription factor in the control of Arabidopsis cell growth and differentiation. Plant cell **16:** 2350-2363

Reichheld JP, Chaubet N, Shen WH, Renaudin JP, Gigot C (1996) Multiple A-type cyclins express sequentially during the cell cycle in Nicotiana tabacum BY2 cells. Proceedings of the National Academy of Sciences **93:** 13819-13824

Renaudin JP, Doonan JH, Freeman D, Hashimoto J, Hirt H, Inzé D, Jacobs T, Kouchi H, Rouzé P, Sauter M (1996) Plant cyclins: a unified nomenclature for plant A-, B-and D-type cyclins based on sequence organization. Plant Mol Biol **32:** 1003-1018

Riou-Khamlichi C, Huntley R, Jacqmard A, Murray JAH (1999) Cytokinin Activation of Arabidopsis Cell Division Through a D-Type Cyclin. Science **283:** 1541-1544

Rossi V, Locatelli S, Lanzanova C, Boniotti MB, Varotto S, Pipal A, Goralik-Schramel M, Lusser A, Gatz C, Gutierrez C (2003) A maize histone deacetylase and retinoblastoma-related protein physically interact and cooperate in repressing gene transcription. Plant Mol Biol **51:** 401-413

Rossignol P, Stevens R, Perennes C, Jasinski S, Cella R, Tremousaygue D, Bergounioux C (2002) AtE2F-a and AtDP-a, members of the E2F family of transcription factors, induce Arabidopsis leaf cells to re-enter S phase. Molecular Genetics and Genomics **266:** 995-1003

Rotman N, Durbarry A, Wardle A, Yang WC, Chaboud A, Faure JE, Berger F, Twell D (2005) A novel class of MYB factors controls sperm-cell formation in plants. Curr Biol **15:** 244-248

Roudier F, Fedorova E, Gyorgyey J, Feher A, Brown S, Kondorosi A, Kondorosi E (2000) Cell cycle function of a Medicago sativa A2-type cyclin interacting with a PSTAIRE-type cyclin-dependent kinase and a retinoblastoma protein. The Plant Journal **23:** 73-83

Sabelli PA, Dante RA, Leiva-Neto JT, Jung R, Gordon-Kamm WJ, Larkins BA (2005) RBR3, a member of the retinoblastoma-related family from maize, is regulated by the RBR1/E2F pathway. Proceedings of the National Academy of Sciences **102:** 13005-13012

Saito K, Nishida KM, Mori T, Kawamura Y, Miyoshi K, Nagami T, Siomi H, Siomi MC (2006) Specific association of Piwi with rasiRNAs derived from retrotransposon and heterochromatic regions in the Drosophila genome. Genes Dev **20:** 2214-2222

Schneidereit A, Scholz-Starke J, Buttner M (2003) Functional Characterization and Expression Analyses of the Glucose-Specific AtSTP9 Monosaccharide Transporter in Pollen of Arabidopsis 1. Plant Physiol **133:** 182-190

Schnittger A, Schöbinger U, Stierhof YD, Hülskamp M (2002) Ectopic B-Type Cyclin Expression Induces Mitotic Cycles in Endoreduplicating Arabidopsis Trichomes. Current Biology **12:** 415-420

Scholz-Starke J, Buttner M, Sauer N (2003) AtSTP6, a New Pollen-Specific H - Monosaccharide Symporter from Arabidopsis. Plant Physiol **131:** 70-77

Sessions A (1997) ETTIN patterns the Arabidopsis floral meristem and reproductive organs. Development **124:** 4481-4491

Shaul O, Mironov V, Burssens S, Van Montagu M, Inze D (1996a) Two Arabidopsis cyclin promoters mediate distinctive transcriptional oscillation in synchronized tobacco BY-2 cells. Proceedings of the National Academy of Sciences **93:** 4868-4872

Shimotohno A, Umeda-Hara C, Bisova K, Uchimiya H, Umeda M (2004) The Plant-Specific Kinase CDKF; 1 Is Involved in Activating Phosphorylation of Cyclin-Dependent Kinase-Activating Kinases in Arabidopsis. Plant Cell **16:** 2954-3006

Sijen T, Fleenor J, Simmer F, Thijssen KL, Parrish S, Timmons L, Plasterk RHA, Fire A (2001) On the Role of RNA Amplification in dsRNA-Triggered Gene Silencing. Cell **107:** 465-476

Smith NA, Singh SP, Wang MB, Stoutjesdijk PA, Green AG, Waterhouse PM (2000) Total silencing by intron-spliced hairpin RNAs. Nature **407:** 319-320

Soni R, Carmichael J, Shah Z, Murray J (1995) A Family of Cyclin D Homologs from Plants Differentially Controlled by Growth Regulators and Containing the Conserved Retinoblastoma Protein Interaction Motif. Plant cell **7:** 85-103

Soppe WJJ, Jacobsen SE, Alonso-Blanco C, Jackson JP, Kakutani T, Koornneef M, Peeters AJM (2000) The Late Flowering Phenotype of fwa Mutants Is Caused by Gain-of-Function Epigenetic Alleles of a Homeodomain Gene. Mol Cell **6:** 791-802

Sorrell DA, Marchbank A, McMahon K, Dickinson JR, Rogers HJ, Francis D (2002) A WEE1 homologue from Arabidopsis thaliana. Planta **215:** 518-522

Stam M, de Bruin R, Kenter S, van der Hoorn RAL, van Blokland R, Mol JNM, Kooter JM (1997) Post-transcriptional silencing of chalcone synthase in Petunia by inverted transgene repeats. The Plant Journal **12:** 63-82

Sun Y, Dilkes BP, Zhang C, Dante RA, Carneiro NP, Lowe KS, Jung R, Gordon-Kamm WJ, Larkins BA (1999) Characterization of maize (Zea mays L.) Wee1 and its activity in developing endosperm. Proceedings of the National Academy of Sciences USA **96:** 4180-4185

Swaminathan K, Yang Y, Grotz N, Campisi L, Jack T (2000) An Enhancer Trap Line Associated with a D-Class Cyclin Gene in Arabidopsis. Plant Physiol **124:** 1658-1667

Tabara H, Sarkissian M, Kelly WG, Fleenor J, Grishok A, Timmons L, Fire A, Mello CC (1999) The rde-1 Gene, RNA Interference, and Transposon Silencing in C. elegans. CELL **99:** 123-132

Takeda T, Amano K, Ohto M, Nakamura K, Sato S, Kato T, Tabata S, Ueguchi C (2006) RNA Interference of the Arabidopsis Putative Transcription Factor TCP16 Gene Results in Abortion of Early Pollen Development. Plant Mol Biol **61:** 165-177

Torres Acosta J, de Almeida Engler J, Raes J, Magyar Z, De Groodt R, Inzé D, De Veylder L (2004) Molecular characterization ofArabidopsisPHO80-like proteins, a novel class of CDKA; 1-interacting cyclins. Cellular and Molecular Life Sciences (CMLS) **61:** 1485-1497

Trehin C, Glab N, Perennes C, Planchais S, Bergounioux C (1999) M phase-specific activation of theNicotiana sylvestris Cyclin B1promoter involves multiple regulatory elements. The Plant Journal **17:** 263-273

Truernit E, Stadler R, Baier K, Sauer N (1999) A male gametophyte-specific monosaccharide transporter inArabidopsis. The Plant Journal **17:** 191-201

Twell D (1995) Diphtheria toxin-mediated cell ablation in developing pollen: Vegetative cell ablation blocks generative cell migration. Protoplasma **187:** 144-154

Twell D (1990) Pollen-specific gene expression in transgenic plants: coordinate regulation of two different tomato gene promoters during microsporogenesis. Development **109:** 705-713

Twell D, Oh S, Honys D (2006) Pollen Development, a Genetic and Transcriptomic View. PLANT CELL MONOGRAPHS **3:** 15-45

Twell D, Park SK, Hawkins TJ, Schubert D, Schmidt R, Smertenko A, Hussey PJ (2002) MOR1/GEM1 plays an essential role in the plant-specific cytokinetic phragmoplast. Nat Cell Biol **4:** 711-714

Twell D, Park SK, Lalanne E (1998) Asymmetric division and cell-fate determination in developing pollen. Trends Plant Sci **3:** 305-310

Umeda M, Umeda-Hara C, Uchimiya H (2000) A cyclin-dependent kinase-activating kinase regulates differentiation of root initial cells in Arabidopsis. PNAS **97:** 13396-13400

Van Tunen A, Mur L, Brouns G, Rienstra J, Koes R, Mol J (1990) Pollen-and Anther-Specific chi Promoters from Petunia: Tandem Promoter Regulation of the chiA Gene. Plant Cell **2:** 393-401

Vandepoele K, Raes J, De Veylder L, Rouze P, Rombauts S, Inze D (2002) Genome-Wide Analysis of Core Cell Cycle Genes in Arabidopsis. Plant Cell **14:** 903-913

Vaucheret H (2006) Post-transcriptional small RNA pathways in plants: mechanisms and regulations. Genes Dev **20:** 759-771

Vaucheret H, Vazquez F, Crete P, Bartel DP (2004) The action of ARGONAUTE1 in the miRNA pathway and its regulation by the miRNA pathway are crucial for plant development. Genes Dev **18:** 1187-1197

Vazquez F, Vaucheret H, Rajagopalan R, Lepers C, Gasciolli V, Mallory AC, Hilbert JL, Bartel DP, Crété P (2004) Endogenous trans-Acting siRNAs Regulate the Accumulation of Arabidopsis mRNAs. Mol Cell **16:** 69-79

Vodermaier HC (2004) APC/C and SCF: Controlling Each Other and the Cell Cycle. Current Biology **14:** 787-796

von Besser K, Frank AC, Johnson MA, Preuss D (2006) Arabidopsis HAP2 (GCS1) is a sperm-specific gene required for pollen tube guidance and fertilization. Development **133:** 4761-4769

Wagner D (2003) Chromatin regulation of plant development. Curr Opin Plant Biol **6:** 20-28

Wang G, Kong H, Sun Y, Zhang X, Zhang W, Altman N, dePamphilis CW, Ma H (2004) Genome-Wide Analysis of the Cyclin Family in Arabidopsis and Comparative Phylogenetic Analysis of Plant Cyclin-Like Proteins 1 [w]. Plant Physiol **135:** 1084-1099

Wang H, Qi Q, Schorr P, Cutler AJ, Crosby WL, Fowke LC (1998) ICK1, a cyclin-dependent protein kinase inhibitor fromArabidopsis thalianainteracts with both Cdc2a and CycD3, and its expression is induced by abscisic acid. The Plant Journal **15:** 501-510

Wang H, Zhou Y, Gilmer S, Whitwill S, Fowke LC (2000) Expression of the plant cyclin-dependent kinase inhibitor ICK1 affects cell division, plant growth and morphology. The Plant Journal **24:** 613-623

Wassenegger M, Heimes S, Riedel L, Sanger HL (1994) RNA-directed de novo methylation of genomic sequences in plants. Cell **76:** 567-576

Waterhouse PM, Graham MW, Wang MB (1998) Virus resistance and gene silencing in plants can be induced by simultaneous expression of sense and antisense RNA. Proceedings of the National Academy of Sciences **95:** 13959-13964

Weingartner M, Criqui MC, Meszaros T, Binarova P, Schmit AC, Helfer A, Derevier A, Erhardt M, Bogre L, Genschik P (2004a) Expression of a Nondegradable Cyclin B1 Affects Plant Development and Leads to Endomitosis by Inhibiting the Formation of a Phragmoplast. Plant cell **16:** 643-657

Weingartner M, Pelayo HR, Binarova P, Zwerger K, Melikant B, de la Torre C, Heberle-Bors E, Bogre L (2003) A plant cyclin B2 is degraded early in mitosis and its ectopic expression shortens G2-phase and alleviates the DNA-damage checkpoint. J Cell Sci **116:** 487-498

Wesley SV, Helliwell CA, Smith NA, Wang MB, Rouse DT, Liu Q, Gooding PS, Singh SP, Abbott D, Stoutjesdijk PA (2001) Construct design for efficient, effective and high-throughput gene silencing in plants. The Plant Journal **27:** 581-590

Weterings K, Schrauwen J, Wullems G, Twell D (1995) Functional dissection of the promoter of the pollen-specific gene NTP303 reveals a novel pollen-specific, and conserved cis-regulatory element. The Plant Journal **8:** 55-63

Wienholds E, Kloosterman WP, Miska E, Alvarez-Saavedra E, Berezikov E, de Bruijn E, Horvitz HR, Kauppinen S, Plasterk RHA (2005) MicroRNA Expression in Zebrafish Embryonic Development. Science **309:** 310-311

Wildwater M, Campilho A, Perez-Perez JM, Heidstra R, Blilou I, Korthout H, Chatterjee J, Mariconti L, Gruissem W, Scheres B (2005) The RETINOBLASTOMA-RELATED Gene Regulates Stem Cell Maintenance in Arabidopsis Roots. Cell **123:** 1337-1349

Xie Z, Allen E, Fahlgren N, Calamar A, Givan SA, Carrington JC (2005a) Expression of Arabidopsis MIRNA Genes. Plant Physiol **138:** 2145-2154

Xie Z, Johansen LK, Gustafson AM, Kasschau KD, Lellis AD, Zilberman D, Jacobsen SE, Carrington JC (2004) Genetic and Functional Diversification of Small RNA Pathways in Plants. PLoS Biology **2:** 104-108

Xing S, Zachgo S (2007) Pollen Lethality: A Phenomenon in Arabidopsis RNA Interference Plants. Plant Physiol **145:** 330-333

Xu H, Davies SP, Kwan BYH, O'Brien AP, Singh M, Knox RB (1993) Haploid and diploid expression of a Brassica campestris anther-specific gene promoter in Arabidopsis and tobacco. Molecular Genetics and Genomics **239:** 58-65

Yu B, Yang Z, Li J, Minakhina S, Yang M, Padgett RW, Steward R, Chen X (2005) Methylation as a Crucial Step in Plant microRNA Biogenesis. Science **307:** 932-935

Yu Y, Steinmetz A, Meyer D, Brown S, Shen WH (2003) The Tobacco A-Type Cyclin, Nicta; CYCA3; 2, at the Nexus of Cell Division and Differentiation. Plant Cell **15:** 2763-2777

Zarsky V, Garrido D, Říhová L, Tupý J, Vicente O, Heberle-Bors E (1992) Derepression of the cell cycle by starvation is involved in the induction of tobacco pollen embryogenesis. Sexual Plant Reproduction **5:** 189-194

Zhou Y, Wang H, Gilmer S, Whitwill S, Keller W, Fowke LC (2002) Control of petal and pollen development by the plant cyclin-dependent kinase inhibitor ICK1 in transgenic Brassica plants. Planta **215:** 248-257

Zilberman D, Cao X, Jacobsen SE (2003) ARGONAUTE4 Control of Locus-Specific siRNA Accumulation and DNA and Histone Methylation. Science **299:** 716-719

Zimmermann P, Hirsch-Hoffmann M, Hennig L, Gruissem W (2004) Genevestigator. Arabidopsis Microarray Database and Analysis Toolbox. Plant Physiol **136:** 2621-2632